Nuclear Science ISBN 92-64-02304-6

Source Convergence in Criticality Safety Analyses

Phase I: Results for Four Test Problems

Roger N. Blomquist
Argonne National Laboratory, United States

Malcolm Armishaw, David Hanlon, and Nigel Smith
SERCO Assurance, United Kingdom

Yoshitaka Naito and Jinan Yang
NAIS Co. Inc, Japan

Yoshinori Mioshi and Toshihiro Yamamoto
Japan Atomic Energy Agency, Japan

Olivier Jacquet and Joachim Miss
Institut de radioprotection et de sûreté nucléaire, France

NEA No. 5431

NUCLEAR ENERGY AGENCY
ORGANISATION FOR ECONOMIC CO-OPERATION AND DEVELOPMENT

ORGANISATION FOR ECONOMIC CO-OPERATION AND DEVELOPMENT

The OECD is a unique forum where the governments of 30 democracies work together to address the economic, social and environmental challenges of globalisation. The OECD is also at the forefront of efforts to understand and to help governments respond to new developments and concerns, such as corporate governance, the information economy and the challenges of an ageing population. The Organisation provides a setting where governments can compare policy experiences, seek answers to common problems, identify good practice and work to co-ordinate domestic and international policies.

The OECD member countries are: Australia, Austria, Belgium, Canada, the Czech Republic, Denmark, Finland, France, Germany, Greece, Hungary, Iceland, Ireland, Italy, Japan, Korea, Luxembourg, Mexico, the Netherlands, New Zealand, Norway, Poland, Portugal, the Slovak Republic, Spain, Sweden, Switzerland, Turkey, the United Kingdom and the United States. The Commission of the European Communities takes part in the work of the OECD.

OECD Publishing disseminates widely the results of the Organisation's statistics gathering and research on economic, social and environmental issues, as well as the conventions, guidelines and standards agreed by its members.

* * *

This work is published on the responsibility of the Secretary-General of the OECD. The opinions expressed and arguments employed herein do not necessarily reflect the official views of the Organisation or of the governments of its member countries.

NUCLEAR ENERGY AGENCY

The OECD Nuclear Energy Agency (NEA) was established on 1st February 1958 under the name of the OEEC European Nuclear Energy Agency. It received its present designation on 20th April 1972, when Japan became its first nonEuropean full member. NEA membership today consists of 28 OECD member countries: Australia, Austria, Belgium, Canada, the Czech Republic, Denmark, Finland, France, Germany, Greece, Hungary, Iceland, Ireland, Italy, Japan, Luxembourg, Mexico, the Netherlands, Norway, Portugal, Republic of Korea, the Slovak Republic, Spain, Sweden, Switzerland, Turkey, the United Kingdom and the United States. The Commission of the European Communities also takes part in the work of the Agency.

The mission of the NEA is:

– to assist its member countries in maintaining and further developing, through international co-operation, the scientific, technological and legal bases required for a safe, environmentally friendly and economical use of nuclear energy for peaceful purposes, as well as

– to provide authoritative assessments and to forge common understandings on key issues, as input to government decisions on nuclear energy policy and to broader OECD policy analyses in areas such as energy and sustainable development.

Specific areas of competence of the NEA include safety and regulation of nuclear activities, radioactive waste management, radiological protection, nuclear science, economic and technical analyses of the nuclear fuel cycle, nuclear law and liability, and public information. The NEA Data Bank provides nuclear data and computer program services for participating countries.

In these and related tasks, the NEA works in close collaboration with the International Atomic Energy Agency in Vienna, with which it has a Cooperation Agreement, as well as with other international organisations in the nuclear field.

FOREWORD

Slow source convergence has long been a challenge in some loosely coupled neutronics problems, ranging from the Whitesides "criticality of the world" problem identified in 1971 to some very recent burn-up credit benchmark calculation comparisons under the auspices of the OECD Nuclear Energy Agency (NEA). In Monte Carlo calculations, slow convergence and statistical fluctuations can combine to produce unreliable source distributions and fission rates as well as underestimates of keff and its uncertainty. This problem is especially important when no symptoms of non-convergence are apparent to the analyst.

To explore these problems for the benefit of the international criticality safety community, the NEA Working Party on Nuclear Criticality Safety established an Expert Group on Source Convergence in Criticality Safety Analysis in the fall of 2000. Aimed at fostering improved robustness of criticality safety analyses with respect to source convergence, the group's first task was to assemble four test problems that represent cases previously encountered in criticality safety analyses. They are intended to be used as a basis for comparison of source convergence performance rather than comparison of physics results. The problems include a reactor fuel storage array, a spent fuel pin array, an aqueous processing system and an array of small fissile components.

In this report on the Phase I work of the Expert Group, the multiple cases of each of these problems have been analysed with a variety of codes to assess vulnerability to slow convergence and/or the statistical fluctuations inherent in Monte Carlo calculations. Their results have been collated and compared.

It is hoped that the development of improved methods to speed convergence or detect non-convergence will emerge from these comparisons and from investigations carried out by the participants and by others. In particular, statistical tests used to detect non-convergence ought to be characterised partly by their reliability measured using the NEA source convergence test problems. The four test problems can also be used to develop source convergence input parameter guidelines for criticality safety codes and as training problems for criticality safety analysts.

This publication is available in colour on the NEA website at:
www.nea.fr/html/science/pubs/2006/nea5431-source.pdf

Acknowledgements

The authors wish to thank D. Mennerdahl, T. Kuroshi, J. Wagner, M. Armishau, J. Miss and Y. Naito for reviewing sections of this report.

TABLE OF CONTENTS

Chapter 1

INTRODUCTION

By R.N. Blomquist

This report describes the Phase I work done by the OECD/NEA Expert Group on Source Convergence in Criticality Safety Analysis under the supervision of the Working Party on Nuclear Criticality Safety during 1999-2005. Phase I consists mostly of specification and analysis of computational test problems of interest to criticality safety analysts that exhibit source convergence difficulties. It is aimed at improving the computational basis of criticality safety analyses.

The practice of criticality safety engineering involves the use of criticality data derived from experiments and associated calculations. A typical analysis will also include calculations solving the neutron transport equation employing either the Monte Carlo method or deterministic methods. Both kinds of calculations require computing the fission distribution iteratively until it is sufficiently converged, and only then extracting the parameters of interest, e.g., the fundamental mode eigenvalue. These calculations begin with a starting source determined by the user or by default in the computer code. Unless there is spatial decoupling between fissionable components with very different spectra, one can expect the neutron spectrum to converge very quickly, so the term "source convergence" in this report refers to spatial fission distributions. A deterministic method is finished when the eigenvalue convergence and source convergence criteria are met. A Monte Carlo method requires statistical sampling after acceptable source convergence has occurred. Optionally, the statistical sampling can be carried out using an initial source distribution from a sufficiently similar earlier calculation. Either way the sampling process is continued until estimated uncertainties are sufficiently small (statistical convergence).

Because the iteration process updates the generation source distribution, the estimated parameters are not independent between generations. For some problems in which the neutronic coupling between multiplying media is very small, the convergence rate of the fission source iterations is extremely slow. Moreover, these calculations are characterized by a strong dependence of the results on the initial source distribution, an indication that source convergence is not achieved. These effects are not problems unless the analyst mistakenly decides the calculation has converged (because there is no apparent change in the solution between iterations). In such cases, the estimated fission distribution will be in error, and in some problems, the eigenvalue can be substantially under-predicted, with adverse implications for the safety analysis.

Our premise is that an eigenvalue produced using an insufficiently converged source is not reliably computed and should not be used in a safety analysis. Whether the source is sufficiently converged depends on the purpose of the calculation and the nature of the system being analysed. A conservatively calculated source can be acceptable where a bounding estimate is satisfactory. However, evaluation of critical experiments and estimation of small reactivity effects should be based on much tighter convergence criteria. Further, the sensitivity of k_{eff} to variations in the fission source can be a consideration. For geometrically simple systems, the traditional way to check source convergence has

been to check k_{eff} convergence for an increasing number of generations and for an increasing number of skipped initial generations. Specific studies of fission source spatial distributions, however, are important for neutronically complicated systems.

It will be seen that the effect on the neutron multiplication factor (k_{eff}) of incomplete convergence or other related computational difficulties sometimes is small. In practice, it is frequently possible to compute a correct k_{eff} without completely converging the fission source distribution. The results discussed in this report, however, show that statistical tests applied to Monte Carlo k_{eff} estimates do not always perform well, nor do eigenvalue convergence tests in deterministic codes.

Compared to deterministic methods, Monte Carlo calculations are more challenged by loosely coupled systems because the method has three features that can prematurely make the source appear converged. First, variance estimators frequently assume zero serial correlation [1,2]. If the source is not converged, this assumption is invalid, and the uncertainties are underestimated. Low and shrinking uncertainties are used by Monte Carlo analysts as indicators of both statistical and source convergence, so any underestimation increases the risk of non-conservative results. Second, the power method on the fission source iteration in Monte Carlo codes is unaccelerated. Deterministic transport codes usually use well-known fission source iteration acceleration methods, but these are not very transferable to Monte Carlo codes because of noise. Although some mitigating algorithms are available [e.g., 1, 3, 4], these are insufficiently effective in severe cases. Finally, Monte Carlo source convergence difficulties can arise because of undersampling in parts of the system [5]. Fortunately, there are several obvious remedies for all three difficulties: (1) perform additional calculations with more histories and/or more neutron generations used to converge the fission source, (2) perform similar calculations with a different initial source and compare the solutions, and (3) apply statistical tests that provide the analyst warnings when the fission source is insufficiently converged.

Which tests and methods are best applied, and how effective they are, is the object of work underway at a variety of institutions with efforts in criticality safety analysis or development of its supporting computational tools. The OECD Nuclear Energy Agency Expert Group on Fission Source Convergence in Criticality Safety Analyses has specified four idealised test problems that represent cases previously encountered in real criticality safety analyses. The Expert Group reviewed the specifications, and various participants performed the specified calculations, along with other calculations felt to be illuminating, and submitted their results to the coordinator for a particular test problem. Chapters 2-5 present the specifications and the four coordinators' reports on the accumulated results.

These problems are intended for evaluation of source convergence algorithms and convergence tests so that investigators working in different institutions can assess method and code performance consistently. Of course, they also should make good test problems for training criticality safety analysts. While retaining the source convergence properties of the original system, their specifications have been modified to exclude proprietary information, to simplify input preparation, and to reduce computation times.

The computational control parameters (number of histories, etc.) included in the specifications are not intended to be recommendations, but are specified merely for consistency of comparisons during the first phase carried out by the members of the Expert Group. In order to highlight convergence problems, some of these parameters are intentionally set to sub-optimal values that would be completely unjustifiable in actual criticality calculations. In comparing results from the participants, the differences in nuclear data, transport equation approximations, and reference solutions have not been examined because they are outside of the scope of the study. Instead, the focus has been on convergence

and statistical behaviour. The test problems will be described in detail in subsequent sections of this report, but their overall characteristics are surveyed here.

Although each problem exhibits slow convergence, undersampling effects, source-related statistical anomalies, or some combination of these effects, the effects of non-convergence on the eigenvalue vary greatly. In general, very slow deterministic convergence occurs because the dominance ratio (the ratio of the second largest to the largest eigenvalue) is nearly 1.0. In these cases, the shift in eigenvalue estimates is small during the course of source iterations. In problems where the dominance ratio is far from unity (say, < 0.96), the shift is larger, but convergence is much faster.

Test problem 1 was submitted by N. Smith (Answers Software, SERCO Assurance), and is described in detail in Chapter 2. It is a fuel storage facility surrounded by concrete on three sides and water on the fourth in which 36 identical fresh fuel assemblies with about 3.5 weight percent enriched UO_2 fuel and Zr clad are stored in an alternating (checkerboard) pattern with empty locations, in a square grid demarcated by 1.0 cm steel plates. The fueled locations consist of a square pin lattice, and all locations are flooded with water. Adjacent fuel assemblies are almost completely decoupled, so deterministic and Monte Carlo calculations suffer from extremely slow convergence. A simplified calculation using VIM established that the probability that a neutron born in one subassembly will cause a fission in a particular adjacent column is about 0.003. To the naïve analyst, the problem layout suggests a uniform guess, but this is quite unrealistic because the converged fission distribution peaks in column 1, row 3 (the upper left corner), the only location bounded on two sides by concrete. For the initial fission sites in the far end to migrate to the reactive corner unit during the source iterations, very many generations will be required. Monte Carlo calculations may also show the effects of undersampling if insufficient numbers of histories per generation are used. The thirty-six cases specified differ only in their initial source distributions, generation sizes, and numbers of skip generations.

Case 27 is used here as a “reference” case. It is specified with uniform initial source, 5 000 histories per generation, skip 100 before tallying. We refer to it because a naïve user might very well select it as the best of all the specified cases, but it will be seen that this parameter set is clearly not good enough. Instead, case 30 [starting source in cell (1,1)] is probably the best of the specified cases. It is similar to what might be chosen as “best” by an experienced analyst [initial source in (1,3)], or by one who studies the physics of the problem or performs a few simple preparatory calculations. When an initial source much closer to the converged one is used, it is possible to converge the fission source with far fewer skipped generations than one needs for a uniform starting source.

Figure 1.1 shows the influence of Monte Carlo computational strategy on estimated fission distributions when a straightforward generation-by-generation power iteration is used and the assumed initial source is uniform. Since the status of the fission source convergence is manifested mainly along the x-axis, we show only the fission fractions for row 3 (along the long concrete face), which includes the location with the most reactive cell. Using a seemingly reasonable set of the specified parameters (case 27: uniform initial source, 5 000 histories per generation, skip 100 before tallying), the most reactive fuel assembly is apparent, but its fission fraction is badly underestimated. As commonly happens for very slowly converging problems, the uncertainties are also underestimated. Increasing the number of histories per generation to 25 000 substantially improves both the cell fission fraction and its uncertainty estimate, but not by enough for the source to be considered converged. (The effect on k_{eff}, however, may not be large at this point). Skipping 500 generations instead of 100, and tallying over 1 000 generations nearly converges the fission distribution sufficiently to determine accurately the additional reactivity due to reflection from two concrete faces.

Figure 1.1 Checkerboard system row 3 fission fractions for 3 cases

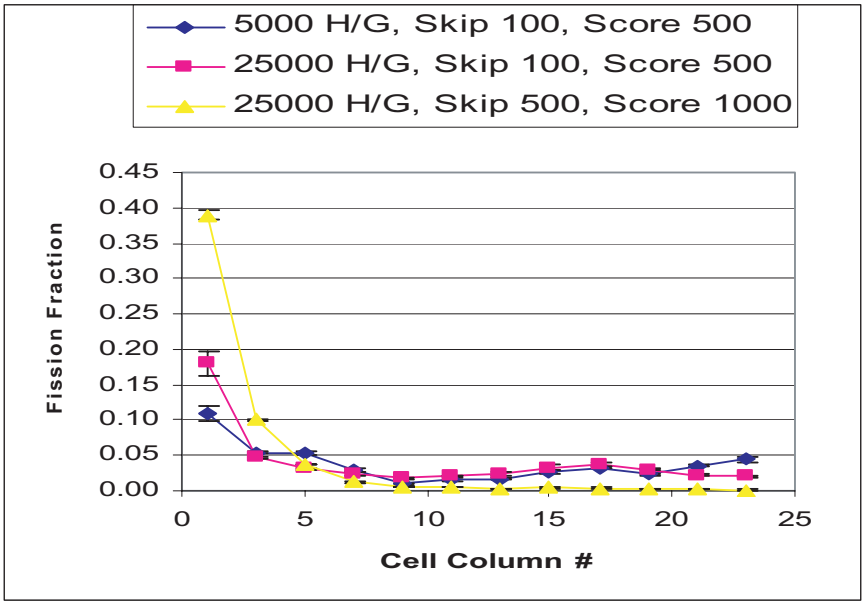

Table 1.1 shows the sensitivity of eigenvalues to the choice of Monte Carlo computational parameters. For each set of calculations (by one code), the range of eigenvalues can be viewed as a crude measure of the uncertainty embodying the combined effects of differing parameters and (sometimes) different pseudorandom number sequences. The Table also shows the differences between the largest eigenvalue and case 27. The last digits of the estimated uncertainties are shown in parentheses. Clearly, the range of eigenvalues substantially exceeds the uncertainties, so these cases are deemed to suffer from insufficient source convergence and/or inaccurate statistical treatment. Statistical tests were unable to detect the eigenvalue drift (typically 0.002) during source iterations. Additional experimentation showed that at least 700 skip generations are required to fully converge the source using conventional power iterations.

Table 1.1 k_{eff} ranges (uncertainties) over all cases, and largest difference with case 27

Participant/Code	Max(k_{eff})–Min(k_{eff})	Max(k_{eff})–Case 27 k_{eff}
ANL/VIM[a]	0.0040 (13)	0.0010 (16)
JAERI/MCNP4B[a]	0.0050 (9)	0.0025 (9)
JNC/KENO-Va[a]	0.0063 (18)	0.0011 (14)
KFKI/MCNP4C[a]	0.0038 (14)	0.0010 (9)
LANL/MCNP4C[a]	0.0053 (12)	0.0023 (6)
ORNL/KENO-Va[a]	0.0043 (10)	0.0000 (10)
Answers/MONK8A[b]	0.0047 (12)	0.0017 (8)
EMS/KENO-Va[a]	0.0065 (18)	0.0025 (14)
IRSN/MORET4[a]	0.0040 (15)	0.0029 (13)
IRSN/MORET4[b]	0.0072 (13)	0.0045 (9)
IRSN/MORET4[c]	0.0015 (9)	0.0015 (7)

[a]conventional power iteration, [b]superhistory method, [c]stratified sampling

Test problem 2 is a flooded infinite lattice of depleted LWR pins, as described in Chapter 3. Six cases are considered which describe various symmetric and non-symmetric axial composition profiles due either to axial enrichment grading or to an idealised burn-up profile. This is a simplified version of the NEA Burn-up Credit (Phase II-A) Test Problem [6]. A 285.7 cm length of high-burn-up, strongly absorbing, low-multiplication fuel in the center decouples the two reactive ends. Because there are only two reactive regions, neither end is unsampled in typical Monte Carlo calculations. Calculations with thousands of histories per generation are effectively unable to generate fissions in the high-burn-up section, so neutron transport between the ends is not successfully simulated. Consequently, the redistribution of fission sites will be effected entirely by action of the fission source algorithm. Even for the cases with a large asymmetry, source convergence is somewhat slow, and it is extremely slow for the nearly symmetric cases. The nearly symmetric cases require about 600 generations for source convergence, and the eigenvalue drift during convergence is about 0.005. The axially symmetric cases appear to produce non-symmetric fission distributions, but they are in fact exhibiting underestimates of fission distribution uncertainties.

Test problem 3 (Chapter 4) models two rectangular tanks of uranyl nitrate solution decoupled by an intervening moderating tank of water similar to the problem described in reference [3]. The structures are omitted, leaving only the solutions. The twelve cases consist of varying the left solution slab thickness to 12, 15, 18, and 20 cm, and the moderating slab to 10, 20, and 30 cm. This problem was originally used to test a fission matrix method [3], which acts as a restoring force to unduly fluctuating fission distributions. Due to relatively good coupling between the end slabs, the cases with the 10 cm water slab did not exhibit major fluctuations in the fission distribution. With 30 cm thick water, however, large asymmetric fluctuations resulted, with fission fraction ratios approaching 10. In the most asymmetric cases, even with a 30 cm water slab, the source required only about 20 generations to converge. The eigenvalue drift during convergence is about 0.01.

One computational difficulty discovered during the study of problem 3 is that homogeneous compositions can exacerbate the additional variance caused by using collisions to generate fission sites, a common Monte Carlo technique [7]. This occurs because the number of collisions that generate potential fission sites varies randomly, and in homogeneous systems every collision occurs with a non-zero fission cross section. When combined with the system's slow convergence, the result is a serious underestimate in reaction rate variances. This was most clearly evident in the moderately decoupled symmetric case (20-30-20) shown in Figure 1.2, when the fission fraction ratios reached 40. Selecting fission sites on absorption in VIM calculations produced a dramatic reduction in the fission distribution variation during the calculation.

Even when 2 000 histories per generation are sampled, undersampling is possible, especially in the most decoupled of the symmetric systems. Increasing the generation size further to 20 000 substantially reduced the fluctuations by reducing statistical variations. For the symmetric configurations, the computed ratios of the fission fractions (theoretically 1.0) have no influence on k_{eff}. To estimate k_{eff} correctly, the calculations need only include the interaction effects between the two multiplying slabs and the correct flux shape within each one.

Figure 1.2 Problem 3 fission fraction ratios for two fission site schemes

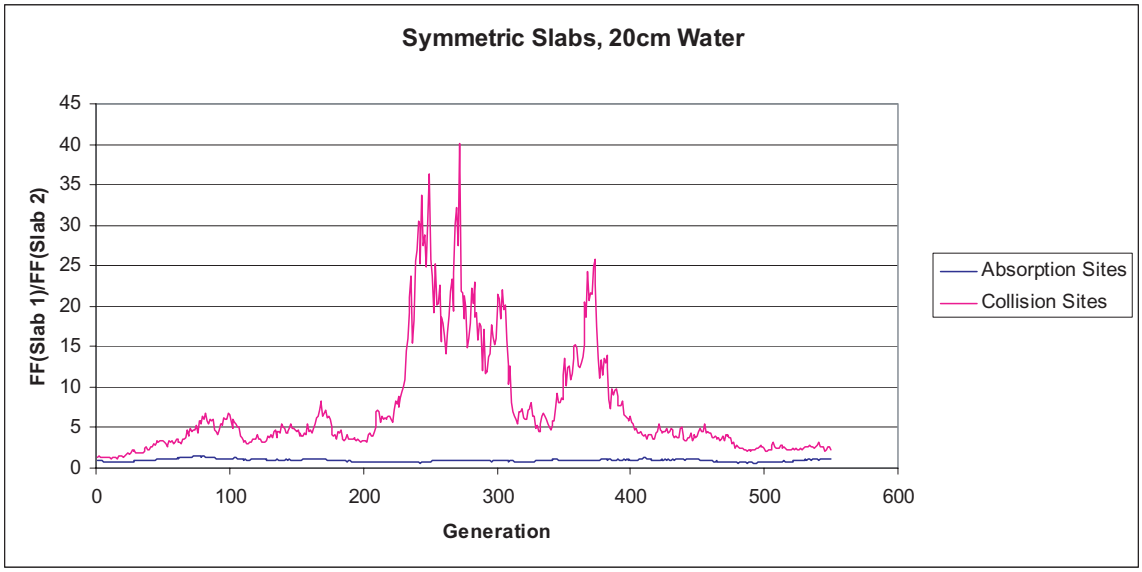

Problem 4 (Chapter 5) is a reduced-scale (5x5x1) version[8] of the 9x9x9 Whitesides problem [5], an array of metal spheres in vacuum. The centre sphere is much larger than the others, so source sites will accumulate in it while the source is converging. Unlike the checkerboard test problem where an essentially one-dimensional array of cells acts to inhibit convergence, each sphere is directly (if weakly) coupled to two to four others in its row and column, and to roughly half of the spheres. The specified initial source contains only 125 neutrons per generation with a single neutron at the centre of each sphere and 101 concentrated at the centre of the lower left corner sphere. This is deliberately chosen to be far from the converged source distribution, possibly resulting in a badly underestimated k_{eff}. Figure 1.3 shows the evolution of the instantaneous fission fraction of the central sphere during each of 10 statistically independent replica calculations. The randomness introduced by undersampling is dramatic, and it is easily reduced by increasing the number of histories per generation. It is clear that this problem does not suffer from slow convergence *per se*; once the central sphere contains a few fission sites, its fission fraction converges rapidly. In fact, this problem converges easily when a uniform initial source is used.

The authors of Chapter 5 compiled information about the codes used for test problem 4. In general, these codes were also used for the other test problems as well.

Test problem 4 can be used to address the question of convergence reliability. Although it will always converge eventually, the number of generations required varies randomly and widely. Accordingly, Monte Carlo results were submitted by each participant for 100 statistically independent replica calculations. This allowed estimation of the probability that the source fails to converge. In 100 replicas, between 100 and 900 skip generations were required to converge the fission source. The eigenvalue drift during convergence is 0.06. Stratified sampling and superhistory powering were found to produce superior convergence performance compared to conventional power iterations, but did not eliminate the possibility of non-convergence.

Figure 1.3. Problem 4 instantaneous fission fraction in central sphere for 10 replicas

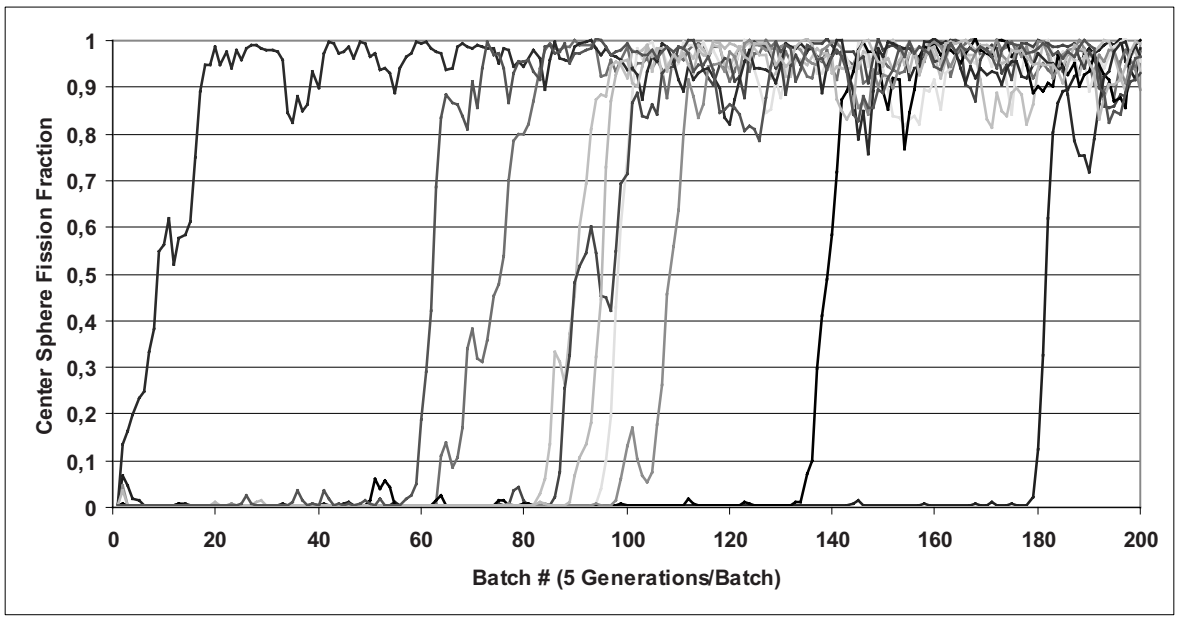

The test problem comparison programme of the expert group has stimulated a useful set of investigations into the algorithms currently used to propagate neutron sources in Monte Carlo calculations. It is common knowledge that understanding the underlying physics of criticality problems is necessary to ensure satisfactory source convergence in criticality calculations. These test problems demonstrate that statistical tests applied to eigenvalue estimates cannot be relied upon to detect inadequate source convergence. Furthermore, statistical tests commonly applied to detect non-convergence are being evaluated, and new ones are being proposed and tested.

References

[1] R.J. Brissenden and A.R. Garlick, "Biases in the Estimation of k_{eff} and its Error by Monte Carlo Methods," Ann. Nucl. Energy, 113, No. 2, pp. 63-83 (1986).

[2] E. Gelbard and Albert Gu, "Biases in Monte Carlo Eigenvalue Calculations," Nucl. Sci. and Eng., 117, pp. 1-9 (1994).

[3] T. Yamamoto, T. Nakamura, and Y. Miyoshi, "Fission Source Convergence of Monte Carlo Criticality Calculations in Weakly Coupled Fissile Arrays," J. of Nucl. Sci. and Tech., Vol. 37, No. 1, pp. 41-45, January, 2000.

[4] A. Mohamed and E. Gelbard, "Stratified Source-Sampling Techniques for Monte Carlo Eigenvalue Analysis," Proc. Int. Conf. On Physics of Nuclear Science and Technology, Hauppage, N.Y., Oct. 5-8, 1998.

[5] E.G. Whitesides, "A Difficulty in Computing the k_{eff} of the World," Trans Am Nucl Soc, 14 No. 2 (1971).

[6] OECD/NEA Expert Group on Burn-up Credit web site at
http://www.nea.fr/html/science/wpncs/buc

[7] “Alternative Implementations of the Monte Carlo Power Method”, by R. N. Blomquist and E. M. Gelbard, Nucl. Sci. Eng., 141, 85-100 (2002).

[8] Kadotani, “Acceleration of Fission Distribution Convergence Using Eigenvectors from Matrix K Calculations in the KENO Code,” ICNC’91, II-1, Oxford, September, 1991.

Chapter 2

THE CHECKERBOARD FUEL STORAGE ARRAY: TEST PROBLEM 1

By M J Armishaw, D Hanlon, N R Smith
Serco Assurance

Overview

The model for Test 1 comprises a notional 24x3 LWR fuel storage rack with fuel elements stored in alternate locations. The fuel elements are ~3.5% enriched-by-weight and are formed from a 15x15 lattice of Zr-clad UO_2. They are located within fully water-flooded steel storage racks surrounded by close-fitting full concrete reflection on three sides, with water on the remaining long side, top and bottom, as shown below. At one institution (ANL), the pin lattice was modelled with volumetric homogenization, with the remaining materials as specified.

Specifications

Material data

Table 2.1 Material atom densities (atoms/barn.cm)

Fuel		Concrete	
^{238}U	2.2380E-02	H	5.5437E-03
O	4.6054E-02	C	6.9793E-03
^{235}U	8.2213E-04	SI	7.7106E-03
		CA	8.9591E-03
		O	4.3383E-02
Water		Iron	
H	6.6706E-02	FE	8.3770E-02
O	3.3353E-02		
Zirconium			
ZR	4.2910E-02		

Geometry

Figure 2.1 describes the problem geometry. The fuel elements are numbered as in a conventional matrix, so that the lowest left-hand fuel element in the figure below is in position (1,1) and the top right-hand fuel element is in position (23,3).

Figure 2.1 Test problem layout

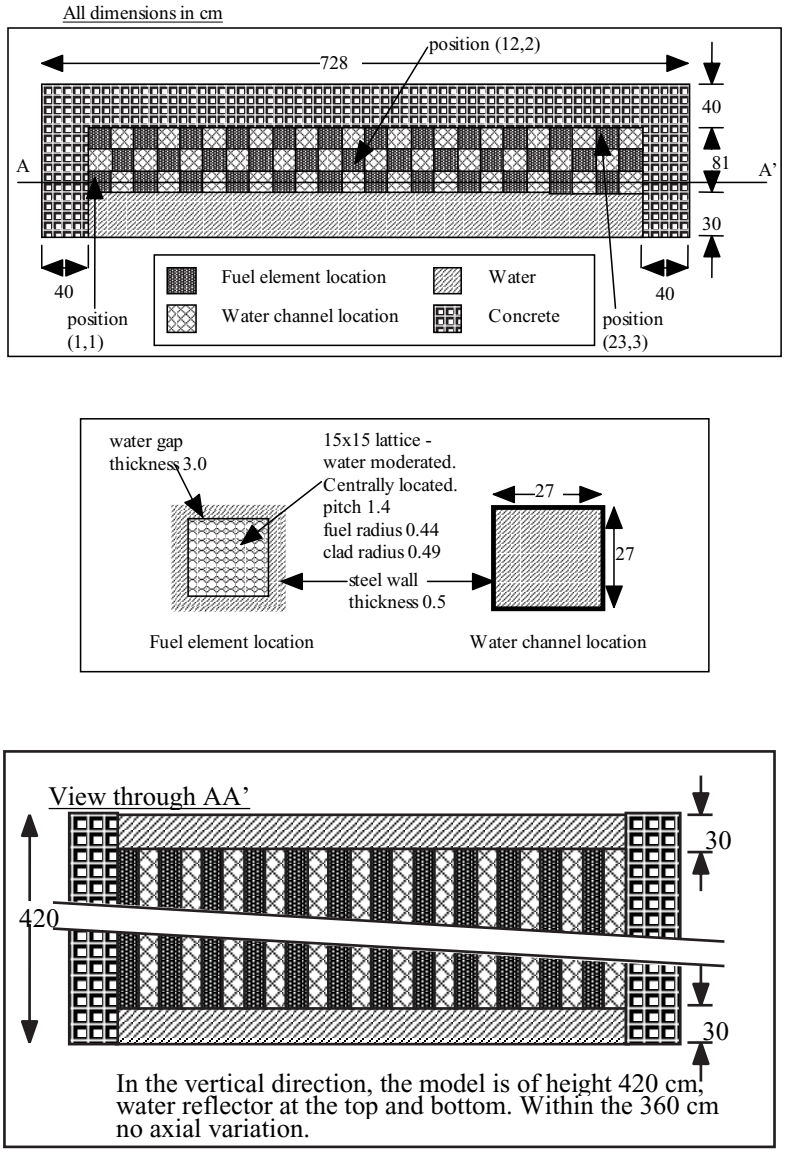

Calculation Cases

Four sets of calculations were required using each of the following starting source distributions:

Uniform over the 36 fuel elements:
All starting source points in location (1,1).
All starting source points in location (23,3).
All starting source points in location (12,2).

Each of the calculations was performed using 500 scored generations, and for each starting source distribution, three different numbers of skipped generations were employed: 20, 40 and 100. In addition, for each combination of initial source and skipped generations, three different numbers of

starting source points per iteration were used: 1 000, 2 000, 5 000. A total of thirty-six calculations, specified in Table 2.2, form a complete set of results.

Table 2.2 Case Monte Carlo control parameters

Case	Starting Source	Skipped Generations	Starting source points
1	Uniform	20	1 000
2	Uniform	40	1 000
3	Uniform	100	1 000
4	Location (1,1)	20	1 000
5	Location (1,1)	40	1 000
6	Location (1,1)	100	1 000
7	Location (23,3)	20	1 000
8	Location (23,3)	40	1 000
9	Location (23,3)	100	1 000
10	Location (12,2)	20	1 000
11	Location (12,2)	40	1 000
12	Location (12,2)	100	1 000
13	Uniform	20	2 000
14	Uniform	40	2 000
15	Uniform	100	2 000
16	Location (1,1)	20	2 000
17	Location (1,1)	40	2 000
18	Location (1,1)	100	2 000
19	Location (23,3)	20	2 000
20	Location (23,3)	40	2 000
21	Location (23,3)	100	2 000
22	Location (12,2)	20	2 000
23	Location (12,2)	40	2 000
24	Location (12,2)	100	2 000
25	Uniform	20	5 000
26	Uniform	40	5 000
27	Uniform	100	5 000
28	Location (1,1)	20	5 000
29	Location (1,1)	40	5 000
30	Location (1,1)	100	5 000
31	Location (23,3)	20	5 000
32	Location (23,3)	40	5 000
33	Location (23,3)	100	5 000
34	Location (12,2)	20	5 000
35	Location (12,2)	40	5 000
36	Location (12,2)	100	5 000

Required output

In addition to identifying information, the participants were asked to submit the information specified in Table 2.3.

Table 2.3 Information to report

Line	Required information
12	Starting source
13	nskip = number of generations skipped before beginning tallies or before convergence:
14	ngen = number of generations tallied
15	nhist = number of histories per generation
16	ngensh = number of generations per superhistory
17	final k_{eff} estimate
18	final k_{eff} estimate uncertainty (one standard deviation)
19	k_{eff} estimate for first supergeneration
20	individual k_{eff} estimate for second supergeneration
…	…
18+ngen	individual k_{eff} estimate for last supergeneration

Cumulative fission fractions *ff(i,g)* in fissionable region *i* and generation g is also an important output. As all computer codes do not have the capability of printing this information for any generation, participants may choose between the following alternatives:

1) Fission fractions are given as average over all generations.
2) Fission fractions are given as average over all active generations.
3) Fission fractions are given at different generation sequences.

Results

Results were received from the participants listed in Table 2.4.

Table 2.4 Participants and codes

Group	Code	Data	Contributor(s)
ANL	VIM	ENDF/B-V	R Blomquist
JAERI	MCNP 4B	JENDL-3.2	T Kuroishi
JNC	KENO-Va	SCALE4.4	S Nobutoshi
KFKI	MCNP 4C	ENDF/B-V&VI	G Hordosy
LANL	MCNP 4C	ENDF/B-VI	F Brown
ORNL	KENO-Va	ENDF/B-V	J Wagner, L Petrie
SERCO Assurance	MONK8A	JEF-2.2	D Hanlon
EMS	KENO-Va	SCALE4.4	D Mennerdahl
IRSN	MORET4	JEF-2.2	J Miss, O Jacquet

Cumulative k_{eff} values were produced for each case for every twenty generations (including during the skipped generations). In addition, the fraction of fission events in each of the thirty-six fuel elements at the end of the calculation was reported.

The k_{eff} versus case number for each of the contributors was plotted (Figure 2.2) to investigate whether there were any effects caused by the control and source parameters. It is important to note that

the final eigenvalues may differ due to differing degrees or rigour in the geometric modelling used, for example the volume-homogenised compositions used in the ANL analyses. Pseudorandom number seeds were not necessarily varied from case to case. When they were not, the difference between (for example) case 2 and case 1 is due only to ignoring the additional skipped generations (21-40) and including the 20 later generations (521-540) in the tallies, i.e., generations 41-520 are identical. Figure 2.2 also shows a pattern across case numbers consistent with consistent seeds, which most or all of the participants used.

Figure 2.2 Final k_{eff} .vs. Case number

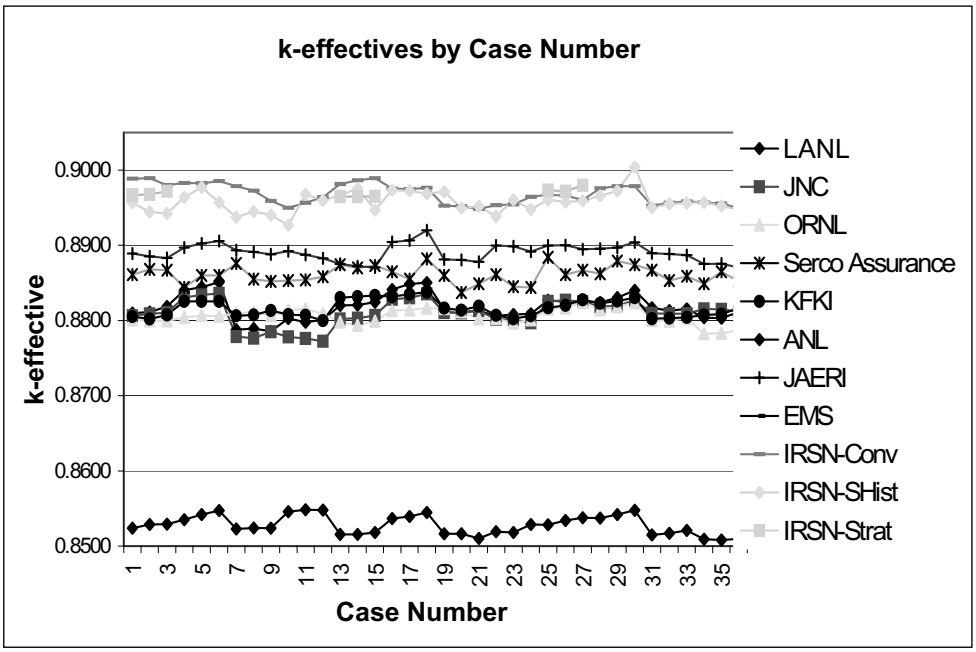

Due to the large amount of data returned, the decision was made to limit the detailed analysis to three cases for each contributor. Of the 36 cases to be run, case 27 was deemed to have the combination of control data most likely to achieve convergence (uniform source, 100 skipped generations and 5 000 source points per iteration), so it was chosen as a reference case. The other two cases chosen were those with the minimum and the maximum k_{eff} for each contributor, which were assumed to be least converged. The selected case numbers (in italics) and the corresponding k_{eff} results are listed in Table 2.5. It should be noted that the maximum and minimum cases in the table are essentially samples from ensembles. Accordingly, there are some instances where the maximum k_{eff} is unexpectedly obtained for a case with an adverse initial source distribution. Which cases produced the maximum k_{eff} is, therefore, displays some randomness, in spite of the fact that one would expect the initial source in (1,1) to be most favorable. To confirm this, a set of VIM calculations were performed, using unique random number seeds and averaged over three like cases that differed only in the number of skipped generations. The three average k_{eff} values for the initial source in (1,1) for 1 000, 2 000, and 5 000 histories per generation, respectively, were always significantly above the averages from the other corresponding cases with other initial sources, which were statistically indistinguishable from each other.

Table 2.5 K_{eff} results for selected cases for each contributor

	Min	Max	Case 27
ANL	0.8508 (0.0006) *35*	0.8548 (0.0015) *11*	0.8538 (0.0006)
JAERI	0.8870 (0.0005) *36*	0.8920 (0.0008) *18*	0.8895 (0.0005)
JNC	0.8773 (0.0013) *11*	0.8836 (0.0013) *6*	0.8825 (0.0006)
KFKI	0.8800 (0.0011) *12*	0.8838 (0.0008) *18*	0.8828 (0.0005)
LANL	0.8773 (0.0011) *10*	0.8826 (0.0004) *30*	0.8803 (0.0004)
ORNL	0.8782 (0.0007) *34*	0.8825 (0.0007) *27*	0.8825 (0.0007)
Serco	0.8837 (0.0010) *20*	0.8884 (0.0006) *25*	0.8867 (0.0006)
EMS	0.8786 (0.0012) *9*	0.8851 (0.0013) *6*	0.8826 (0.0005)
IRSN-Conv	0.8949 (0.0009) *21*	0.8989 (0.0012) *2*	0.8960 (0.0005)
IRSN-SHist	0.8931 (0.0013) *10*	0.9003 (0.0005) *30*	0.8958 (0.0007)
IRSN-Strat	0.8965 (0.0008) *13*	0.8980 (0.0005) *27*	0.8965 (0.0015)

In the case of the IRSN results, there are three fission source algorithms for the MORET4 code: conventional, superhistory and stratified sampling (only a subset of the cases were run using the last method). In this paper, only the conventional results have been examined because they appear to give the least variation between the maximum and minimum values of k_{eff}.

Having identified three cases for each contributor, the individual k_{eff} for each supergeneration (comprising 20 generations) was plotted to investigate the variation in k_{eff} as the runs progress. The plots for each of the contributors are shown in Figures 2.3 to 2.10 inclusive. Inspection of these plots shows that any trends in k_{eff} over the course of the calculations are difficult or impossible to discern.

The final k_{eff} supplied by JAERI for each of the cases was based on a combination of the collision, absorption, and track length, but individual k_{eff} data was only supplied for the three estimators separately. The decision was made to use the absorption estimator data for the plots because this showed the least variation from the final results. No generation data were provided with the final KFKI results, hence their omission from the figures.

The cumulative fission fractions in each element at the end of each case were also requested to provide some insight into how the source distribution has changed from the initial source guess. These results are listed in Tables 2.6 to 2.14 inclusive. Each table header gives the case number, the total number of generations run, the number of skipped generations, the number of histories per generation, and the initial source position.

Figure 2.3 ANL individual k_{eff} .vs. generation number

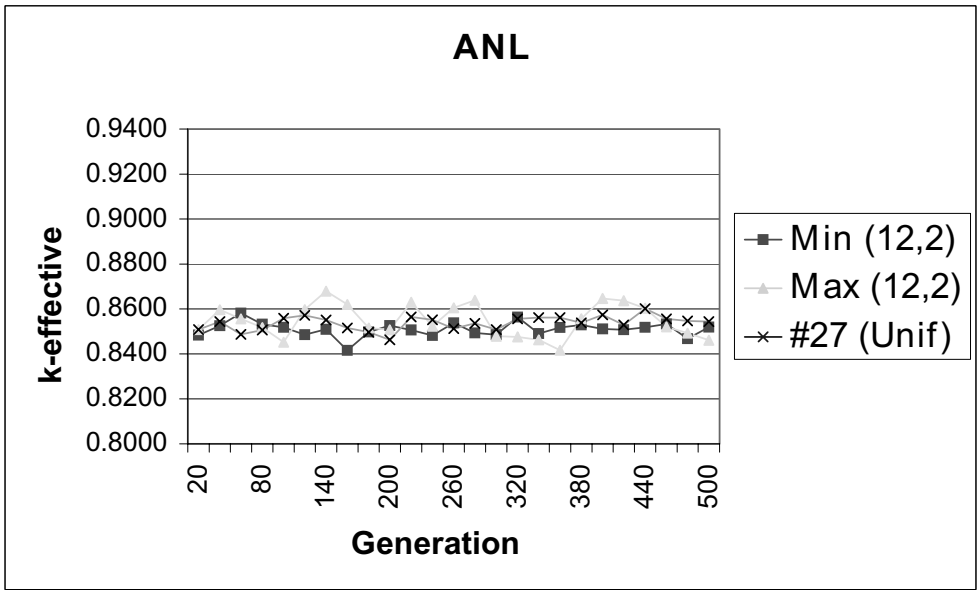

Figure 2.4 JAERI individual k(abs) .vs. generation number

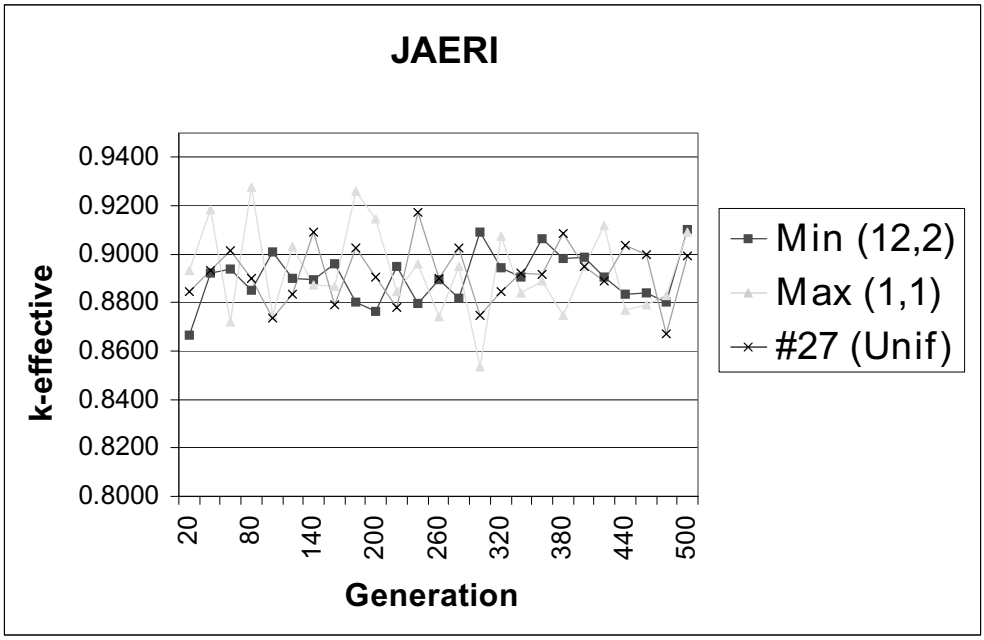

Figure 2.5 Plot of JNC individual k_{eff} .vs. generation number

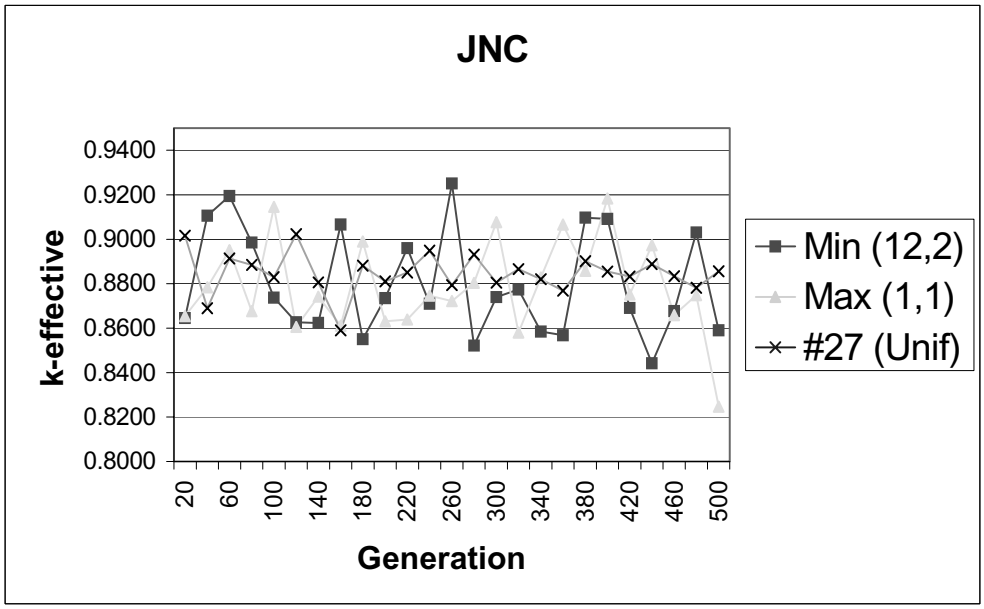

Figure 2.6 Plot of LANL individual k_{eff} .vs. generation number

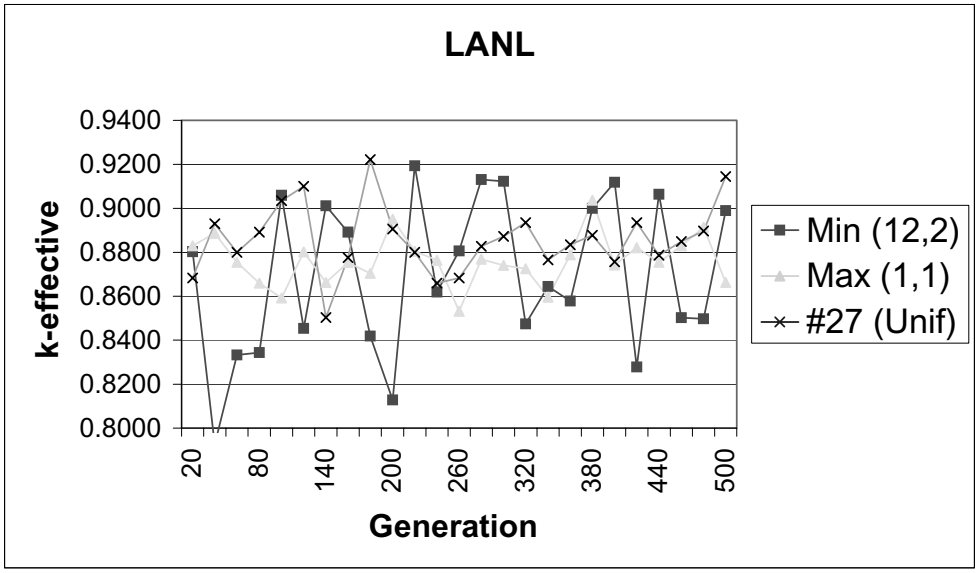

Figure 2.7 Plot of ORNL individual k_{eff} .vs. generation number

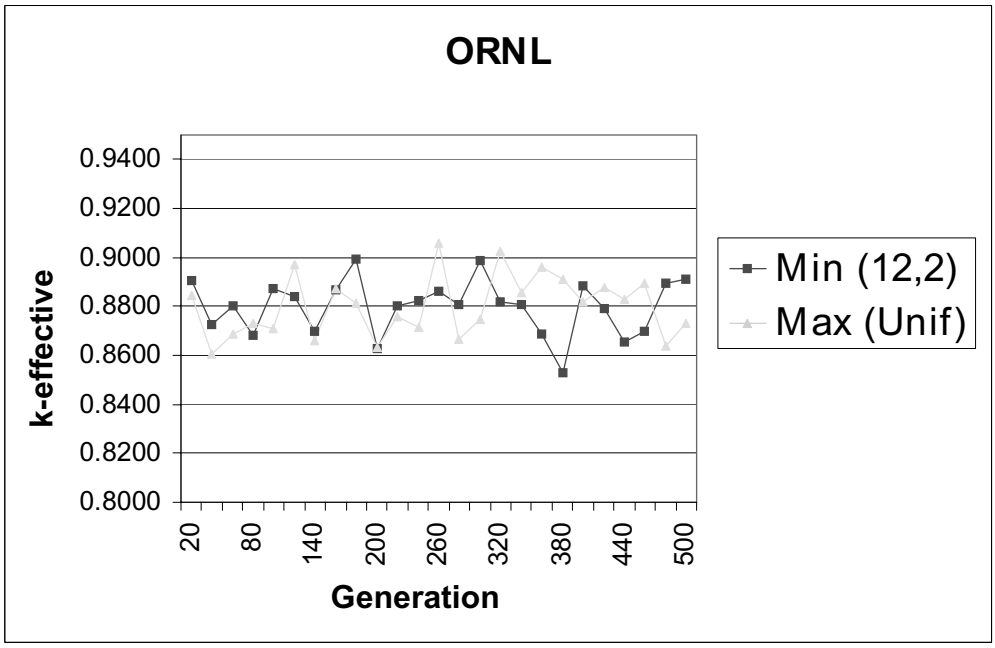

Figure 2.8 Plot of Serco Assurance individual k_{eff} .vs. generation number

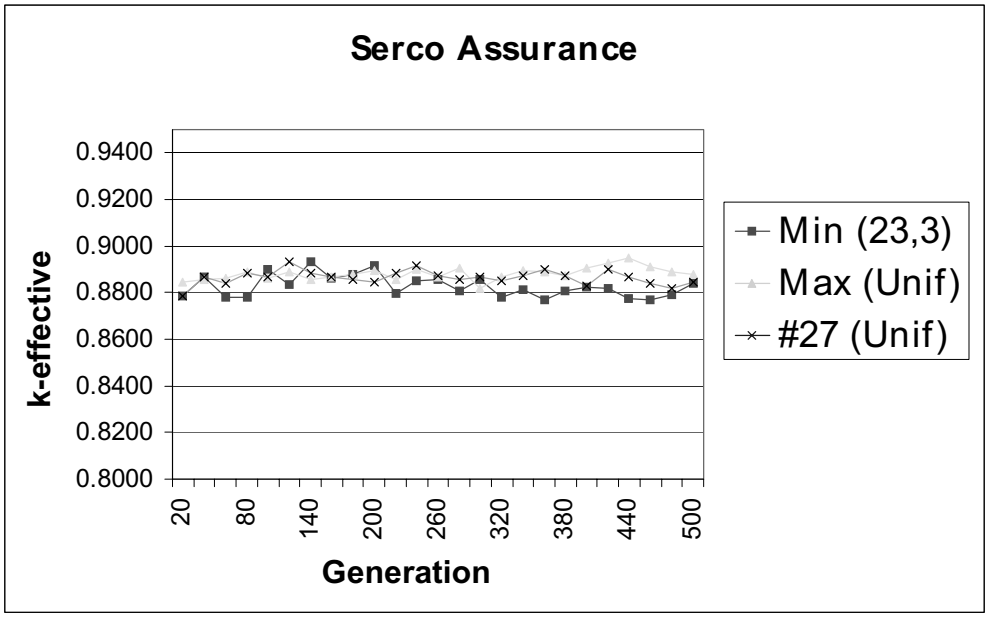

Figure 2.9 Plot of EMS individual k_{eff} .vs. generation number

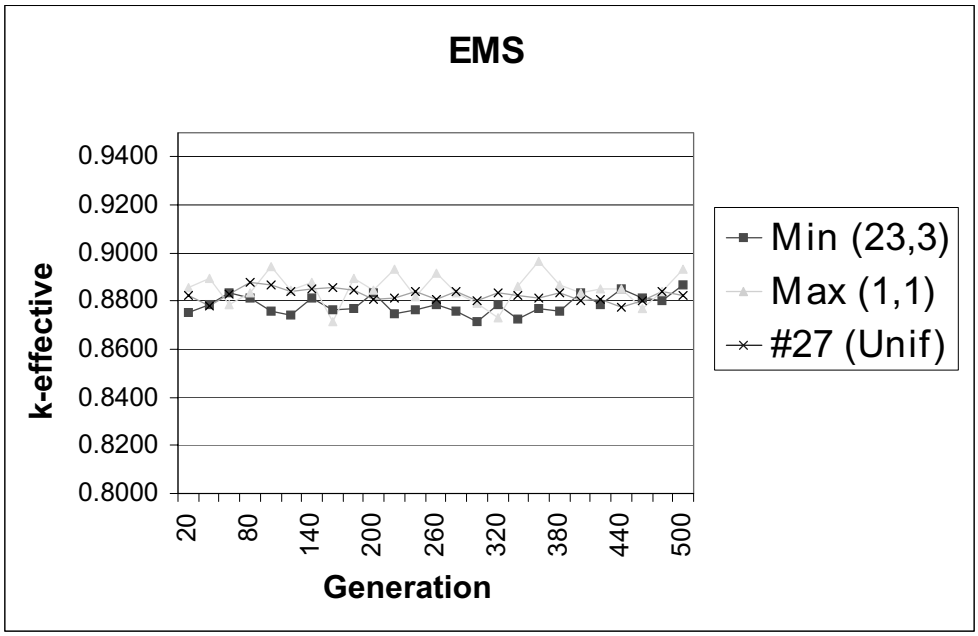

Figure 2.10 Plot of IRSN individual k_{eff} .vs. generation number

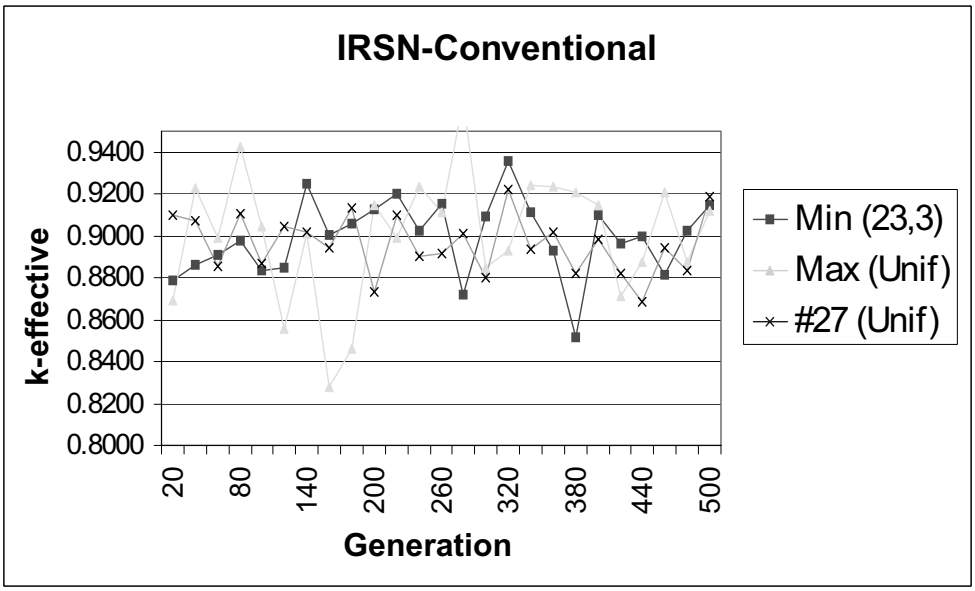

Table 2.6 ANL cumulative fission fractions (%)

case 35	540	40	5000	(12,2)																		
0.00		0.00		0.04		1.25		3.52		11.15		12.96		7.87		4.13		0.94		0.60		0.12	
	0.00		0.01		0.25		1.33		5.59		13.39		7.86		4.73		2.11		0.75		0.14		0.01
0.00 (1,1)		0.00		0.07		0.21		1.83		5.79		6.56		3.35		2.59		0.67		0.16		0.01	

case 11	540	40	1000	(12,2)																		
0.00		0.00		0.30		3.99		5.31		14.08		13.26		3.64		0.48		0.01		0.00		0.00	
	0.00		0.02		1.52		4.66		9.63		12.92		6.45		1.06		0.07		0.00		0.00		0.00
0.00		0.00		0.05		1.43		3.97		8.84		6.07		1.74		0.49		0.00		0.00		0.00	

case 27	600	100	5000	Unif																		
0.15.00		6.55		4.93		4.67		2.32		2.12		1.87		2.08		2.10		3.63		2.39		0.96	
	7.18		5.00		3.77		3.40		1.65		1.67		1.78		1.64		2.67		2.36		1.28		0.60
0.0271		2.71		2.59		1.91		1.39		1.11		0.92		1.40		0.85		1.38		0.85		0.58	

Table 2.7 JAERI cumulative fission fractions (%)

case 36	600	100	5000	(12,2)																		
0.00		0.14		0.62		1.56		7.17		13.28		2.21		5.45		2.06		0.51		0.00		0.00	
	0.00		0.48		0.86		4.33		7.50		12.78		7.28		2.22		0.62		0.18		0.00		0.00
0.00 (1,1)		0.13		0.67		1.38		2.77		6.76		5.98		2.18		0.49		0.21		0.00		0.00	

case 18	600	100	2000	(1,1)																		
46.79		10.03		3.39		0.31		0.00		0.00		0.00		0.00		0.00		0.00		0.00		0.00	
	15.32		4.57		0.71		0.19		0.00		0.00		0.00		0.00		0.00		0.00		0.00		0.00
12.53		3.83		1.85		0.41		0.00		0.00		0.00		0.00		0.00		0.00		0.00		0.00	

case 27	600	100	5000	Unif																		
0.21. 84		5.34		2.35		1.69		1.38		1.33		2.73		1.66		1.01		5.77		4.10		3.36	
	6.95		3.12		1.49		1.12		1.28		2.30		2.19		1.35		1.94		3.78		2.72		1.95
2.86		2.60		1.11		0.60		0.42		1.02		1.52		1.58		1.07		1.23		2.23		1.01	

Table 2.8 JNC cumulative fission fractions (%)

case 11	540	40	1000	(12,2)																			
0.00		0.01		0.92		7.39		9.34		10.73		12.08		1.27		0.27		0.00		0.00		0.00	
	0.00		0.13		2.84		6.56		13.70		10.04		5.06		0.55		0.02		0.00		0.00		0.00
0.00 (1,1)		0.00		0.33		2.28		5.17		6.84		3.63		0.78		0.07		0.00		0.00		0.00	

case 6	600	100	1000	(1,1)																			
42.82		9.22		3.26		1.88		0.01		0.00		0.00		0.00		0.00		0.00		0.00		0.00	
	15.84		7.12		1.17		0.31		0.00		0.00		0.00		0.00		0.00		0.00		0.00		0.00
9.01		4.88		4.29		0.16		0.02		0.00		0.00		0.00		0.00		0.00		0.00		0.00	

case 27	600	100	5000	Unif																			
16.11		4.69		1.63		2.54		2.05		2.27		1.30		2.66		2.95		4.91		5.57		2.67	
	6.54		3.03		1.66		1.60		1.45		1.01		1.27		2.45		3.23		4.16		3.41		1.59
3.03		3.33		1.41		0.78		0.99		0.74		0.77		1.24		1.23		2.10		2.53		1.10	

Table 2.9 LANL cumulative fission fractions (%)

case 10	520	20	1000	(12,2)																	
0.01		1.91		5.29		2.49		10.29		16.06		7.14		0.68		0.00		0.00		0.00		0.00	
	0.46		1.75		3.06		3.84		10.24		14.44		3.05		0.14		0.00		0.00		0.00		0.00
0.04 (1,1)		0.19		0.54		1.62		5.21		7.06		4.22		0.29		0.00		0.00		0.00		0.00	

case 30	600	100	5000	(1,1)																	
40.18		11.56		2.89		0.56		0.09		0.00		0.00		0.00		0.00		0.00		0.00		0.00	
	17.65		5.76		0.92		0.16		0.01		0.00		0.00		0.00		0.00		0.00		0.00		0.00
12.62		5.59		1.76		0.18		0.07		0.00		0.00		0.00		0.00		0.00		0.00		0.00	

case 27	600	100	5000	Unif																	
9.99		5.17		3.84		2.79		3.23		5.17		1.57		0.53		1.73		1.87		3.20		4.58	
	4.84		2.60		2.57		2.58		3.72		3.49		1.07		1.02		1.74		2.22		3.89		5.77
3.60		1.61		1.12		1.49		1.24		2.97		1.35		0.86		0.44		1.74		2.10		2.32	

Table 2.10 ORNL cumulative fission fractions (%)

case 34	520	20	5000	(12,2)																			
0.00		0.00		0.00		0.00		0.02		0.05		0.08		0.04		0.01		99.52		0.00		0.00	
	0.00		0.00		0.00		0.00		0.03		0.07		0.06		0.03		0.00		0.00		0.00		0.00
0.00 (1,1)		0.00		0.00		0.00		0.01		0.03		0.03		0.02		0.00		0.00		0.00		0.00	

case 27	600	100	5000	Unif																			
41.85		8.27		4.54		0.99		0.51		0.28		0.16		0.22		0.22		0.03		0.02		0.01	
	15.36		4.88		1.70		0.47		0.37		0.15		0.13		0.28		0.11		0.02		0.01		0.01
10.55		5.90		1.78		0.58		0.23		0.11		0.04		0.09		0.11		0.03		0.01		0.00	

Table 2.11 Serco Assurance cumulative fission fractions (%)

case 20	540	40	2000	(23,3)																		(23,3)	
0.00		0.00		0.00		0.00		0.00		0.00		0.00		0.00		0.00		0.72		12.52		26.85	
	0.00		0.00		0.00		0.00		0.00		0.00		0.00		0.00		0.22		4.41		19.74		15.49
0.00 (1,1)		0.00		0.00		0.00		0.00		0.00		0.00		0.00		0.00		1.08		9.77		9.19	

case 25	520	20	5000	Unif																			
20.00		5.22		2.46		2.98		1.49		1.27		3.07		2.10		2.96		3.43		2.49		2.10	
	7.15		2.79		2.38		1.22		1.46		2.21		3.29		1.66		1.55		2.68		2.27		2.15
2.90		2.35		2.46		0.91		0.91		1.66		1.52		2.38		0.72		0.83		1.71		1.30	

case 27	600	100	5000	Unif																			
12.60		5.62		3.30		1.05		1.11		2.44		2.63		1.88		2.91		5.40		2.99		4.40	
	5.54		3.68		0.83		0.86		1.50		2.41		2.52		1.39		4.07		2.74		4.35		4.07
2.16		3.32		1.27		0.72		0.55		0.69		1.27		0.97		1.72		1.72		1.69		3.60	

Table 2.12 EMS cumulative fission fractions (%)

case 9	600	100	1000	(23,3)																			
0.00		0.00		0.00		0.00		0.00		0.00		0.00		0.03		1.21		1.45		16.64		18.52	
	0.00		0.00		0.00		0.00		0.00		0.00		0.00		0.19		1.52		9.42		14.15		18.05
0.00 (1,1)		0.00		0.00		0.00		0.00		0.00		0.00		0.01		0.72		2.21		8.08		7.80	

case 6	600	100	1000	(1,1)																			
45.47		12.65		3.82		0.12		0.00		0.00		0.00		0.00		0.00		0.00		0.00		0.00	
	17.67		4.91		0.93		0.02		0.00		0.00		0.00		0.00		0.00		0.00		0.00		0.00
9.72		3.63		0.80		0.24		0.00		0.00		0.00		0.00		0.00		0.00		0.00		0.00	

case 27	600	100	5000	Unif																			
19.98		8.58		5.00		2.33		0.77		1.95		1.05		1.02		0.53		1.40		2.89		6.73	
	9.69		3.94		3.16		0.92		0.98		0.89		0.98		0.54		0.60		1.21		3.20		6.17
4.13		2.67		1.35		1.34		0.67		0.33		0.66		00.30		0.25		0.43		0.91		2.45	

Table 2.13 IRSN conventional cumulative fission fractions (%)

case 21	600	100	2000	(23,3)																		
0.00		0.00		0.00		0.00		0.00		0.00		0.00		0.05		1.47		4.27		8.26		23.76	
	0.00		0.00		0.00		0.00		0.00		0.00		0.00		0.37		1.54		4.96		10.88		26.10
0.00 (1,1)		0.00		0.00		0.00		0.00		0.00		0.00		0.07		0.53		2.61		3.69		11.43	

case 15	600	100	2000	Unif																		
21.52		5.60		0.88		3.20		5.76		5.87		0.88		0.52		0.77		0.21		0.23		0.00	
	8.63		3.41		2.77		6.81		4.31		2.24		1.30		0.51		0.22		0.15		0.25		0.00
6.60		4.02		2.67		2.52		5.07		0.86		0.39		0.34		0.81		0.33		0.35		0.01	

case 27	600	100	5000	Unif																		
8.51		6.62		5.03		1.54		0.72		1.53		2.19		3.07		6.16		2.39		2.64		1.60	
	4.89		4.51		3.04		0.78		0.84		0.88		2.69		4.16		5.53		2.57		2.07		1.01
3.39		3.28		2.60		1.17		1.39		0.24		1.23		2.40		3.00		3.02		1.75		1.57	

Table 2.14 KFKI cumulative fission fractions (%)

case 12	600	100	1000	(12,2)																		
0.00		0.00		0.00		0.10		2.98		14.83		10.45		5.85		4.16		2.75		0.46		0.02	
	0.00		0.00		0.00		1.17		5.82		6.82		5.53		7.93		4.90		2.37		0.35		0.00
0.00 (1,1)		0.00		0.00		0.16		2.24		2.77		3.42		6.52		4.40		2.62		1.33		0.06	

case 18	600	100	2000	(1,1)																		
32.18		13.53		7.24		0.67		0.05		0.00		0.00		0.00		0.00		0.00		0.00		0.00	
	16.75		6.69		2.62		0.11		0.00		0.00		0.00		0.00		0.00		0.00		0.00		0.00
10.15		7.09		2.09		0.68		0.15		0.00		0.00		0.00		0.00		0.00		0.00		0.00	

case 27	600	100	5000	Unif																		
9.33		6.24		6.07		4.45		1.86		2.55		2.34		1.74		1.63		4.42		3.11		2.33	
	5.26		4.46		4.64		3.72		1.44		1.91		2.00		2.05		2.19		4.11		1.85		1.54
2.11		1.74		1.98		2.63		1.14		1.13		0.88		0.87		1.91		1.92		1.55		0.88	

Conclusions

Inspection of the plot of k_{eff} versus case number for all the contributors shows there is a significant variation in k_{eff} with starting source position. The plot shows a less marked variation with the number of skipped generations and the number of starting source points per iteration. There are some patterns visible in the plots of k_{eff} versus case number, with a correlation between the final value of k_{eff} and the initial source distribution. K_{eff} values from an initial source in position (1,1) appear to be higher than those from a flat source distribution which are in turn higher than those values obtained from a start in positions (12,2) and (23,3).

The distribution of cumulative fission fractions by element shows large variations. In some cases only a few elements adjacent to the starting point position have been sampled, leading to a potentially biased value for k_{eff}. In general, where the source guess is limited to a single element, the fission fractions remain concentrated near to the initial source guess. Where the initial source distribution was uniformly spread across the model, we see more of a migration to the more reactive components. A failure to sample every part of the system is not necessarily due to a problem (it could be the result of successful convergence). In this case we know what the distribution should be: almost half of the fissions occur in the corner position (1,3) and essentially the rest in the neighboring positions. Significant fission fractions in other positions may indicate incomplete source convergence.

Two groups of methods can be identified based on the results. KENOVa and MCNP4C give similar results concerning source convergence to position (1,3) when the initial source was in position (1,1). The codes MONK8A, MORET4 and VIM do not find the correct source distribution as easily. The more complicated sampling algorithms in the latter codes seem to slow convergence. Later calculations with VIM, using more histories, supported the results by KENOVa and MCNP4C. Two further studies which might prove interesting would be: firstly to inspect the fission fraction of all those cases which gave the "correct" k_{eff}; secondly to determine whether any cases with apparently suitable fission fraction distributions gave an inappropriate k_{eff}. These studies would demonstrate whether the distribution of fission fractions could be used as a measure of convergence – bearing in mind that for the practical use of this method some idea of the correct distribution would be needed beforehand. In criticality safety assessment, the analyst normally has a good idea of the correct distribution based on experience and on preliminary calculations of simpler systems.

Part of the remit for this work was to offer guidance to analysts so they could identify when a case has failed correctly to converge. From the results available here, the most useful, though not infallible, indicator is the cumulative fission fractions. There are two steps in a Monte Carlo evaluation. The first, fission source convergence, is to determine a converged fission source. This can be done in various ways, including using previous experience and preparatory calculations using different initial sources. The second step, statistical convergence, is to use a sufficiently converged source as an initial source for a purely statistical calculation of k_{eff}. If, in spite of this, the second step results in a significant deviation between the initial source and the final source, further evaluation is in order.

All of the codes used have shown some degree of inability to cope with this test, particularly where the initial source has been poorly specified. All of the calculation cases have fixed specifications and none of them are typical for an acceptable criticality safety application of the codes used. The code user must be expected to understand both the physics of the problem as well as the capabilities and limitations of the code. Convergence problems need to be compensated by skepticism of one's own results, independent internal review, and through the licensing process.

The increasing power of computers is leading to ever more criticality cases being run, often to reduce the potential for mistakes in a single calculation. This is a great benefit for safety since many extra "what if"-calculations can be carried out to reduce uncertainties and to increase understanding. Even so, the codes need to include some sort of automated checking to advise when convergence may be failing. It is vitally important that this work should continue, with the aim of enabling us to provide the information both analysts and developers need to identify when these problems occur.

Chapter 3

PIN-CELL ARRAY WITH IRRADIATED FUEL: TEST PROBLEM 2

By Yoshitaka Naito, Jinan Yang (NAIS Co. Inc.)

Overview

The test problem "Pin-cell array with irradiated fuel" is a problem which has been chosen for the purpose of studying the source convergence for Monte Carlo calculations applied to LWR spent fuel pools. The composition of LWR spent fuel consists of more reactive, low burn-up end regions separated by a long, less active, high burnup region. Such a configuration is similar to two loosely coupled reactors, for which it is difficult to obtain source convergence using the Monte Carlo method. Moreover, if the axial profile of the fuel composition is asymmetric (as it is in discharged fuel), the source distribution will be quite different from that obtained from a case with symmetrical composition. In such a case, it is difficult to determine whether the source is converged or not, and it is difficult to determine an adequate number of skip cycles. This test problem was originally formulated by modifying an OECD/NEA burn-up credit problem[1] Phase IIA on the effect of axial burn-up profiles.

Specifications

Geometry

These tests are composed of an infinite fuel pin array in water. Figure 3.1 depicts the horizontal geometry of the unit cell, and Figure 3.2 depicts the axial geometry, including the division of the fuel material into 9 regions. A reflecting boundary condition is assumed at the boundary of the square cell of water.

Material

The atom densities of the fuel types for fresh fuel and structural materials are given in Table 3.1, while the atom densities of the fuel at various burnups are given in Table 3.2.

Case identification

Six cases of test problems are identified for solving source convergence problems on criticality analyses. The fuel composition axial distributions are defined in Table 3.3 using abbreviations (NU for natural uranium, EU45 for 4.5% enriched fresh uranium, EU40 for 4.0% enriched fresh uranium, B21 for 21GWD/MTU burn-up fuel, etc.).

Cases 1_1 through 1_3 contain fresh fuel only. The two end parts of the fuel rod are separated by a central natural uranium region. Both axially symmetric (Case 1_1) and asymmetric (Cases 1_2, 1_3) configurations of the fuel rod are proposed. This is based on the fact that a highly asymmetric power distribution appears in a weakly coupled asymmetric reactor core. Cases 2_1 through 2_3 are composed of irradiated fuels. Similarly, both axially symmetric (Case 2_1) and asymmetric (Cases 2_2, 2_3) configurations of the fuel rod are specified.

Figure 3.1 Horizontal configuration of unit cell

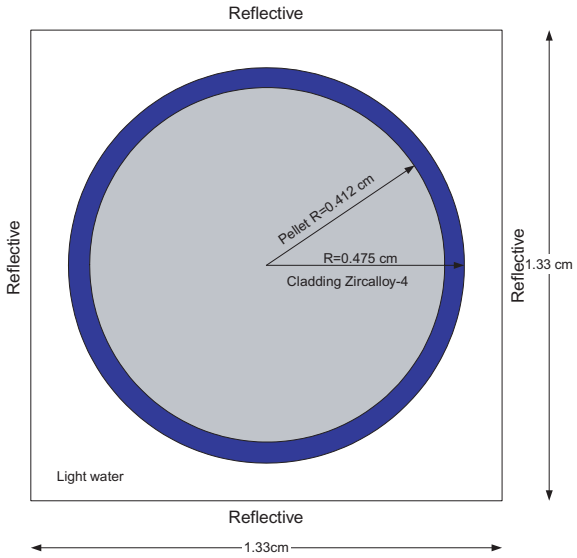

Figure 3.2 Vertical cross-section

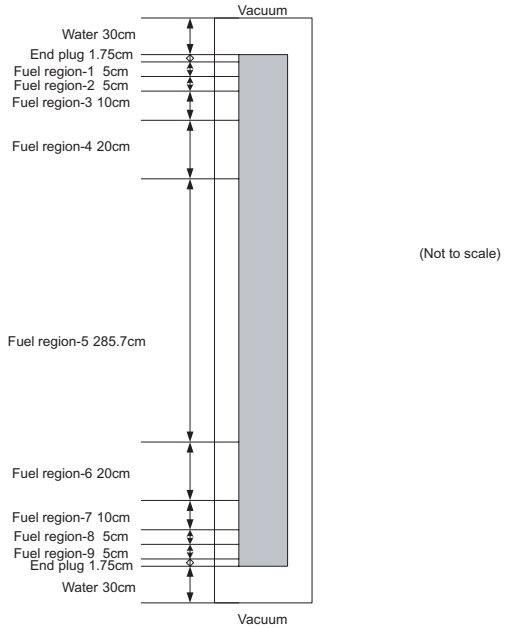

Table 3.1 Atom densities (atoms/barn-cm) for fresh fuel

Fuel-type	EU45
Fresh fuel U(4.5wt.%)O_2 enriched	
^{234}U	8.4100E-06
^{235}U	1.0526E-03
^{236}U	6.4752E-06
^{238}U	2.2042E-02
O	4.6219E-02
Fuel-type	**EU40**
Fresh fuel U(4.0wt.%)O_2 enriched	
^{234}U	7.5481E-06
^{235}U	9.3949E-04
^{238}U	2.2256E-02
O	4.6405E-02
Fuel-type NU	
U (natural)O_2	
^{234}U	1.2757E-06
^{235}U	1.6700E-04
^{238}U	2.3026E-02
O	4.6388E-02
Zircalloy-4	
Cr	7.5891E-05
Fe	1.4838E-04
Zr	4.2982E-02
Light Water 25deg.C	
H	6.6658E-02
O	3.3329E-02

Table 3.2 Atom densities (atoms/barn-cm) of irradiated fuels ^{239}Pu

Fuel-Type	B21G	B24G	B30G	B40G	B55G
	4.5 wt% ^{235}U 21.57 GWD/MTU	4.5 wt% ^{235}U 24.023 GWD/MTU	4.5 wt% ^{235}U 30.580 GWD/MTU	4.5 wt% ^{235}U 40.424 GWD/MTU	4.5 wt% ^{235}U 54.605 GWD/MTU
^{234}U	6.4862E-06	6.2881E-06	5.7868E-06	5.1152E-06	4.3280E-06
^{235}U	5.6757E-04	5.2562E-04	4.2455E-04	3.0002E-04	1.7108E-04
^{236}U	9.4556E-05	1.0155E-04	1.1763E-04	1.3534E-04	1.4897E-04
^{238}U	2.1732E-02	2.1693E-02	2.1585E-02	2.1413E-02	2.1142E-02
^{238}Pu	1.1322E-06	1.4876E-06	2.7262E-06	5.3656E-06	1.0471E-05
^{239}Pu	1.2591E-04	1.3161E-04	1.4249E-04	1.5064E-04	1.5300E-04
^{240}Pu	2.6395E-05	2.9965E-05	3.9140E-05	5.1484E-05	6.5540E-05
^{241}Pu	1.3614E-05	1.5953E-05	2.1863E-05	2.9175E-05	3.6032E-05
^{242}Pu	2.2623E-06	3.0335E-06	5.6472E-06	1.0893E-05	2.0303E-05
^{241}Am	4.0266E-06	4.7603E-06	6.6579E-06	9.0866E-06	1.1405E-05
^{243}Am	2.6222E-07	3.9809E-07	9.7353E-07	2.5108E-06	6.1550E-06
^{237}Np	6.8089E-06	7.9041E-06	1.0948E-05	1.5602E-05	2.1806E-05
^{95}Mo	3.1530E-05	3.4781E-05	4.3130E-05	5.4806E-05	6.9892E-05
^{99}Tc	3.0319E-05	3.3465E-05	4.1531E-05	5.2746E-05	6.6975E-05
^{101}Ru	2.7452E-05	3.0548E-05	3.8751E-05	5.0881E-05	6.7875E-05
^{103}Rh	1.7260E-05	1.9008E-05	2.3371E-05	2.9057E-05	3.5406E-05
^{109}Ag	1.8879E-06	2.2230E-06	3.1774E-06	4.7134E-06	6.9836E-06
^{133}Cs	3.3140E-05	3.6549E-05	4.5257E-05	5.7263E-05	7.2263E-05
^{147}Sm	6.4488E-06	6.9339E-06	8.0315E-06	9.2075E-06	1.0106E-05
^{149}Sm	1.9390E-07	1.9611E-07	1.9935E-07	1.9993E-07	1.9259E-07
^{150}Sm	7.1174E-06	8.0472E-06	1.0496E-05	1.3997E-05	1.8627E-05
^{151}Sm	5.7531E-07	6.0064E-07	6.6160E-07	7.3765E-07	8.1779E-07
^{152}Sm	3.0178E-06	3.3473E-06	4.1844E-06	5.3316E-06	6.7637E-06
^{143}Nd	2.5793E-05	2.8067E-05	3.3502E-05	3.9984E-05	4.5992E-05
^{145}Nd	1.8633E-05	2.0504E-05	2.5263E-05	3.1783E-05	3.9892E-05
^{153}Eu	2.0026E-06	2.3329E-06	3.2546E-06	4.6705E-06	6.5858E-06
^{155}Gd	1.1986E-07	1.4386E-07	2.2155E-07	3.6871E-07	6.0862E-07
O	4.6219E-02	4.6219E-02	4.6219E-02	4.6219E-02	4.6219E-02

Table 3.3 Fuel composition identification for each region

	Case1_1	Case1_2	Case1_3	Case2_1	Case2_2	Case2_3
Region	**Fuel-type**	**Fuel-type**	**Fuel-type**	**Fuel-type**	**Fuel-type**	**Fuel-type**
1	EU45	EU45	EU45	B21G	B21G	B21G
2	EU45	EU45	EU45	B24G	B24G	B24G
3	EU45	EU45	EU45	B30G	B30G	B30G
4	EU45	EU45	EU45	B40G	B40G	B40G
5	NU	NU	NU	B55G	B55G	B55G
6	EU45	EU40	EU45	B40G	B55G	B40G
7	EU45	EU40	EU45	B30G	B40G	B30G
8	EU45	EU40	EU40	B24G	B30G	B30G
9	EU45	EU40	EU40	B21G	B24G	B24G

Calculation control parameters

To calculate eigenvalue problems by the Monte Carlo method, the following data must be input: the starting source, the number of generations skipped before beginning tallies (nskip), the number of generations tallied (ngen), and the number of histories per generation (nhist). The data on ngen and nhist are fixed as 100 and 100 000 for our test calculation, respectively. To determine a realistic nskip value, the test problems were solved with the Monte Carlo code MCNP. The relations between k_{eff} (standard deviation) and nskip are shown in Figures 3.3-3.9. From these figures, one can see an nskip of 200 is necessary to obtain a stable k_{eff} for cases 1_1, 1_2, 2_1 and 2_2. For cases 1_3 and 2_3, a much larger nskip seems to be required. For our calculations, we have fixed nskip at 200 and ngen at 1 000 to compare with calculation results from each participant.

Required output

In addition to identifying information, the participants were asked to submit the information specified in Table 3.4.

Table 3.4 Information to report

Line	Required information
12	Starting source
13	nskip = number of generations skipped before beginning tallies or before convergence:
14	ngen = number of generations tallied
15	nhist = number of histories per generation
16	ngensh = number of generations per superhistory
17	final k_{eff} estimate
18	final k_{eff} estimate uncertainty (one standard deviation)
19	k_{eff} estimate for first supergeneration
20	individual k_{eff} estimate for second supergeneration
…	….
18+ngen	individual k_{eff} estimate for last supergeneration

Cumulative fission fractions *ff(i,g)* in fissionable region *i* in generation *g* is also an important output. As all computer codes do not have the capability of printing this information for any generation, participants may choose between the following alternatives:

1) Fission fractions are given as average over all generations.
2) Fission fractions are given as average over all active generations.
3) Fission fractions are given at different generation sequences.

Results

Participants

The eight groups and the calculational control parameters each group used are shown in Table 3.5.

Table 3.5. Contact persons and calculation control parameters

Institution	Los Alamos National Laboratory	KFKI Atomic Energy Research Institute	Japan Nuclear Cycle Development Institute	Oak Ridge National Laboratory
Contact Person	Avneet Sood	Gabor Hordosy	Nobutoshi Shirai	John Wagner
E-mail address	asood@lanl.gov	hordosy@sunserv.kfki.hu	shirai@tokai.jnc.go.jp	wagnerjc@ornl.gov
Voice phone number	505.667.2119	3613922222 ext 3442	81-29-282-1111 (ext.71311)	865-241-3570
FAX phone number	505.665.3046	3613959293	81-29-282-7839	865-576-3513
Code name	MCNP4C2	MCNP4B	SCALE-4.4 (CSAS25/KENO-V.a)	KENO-V.a
Code type	Monte Carlo	Monte Carlo	Monte Carlo	Monte Carlo
Cross section library source	ENDF-V and ENDF-VI	ENDF-B/VI, ENDF/B-V	44groupndf5 library	238-group library (ENDF/B-V)
Starting source	Uniform	Uniform	Flat	Uniform
Nskip	200	200	200	200
Ngen	1 000	1 000	1 000	1 000
nhist	100 000	100 000	100 000	100 000
ngensh	1	No superhistory	1	1

Table 3.5 Contact persons and calculation control parameters *(continued)*

Institution	E.Mennerdahl Systems	Argonne National Laboratory	NAIS Co. inc.	Institut de Radioprotection et de Surete Nucleaire
Contact Person	Dennis Mennerdahl	R. N. Blomquist	Yoshitaka NAITO	Joachim Miss
E-mail address	dennis.mennerdahl @ems.se	RNBlomquist@anl. gov	ynaito@nais.ne.jp	Joachim.miss@irsn. fr
Voice phone number	+46(8)7565812	630-252-8423	81-29-270-5000	331 58 35 89 15
FAX phone number	+46(8)7565872	630-252-4500	81-29-270-5001	331 46 57 29 98
Code name	SCALE 4.4, CSASI+KENOVa	VIM	MCNP4B2	MORET4A6
Code type	Monte Carlo	Monte Carlo	Monte Carlo	Monte Carlo
Cross section library	238 group library	ENDF/B-V	ENDF-V and ENDF-VI	CEA93 library
Starting source	Uniform	Uniform	Uniform	Uniform
Nskip	200	200	200	200
Ngen	1 000	1 000	1 000	1 000
nhist	100 000	10 000	10 000	100 000
ngensh	20	1	1	1

Comparison of computed results

The computed results are summarized into Tables 3.6-3.11. The evolution of k_{eff} for a set of sample calculations is shown in Figures 3.3-3.8.

Table 3.6 Calculated k_{eff} and fission fractions for Case1_1

Institution	Los Alamos National Laboratory	KFKI Atomic Energy Research Institute	Japan Nuclear Cycle Development Institute	Oak Ridge National Laboratory
Case name	Case 1_1	Case 1_1	Case 1_1	Case 1_1
Final k_{eff} estimate	1.34253	1.34264	1.34305	1.33979
Final k_{eff} estimate uncertainty	0.00006	6.00E-05	0.00008	0.00008
Region 1	1.87550E-02	3.91486E-02	4.52776E-02	4.3021E-02
Region 2	2.02700E-02	4.21925E-02	4.88654E-02	4.6327E-02
Region 3	5.12460E-02	1.06899E-01	1.23826E-01	1.1722E-01
Region 4	9.48110E-02	1.97916E-02	2.29393E-01	2.1692E-01
Region 5	3.58850E-02	8.31008E-02	8.30461E-02	8.3417E-02
Region 6	3.99250E-01	2.71980E-01	2.40830E-01	2.5277E-01
Region 7	2.15740E-01	1.46937E-01	1.29959E-01	1.3638E-01
Region 8	8.51500E-02	5.80153E-02	5.12630E-02	5.3884E-02
Region 9	7.88970E-02	5.38105E-02	4.75425E-02	5.0056E-02

Table 3.6 Calculated k_{eff} and fission fractions for Case1_1 *(continued)*

Institution	E.Mennerdahl Systems	Argonne National Laboratory	NAIS Co. inc.	Institut de Radioprotection et de Sûreté Nucléaire
Case name	Case1_1	Case1_1	Case1_1	Case1_1
Final k_{eff} estimate	1.33757	1.3413	1.34226	1.34239
Final k_{eff} estimate uncertainty	0.00008	0.0003	0.0002	0.00006
Region 1	0.0377	0.0645	4.161269E-02	4.66E-02
Region 2	0.0409	0.0695	4.475076E-02	5.03E-02
Region 3	0.1053	0.1768	1.134248E-01	1.263E-01
Region 4	0.1983	0.33	2.110497E-01	2.218E-01
Region 5	0.0848	0.0863	8.383544E-02	5.7E-02
Region 6	0.2755	0.1397	2.590542E-01	2.484E-01
Region 7	0.1468	0.0756	1.399368E-01	1.413E-01
Region 8	0.0575	0.0298	5.515876E-02	5.630E-02
Region 9	0.0532	0.0277	5.117687E-02	5.200E-02

Table 3.7 Calculated k_{eff} and fission fractions for Case1_2

Institution	Los Alamos National Laboratory	KFKI Atomic Energy Research Institute	Japan Nuclear Cycle Development Institute	Oak Ridge National Laboratory
Case name	Case 1_2	Case 1_2	Case 1_2	Case 1_2
Final k_{eff} estimate	1.34223	1.34225	1.34306	1.33952
Final k_{eff} estimate uncertainty	0.00007	7.00E-05	0.00009	0.00008
Region 1	9.19800E-02	9.26450E-02	9.26474E-02	9.2959E-02
Region 2	9.91660E-02	9.98812E-02	9.99308E-02	1.0011E-01
Region 3	2.51210E-01	2.52960E-01	2.52991E-01	2.5321E-01
Region 4	4.65240E-01	4.68390E-01	4.68801E-01	4.6927E-01
Region 5	8.35530E-02	8.33375E-02	8.28973E-02	8.3602E-02
Region 6	4.54010E-03	1.43151E-03	1.38786E-03	4.4070E-04
Region 7	2.45240E-03	7.67683E-04	7.61299E-04	2.3848E-04
Region 8	9.67970E-04	3.05382E-04	3.04234E-04	9.4802E-05
Region 9	8.94280E-04	2.81551E-04	2.76754E-04	8.8508E-05

Table 3.7 Calculated k_{eff} and fission fractions for Case1_2 *(continued)*

Institution	E.Mennerdahl Systems	Argonne National Laboratory	NAIS Co. inc.	Institut de Radioprotection et de Sûreté Nucléaire
Case name	Case 1_2	Case 1_2	Case 1_2	Case 1_2
Final k_{eff} estimate	1.33746	1.341	1.34196	1.34213
Final k_{eff} estimate uncertainty	0.00008	0.0003	0.00019	0.00006
Region 1	0.0905	0.0921	9.284588E-02	9.82E-02
Region 2	0.0981	0.0993	9.996385E-02	1.062E-01
Region 3	0.2528	0.252	2.522006E-01	2.666E-01
Region 4	0.4738	0.4679	4.682112E-01	4.688E-01
Region 5	0.0848	0.0863	8.377238E-02	5.7E-02
Region 6	0.0000	0.0013	1.537920E-03	1.6E-03
Region 7	0.0000	0.0007	8.300267E-04	9.0E-04
Region 8	0.0000	0.0002	3.381075E-04	4.0E-04
Region 9	0.0000	0.0002	3.000915E-04	3.0E-04

Table 3.8 Calculated k_{eff} and fission fractions for Case1_3

Institution	Los Alamos National Laboratory	KFKI Atomic Energy Research Institute	Japan Nuclear Cycle Development Institute	Oak Ridge National Laboratory
Case name	Case 1_3	Case 1_3	Case 1_3	Case 1_3
Final k_{eff} estimate	1.34093	1.34209	1.34259	1.33911
Final k_{eff} estimate uncertainty	0.00006	6.00E-05	0.00008	0.0001
Region 1	5.31020E-02	7.40016E-02	7.83337E-02	8.3149E-02
Region 2	5.71060E-02	7.97469E-02	8.43914E-02	8.9610E-02
Region 3	1.44860E-01	2.01859E-01	2.13612E-01	2.2666E-01
Region 4	2.68510E-01	3.74426E-01	3.95437E-01	4.2021E-01
Region 5	8.44740E-02	8.35739E-02	8.32011E-02	8.3810E-02
Region 6	2.04310E-01	9.71287E-02	7.54691E-02	5.0521E-02
Region 7	1.08910E-01	5.19094E-02	4.03685E-02	2.6795E-02
Region 8	4.09380E-02	1.94226E-02	1.51782E-02	1.0020E-02
Region 9	3.78000E-02	1.79315E-02	1.40090E-02	9.2240E-03

Table 3.8 Calculated k_{eff} and fission fractions for Case1_3 *(continued)*

Institution	E.Mennerdahl Systems	Argonne National Laboratory	NAIS Co. inc.	Institut de Radioprotection et de Sûreté Nucléaire
Case name	Case1_3	Case1_3	Case1_3	Case1_3
Final k_{eff} estimate	1.33697	1.341	1.34122	1.34185
Final k_{eff} estimate uncertainty	0.00009	0.0003	0.00019	0.00006
Region 1	0.0842	0.0762	6.693398E-02	8.48E-02
Region 2	0.0910	0.0823	7.218831E-02	9.17E-02
Region 3	0.2333	0.2089	1.819082E-01	2.304E-01
Region 4	0.4391	0.3904	3.367847E-01	4.046E-01
Region 5	0.0851	0.0865	8.428891E-02	5.72E-02
Region 6	0.0352	0.081	1.347575E-01	6.66E-02
Region 7	0.0189	0.0432	7.136669E-02	3.74E-02
Region 8	0.0069	0.0163	2.682479E-02	1.42E-02
Region 9	0.0063	0.0152	2.494691E-02	1.31E-02

Table 3.9 Calculated k_{eff} and fission fractions for Case2_1

Institution	Los Alamos National Laboratory	KFKI Atomic Energy Research Institute	Japan Nuclear Cycle Development Institute	Oak Ridge National Laboratory
Case name	Case 2_1	Case 2_1	Case 2_1	Case 2_1
Final k_{eff} estimate	1.05324	1.05337	1.05703	1.04964
Final k_{eff} estimate uncertainty	0.00006	6.00E-05	0.00007	0.00007
Region 1	3.01990E-02	5.09458E-02	5.05222E-02	5.0738E-02
Region 2	2.98640E-02	5.03599E-02	5.02228E-02	5.0144E-02
Region 3	6.43580E-02	1.08810E-01	1.09388E-01	1.0897E-01
Region 4	9.81180E-02	1.66640E-01	1.68908E-01	1.6824E-01
Region 5	2.45300E-01	2.46649E-01	2.48539E-01	2.4903E-01
Region 6	2.34520E-01	1.66340E-01	1.66206E-01	1.6591E-01
Region 7	1.53970E-01	1.08788E-01	1.07429E-01	1.0749E-01
Region 8	7.14230E-02	5.04173E-02	4.92442E-02	4.9458E-02
Region 9	7.22540E-02	5.10501E-02	4.95397E-02	5.0002E-02

Table 3.9 Calculated k_{eff} and fission fractions for Case2_1 *(continued)*

Institution	E.Mennerdahl Systems	Argonne National Laboratory	NAIS Co. inc.	Institut de Radioprotection et de Sûreté Nucléaire
Case name	Case2_1	Case2_1	Case2_1	Case2_1
Final k_{eff} estimate	1.05243	1.0569	1.05329	1.05625
Final k_{eff} estimate uncertainty	0.00006	0.0002	0.00021	0.00005
Region 1	0.0575	0.0526	6.968193E-02	5.41E-02
Region 2	0.0575	0.052	6.885718E-02	5.41E-02
Region 3	0.1280	0.1123	1.487830E-01	1.179E-01
Region 4	0.2009	0.1707	2.274839E-01	1.822E-01
Region 5	0.2584	0.2462	2.470891E-01	2.527E-01
Region 6	0.1349	0.1625	1.053092E-01	1.513E-01
Region 7	0.0856	0.1057	6.865237E-02	9.79E-02
Region 8	0.0385	0.0489	3.182848E-02	4.49E-02
Region 9	0.0386	0.0492	3.231483E-02	4.48E-02

Table 3.10 Calculated k_{eff} and fission fractions for Case2_2

Institution	Los Alamos National Laboratory	KFKI Atomic Energy Research Institute	Japan Nuclear Cycle Development Institute	Oak Ridge National Laboratory
Case name	Case 2_2	Case 2_2	Case 2_2	Case 2_2
Final k_{eff} estimate	1.05322	1.05342	1.05708	1.04966
Final k_{eff} estimate uncertainty	0.00006	6.00E-05	0.00006	0.00006
Region 1	1.02380E-01	1.01969E-01	1.00301E-01	1.0055E-01
Region 2	1.01030E-01	1.00698E-01	9.96651E-02	9.9501E-02
Region 3	2.18000E-01	2.17456E-01	2.16940E-01	2.1633E-01
Region 4	3.32620E-01	3.32619E-01	3.34826E-01	3.3431E-01
Region 5	2.45970E-01	2.47258E-01	2.48262E-01	2.4932E-01
Region 6	3.30730E-06	9.33218E-08	1.67640E-06	9.9133E-07
Region 7	1.40840E-06	0.0	8.46239E-07	1.9887E-07
Region 8	7.94680E-07	0.0	3.15369E-07	1.1715E-07
Region 9	7.66240E-07	0.0	3.52256E-07	1.4242E-07

Table 3.10 Calculated k_{eff} and fission fractions for Case2_2 *(continued)*

Institution	E.Mennerdahl Systems	Argonne National Laboratory	NAIS Co. inc.	Institut de Radioprotection et de Sûreté Nucléaire
Case name	Case2_2	Case2_2	Case2_2	Case2_2
Final k_{eff} estimate	1.05241	1.0572	1.05309	1.05634
Final k_{eff} estimate uncertainty	0.00006	0.0002	0.0002	0.00005
Region 1	0.0959	0.1012	1.029274E-01	9.89E-02
Region 2	0.0967	0.1004	1.013878E-01	9.90E-02
Region 3	0.2127	0.2173	2.185235E-01	2.156E-01
Region 4	0.3352	0.3324	3.330178E-01	3.333E-01
Region 5	0.2595	0.2488	2.441426E-01	2.532E-01
Region 6	0.0000	0	9.243254E-07	0
Region 7	0.0000	0	1.410689E-08	0
Region 8	0.0000	0	6.376319E-09	0
Region 9	0.0000	0	2.165536E-08	0

Table 3.11 Calculated k_{eff} and fission fractions for Case2_3

Institution	Los Alamos National Laboratory	KFKI Atomic Energy Research Institute	Japan Nuclear Cycle Development Institute	Oak Ridge National Laboratory
Case name	Case 2_3	Case 2_3	Case 2_3	Case 2_3
Final k_{eff} estimate	1.05271	1.05302	1.05682	1.04933
Final k_{eff} estimate uncertainty	0.00007	6.00E-05	0.00007	0.00009
Region 1	9.43440E-02	9.80849E-02	9.69295E-02	9.7116E-02
Region 2	9.31170E-02	9.69766E-02	9.63163E-02	9.5978E-02
Region 3	2.00960E-01	2.09717E-01	2.09943E-01	2.0888E-01
Region 4	3.06750E-01	3.20376E-01	3.24437E-01	3.2352E-01
Region 5	2.47680E-01	2.47161E-01	2.49158E-01	2.5053E-01
Region 6	2.64740E-02	1.27958E-02	1.08240E-02	1.1150E-02
Region 7	1.65290E-02	8.01550E-03	6.66963E-03	6.9006E-03
Region 8	6.92930E-03	3.37759E-03	2.81745E-03	2.9185E-03
Region 9	7.21060E-03	3.49509E-03	2.90325E-03	3.0062E-03

Table 3.11 Calculated k_{eff} and fission fractions for Case2_3 *(continued)*

Institution	E.Mennerdahl Systems	Argonne National Laboratory	NAIS Co. inc.	Institut de Radioprotection et de Sûreté Nucléaire
Case name	Case2_3	Case2_3	Case2_3	Case2_3
Final k_{eff} estimate	1.05203	1.0565	1.05345	1.05615
Final k_{eff} estimate uncertainty	0.00009	0.0002	0.0002	0.00005
Region 1	0.0955	0.0967	9.962111E-02	9.59E-02
Region 2	0.0954	0.0959	9.860388E-02	9.59E-02
Region 3	0.2121	0.2066	2.128503E-01	2.091E-01
Region 4	0.3348	0.3159	3.249325E-01	3.226E-01
Region 5	0.2604	0.2501	2.465805E-01	2.533E-01
Region 6	0.0008	0.0162	8.088689E-03	1.09E-02
Region 7	0.0005	0.01	5.034129E-03	6.7E-03
Region 8	0.0002	0.0042	2.103446E-03	2.8E-03
Region 9	0.0002	0.0044	2.185480E-03	2.9E-03

Figure 3.3 The skip cycles effect on the values of K_{eff} and standard deviations obtained from 1 000 active cycles for Case1_1

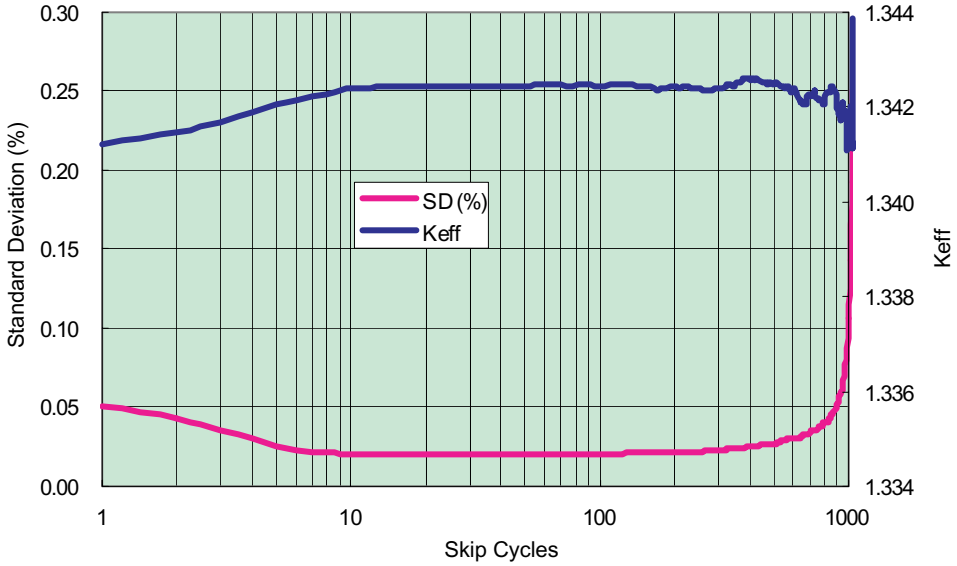

Figure 3.4 The skip cycles effect on the values of K_{eff} and standard deviations obtained from 1 000 active cycles for Case1_2

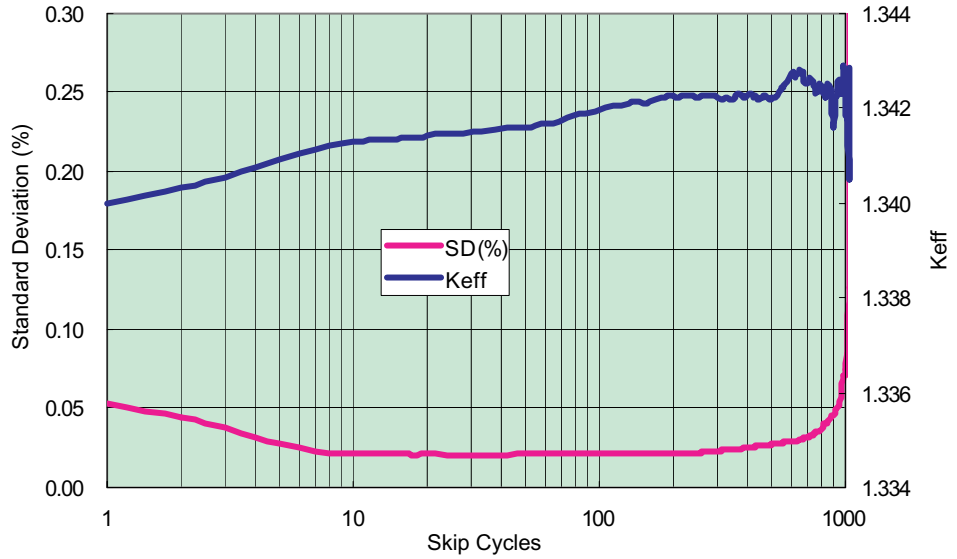

Figure 3.5 The skip cycles effect on the values of K_{eff} and standard deviations obtained from 1 000 active cycles for Case1_3

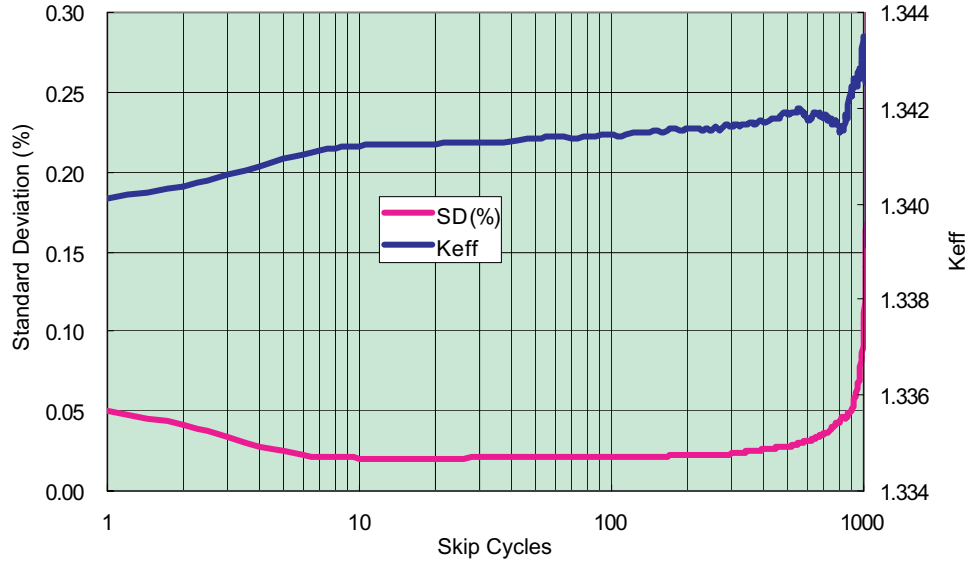

Figure 3.6 The skip cycles effect on the values of K_{eff} and standard deviations obtained from 1 000 active cycles for Case2_1

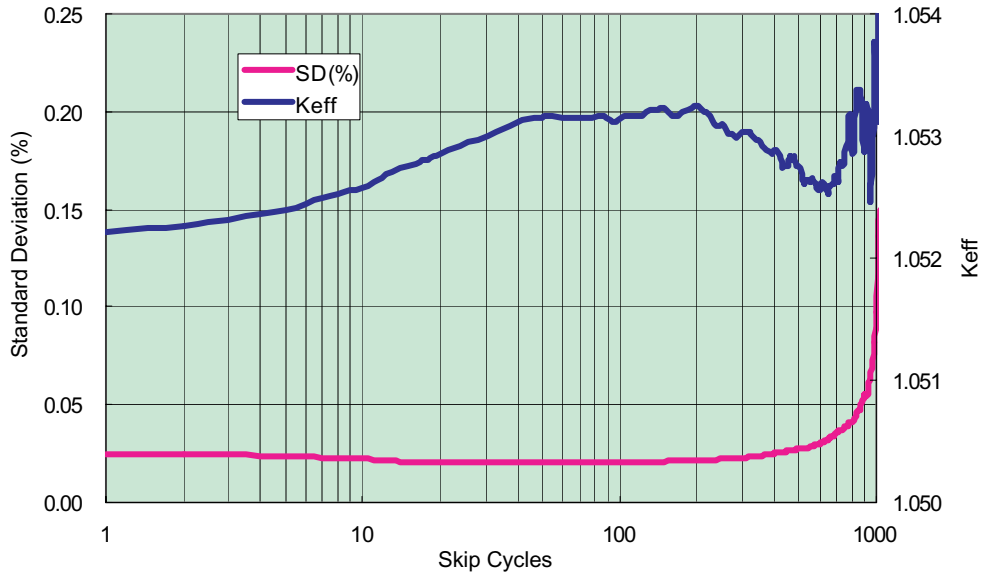

Figure 3.7 The skip cycles effect on the values of K_{eff} and standard deviations obtained from 1 000 active cycles for Case2_2

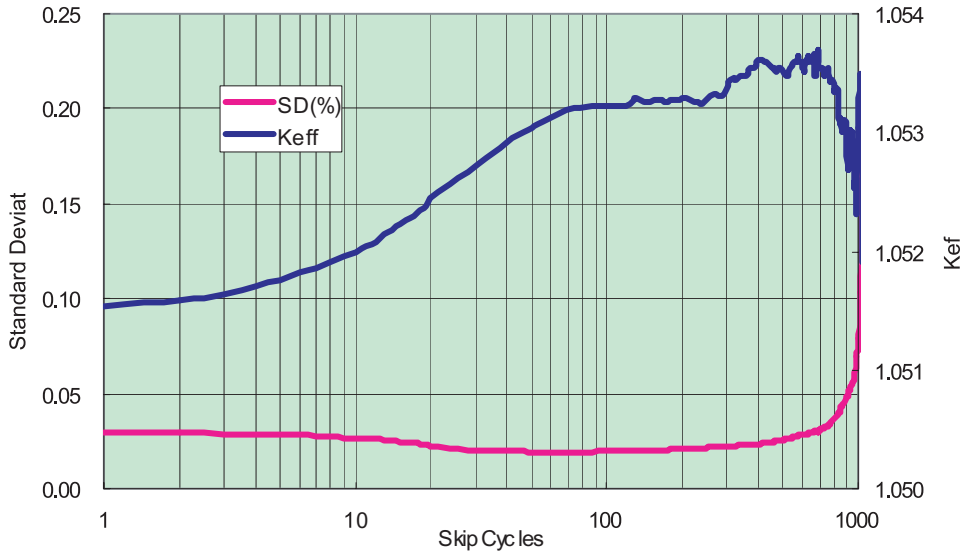

Figure 3.8 The skip cycles effect on the values of K_{eff} and standard deviations obtained from 1 000 active cycles for Case2_3

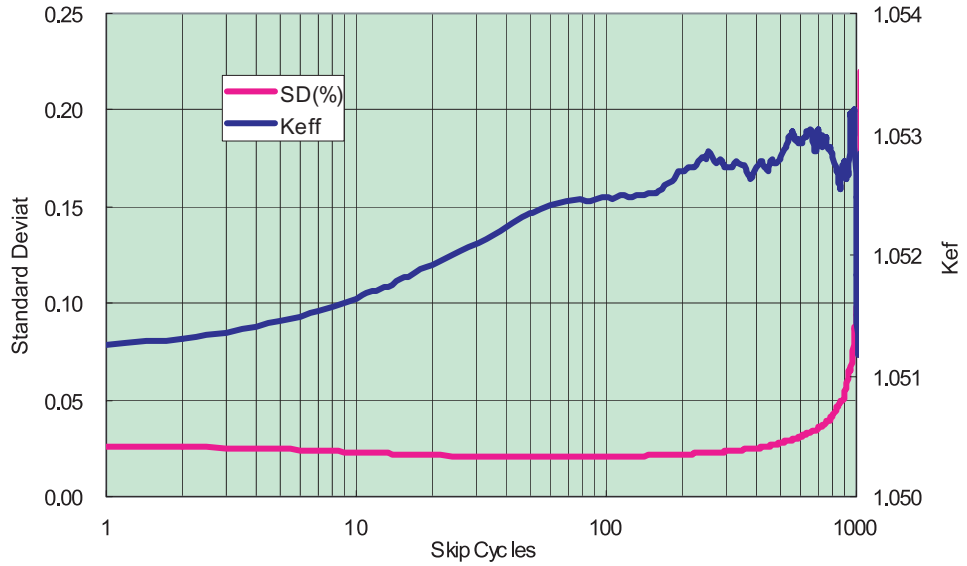

Conclusions

Test problems No.2 were calculated with several Monte Carlo codes, that is, MCNP, KENO, VIM and MORET. The final k_{eff}'s computed with each code show similar values. The differences probably stem from the cross section libraries used by the various codes. The calculation control parameters proposed by the problem coordinator, i.e. the number of generations skipped before beginning tallies, the number of generations tallied, and the number of histories per generation, require time-consuming computation.

In cases 1_1 and 2_1, axial material distributions are symmetrical, so that axial fission fraction distribution should appear symmetrical. The fission fractions calculated with MCNP by LANL and NAIS, appear to deviate from a symmetrical distribution. KENO calculations by JNC and EMS show symmetrical fission fraction distributions in these cases. The multiplication factor for these cases should decrease in the order of cases 1_1, 1_3, and 1_2,on physical grounds. k_{eff} results from ORNL and NAIS do show 1_3 smaller than case 1_2. The values of k(1_3) and k(1_2) are 1.33911±0.0001 and 1.33952±0.00008 (ORNL), and 1.34122±0.00019 and 1.34196±0.00019 (NAIS). This inversion seems to come from an error in the source distribution, that is, the source of the bottom part in case 1_3 is estimated to be larger than the final values. In case 1_2, the reactivity of the bottom part is so small that source in that part soon becomes small through the effects of generation cycles. However, in case 1_3, the reactivity of the bottom part is not as small, so that many more cycles are necessary to decrease the source to the same level. This means that to obtain the final source distribution in such a case as 1_3, where the core configuration is slightly asymmetrical, requires a larger number of generation cycles, which is evident by the results shown in Figure 3.3.

Discussion

In our test specifications, the number of skip cycles is given by the problem coordinator. When convergence is slow, it is very important to determine the number of skip cycles for Monte Carlo calculations. One basic assumption that is made for good criticality calculations is that the fundamental spatial mode for the fission source is achieved during the inactive cycles. In other words, the neutron source distribution has essentially reached stability after enough inactive cycles have been skipped.

To obtain a reasonable number of skip cycles, we have tried an idea as follows. For example, we take average of k_{eff} values over 10 cycles, i.e., one batch of 10 k_{eff} cycles with 10000 particles per cycles. Then the difference between adjacent k_{eff}'s is scanned over the series of 50 batches. When the k_{eff} differences *(AVSQ(n))* curve falls within the limits –1.0E-3 to 1.0E-03, "stability" is assumed to be reached. By this method, a reasonable skip number is expected to be obtained. Here, we define

$$AVSQ\,(n) = \frac{AV\,(n+1) - AV\,(n)}{0.5(AV\,(n+1) + AV\,(n))}$$

and

$$AV\,(a) = 0.1 \sum_{i=10(n-1)+1}^{10n} \mathrm{k_{eff}}\,(\mathrm{i})$$

The *AVSQ(n)* value obtained from above equation is shown in Figure 3.9(a) for case 2_3.The relative k_{eff} difference, AVSQ, falls within limits ±1.0E-03 after 100 start cycle, where k_{eff}'s are

averaged over adjacent 10 cycles. However, from Figure 3.9(b-c), we note that, because of the low speed of convergence by cycles, the k_{eff} still remains far from the approximate final k_{eff} 1.05345, as shown in Table 3.11.

Figure 3.9(a) Relative K_{eff} difference obtained from each batch of 10 k_{eff} cycles for Case2_3

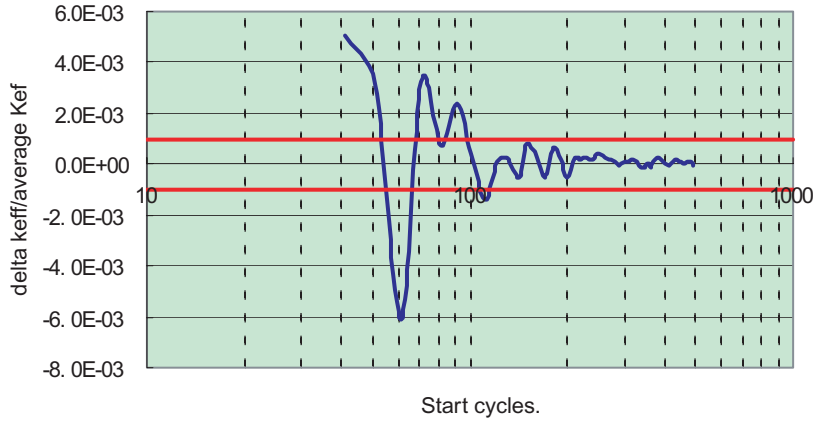

Figure3.9(b) The K_{eff} and standard deviation of each batch for Case2_3

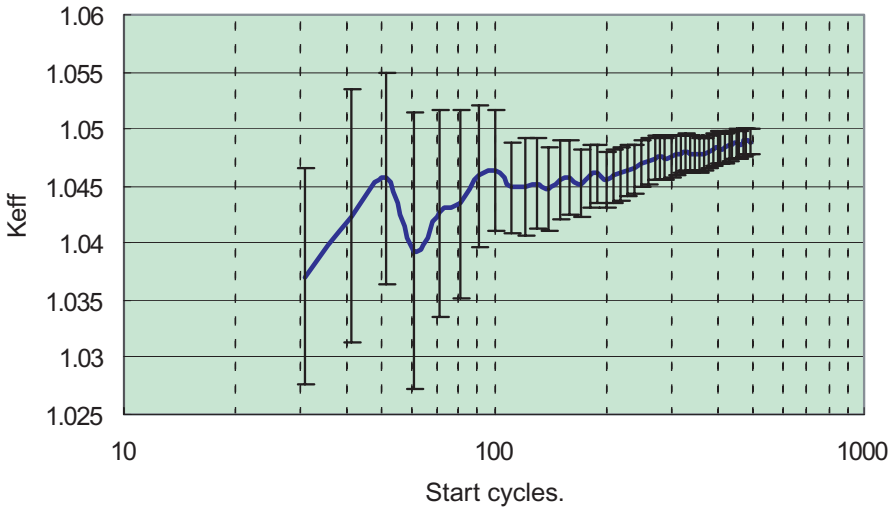

Figure 3.9(c) The K_{eff} and standard deviation of each batch for Case2_3

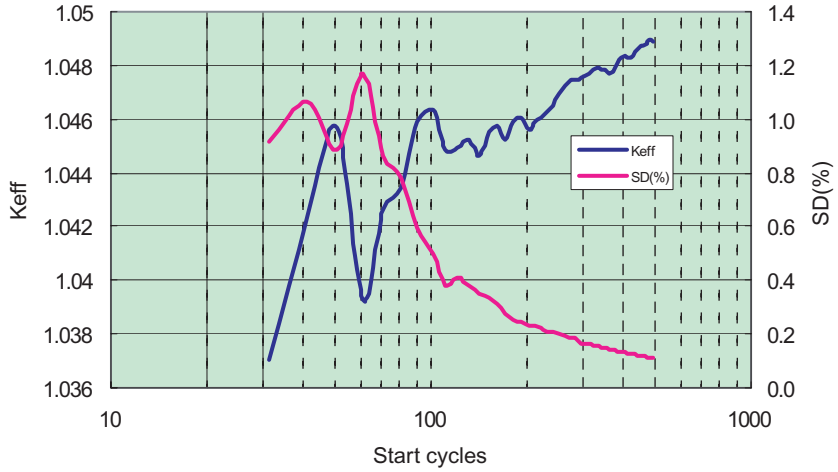

As shown above, it is not so easy to determine whether the source iteration has converged or not. When analyzing systems such as these, it is important to: (a) find a method to determine source iteration convergence, and (b) obtain the necessary number of skip cycles. We know the final k_{eff}'s of the test problems through time-consuming computation; we would like to obtain these k_{eff}'s in a shorter computing time.

References

[1] M. Takano and H. Okuno, "OECD/NEA Burn-up Credit Criticality Test Result of Phase II-A", NEA/NSC/DOC (96)01, JAERI Research 96-003 (1996).

Chapter 4

LOOSELY COUPLED URANYL NITRATE SOLUTION SLABS: TEST PROBLEM 3

Yoshinori Miyoshi, Toshihiro Yamamoto
Japan Atomic Energy Research Institute

Overview

Two fissile units (Unit 1 and Unit 2) are separated by a slab of water. The fuel is 10 wt.% enriched uranyl nitrate aqueous solution [1]. The uranium concentration is 300 gU/L, and the nitric acid molarity is 1.0 mol/L. The thickness of unit 2 is fixed at 20 cm. The thicknesses of unit 1 are varied, as are the water thicknesses.

Specifications

Material

The material compositions are shown in Table 4.1.

Table 4.1 Material specifications (at/b-cm)

Uranyl Solution	
H	5.9347E-02
N	2.1220E-03
O	3.7258E-02
^{235}U	7.6864E-05
^{238}U	6.8303E-04
Water	
H	6.6658E-02
O	3.3329E-02

Geometry

Figure 4.1 describes the problem geometry. Unit 1 and unit 2 have the same composition (see table above), the difference between fissile units being the thickness. Table 4.2 gives the thicknesses for the studied cases.

Figure 4.1 Problem geometry

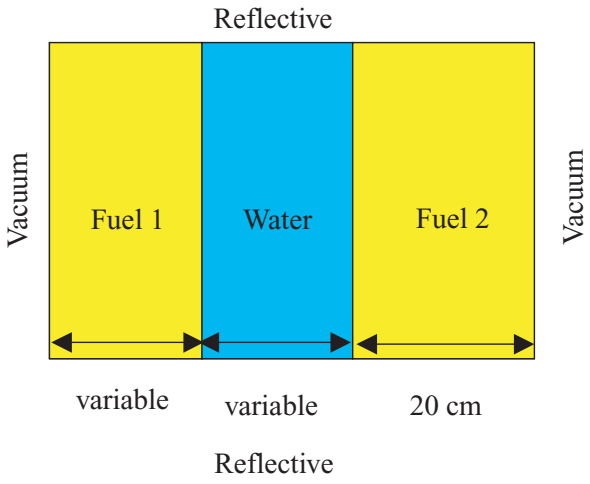

Cases

Table 4.2 Dimension specifications of cases (cm)

Case	Unit #		Water Gap
	1	2	
1	20	20	30
2	18	20	30
3	15	20	30
4	12	20	30
5	20	20	20
6	18	20	20
7	15	20	20
8	12	20	20
9	20	20	10
10	18	20	10
11	15	20	10
12	12	20	10

Calculational parameters

- 2 000 neutrons per generation;
- 50 skip generations;

- 550 active generations;
- flat initial source;

Required output

In addition to identifying information, the participants were asked to submit the information specified in Table 4.3.

Table 4.3 Information to report

Line	Required information
12	Starting source
13	nskip = number of generations skipped before beginning tallies or before convergence:
14	ngen = number of generations tallied
15	nhist = number of histories per generation
16	ngensh = number of generations per superhistory
17	final k_{eff} estimate
18	final k_{eff} estimate uncertainty (one standard deviation)
19	k_{eff} estimate for first supergeneration
20	individual k_{eff} estimate for second supergeneration
18+ngen	individual k_{eff} estimate for last supergeneration

Cumulative fission fractions ff(i,g) in fissionable region i in generation g is also an important output. As all computer codes do not have the capability of printing this information for any generation, participants may choose between the following alternatives.

1) Fission fractions are given as average over all generations

2) Fission fractions are given as average over all active generations

3) Fission fractions are given at different generation sequences

Results

Six organizations took part and four Monte Carlo codes, VIM, MCNP, MORET and KENO-V.a with 27-group ENDF/B-IV or 238-group ENDF-B/V cross sections in SCALE 4.4, were applied. A deterministic method with XSDRNPM in SCALE 4.4 was also applied for comparison of the results. All Monte Carlo codes used conventional power iteration methods except for a super history technique in MORET.

To investigate a coupling intensity among array of units, it is proposed in this problem that coupling coefficients be introduced. The coupling coefficient *Pij* is defined as the expectation value that a fission neutron in unit i gives rise to a next generation fission neutron in unit *j*. A coupling coefficient matrix is defined for two unit array system as

$$\begin{bmatrix} P_{11} & P_{21} \\ P_{12} & P_{22} \end{bmatrix} \begin{bmatrix} S_1 \\ S_2 \end{bmatrix} = k_{eff} \begin{bmatrix} S_1 \\ S_2 \end{bmatrix}. \quad (1)$$

S_1 and S_2 are fission sources in units 1 and 2, respectively. These coupling coefficients can be obtained by Monte Carlo method such as KENO and MCNP. KENO has a capability to give coupling coefficients after a criticality calculation by invoking a relevant code option. KENO, however, only has a capability to give the standard deviations for the largest coupling coefficients. MCNP is capable of calculating coupling coefficients and their standard deviations by storing a fission source distribution obtained by a criticality calculation.

Equation (1) has two eigenvalues. The larger one, k_0, is the eigenvalue for a fundamental mode and the smaller one, k_1, is for the first harmonic. The elements of the fission probability matrix are calculated for a fundamental mode flux distribution. Thus, the first harmonic is significant if a neutron interaction between the units 1 and 2 does not affect the fission source distribution in each unit. As the thickness of the interstitial water decreases, the k_1 obtained by the eigenvalue matrix equation becomes incorrect. The ratio k_1/k_0 (i.e., dominance ratio) of a symmetric weak interaction system such as Case 1 is close to unity. When the dominance ratio is close to unity, the decay of higher-harmonics during the source iteration process is very slow. If a statistical fluctuation is not negligible compared with $1\text{-}k_1/k_0$, it is difficult to reach a converged fission source distribution. In other words, the statistical uncertainty of k_1/k_0 comparable to k_1/k_0 makes the convergence of the system difficult. Using the coupling coefficient matrix, it is possible to discuss the fission convergence problem quantitatively.

Tables 4.4, 4.5 and 4.6, show the coupling coefficients and matrix eigenvalues for all 12 cases. These results were calculated by MCNP 4B. In case 1 (30 cm water separator), the coupling coefficients P_{12} (or P_{21}) between the units 1 and 2 are approximately 0.0012, and two units are almost isolated, while the self-coupling coefficient of the unit 1, P_{11} (or P_{22}), is 0.935. Thus, the k_{eff} of the system was mostly dominated by a single unit, regardless of the fission source distribution. This means that, even if all neutrons are started in one of the units and the chain reaction never reaches the other unit, the k_{eff} would be substantially correct.

Although the converged fission source ratio between the two symmetrical units is supposed to be unity, it was as large as 5 in an MCNP calculation during the iterations of generation as shown in Figure 4.2. On the other hand, a thinner water layer makes the fission source more stable, also shown in Figure 4.2 The frequency distribution of the fission source fraction in the unit 1, which was obtained by 50 replica calculations, is shown in Figure 4.3. The distribution exhibits large variations from 0.2 to 0.8 as compared to the exact solution of 0.5. Due to the weak interaction between the units, each unit behaves independently of the other unit. The broadening of the fission fraction ratio distribution can be reduced by decreasing the standard deviations of P_{11} and P_{22}, easily done by increasing the neutrons per generation (based on the central limit theorem). It has already been demonstrated [1] that an anomalous fission source distribution in a symmetrical array system does not affect the system k_{eff}. Figure 4.4 shows a fission source ratio transition with an increased number of neutrons per generation. With 10 000 neutrons per generation, the fission source ratio in each generation is largely improved. The discussion on the increased number of neutrons per generation for KENO V.a is presented in Appendix 4.a.

Table 4.4 Coupling coefficients for 30 cm thickness water

	Coupling coefficients				Matrix eigenvalue	
Case	P_{11}	P_{12}	P_{21}	P_{22}	k_0	k_1
1	0.9354 ±0.0017	0.0012 ±0.00006	0.0011 ±0.00006	0.9362 ±0.0020	0.9370 ±0.0014	0.9346 ±0.0014
2	0.8903 ±0.0094	0.0008 ±0.00026	0.0012 ±0.00004	0.9336 ±0.0010	0.9336 ±0.0067	0.8903 ±0.0067
3	0.8105 ±0.0130	0.0021 ±0.00068	0.0012 ±0.00004	0.9339 ±0.0009	0.9339 ±0.0092	0.8105 ±0.0092
4	0.6956 ±0.0156	0.0017 ±0.00068	0.0010 ±0.00004	0.9338 ±0.0009	0.9338 ±0.0111	0.6955 ±0.0111

Table 4.5 Coupling coefficients for 20 cm thickness water

	Coupling coefficients				Matrix eigenvalue	
Case	P_{11}	P_{12}	P_{21}	P_{22}	k_0	k_1
5	0.9342 ±0.0017	0.0065 ±0.00015	0.0064 ±0.00013	0.9355 ±0.0016	0.9413 ±0.0012	0.9284 ±0.0012
6	0.8884 ±0.0038	0.0079 ±0.00034	0.0066 ±0.00011	0.9370 ±0.0011	0.9380 ±0.0028	0.8874 ±0.0028
7	0.8078 ±0.0055	0.0082 ±0.00055	0.0061 ±0.00009	0.9329 ±0.0010	0.9333 ±0.0039	0.8074 ±0.0039
8	0.7049 ±0.0071	0.0112 ±0.00083	0.0059 ±0.00009	0.9339 ±0.0010	0.9342 ±0.0051	0.7046 ±0.0051

Table 4.6 Coupling coefficients for 10 cm thickness water

	Coupling coefficients				Matrix eigenvalue	
Case	P_{11}	P_{12}	P_{21}	P_{22}	k_0	k_1
9	0.9313 ±0.0017	0.0436 ±0.00037	0.0441 ±0.00037	0.9329 ±0.0017	0.9760 ±0.0012	0.8882 ±0.0012
10	0.8878 ±0.0019	0.0494 ±0.00045	0.0424 ±0.00035	0.9322 ±0.0013	0.9609 ±0.0013	0.8590 ±0.0013
11	0.8099 ±0.0025	0.0619 ±0.00066	0.0403 ±0.00033	0.9365 ±0.0012	0.9538 ±0.0018	0.7926 ±0.0018
12	0.7025 ±0.0030	0.0730 ±0.00091	0.0381 ±0.00032	0.9326 ±0.0012	0.9441 ±0.0022	0.6909 ±0.0022

Figure 4.2　Fission source ratios of Cases 1, 5 and 9

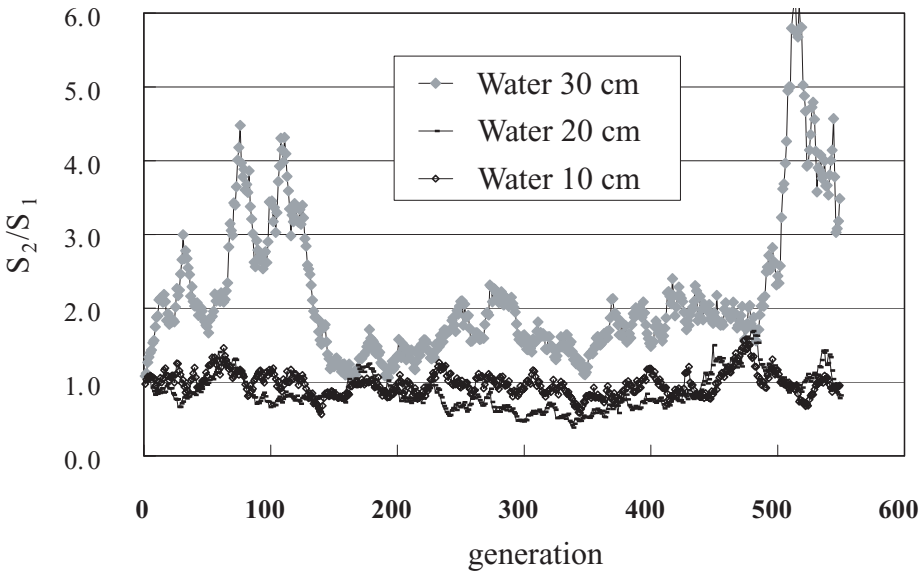

Figure 4.3　Frequency distribution of S1/(S1+S2) of Case 1

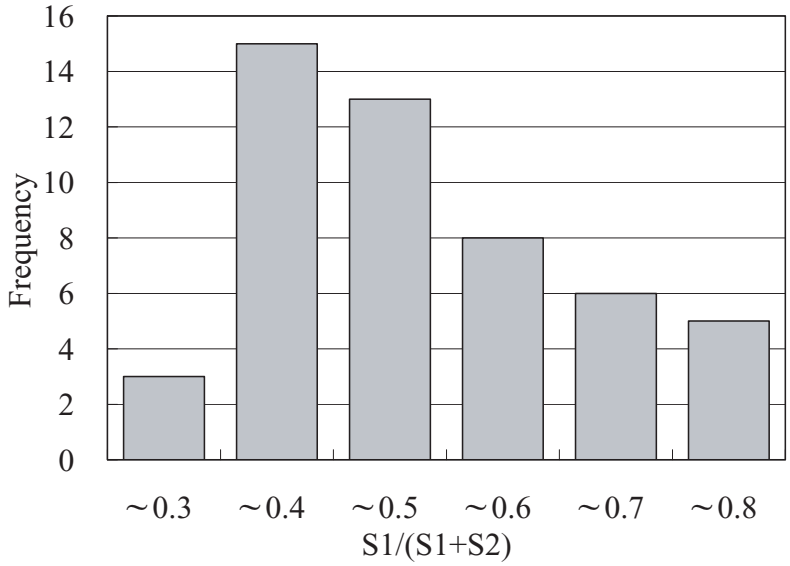

Figure 4.4 Fission source ratios with different neutrons per generation in Case 1

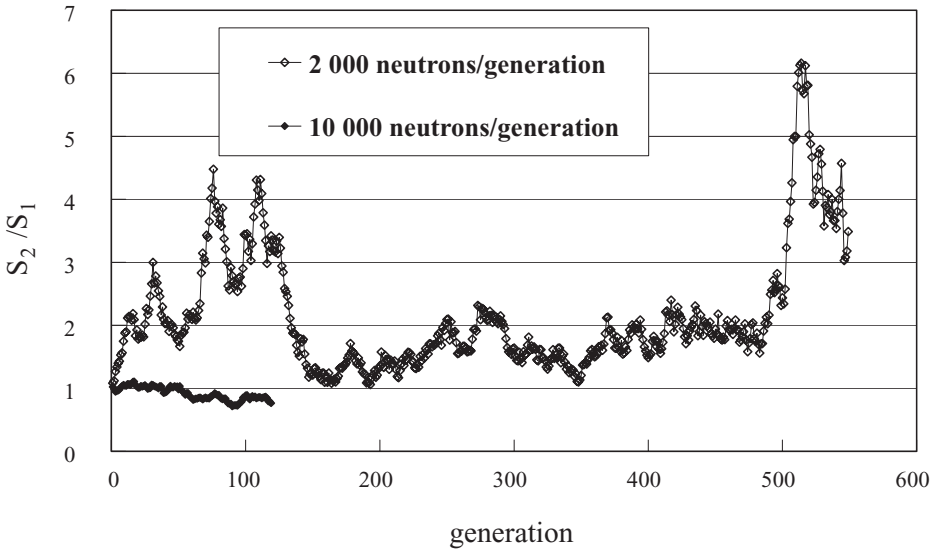

Slight asymmetry in a weakly coupling fissile array (Case 2) makes a large difference in fission source allocation. The smaller unit contributes little to k_{eff} of the array system in this situation since the k_{eff} is dominated by the larger unit. The fission source ratios in the Cases 2, 3, 4 are stable during the generations due to the asymmetry in spite of the weak neutron interaction. The dominance ratio k_1/k_0 of case 2 is 0.95 and this ratio is significantly smaller than unity. Figure 4.5 shows a fission source ratio S_2/S_1 transition for Case 2, and the fission source is found to show a relatively stable convergence around 50. Occasionally, large deviations of the S_2/S_1 occur due to the small number of fission source sites in unit 1.

Figure 4.5 Fission source ratio of Case 2

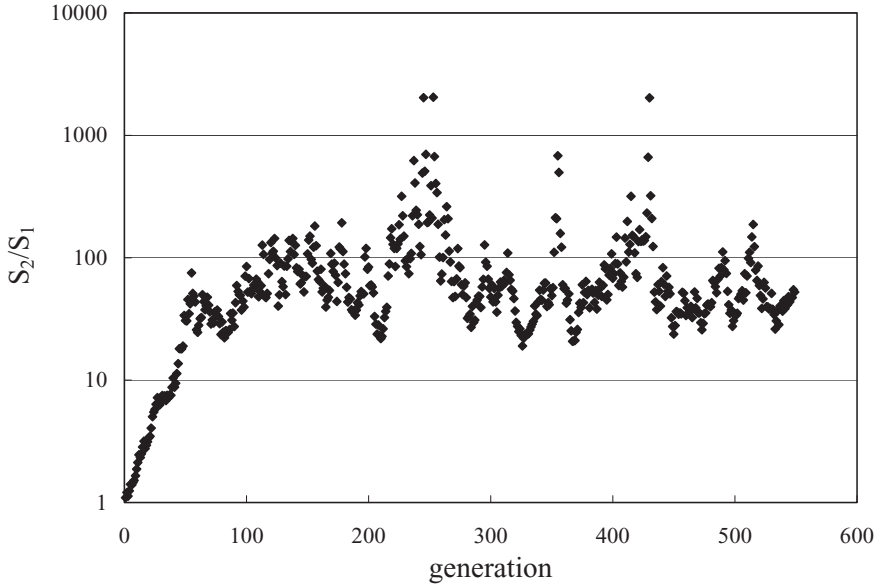

As the thickness of the water slab is reduced, the neutron interaction between the units becomes larger and the fission source distribution during the generations becomes more stable even in a symmetric system. Take, for example, in Case 9 (10 cm water separator), $P_{12}=P_{21}=0.044$. This symmetric system has a dominance ratio that is much smaller than in case 1, and has a sufficient restoring force to make the fission source allocation the appropriate one. The fission source ratio S2/S1 averaged over the whole generations in Case 9 is approximately 0.96, which is much better than in case 1.

Figure 4.6 shows the number of fission neutrons in both units of Case 4 when the number of neutrons per generation was only 100 and they were all started in the less reactive unit 1 at the first generation. This figure shows that the more reactive unit was sampled after the fourth generation. Despite the larger interstitial water thickness and the small number of neutrons per generation, we did not encounter a phenomenon of so-called "lost unit". As the number of neutrons increases, the probability of "lost unit" decreases. Thus, MCNP and other Monte Carlo codes using the same algorithm of fission source site determination hardly have an opportunity to have a "lost unit" during the criticality calculations.

Figure 4.6 Fission neutron distribution of Case 4 when all neutrons start in the less reactive unit

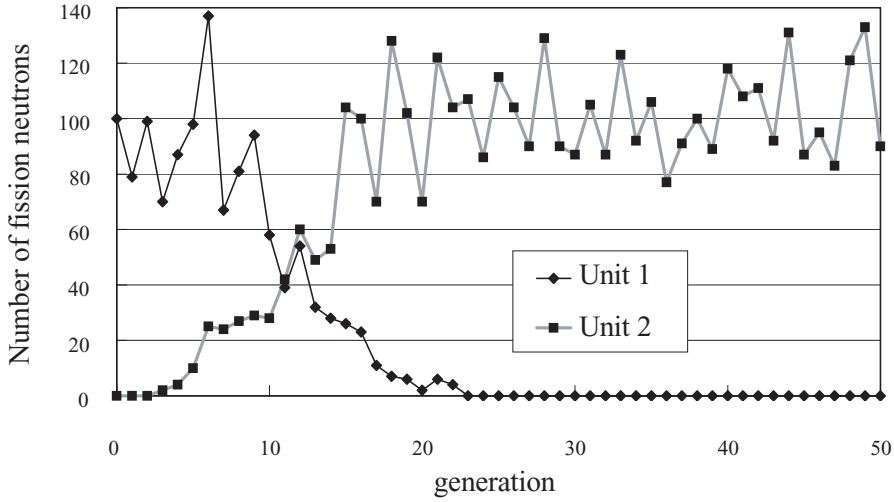

Comparison among several Monte Carlo Codes

Participants and the codes used are given in Table 4.7. Table 4.8 shows that the fission source ratios, S_2/S_1, obtained by one million history criticality calculations (2 000 neutrons per generation and 500 generations) of several Monte Carlo codes. For comparison, the results of a deterministic code XSDRNPM are given as well. XSDRNPM used the 44-group cross-sections. The results of Monte Carlo codes are from only one replica calculation. Note that the ratios in symmetric weakly coupled cases (i.e., cases 1 and 5) may change drastically around unity by using different random number sequences.

Table 4.7 List of participants and calculation tools

Name	Code	Cross-section library
R.Blomquist	VIM	ENDF/B-V
J.Wagner	KENO V.a	238Gr. ENDF/B-V
D.Mennerdahl	KENO V.a & XSDRNPM	238Gr. ENDF/B-V
N.Shirai	KENO V.a	27Gr. ENDF/B-IV
J.Miss, O.Jacquet	MORET4	172Gr. CEA93 JEF2.2
R.Little	MCNP 4C	ENDF/B-VI
T.Yamamoto	MCNP 4B	JENDL-3.2

Table 4.8 Fission source ratio S_2/S_1 by one million history calculations

Case	Unit		Water	S_2/S_1							
	1	2	(cm)	XSDR NPM	MORET		MCNP	KENO		VIM	VIM
	cm	cm		44Gr.	C.M*	S.H **		238Gr	27Gr	collision	absorp tion
1	20	20	30	1.00	0.93	0.96	1.9	1.3	1.2	5.1	0.94
2	18	20	30	34	47	33	52	31	28	35	35
3	15	20	30	110	132	101	111	110	107	99	99
4	12	20	30	219	203	217	196	226	219	226	200
5	20	20	20	1.00	1.02	1.08	0.82	0.91	0.86	0.83	1.12
6	18	20	20	7.1	7.3	7.3	8.1	7.3	7.6	7.5	6.6
7	15	20	20	21	20	20	20	21	20	21	21
8	12	20	20	40	36	38	40	40	39	42	39
9	20	20	10	1.00	1.04	0.98	0.96	0.99	1.07	1.03	1.04
10	18	20	10	1.7	1.7	1.7	1.8	1.7	1.8	1.7	1.7
11	15	20	10	3.5	3.4	3.4	3.5	3.6	3.7	3.6	3.5
12	12	20	10	6.3	6.1	6.0	6.4	6.3	6.3	6.4	6.4

*Conventional method of MORET.

**Super history technique with 10 generations per superhistory stage.

The fission source ratios S_2/S_1 by XSDRNPM seem to agree with Monte Carlo. It is suggested that a deterministic code does not always give a true fission source distribution for a weakly coupled systems. The fission source ratio by a deterministic method is very sensitive to the mesh size especially for a weak interaction system. More studies are needed to discuss the fission source convergence of deterministic codes on these test problems.

In the VIM calculations, two algorithms for source site determination (collision-based and absorption-based) were tried [2]. The collision-based algorithm was the original technique used in VIM, which now uses absorptions. Relatively good agreement in the fission source ratios among several codes were found except in the VIM collision-based algorithm result for Case 1. Judging from the standard deviations of S_2/S_1, the VIM absorption-based algorithm is the best among the codes in Table 4.8, and KENO is a little better than MCNP. Figure 4.7 shows the fission source ratio fluctuations for case 1 obtained by both VIM algorithms and MCNP. Extreme deviations from 1.0 were found in the VIM collision-based results. MCNP uses a collision-based algorithm similar to that used in VIM, except the number of particles is not fixed. It is the product of the number of starting particles per

generation and the particle weight that is fixed throughout the generations. On the other hand, the result by the VIM absorption-based algorithm is better than its collision-based algorithm and MCNP. The collision-based algorithm used for the generation of source sites would increase the magnitude of fluctuations in the fission source distribution caused by the variability in the number of collisions per particle [2]. This is especially true in homogeneous media where the fissionable material is mixed with other materials as in this test problem.

Figure 4.7 Fission source ratio of case 1 by MCNP and VIM

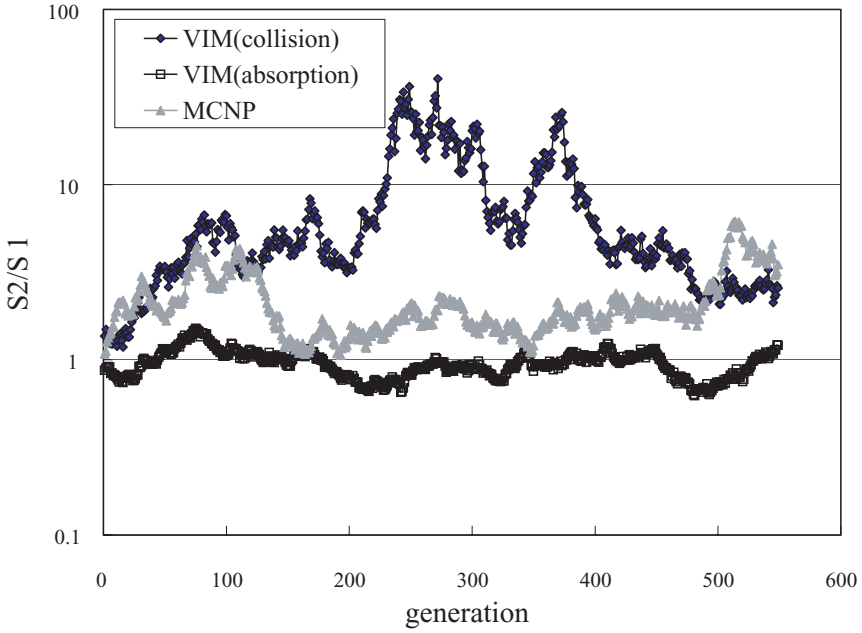

Table 4.9 shows the coupling coefficients calculated by KENO V.a and 27 group ENDF/B-IV. These coupling coefficients are almost comparable to those obtained by MCNP. There seem also to be no conspicuous differences in the fission source convergence between KENO and MCNP. Figure 4.8 shows the calculated k_{eff}'s by different codes. It can be seen from this figure that the calculations were carried out correctly. The overestimations of MCNP are caused by the library JENDL-3.2, which gives higher k_{eff}'s for homogeneous enriched uranium solution systems.

Table 4.9 Fission probability matrix elements by KENO V.a

Case	Fission probability matrix				Eigenvector ratio
	P_{11}	P_{12}	P_{21}	P_{22}	S_2/S_1
1	0.930	0.0013	0.0012	0.930	1.14
2	0.884	0.0011	0.0012	0.929	36.8
3	0.805	0.0019	0.0011	0.931	109
4	0.690	0.0015	0.0010	0.930	227
5	0.930	0.0063	0.0063	0.928	0.87
6	0.884	0.0074	0.0062	0.930	7.50
7	0.806	0.0087	0.0060	0.930	20.7
8	0.704	0.0105	0.0056	0.929	39.7
9	0.926	0.0433	0.0432	0.927	1.01
10	0.884	0.0492	0.0415	0.929	1.76
11	0.803	0.0607	0.0398	0.930	3.61
12	0.704	0.0713	0.0376	0.929	6.29

Figure 4.8 Calculated k_{eff}'s

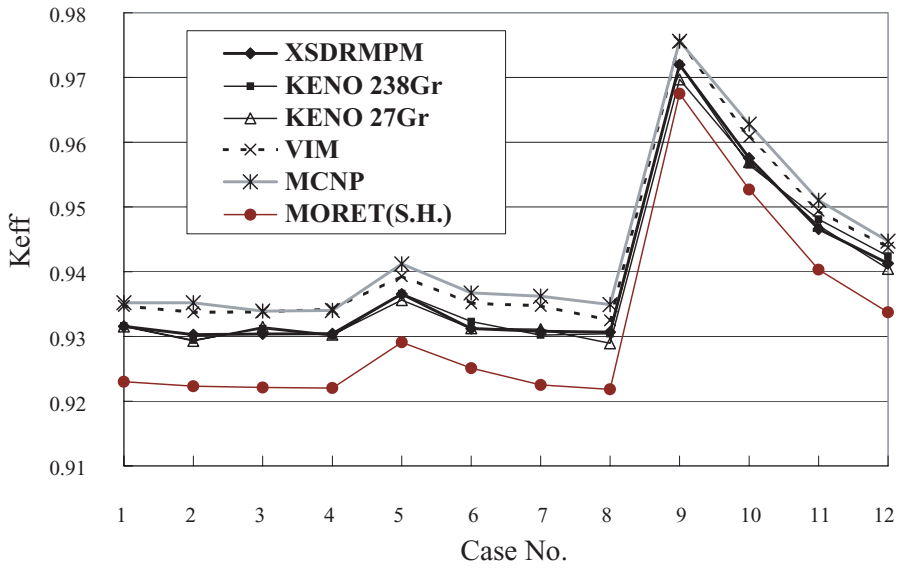

MORET used three techniques to determine the fission source sites: the conventional power method, stratified source sampling, and the superhistory method. The fission fractions of unit 1 for case 1 obtained by eleven replica calculations using the three techniques are shown in Figure 4.9. In the superhistory technique, 10 generations correspond to one superhistory stage. The fluctuation of the fission fraction through the replica calculations is the smallest with the superhistory technique. The stratified source sampling technique may not be superior to the conventional method. This is to be expected because neither unit is likely to be lost in this test problem.

Figure 4.9 Fission fraction of Unit 1 by three techniques of MORET

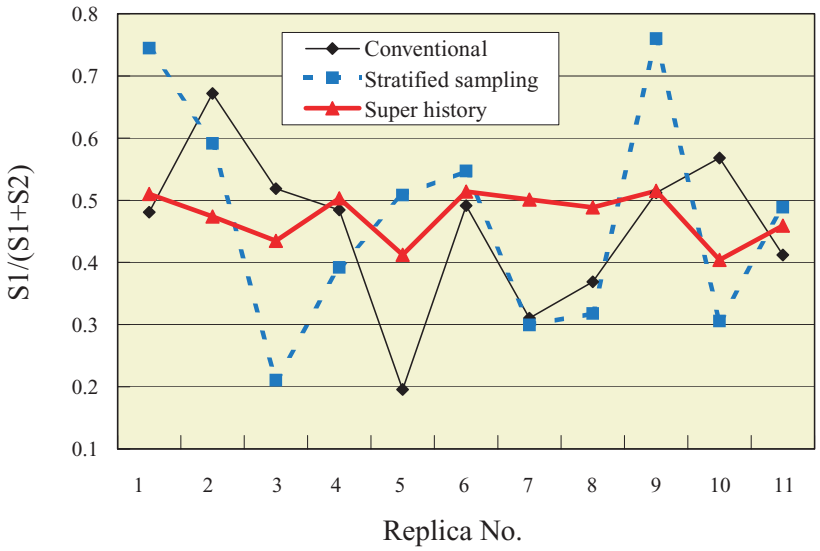

Conclusions

Calculating coupling coefficients among fissile array of units is very powerful tool for discussing the problem of fission source convergence. By solving a matrix eigenvalue equation, we can easily compute the largest and the second-largest eigenvalues, and the ratio of the two eigenvalues (dominance ratio).

No units were “lost” even with 30 cm thickness water and 100 neutrons per generation.

While the VIM collision-based algorithm seems not to be suitable for Case 1 of this test problem, the absorption-based algorithm is expected to reduce fission source fluctuations in a symmetric, weakly interacting system.

The superhistory algorithm can improve the fission source convergence of this test problem, having an effect similar to increasing the number of neutrons per generation.

References

[1] T. Yamamoto, T. Nakamura, Y. Miyoshi, “Fission Source Convergence of Monte Carlo Criticality Calculations in Weakly Coupled Fissile Arrays,” J.Nucl.Sci.Technol., **37**, 41 (2000).

[2] R.N. Blomquist, E.M. Gelbard, “Alternative Implementation of the Monte Carlo Power Method,” Nucl.Sci.Eng., **141**, 85 (2002).

Appendix 4.a

To confirm the report results in Figure 4.4, a similar study of 50 replicas for case 1 was made, using KENOVa and given statistical specifications: 2 000 neutrons per generations (NPG), 500 active generations and 50 skipped generations. In a second series of calculations, the specifications were changed to 20 000 neutrons per generations, 50 active generations and 5 skipped generations. This means identical numbers of active and skipped neutrons. The results are given in Figure 4.a.1 below. The standard deviations for k_{eff} were similar while those for S_1 and S_2 were lower. A significant improvement is obtained when the number of neutrons per generation is increased. However, depending on for what purpose the S_2/S_1 ratios are generated, the statistical model could be improved further. More generations for a 2 000 NPG case were attempted (up to 11 000 active generations) and improved the results, but only very slowly. The Expert Group should study the optimization of statistics further.

Figure 4.a.1 Effect of generation size on source fluctuations (Case 1)

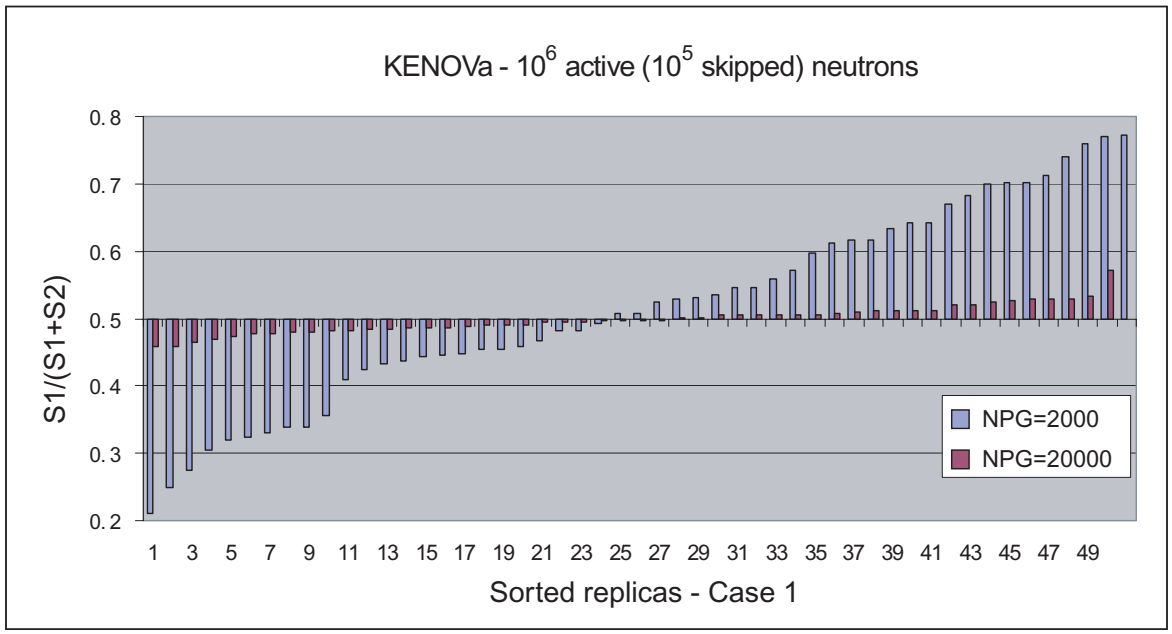

Chapter 5

ARRAY OF INTERACTING SPHERES: TEST PROBLEM 4

By Olivier Jacquet and Joachim Miss (IRSN, France)

Overview

Test problem 4 is an unreflected 5 x 5 x 1 array of metal spheres in air in which the initial source is chosen to be far from the converged source distribution. The greatest part of the neutrons is placed in one of the least reactive units. Moreover, an insufficient number of histories per cycle (125) is intentionally chosen to amplify the effects of under-sampling. In those conditions, the source convergence process requires a large number of cycles before the most reactive unit is correctly sampled. As the number of cycles is intentionally limited to 1 000 (with 0 cycle skipped), 1 200 (with 200 cycles skipped) or 1 400 (with 400 cycles skipped), the final k_{eff} (cumulative over the active cycles) may be underestimated for two reasons:

1) Either the source convergence has not been achieved, i.e. the most reactive unit is still under-sampled at the end of the simulation; in the worst case, the most reactive unit may be deserted and may stayed unvisited, leading to a wrong convergence.
2) Either the source convergence has been achieved and the number of initial cycles skipped is not sufficient.
3) The test problem aims at testing the robustness of the criticality codes to converge to the correct distribution of sources when the initial guess is not realistic.

Specifications

Geometry

The test problem geometry is shown in Figure 5.1.

Figure 5.1

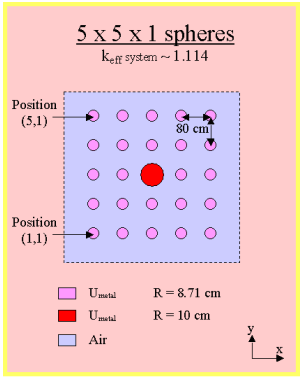

A lattice of 5 x 5 x 1 highly enriched uranium metal spheres separated by air is considered. The center-to-center distance between spheres is 80 cm. All the spheres have the same composition (see Table 5.1 Fuel and air compositions (in atoms/barn-cm)). The radius of the central sphere is 10 cm and the radius of the other spheres is 8.71 cm. Table 5.2. Specification of replica calculations. The spheres are numbered as in a conventional matrix, so that the lowest left-hand sphere in the figure below is in position (1,1) and the top right-hand sphere is in position (5,5). The test is a modified version of the configuration studied by Kadotani *et al.* [1].

Material

Table 5.1 Fuel and air compositions (in atoms/barn-cm)

High enriched uranium metal:	
^{235}U	4.549E-02
^{238}U	2.560E-03
Air	
N	4.3250E-5
O	1.0810E-5

Required calculations

Calculations were to be performed using 125 histories per cycle, 1000 active cycles and the following source distribution:

- 101 neutrons in the centre of sphere (1,1),
- 1 neutron in the centre of each of the other 24 spheres.

100 replicas were to be run, (using different random number sequences) for three numbers of passive cycles (preceding the 1 000 active generations): 0, 200 and 400, leading to a total number of 300 calculations.

Table 5.2 Specification of replica calculations

Case	Random number sequence	Skipped Cycles
1	#1	0
2	#1	200
3	#1	400
4	#2	0
5	#2	200
6	#2	400
...	...	...
298	#100	0
299	#100	200
300	#100	400

Moreover a reference calculation was to be run with adequate source convergence and statistical accuracy.

In addition to identifying information, the participants were asked to submit the information specified in Table 2.3.

For each of the 300 cases

- the final k_{eff} estimate (cumulative over the active cycles, i.e. 1000 active generations) and its standard deviation
- the k_{eff} estimate of each single active cycle (as much values as the number of cycles: 1000 values if the number of generation per cycle is equal to 1, and less if the number of generation per cycle is greater than 1)
- the final fission fractions (cumulative over the active cycles, i.e. 1000 active generations), and their standard deviation, of only 3 spheres:
  - sphere (1,1): where the majority of neutrons are emitted at first generation
  - sphere (3,3): the central sphere
  - sphere (5,5): to compare with the fission fraction of sphere (1,1)
- the results of the convergence tests performed by the code

For the reference calculation

- the description of the calculation (strategy used, number of passive stages, number of active stages, number of generations per stage, number of neutrons per generation...)
- the final k_{eff} estimate and its standard deviation
- the final fission fractions (with their standard deviation) of the 3 spheres: (1,1), (3,3) and (5,5).
- the results of the convergence tests performed by the code

Submission format

In addition to identifying information, the participants were asked to submit the information specified in Table 5.3 for each of the 300 cases. Additional information about the algorithms and methods used in the codes, e.g., survival biasing, was requested.

Table 5.3 Information to report

Line Number	Required information
12	Starting source
13	nskip = number of stages skipped before beginning tallies
14	nstage = number of stages tallied
15	nhist = number of histories per generation
16	ngenst = number of generations per stage
17	final k_{eff} estimate
18	final k_{eff} estimate uncertainty (one standard deviation)
19	individual k_{eff} estimate at first stage
20	individual k_{eff} estimate at second stage (not cumulative)
...	
18+nstage	individual k_{eff} estimate at last stage (not cumulative)
18+nstage+1	final fission fraction of sphere (1,1)
18+nstage+2	standard deviation of final fission fraction of sphere (1,1)
18+nstage+3	final fission fraction of sphere (3,3)
18+nstage+4	standard deviation of final fission fraction of sphere (3,3)
18+nstage+5	final fission fraction of sphere (5,5)
18+nstage+6	standard deviation of final fission fraction of sphere (5,5)
18+nstage+7	results of convergence tests (as many lines as necessary)
...	

Results

Table 5.4 Contributors, codes, and libraries

Group	Contributor	Code	Cross-sections Library
ANL	Roger Blomquist	VIM	ENDF/B-V continuous library
EMS	Dennis Mennerdahl	SCALE-4.4 (CSASI/KENO-V.a)	238-group based on ENDF/B-V continuous library
IPPE	Alexander Blyskavka and Tatiana Ivanova	CONSYST* / SCALE-4.3 (KENO-V.a)	299-group ABBN-93 based on FOND-2.2 continuous library
IRSN	Joachim Miss	MORET 4.A.6	16-group Hansen & Roach
JNC	Nobutoshi Shirai	SCALE-4.4 (CSAS25/KENO-V.a)	27-group based on ENDF/B-IV continuous library
LANL	Robert Little	MCNP4C2	ENDF/B-VI continuous library
ORNL	John Wagner	SCALE-4.4a (CSAS25/KENO-V.a)	238-group based on ENDF/B-V continuous library

* CONSYST is a code for cross-section preparation developed at IPPE [2].

All the contributors used a conventional strategy (no superhistory method, no use of the fission matrix method, and no stratified sampling). All the simulations consisted of 1 000 active cycles (1 generation per cycle) with a variable number of inactive cycles preceding the active cycles. Each contributor ran 100 replicas with 0 inactive cycle, 100 replicas with 200 inactive cycles and 100 replicas with 400 inactive cycles.

Sample input files are grouped in Appendix 5.a. Comments of some of the contributors are grouped in Appendix 5.b.

Review of Codes

The main features of the codes used by the contributors on this specific test are summed up in the Tables 5.5 and 5.6. The options of the codes that were not used are not mentioned.

Table 5.5 Main features of the codes

	KENO	MCNP	MORET	VIM
neutrons can survive absorption	yes neutron weight adjusted at each collision by a non-absorption factor and checked against a weight high value to see if the particle should be split, and against a weight low value (0.333) to see if Russian roulette should be played	yes neutron weight adjusted at each collision by a non-absorption factor and checked against a low value (0.25) to see if Russian roulette should be played	no	no
cycle k_{eff} estimator (1)	source-collision	source-collision	balance-track-length	source-track-length
final k_{eff} estimator (1) (average of cycle k_{eff} estimates)	collision estimator	combination of 3 k_{eff} estimators: source-collision source-track-length source-absorption	general combination [3] of 5 k_{eff} estimators: source (collision, track-length, absorption), balance (collision, track-length) and 2 control variables: neutron balance (1) estimated with collision estimator and track-length estimator	combination of 2 k_{eff} estimators: source-track-length and source-absorption
final fission fraction estimator	collision	track-length	track-length	track-length

Table 5.5 Main features of the codes *(continued)*

	KENO	MCNP	MORET	VIM
final k_{eff} standard deviation estimator		combined estimator uses correlation between different estimators at each cycle	no correlation assumed between cycles	combined estimator uses correlation between different estimators at each cycle
	SCALE-4.3: no batching SCALE-4.4: batch estimate, described by Gelbard and Prael [4], batch size selected to maximum the standard deviation estimate	no batching	no batching	no batching
final fission fraction standard deviation estimator	no correlation assumed	no correlation assumed	no correlation assumed	no correlation assumed
	no batching	no batching	no batching	batching (10 cycles = 1 batch)
convergence tests	data presented for the user to aid in making such a decision	cumulative k_{eff}s printed, as are k_{eff}s when more early generations are skipped	cumulative k_{eff}s printed	cumulative k_{eff}s printed, as are k_{eff}s when more early generations are skipped
	normality of the cycle k_{eff} distribution tested using a chi-square test	comparison of first half and second half means of active cycle k_{eff} normality test	normality of the cycle k_{eff} distribution tested using a chi-square test (for each k_{eff} estimator)	comparison of first half and second half means of active cycle k_{eff} (for each k_{eff} estimator: analog, track length, collision) if difference > 2 sigma, the test is failed
		report of fissionable regions which had no fission sites	report of fissionable regions which had no fission sites	

(1) 2 kinds of keff estimator are used:
– source: keff = fission production / source
– balance: keff = fission production / neutron balance
Neutron balance is defined as (absorption + leakage – excess). Its expected value is the total source weight.

The balance estimators are only used in MORET.

Table 5.6 Source distribution estimation in the different codes

	KENO	MCNP	MORET conventional strategy	VIM
event at which sites are created	collision	collision	collision	absorption
number of sites created	n = INT(Ws(i)+ξ) $W_s(i) = \frac{\upsilon\Sigma_{f_i}}{r_k \cdot \Sigma_{t_i}} W_i$ Wi: neutron weight rk: reduced value of k, constant ξ: random number	n = INT(Ws(i)+ξ) $W_s(i) = \frac{\upsilon\Sigma_{f_i}}{k \cdot \Sigma_{t_i}} W_i$ Wi: neutron weight k: constant ξ: random number	n = 1	n = INT(Ws(i)+ξ) $W_s(i) = \frac{\upsilon\Sigma_{f_i}}{k \cdot \Sigma_{a_i}} W_i$ Wi: neutron weight k: constant ξ: random number
sites weight	1	$W_s(i)/n$	$W_s(i) = \frac{\nu\Sigma_{f_i}}{\Sigma_{t_i}} W_i$ Wi: neutron weight	1
starters number	constant number M0	constant total weight M0	constant total weight M0	constant number M0
starters sampling algorithm	if more than M0 sites, site bank sampled without replacement for M0 starters (sites may be used more than once) if exactly M0 sites, each site used once if less than M0 sites, all sites used, and starters randomly sampled without replacement to get the rest of the starters	all the sites are used	respects the proportion PV of fission in each volume V $P_v = \frac{\sum_{\text{collisions in V}} W_s(i)}{\sum_{\text{all collisisons}} W_s(i)} M_0$ $M_V = \text{NINT}(P_V)$ MV starters in volume V sampled from the sites in volume V, the probability to pick a site is proportional to its weight (sites may be used more than once)	if more than M0 sites, site bank sampled without replacement for M0 starters (sites may be used more than once) if exactly M0 sites, each site used once if less than M0 sites, all sites used, and starters randomly sampled without replacement to get the rest of the starters
starters weight	1	$\frac{W_s(i)/n}{\sum_{\text{sites}} W_s(i)/n} M_0$	if MV differs from 0, all starters in volume V have the weight $\frac{P_V}{M_V}$ the weights of all starters are multiplied by the same correction factor so that the total weight of all starters is equal to M0	1

Reference calculations

Each contributor submitted a reference calculation. The two following tables give their main characteristics and the results obtained: final k_{eff} and fission fractions.

Table 5.7 Characteristics of the reference calculations

Contributor	Cycles	Histories per cycle	Skipped cycles	Active histories	Initial source
ANL / VIM	6,000	20,000	1,000	100 million	uniform inside the spheres
EMS / KENO	11,000	10,000	1,000	100 million	flat source distributed over all fissile material
IPPE / KENO	11,000	10,000	1,000	100 million	all neutrons in the center of the central sphere
IRSN / MORET	11,000	10,000	1,000	100 million	93% neutrons are started uniformly in the sphere (3,3)
JNC / KENO	11,000	10,000	1,000	100 million	91% neutrons are started uniformly in the sphere (3,3).
LANL / MCNP	6,000	10,000	1,000	50 million	equal in each of the 25 spheres
ORNL / KENO	11,000	10,000	1,000	100 million	starting points chosen according to a cosine distribution throughout the problem; points that are not in fissile material are discarded. KENO option NST=1 (start type 1)

Table 5.8 Reference k_{eff} and fission fractions

Contributor	Reference k_{eff}	Reference Fission Factions		
		Sphere (1,1)	Sphere (3,3)	Sphere (5,5)
ANL / VIM	1.11370 ± 0.00008	1.01.10-4 ± 3.10-5	0.90851 ± 4.10-4	1.01.10-4 ± 3.10-5
EMS / KENO	1.11234 ± 0.00009	2.60.10-4 ± 3.85.10-6	0.90904 ± 9.09.10-5	2.50.10-4 ± 3.63.10-6
IPPE / KENO	1.11287 ± 0.00008	2.39.10-4 ± 3.58.10-6	0.91116 ± 9.11.10-5	2.36.10-4 ± 3.64.10-6
IRSN / MORET	1.11362 ± 0.00008	2.31.10-4 ± 4.10-6	0.90985 ± 1.16.10-4	2.31.10-4 ± 4.10-6
JNC / KENO	1.12172 ± 0.00009	2.58.10-4 ± 2.03.10-6	0.90874 ± 1.13.10-4	2.55.10-4 ± 2.09.10-6
LANL / MCNP	1.11294 ± 0.00009	2.54.10-4 ±	0.91062 ±	2.54.10-4 ±
ORNL / KENO	1.11242 ± 0.00009	2.51.10-4 ± 3.72.10-6	0.90815 ± 9.08.10-5	2.51.10-4 ± 3.55.10-6

Analysis of the final values of k_{eff} and fission fraction of the central sphere

Final k_{eff}

For each contribution, the 100 final k_{eff} values and their standard deviations, obtained with 0, 200, 400 inactive cycles, are plotted in the figures grouped in 5.c.

Table 5.9 to Table 5.15 give the dispersion of the final k_{eff} values and of their standard deviations, as they are computed by the codes.

- min: minimum value of the 100 final k_{eff} values and of their standard deviations,
- mean: mean value of the 100 final k_{eff} values and of their standard deviations,
- median: median value of the 100 final k_{eff} values and of their standard deviations,
- max: maximal value of the 100 final k_{eff} values and of their standard deviations.

Table 5.9 Final k_{eff} – ANL / VIM

	0 inactive cycle		200 inactive cycles		400 inactive cycles	
	k_{eff}	std	k_{eff}	std	k_{eff}	std
min	1.02769	0.00207	1.05096	0.00208	1.07347	0.00209
mean	1.09369	0.00248	1.10686	0.00228	1.11112	0.00223
median	1.09952	0.00248	1.11133	0.00224	1.11223	0.00221
max	1.11513	0.00284	1.12046	0.00273	1.11937	0.00271

Table 5.10 Final k_{eff} – EMS / KENO (SCALE-4.4)

	0 inactive cycle		200 inactive cycles		400 inactive cycles	
	k_{eff}	std	k_{eff}	std	k_{eff}	std
min	1.04589	0.00263	1.06472	0.00234	1.08410	0.00223
mean	1.09283	0.00548	1.10605	0.00362	1.10993	0.00307
median	1.09714	0.00566	1.11049	0.00291	1.11106	0.00285
max	1.11458	0.00842	1.11768	0.00782	1.11805	0.00702

Table 5.11 Final k_{eff} – IPPE / KENO (SCALE-4.3)

	0 inactive cycle		200 inactive cycles		400 inactive cycles	
	k_{eff}	std	k_{eff}	std	k_{eff}	std
min	1.03284	0.00210	1.05521	0.00207	1.07466	0.00205
mean	1.09209	0.00247	1.10543	0.00228	1.10994	0.00221
median	1.09733	0.00244	1.10985	0.00222	1.11081	0.00218
max	1.11299	0.00287	1.11692	0.00284	1.11974	0.00273

Table 5.12 Final k_{eff} – IRSN / MORET

	0 inactive cycle		200 inactive cycles		400 inactive cycles	
	k_{eff}	std	k_{eff}	std	k_{eff}	std
min	1.03042	0.00208	1.05380	0.00201	1.07712	0.00199
mean	1.09197	0.00242	1.10641	0.00222	1.11167	0.00215
median	1.09731	0.00241	1.11089	0.00216	1.11292	0.00213
max	1.11185	0.00275	1.11766	0.00281	1.11851	0.00267

Table 5.13 Final k_{eff} – JNC / KENO (SCALE-4.4)

	0 inactive cycle		200 inactive cycles		400 inactive cycles	
	k_{eff}	std	k_{eff}	std	k_{eff}	std
min	1.02354	0.00265	1.04658	0.00239	1.06878	0.00236
mean	1.10139	0.00553	1.11539	0.00353	1.11910	0.00305
median	1.10384	0.00585	1.11898	0.00294	1.12034	0.00285
max	1.12338	0.00870	1.12608	0.00789	1.12679	0.00798

Table 5.14 Final k_{eff} – LANL / MCNP

	0 inactive cycle		200 inactive cycles		400 inactive cycles	
	k_{eff}	std	k_{eff}	std	k_{eff}	std
min	1.05756	0.00186	1.07862	0.00179	1.09798	0.00177
mean	1.09302	0.00219	1.10615	0.00197	1.11087	0.00188
median	1.09742	0.00217	1.10946	0.00190	1.11101	0.00187
max	1.11484	0.00259	1.11667	0.00248	1.11779	0.00208

Table 5.15 Final k_{eff} – ORNL / KENO (SCALE-4.4a)

	0 inactive cycle		200 inactive cycles		400 inactive cycles	
	k_{eff}	std	k_{eff}	std	k_{eff}	std
min	1.04362	0.00283	1.06553	0.00246	1.08819	0.00238
mean	1.09227	0.00561	1.10589	0.00361	1.11018	0.00288
median	1.09587	0.00572	1.10874	0.00293	1.11072	0.00277
max	1.11259	0.00820	1.11504	0.00794	1.11665	0.00673

Observations

Since all the minimum k_{eff} values obtained are greater than 1.007, which is approximately the k_{eff} of the system without the central sphere, no wrong convergence was obtained, i.e. the central sphere was always sampled, i.e. in the conditions of calculation (125 neutrons per cycle), the central sphere never stayed unvisited during the first 1 000 cycles.

If more replicas had been run, maybe some of them would have been unconverged.

The final k_{eff} values are biased (underestimated) only due to the presence of an initial transient during which the distribution of sources is not converged (the most reactive sphere is under-sampled).

As expected, the greater the number of inactive cycles (i.e. the smaller the size of transient in the active cycles):

- the greater the final k_{eff} values (since the k_{eff} is initially underestimated),
- the lower the standard deviation values.

The three minimum final k_{eff} values obtained with MCNP (1.05756, 1.07862, 1.09798) are systematically higher than those obtained with the three other codes: KENO, MORET, VIM, whatever

the number of inactive cycles is. The origin of such a difference should be investigated.

As far as standard deviations are concerned, the results can be grouped into three categories, from the lowest to the highest values:

1) MCNP,

2) MORET, VIM, KENO (SCALE-4.3),

3) KENO (SCALE-4.4).

Two reasons can explain the fact that the standard deviations estimated with KENO (SCALE-4.4) are higher than with the three other codes:

1) Contrarily to the three other codes, KENO in the version 4.4 of SCALE takes into account correlations between cycles. The standard deviation of k_{eff} is computed using a batched estimate[5] in which the batch size is automatically determined by the code to maximum the standard deviation estimate.

2) Contrarily to the three other codes, KENO does not compute combinations of several k_{eff} estimators (three in MCNP, five in MORET, two in VIM). Moreover, the collision estimator used by KENO is not the better one for test 4.

The difference between MCNP and the 2 other codes MORET and VIM should be investigated.

Table 5.16 compares the external standard deviations (defined below) and the ratios of the external standard deviation over the mean value of the 100 standard deviations. The external standard deviation ("external std" in the table) of final k_{eff} is calculated from the observed scatter of the population of replica final k_{eff}, i.e. the standard deviation of 100 final k_{eff} values.

The ratio of the external standard deviation over the mean value of the 100 standard deviations ("external std mean std" in the table) gives some indication of the Monte Carlo underestimation of the individual eigenvalue uncertainties. The theoretical value of this ratio is 1 if the cycle k_{eff} series are stationary and if the standard deviations of the individual final k_{eff} are correctly estimated. When the two conditions are fulfilled, the internal standard deviation of a single calculation reflects perfectly the external standard deviation (i.e. the scatter) of a set of replicas.

This is precisely what we can observe in Table 5.16:

1) The ratio "external standard deviation over mean standard deviation" is all the lower when as the number of inactive cycles is higher.

2) The ratio tends to be smaller with the three contributions based on KENO of SCALE-4.4 which uses a better estimator of the final k_{eff} standard deviation than the conventional estimator assuming no correlation between cycles.

Table 5.16 External standard deviation of Final k_{eff} and comparison with the mean standard deviation

	0 inactive cycle		200 inactive cycles		400 inactive cycles	
	external std	external std / mean std	external std	external std / mean std	external std	external std / mean std
ANL / VIM	0.01701	6.87117	0.01212	5.30638	0.00644	2.89195
EMS / KENO	0.01616	2.94974	0.01157	3.19802	0.00574	1.87304
IPPE / KENO	0.01800	7.28093	0.01299	5.70187	0.00725	3.27686
IRSN / MORET	0.01660	6.85847	0.01181	5.31800	0.00609	2.82804
JNC / KENO	0.01676	3.03301	0.01241	3.51017	0.00748	2.45214
LANL / MCNP	0.01423	6.49581	0.00909	4.61621	0.00317	1.68318
ORNL / KENO	0.01454	2.59084	0.00919	2.54503	0.00399	1.38408

The external standard deviation is reduced as the number of inactive cycles is increased. The dispersion of the results decreases due to the elimination of part of the transient in the active cycles.

The external standard deviation values can be grouped into two categories, from the lowest to the highest:

1) MCNP, KENO (SCALE-4.4a: ORNL),

2) KENO (SCALE-4.4: EMS, JNC), MORET, VIM, KENO (SCALE-4.3: IPPE).

The three external standard deviations of final k_{eff} values obtained with MCNP are systematically lower than with the three other codes: KENO, MORET, VIM, whatever the number of inactive cycles is.

This observation is probably linked to the fact that the three minimum final k_{eff} values obtained with MCNP are systematically higher than with the three other codes.

The various observations concerning the results obtained with MCNP highlight the smallest dispersion. A plausible explanation is the fact that neutrons can survive absorption in MCNP tending to decrease the variance per history. It should be noticed that KENO has the same feature as MCNP (but the default threshold of the Russian roulette is 0.333 in KENO as compared to 0.25 in MCNP) whereas in MORET and VIM, neutrons do not survive absorption

Surprisingly, the scatter of the results obtained by the four users of KENO is not the same. It should be noted that the scatter of the results obtained by ORNL tends to be significantly lower.

The four users of KENO did not use the same cross-sections library or the same code for the cross-sections preparation (different versions of CSAS or CONSYST for IPPE) but is it the only origin of that difference? Generally they used the same options (in particular the same threshold of the Russian roulette), with the exception that IPPE and ORNL used P5, as compared to P3 for EMS, and with the exception that IPPE used the version 4.3 of SCALE in which the batching was not available.

The most appropriate comparison is between EMS (SCALE-4.4 with 238-group library) and ORNL (SCALE-4.4a with 238-group library). The others used considerably different cross-section libraries, the effects of which are difficult to comment on. With regard to the differences between EMS and ORNL results, the differences could be due to a variety of changes between SCALE-4.4 and

SCALE-4.4a, most likely related to the cross-section/material processing routines, for example changes in NITAWL, the cross-section library, or the Standard Composition Library. No significant changes were made to KENO V.a between SCALE-4.4 and SCALE-4.4a.

The potential for differences due to P_3 (EMS) and P_5 (ORNL) scattering treatment (both using discrete angle scattering) has been investigated. New results based on P_3 still obtained with SCALE 4.4a have been submitted by ORNL and analyzed (Tables 5.17 and 5.18). The scatter of these results is more important than with P_5 and is closer to the scatter of the other contributions obtained with SCALE. A further study should be carried out to provide an explanation to this point.

Table 5.17 Final k_{eff} – ORNL / KENO (SCALE-4.4a) – Submission based on P3

	0 inactive cycle		200 inactive cycles		400 inactive cycles	
	k_{eff}	std	k_{eff}	std	k_{eff}	std
min	1.01716	0.00285	1.04145	0.00238	1.06409	0.00237
mean	1.09176	0.00561	1.10567	0.00360	1.10945	0.00307
median	1.09683	0.00557	1.11002	0.00295	1.11087	0.00286
max	1.11303	0.00860	1.11777	0.00843	1.11803	0.00843

Table 5.18 External standard deviation of Final k_{eff} and comparison with the mean standard deviation ORNL / KENO (SCALE-4.4a) – Submission based on P3

	0 inactive cycle		200 inactive cycles		400 inactive cycles	
	external std	external std / mean std	external std	external std / mean std	external std	external std / mean std
ORNL / KENO	0.01789	3.18841	0.01330	3.69509	0.00770	2.50557

Final Fission Fraction of the Central Sphere

For each contribution, the 100 final fission fractions values of the central sphere and their standard deviations, obtained with 0, 200, 400 inactive cycles, are plotted in the figures of 5.d.

Tables 5.19 to 5.25 give the dispersion of the final fission fractions values of the central sphere and of their standard deviations, as they are computed by the codes, when this information is available.

- min: minimum value of the 100 final fission fractions values of the central sphere and of their standard deviations,
- mean: mean value of the 100 final fission fractions values of the central sphere and of their standard deviations,
- median: median value of the 100 final fission fractions values of the central sphere and of their standard deviations,
- max: maximal value of the 100 final fission fractions values of the central sphere and of their standard deviations.

Table 5.19 Final fission fraction of central sphere (ffcs) – ANL / VIM

	0 inactive cycle		200 inactive cycles		400 inactive cycles	
	f.f.c.s.	std	f.f.c.s.	std	f.f.c.s.	std
min	0.23562	0.01213	0.42061	0.00479	0.59765	0.00422
mean	0.75224	0.03040	0.85959	0.01446	0.89322	0.00909
median	0.79435	0.03118	0.89608	0.00799	0.90327	0.00725
max	0.89897	0.04737	0.92608	0.04711	0.92865	0.04476

Table 5.20 Final fission fraction of central sphere – EMS / KENO

	0 inactive cycle		200 inactive cycles		400 inactive cycles	
	f.f.c.s.	std	f.f.c.s.	std	f.f.c.s.	std
min	0.34505	0.00416	0.52477	0.00248	0.70269	0.00240
mean	0.75607	0.00977	0.86243	0.00490	0.89371	0.00351
median	0.78411	0.01024	0.89596	0.00313	0.90410	0.00297
max	0.89544	0.01503	0.92448	0.01453	0.92657	0.01232

Table 5.21 Final fission fraction of central sphere – IPPE / KENO

	0 inactive cycle		200 inactive cycles		400 inactive cycles	
	f.f.c.s.	std	f.f.c.s.	std	f.f.c.s.	std
min	0.25534	0.00354	0.44190	0.00249	0.61759	0.00248
mean	0.75368	0.00980	0.85950	0.00517	0.89359	0.00358
median	0.79526	0.00971	0.89837	0.00306	0.90452	0.00294
max	0.90829	0.01576	0.92321	0.01507	0.92592	0.01402

Table 5.22 Final fission fraction of central sphere – IRSN / MORET

	0 inactive cycle		200 inactive cycles		400 inactive cycles	
	f.f.c.s.	std	f.f.c.s.	std	f.f.c.s.	std
min	0.23630	0.00390	0.42070	0.00150	0.60480	0.00150
mean	0.73365	0.01009	0.85959	0.00482	0.90227	0.00276
median	0.78155	0.00975	0.90500	0.00245	0.91435	0.00215
max	0.90220	0.01440	0.93190	0.01390	0.93490	0.01320

Table 5.23 Final fission fraction of central sphere – JNC / KENO

	0 inactive cycle		200 inactive cycles		400 inactive cycles	
	f.f.c.s.	std	f.f.c.s.	std	f.f.c.s.	std
min	0.10734	0.00336	0.29248	0.00310	0.47479	0.00308
mean	0.75325	0.00486	0.86560	0.00361	0.89214	0.00332
median	0.77401	0.00507	0.89926	0.00321	0.90146	0.00320
max	0.90383	0.00636	0.92688	0.00609	0.92191	0.00617

Table 5.24 Final fission fraction of central sphere – LANL / MCNP

	0 inactive cycle		200 inactive cycles		400 inactive cycles	
	f.f.c.s.	**std**	**f.f.c.s.**	**std**	**f.f.c.s.**	**std**
min	0.48820	not available	0.66148	not available	0.82961	not available
mean	0.75212	not available	0.86642	not available	0.90157	not available
median	0.78086	not available	0.89542	not available	0.90493	not available
max	0.90206	not available	0.93093	not available	0.93243	not available

Table 5.25 Final fission fraction of central sphere – ORNL / KENO

	0 inactive cycle		200 inactive cycles		400 inactive cycles	
	f.f.c.s.	**std**	**f.f.c.s.**	**std**	**f.f.c.s.**	**std**
min	0.37848	0.00440	0.56224	0.00230	0.73716	0.00240
mean	0.75460	0.00985	0.86327	0.00511	0.89728	0.00324
median	0.78439	0.01010	0.89152	0.00331	0.90295	0.00293
max	0.89755	0.01491	0.92140	0.01456	0.92239	0.01179

Observations

The review of the minimum fission fraction values of central sphere leads to the same conclusion as the review of the final k_{eff} values: the central sphere never stayed unsampled during the first 1 000 cycles. The final fission fraction values are underestimated only due to the presence of an initial transient during which the most reactive sphere is under-sampled.

As expected, the greater the number of inactive cycles (i.e. the smaller the portion of the transient remaining in the active cycles):

- the greater the final fission fraction values in central sphere,
- the lower the standard deviation values.

The three minimum final fission fraction values of the central sphere obtained with MCNP (0.48820, 0.66148, 0.82961) are systematically higher than with the three other codes: KENO, MORET, VIM, whatever the number of inactive cycles is. The origin of such a difference should be investigated.

As far as standard deviations are concerned, the results can be grouped into two categories, from the lowest to the highest values:

1) KENO, MORET,

2) VIM.

MCNP standard deviations of final fission fractions were not reported.

In KENO and MORET, the standard deviation of fission fraction is computed assuming no correlation between cycles. In VIM, no correlation is assumed but the cycle fission fractions are batched into batches of 10 generations, giving more reliable estimations of the uncertainty. Table 5.26

compares the external standard deviations and the ratios of the external standard deviation to the mean value of the 100 standard deviations.

- external std: external standard deviation, i.e. standard deviation of the 100 final fission fraction values of the central sphere,

- external std / mean std: ratio of the external standard deviation over the mean value of the 100 standard deviations.

Table 5.26 External standard deviation of Final fission fraction of central sphere and comparison with the mean standard deviation

	0 inactive cycle		200 inactive cycles		400 inactive cycles	
	external std	external std / mean std	external std	external std / mean std	external std	external std / mean std
ANL / VIM	0.13080	4.30256	0.09074	6.27639	0.04355	4.78877
EMS / KENO	0.12586	12.88185	0.08685	17.71504	0.03921	11.17409
IPPE / KENO	0.13823	14.10121	0.09572	18.50083	0.04936	13.79466
IRSN / MORET	0.13777	13.65097	0.09955	20.63692	0.04892	17.75590
JNC / KENO	0.13434	27.62283	0.09846	27.30115	0.05746	17.29368
LANL / MCNP	0.11002	not available	0.06666	not available	0.01658	not available
ORNL / KENO	0.11231	11.39884	0.06787	13.28925	0.02535	7.83212

The external standard deviation is reduced as the number of inactive cycles is increased due to the reduction of the length of the transient in the active cycles. The external standard deviation values can be grouped into two categories, from the lowest to the highest:

1) MCNP, KENO (SCALE-4.4a: ORNL),

2) KENO (SCALE-4.4: EMS, JNC), KENO (SCALE-4.3: IPPE), VIM, MORET.

The three external standard deviations of final fission fraction values of the central sphere obtained with MCNP are systematically lower than with the three other codes: KENO, MORET, VIM, whatever the number of inactive cycles is. This observation is probably related to the fact that the three minimum final fission fraction values of the central sphere obtained with MCNP are systematically higher (more converged) than with the three other codes.

As for the final k_{eff} values, the various observations obtained with MCNP display the smallest dispersion. A plausible explanation is the fact that neutrons can survive absorption in MCNP tending to decrease the variance per history. KENO has the same feature but the default threshold of the Russian roulette is 0.333 in KENO as compared to 0.25 in MCNP.

Despite the fact that neutrons do not survive absorption in MORET and VIM, the scatter of the results obtained with both those codes is of the same order than with KENO of the versions 4.3 and 4.4 of SCALE. (It should be noted that the scatter of the results obtained by ORNL with KENO of SCALE-4.4a tends to be significantly lower but an additional analysis shows that this difference could be due to the anisotropic scattering treatment). This may imply that another factor causes the smaller scatter of results obtained with MCNP. It may also be that in MCNP all fission sites obtained during a cycle are used as starters of the following cycle.

The values of the ratio “external standard deviation over mean standard deviation” are much higher than for the final k_{eff} and are very far from the theoretical value of 1. This can be explained by the fact that the dispersion due to the presence of the transient is larger for the fission fractions of the central sphere than for the k_{eff}: during the transient, k_{eff} varies from around 1.0 to around 1.1 whereas fission fraction of central sphere varies from around 0.0 to around 0.9. The batching used in VIM for the estimation of the standard deviation of fission fractions tends to decrease the value of the ratio. Nevertheless this ratio is still much larger than 1. This may imply two things:

1) the size of the batches (10) is not sufficient to eliminate the correlations between the batches,

2) the transient in the cycle fission fraction series is still significant even with 400 inactive cycles (the duration of the transient varies widely from replica to replica, the fission source nearly converged after as few as 50 generations, or as many as 950 generations).

Conclusion

This test problem provides a rather difficult situation where the number of neutrons per generation was kept quite small (125 neutrons), the initial source was intentionally chosen to concentrate on less reactive units, and the coupling between the units is low. Despite that, the calculations made with a variety of codes and hundred replicas did not exhibit a single situation where the central, most reactive sphere remained undersampled during more than 1 000 cycles. Of course, if more replicas had been run, or if less than 1 000 active cycles had been run, some replicas would probably have failed in this way. Nevertheless this observation suggests that the convergence property of Monte Carlo powering algorithm leads to a source distribution close enough to the true solution to avoid the risk of large under-estimation. If a sufficient number of cycles is run, the main problem seems to be more in the detection of this convergence and the possibility to use reliable algorithms to truncate the transient.

The final values of k_{eff} and fission fraction of central sphere are underestimated only due to the presence in the active cycles of an initial transient during which the distribution of sources is not converged (the most reactive sphere is under-sampled). The greater the number of inactive cycles (i.e. the smaller the size of transient in the active cycles):

- the greater the final values of k_{eff} and fission fraction of central sphere,
- the lower the standard deviation values.

400 inactive cycles are generally insufficient for the configuration studied in this test, especially so for the bad initial source guess. The effect of the transient is still visible when observing the ratio "external standard deviation over mean standard deviation" of the fission fraction of central sphere.

The results obtained with MCNP highlight the smallest dispersion of the final values of k_{eff} and fission fraction of central sphere. A plausible explanation, but maybe not the only one, is the fact that neutrons can survive absorption in MCNP as in KENO. The threshold of the Russian roulette is 0.25 in MCNP and 0.333 in KENO. As a consequence the histories of neutrons are longer in MCNP than in KENO and histories in KENO are longer than in VIM or MORET since neutrons do not survive absorption in those two codes. Nevertheless, the dispersions of the results differ according to the user of KENO. It should be noted that the scatter of the results obtained by ORNL tends to be significantly lower but an additional analysis has shown that this difference could be due not only to different cross-sections libraries but also, in a great part, to the anisotropic scattering treatment. Further investigation is needed to explain the origins of the differences. Another plausible explanation to investigate is the

fact that in MCNP all fission sites obtained during a cycle are used as starters of the following cycle. In fact, a great variety of parameters (like the anisotropic scattering treatment) should be studied independently to identify their impact on the dispersion of the results.

Finally, more reliable estimations of uncertainties are obtained when correlations between generations are taken into account in the calculation of k_{eff} standard deviation. In this respect, the methods implemented in KENO (automated, batched estimate) and VIM (batching method) lead to improved results compared to the standard method where inter-generation correlation are ignored.

Analysis of the cycle k_{eff} series

In the previous section, it was observed that, if a sufficient number of cycles are run, sources converge to the correct distribution. In this case, the main problem is to remove the initialization bias. One method would be to detect when the cycle fission fractions series become stationary, but we do not normally have cycle-by-cycle estimates of the fission fractions. Nevertheless, the utility of test problem 4 is in the fact that k_{eff} is very sensitive to the source distribution.

The main analysis has been focused on the cycle k_{eff} series provided by each contributor. An algorithm has been used to automatically suppress the transient in each cycle k_{eff} series. It should be recalled that the cycle k_{eff} estimator considered differs form one code to another:

- KENO: source-collision,
- MCNP: source-collision,
- MORET: balance-track-length,
- VIM: source-track-length.

Refer to the Specifications/Required Information about Codes (above).

As the test problem 4 configuration includes unmoderated and unreflected fissionable material, the mean free path of neutrons is large compared to the sphere dimensions and as a consequence the average number of collisions is very low. To get acceptable statistics the collision estimators require more neutron histories than the track-lengths estimators. This is why, in the framework of this test, the track-length k_{eff} estimator is the best one, i.e. its uncertainties tend to be the lowest, all other things being equal. In contrast, the uncertainties of the collision estimators tend to be the highest. In addition, "balance" estimators usually have lower uncertainties than "source" estimators, all other things being equal.

Automatic transient suppression

Stationarity detection test

As illustrated in Appendix 5.e, many tests can be performed to determine if the cycle k_{eff} series is stationary [6]. We have used an association of the modified Schruben test and of the Vassilacopoulos test, designed for the detection of negative transients (initial underestimation of the k_{eff}), both described in Appendix 5.e. The stationarity assumption is rejected if it is rejected by one of the two tests. The level of significance of the modified Schruben test is α = 5%. The level of significance of the Vassilacopoulos test is α = 2.5%. Table 5.27 gives the percentage of replicas non-stationary using this combination of tests.

Table 5.27 Percentage of replicas non-stationary using a combination of the modified Schruben test and of the Vassilacopoulos test

	0 inactive cycle	200 inactive cycles	400 inactive cycles
ANL / VIM	87	38	19
EMS / KENO	91	38	19
IPPE / KENO	97	36	19
IRSN / MORET	98	47	24
JNC / KENO	90	38	20
LANL / MCNP	94	43	11
ORNL / KENO	96	44	17

Principle of automatic transient suppression [7]

The stationary detection test is first applied on the whole cycle k_{eff} series. If the stationarity is not detected then a fixed number of cycles is removed from the beginning of the series. We have chosen cutting 5% of the initial length of the series, i.e. 50 cycles. Then, the stationary detection test is performed on the new series (computation of the statistic, of the p-value, comparison with the level of significance). The tests and truncations are performed until stationarity detection.

See the tables in Appendix 5.f for the number of active cycles removed until detection of stationarity for the 300 replicas provided by each contributor (100 with 0 inactive cycle, 100 with 200 inactive cycle, 100 with 400 inactive cycle).

Standard deviation calculation

For each cycle k_{eff} series provided by each contributor, the same method is applied to compute the standard deviation of the final k_{eff} after suppression of the transient. The method used is a modification of the method presented by Ueki et al. [8]. For details, refer to Appendix 5.g.

Final k_{eff} after automatic suppression of transient active cycles

For each contribution, the 100 final k_{eff} values and their standard deviations, obtained with 0, 200, 400 inactive cycles, are plotted in the figures grouped in Appendix 5.h. Tables 5.28 to 5.34 give the dispersion of the final k_{eff} values and of their standard deviations after the application of the automatic suppression of transient active cycles. This time, for all the replicas of each contribution, the standard deviations are recomputed with the same method.

- min: minimum value of the 100 final k_{eff} values and of their standard deviations,
- mean: mean value of the 100 final k_{eff} values and of their standard deviations,
- median: median value of the 100 final k_{eff} values and of their standard deviations,
- max: maximal value of the 100 final k_{eff} values and of their standard deviations.

The scatter of final k_{eff} values after the automatic suppression of transient active cycles, as illustrated by the figures and tables, allows to note the powerfulness of the automatic suppression of transient.

Table 5.28 Final k_{eff} after automatic suppression of transient active cycles – ANL / VIM

	0 inactive cycle		200 inactive cycles		400 inactive cycles	
	k_{eff}	std	k_{eff}	std	k_{eff}	std
min	1.09909	0.00280	1.10280	0.00254	1.10428	0.00253
mean	1.11176	0.00381	1.11231	0.00342	1.11250	0.00327
median	1.11206	0.00376	1.11247	0.00339	1.11256	0.00323
max	1.12527	0.00748	1.12259	0.00505	1.12072	0.00434

Table 5.29 Final k_{eff} after automatic suppression of transient active cycles – EMS / KENO

	0 inactive cycle		200 inactive cycles		400 inactive cycles	
	k_{eff}	std	k_{eff}	std	k_{eff}	std
min	1.10103	0.00219	1.10182	0.00209	1.10048	0.00207
mean	1.11085	0.00313	1.11122	0.00287	1.11152	0.00278
median	1.11094	0.00299	1.11139	0.00281	1.11166	0.00271
max	1.11898	0.00739	1.12246	0.00512	1.11986	0.00501

Table 5.30 Final k_{eff} after automatic suppression of transient active cycles – IPPE / KENO

	0 inactive cycle		200 inactive cycles		400 inactive cycles	
	k_{eff}	std	k_{eff}	std	k_{eff}	std
min	1.10365	0.00220	1.10418	0.00206	1.10486	0.00194
mean	1.11173	0.00314	1.11182	0.00281	1.11190	0.00269
median	1.11162	0.00306	1.11156	0.00276	1.11192	0.00265
max	1.12159	0.00603	1.12289	0.00430	1.12265	0.00361

Table 5.31 Final k_{eff} after automatic suppression of transient active cycles – IRSN / MORET

	0 inactive cycle		200 inactive cycles		400 inactive cycles	
	k_{eff}	std	k_{eff}	std	k_{eff}	std
min	1.10536	0.00207	1.10693	0.00202	1.10713	0.00214
mean	1.11314	0.00333	1.11337	0.00295	1.11387	0.00292
median	1.11355	0.00317	1.11297	0.00282	1.11379	0.00285
max	1.12398	0.00651	1.12456	0.00642	1.13696	0.00675

Table 5.32 Final k_{eff} after automatic suppression of transient active cycles – JNC / KENO

	0 inactive cycle		200 inactive cycles		400 inactive cycles	
	k_{eff}	std	k_{eff}	std	k_{eff}	std
min	1.10576	0.00227	1.11323	0.00201	1.11342	0.00209
mean	1.12035	0.00331	1.12109	0.00288	1.12101	0.00275
median	1.12024	0.00300	1.12098	0.00271	1.12126	0.00269
max	1.13032	0.01520	1.13834	0.00768	1.13002	0.00604

Table 5.33 Final k_{eff} after automatic suppression of transient active cycles – LANL / MCNP

	0 inactive cycle		200 inactive cycles		400 inactive cycles	
	k_{eff}	std	k_{eff}	std	k_{eff}	std
min	1.09930	0.00237	1.10191	0.00219	1.10157	0.00214
mean	1.11141	0.00330	1.11150	0.00291	1.11146	0.00278
median	1.11119	0.00321	1.11118	0.00287	1.11112	0.00279
max	1.12709	0.00570	1.12244	0.00504	1.11759	0.00388

Table 5.34 Final k_{eff} after automatic suppression of transient active cycles – ORNL / KENO

	0 inactive cycle		200 inactive cycles		400 inactive cycles	
	k_{eff}	std	k_{eff}	std	k_{eff}	std
min	1.10262	0.00232	1.10373	0.00221	1.10492	0.00208
mean	1.11091	0.00315	1.11052	0.00280	1.11116	0.00274
median	1.11091	0.00300	1.11014	0.00272	1.11094	0.00265
max	1.12550	0.00774	1.11685	0.00390	1.12150	0.00584

Table 5.35 compares the external standard deviations and the ratios of the external standard deviation over the mean value of the 100 standard deviations, after automatic suppression of transient active cycles:

- external std: external standard deviation, i.e. standard deviation of the 100 final k_{eff} values,
- external std / mean std: ratio of the external standard deviation over the mean value of the 100 standard deviations.

Table 5.35 External standard deviation of Final k_{eff} and comparison with the mean standard deviation after automatic suppression of transient active cycles

	0 inactive cycle		200 inactive cycles		400 inactive cycles	
	external std	external std / mean std	external std	external std / mean std	external std	external std / mean std
ANL / VIM	0.00474	1.24395	0.00410	1.19708	0.00388	1.18821
EMS / KENO	0.00350	1.11988	0.00349	1.21506	0.00345	1.23948
IPPE / KENO	0.00351	1.11744	0.00316	1.12235	0.00296	1.09806
IRSN / MORET	0.00371	1.11373	0.00332	1.12779	0.00364	1.24689
JNC / KENO	0.00388	1.17451	0.00376	1.30360	0.00318	1.15472
LANL / MCNP	0.00426	1.29241	0.00329	1.12904	0.00289	1.03911
ORNL / KENO	0.00402	1.27407	0.00309	1.10487	0.00297	1.08538

Table 5.35 should be compared with Table 5.16, corresponding to the final k_{eff} and their standard deviation provided by the contributors, as they were computed by the codes. This time, the ratios "external standard deviation over the mean standard deviation" are closer to 1. This comes from:

- the suppression of transient,
- the improved calculation of the final k_{eff} standard deviations taking into account correlations.

Other statistical tests performed

In this section, two commonly used statistical tests are tried with the cycle k_{eff} series provided by the contributors, before and after the automatic suppression of the transient active cycles.

These two tests are not necessarily implemented in the same way here as in the codes.

Cycle values normally distributed

In the MORET code, the cycle k_{eff} values are divided into 12 bins based on the mean value *mu* and the standard deviation *sigma* of the entire cycle k_{eff} series:

- 10 bins of width *sigma* between *mu* – 2.5 *sigma* and *mu* + 2.5 *sigma*,
- 1 bin between 0 and *mu* – 2.5 *sigma*,
- 1 bin between *mu* + 2.5 *sigma* and infinity.

We observe that such a definition of bins does not allow an efficient detection of transients. Most of the replicas obtained with MORET passed the normality test. Two main reasons can be proposed:

- firstly, *mu* and *sigma* are computed on the basis of the whole series; they can be strongly biased by the presence of a transient,
- secondly, there are too many bins near the center and not enough bins in the tails of the distribution.

This is why we have chosen here to divide the cycle k_{eff} values of the whole series into 12 bins based on the mean value *mu* and the standard deviation *sigma* of the cycle k_{eff} values of the second half of the cycle k_{eff} series:

- 10 bins of width *sigma* between *mu* – 5 *sigma* and *mu* + 5 *sigma*,
- 1 bin between 0 and *mu* – 5 *sigma*,
- 1 bin between *mu* + 5 *sigma* and infinity.

This time, *mu* and *sigma* are less affected by the presence of a transient and the number of bins in the tails is more important. This choice may be not pertinent because the expected frequency of the extreme bins is too low: the normality hypothesis may be rejected too frequently.

The observed frequencies of the 12 bins are compared with the expected frequencies of the 12 bins in the case of the normal law N(0,1), using the statistic:

$$d^2 = \sum_{i=1}^{12} \frac{(f_o(i) - f_e(i))^2}{f_e(i)}$$

If the cycle values are normally distributed, the statistic d^2 tends to be distributed as a chi-square.

In the test implemented in the MORET code, the number of degrees of freedom is 9 because there are 12 bins, in which a fixed number of values are divided, and 2 parameters are estimated: the sample mean and the sample standard deviation.

In the test proposed here, the number of degrees of freedom is difficult to determine because the 2 estimated parameters *mu* and *sigma* are not based on the whole sample. The real degree of freedom is probably between 9 and 11. We have chosen the value 11 which leads to rejection less often than the value 9.

The normality test is based on the statistic d^2. The p-value of the test is the probability of getting a value more extreme than d^2 under the hypothesis of a chi-squared distribution with 11 degrees of freedom for d^2.

The null hypothesis of the test (the cycle values are normally distributed) is rejected if the p-value is lower than 0.05.

Tables 5.36 and 5.37 give the percentage of the replicas with cycle values not normally distributed respectively before and after the automatic suppression of the transient active cycles.

Table 5.36 Percentage of the replicas with cycle values not normally distributed before automatic suppression of transient active cycles

	0 inactive cycles	200 inactive cycles	400 inactive cycles
ANL / VIM	74	37	21
EMS / KENO	88	19	12
IPPE / KENO	84	32	16
IRSN / MORET	87	33	16
JNC / KENO	89	25	9
LANL / MCNP	87	33	13
ORNL / KENO	89	36	11

Before the automatic suppression of the transient, the percentage of replicas with cycle values not normally distributed decreases when the number of inactive cycles increases. The test is efficient but not as much as the stationarity test (refer to Table 5.37).

Table 5.37 Percentage of the replicas with cycle values not normally distributed after automatic suppression of transient active cycles

	0 inactive cycles	200 inactive cycles	400 inactive cycles
ANL / VIM	12	15	15
EMS / KENO	12	6	4
IPPE / KENO	9	8	9
IRSN / MORET	6	6	9
JNC / KENO	9	3	4
LANL / MCNP	8	6	8
ORNL / KENO	8	11	9

After the automatic suppression of the transient, the percentage of replicas with cycle values not normally distributed is low and rather independent of the number of inactive cycles but greater than the level of significance of the test (5 %) (especially in the case of ANL / VIM). This is what we expected due to the too low expected frequencies of the extreme bins. Nevertheless, the normality test seems to confirm that the transient has been correctly removed from each replica.

Comparison of the mean values of the two halves

Let *mu1* and *sigma1*, *mu2* and *sigma2* denote the mean values and the standard deviations of the mean of the first and second halves of the series. *Sigma1* and *sigma2* are computed using a modification of the method of Ueki et al [8] (refer to Appendix 5.g). If the two halves of the series have the same mean (this can be expected when the source is stationary), $\Delta = \frac{mu_2 - mu_1}{\sqrt{sigma_1^{\,2} + sigma_2^{\,2}}}$ tends to be normally distributed with a meanvalue of 0 and a standard deviation of 1. The comparison of the halves means test is based on the statistic Δ. The p-value of the test is the probability of getting a value more extreme than Δ, in absolute value, under the hypothesis of normality for Δ. The null hypothesis of the test (the two halves of the series have the same mean) is rejected if the p-value is lower than 0.05. Tables 5.38 and 5.39 give the percentage of the replicas with the two halves' means different before and after the automatic suppression of the transient active cycles, respectively.

Table 5.38 Percentage of the replicas with the two halves means different before automatic suppression of transient active cycles

	0 inactive cycles	200 inactive cycles	400 inactive cycles
ANL / VIM	62	19	10
EMS / KENO	63	23	12
IPPE / KENO	67	22	13
IRSN / MORET	69	29	14
JNC / KENO	66	23	8
LANL / MCNP	62	26	9
ORNL / KENO	72	26	11

Before the automatic suppression of the transient, the percentage of replicas with the two halves means different decreases when the number of inactive cycles increases but seems to be independent of the contributor. The comparison of the two halves means does not allow detecting as much non-stationary series as the stationary detection test (refer to Table 5.27).

Table 5.39 Percentage of the replicas with the two halves means different after automatic suppression of transient active cycles

	0 inactive cycles	200 inactive cycles	400 inactive cycles
ANL / VIM	4	2	3
EMS / KENO	2	6	5
IPPE / KENO	0	2	5
IRSN / MORET	3	5	5
JNC / KENO	4	3	3
LANL / MCNP	0	2	7
ORNL / KENO	0	4	4

After the automatic suppression of the transient, the percentage of replicas with the two halves means different is of the order of the level of significance of the test, whatever the number of inactive cycle is and for each contributor. The transient seems to have been correctly removed from each replica.

Comparison of the distribution of $(k_{eff} - k_{eff,ref}) / \sqrt{(std^2 + std_{ref}^2)}$ with normal law N(0,1) after automatic suppression of transient active cycles

Let $k_{eff,ref}$ and stdref denote the final k_{eff} and the standard deviation of the final k_{eff} of the reference calculation. These values are provided by contributor in Table 5.8. Let k_{eff} and std denote the final k_{eff} and the standard deviation of the final k_{eff} of a replica after the automatic suppression of transient active cycles. The standard deviations are computed according the modified method of Ueki et al. detailed in Appendix 5.g. If the initial transient is entirely removed from each replica and if the standard deviation of the final k_{eff} of each replica is correctly computed (taking into account correlations between cycles), the set of values $(k_{eff} - k_{eff,ref}) / \sqrt{(std^2 + stdref^2)}$ should be distributed as the normal law N(0,1).

The values $(k_{eff} - k_{eff,ref}) / \sqrt{(std^2 + stdref^2)}$ are divided into 6 bins:

- 4 bins of width 1 between –2 and 2,
- 1 bin between –infinity and –2,

- 1 bin between 2 and infinity,

but also into 2 bins:

- the bin of negative values: $(k_{eff} - k_{eff,ref}) < 0$,
- the bin of positive values: $(k_{eff} - k_{eff,ref}) > 0$.

Tables 5.40 to 5.46 give the observed frequencies of the values $(k_{eff} - k_{eff,ref}) / \sqrt{(std^2 + stdref^2)}$ divided into 6 bins and 2 bins, after the automatic suppression of transient active cycles, in comparison with the expected frequencies in the case of the normal law N(0,1). The histograms corresponding to these tables are grouped in Appendix 5.i.

Table 5.40 Distribution of $(k_{eff} - k_{eff,ref}) / \sqrt{(std^2 + std_{ref}^2)}$ after automatic suppression of transient active cycles – ANL / VIM

	Observed frequencies			Expected freq.
bins	**0 inactive cycle**	**200 inactive cycles**	**400 inactive cycles**	**normal law N(0,1)**
< -2	12	10	12	2.27501
[-2;-1]	15	17	20	13.59052
[-1;0]	40	40	29	34.13447
[0;1]	24	19	24	34.13447
[1;2]	7	12	14	13.59052
> 2	2	2	1	2.27501
< 0	67	67	61	50.00000
> 0	33	33	39	50.00000
total	100	100	100	100.00000

Table 5.41 Distribution of $(k_{eff} - k_{eff,ref}) / \sqrt{(std^2 + std_{ref}^2)}$ after automatic suppression of transient active cycles – EMS / KENO

	Observed frequencies			Expected freq.
bins	**0 inactive cycle**	**200 inactive cycles**	**400 inactive cycles**	**normal law N(0,1)**
< -2	11	8	7	2.27501
[-2;-1]	21	23	22	13.59052
[-1;0]	27	30	29	34.13447
[0;1]	37	27	29	34.13447
[1;2]	2	10	11	13.59052
> 2	2	2	2	2.27501
< 0	59	61	58	50.00000
> 0	41	39	42	50.00000
total	100	100	100	100.00000

Table 5.42 Distribution of $(k_{eff} - k_{eff,ref}) / \sqrt{(std^2 + std_{ref}^2)}$ after automatic suppression of transient active cycles – IPPE / KENO

	Observed frequencies			Expected freq.
bins	0 inactive cycle	200 inactive cycles	400 inactive cycles	normal law N(0,1)
< -2	10	7	6	2.27501
[-2;-1]	20	25	27	13.59052
[-1;0]	34	34	29	34.13447
[0;1]	26	22	27	34.13447
[1;2]	9	11	10	13.59052
> 2	1	1	1	2.27501
< 0	64	66	62	50.00000
> 0	36	34	38	50.00000
total	100	100	100	100.00000

Table 5.43 Distribution of $(k_{eff} - k_{eff,ref}) / \sqrt{(std^2 + std_{ref}^2)}$ after automatic suppression of transient active cycles – IRSN / MORET

	Observed frequencies			Expected freq.
bins	0 inactive cycle	200 inactive cycles	400 inactive cycles	normal law N(0,1)
< -2	4	3	1	2.27501
[-2;-1]	23	19	17	13.59052
[-1;0]	27	32	31	34.13447
[0;1]	29	30	35	34.13447
[1;2]	13	13	14	13.59052
> 2	4	3	2	2.27501
< 0	54	54	49	50.00000
> 0	46	46	51	50.00000
total	100	100	100	100.00000

Table 5.44 Distribution of $(k_{eff} - k_{eff,ref}) / \sqrt{(std^2 + std_{ref}^2)}$ after automatic suppression of transient active cycles – JNC / KENO

	Observed frequencies			Expected freq.
bins	0 inactive cycle	200 inactive cycles	400 inactive cycles	normal law N(0,1)
< -2	6	9	8	2.27501
[-2;-1]	22	15	19	13.59052
[-1;0]	37	34	29	34.13447
[0;1]	26	26	30	34.13447
[1;2]	9	15	13	13.59052
> 2	0	1	1	2.27501
< 0	65	58	56	50.00000
> 0	35	42	44	50.00000
total	100	100	100	100.00000

Table 5.45 Distribution of $(k_{eff} - k_{eff,ref}) / \sqrt{(std^2 + std_{ref}^2)}$ after automatic suppression of transient active cycles –LANL / MCNP

	Observed frequencies			Expected freq.
bins	**0 inactive cycle**	**200 inactive cycles**	**400 inactive cycles**	**normal law N(0,1)**
< -2	6	6	7	2.27501
[-2;-1]	30	31	26	13.59052
[-1;0]	36	31	38	34.13447
[0;1]	17	25	21	34.13447
[1;2]	8	5	8	13.59052
> 2	3	2	0	2.27501
< 0	72	68	71	50.00000
> 0	28	32	29	50.00000
total	100	100	100	100.00000

Table 5.46 Distribution of $(k_{eff} - k_{eff,ref}) / \sqrt{(std^2 + std_{ref}^2)}$ after automatic suppression of transient active cycles – ORNL / KENO

	Observed frequencies			Expected freq.
bins	**0 inactive cycle**	**200 inactive cycles**	**400 inactive cycles**	**normal law N(0,1)**
< -2	12	11	7	2.27501
[-2;-1]	25	29	26	13.59052
[-1;0]	26	28	37	34.13447
[0;1]	27	28	20	34.13447
[1;2]	9	4	10	13.59052
> 2	1	0	0	2.27501
< 0	63	68	70	50.00000
> 0	37	32	30	50.00000
total	100	100	100	100.00000

In order to compare the distribution of the values $(k_{eff} - k_{eff,ref}) / \sqrt{(std^2 + stdref^2)}$ with the normal law N(0,1), the following statistic is computed:

$$d_n^2 = \sum_{i=1}^{n} \frac{(f_{o,n}(i) - f_{e,n}(i))^2}{f_{e,n}(i)}$$

- n being the number of bins (n being 2 or 6),
- $f_{o,n}$ are the observed frequencies of the *n* bins,
- $f_{e,n}$ are the expected frequencies of the *n* bins in the case of the normal law N(0,1).

If the values $(k_{eff} - k_{eff,ref}) / \sqrt{(std^2 + stdref^2)}$ are normally distributed, the statistic d_n^2 tends to be distributed as a chi-square with n-1 degrees of freedom. The null hypothesis (the values $(k_{eff} - k_{eff,ref}) / \sqrt{(std^2 + std_{ref}^2)}$ are normally distributed) is rejected if the p-value (probability of getting a value more extreme than d_n^2, under the hypothesis of a chi-squared distribution with n-1 degrees of freedom for d_n^2) is lower than 0.05.

Tables 5.47 and 5.48 give the results of the chi-square tests respectively with 1 degree and 5 degrees of freedom. Bold numbers in these tables indicate the acceptance of the normality hypothesis.

Table 5.47 Comparison of the distribution of $(k_{eff} - k_{eff,ref}) / \sqrt{(std^2 + std_{ref}^2)}$ with the normal law N(0,1) – 2 bins – Chi square test with 1 degree of freedom Normality hypothesis is accepted if p-value > 0.05 ($d_2^2 < 3.84$)

	0 inactive cycle		200 inactive cycles		400 inactive cycles	
	d_2^2	p-value	d_2^2	p-value	d_2^2	p-value
ANL / VIM	11.56	6.74E-04	11.56	6.74E-04	4.84	2.78E-02
EMS / KENO	**3.24**	**7.19E-02**	4.84	2.78E-02	**2.56**	**1.10E-01**
IPPE / KENO	7.84	5.11E-03	10.24	1.37E-03	5.76	1.64E-02
IRSN / MORET	**0.64**	**4.24E-01**	**0.64**	**4.24E-01**	**0.04**	**8.41E-01**
JNC / KENO	9.00	2.70E-03	**2.56**	**1.10E-01**	**1.44**	**2.30E-01**
LANL / MCNP	19.36	1.08E-05	12.96	3.18E-04	17.64	2.67E-05
ORNL / KENO	6.76	9.32E-03	12.96	3.18E-04	16.00	6.33E-05

Table 5.48 Comparison of the distribution of $(k_{eff} - k_{eff,ref}) / \sqrt{(std^2 + std_{ref}^2)}$ with the normal law N(0,1) – 6 bins – Chi square test with 5 degree of freedom Normality hypothesis is accepted if p-value > 0.05 ($d_6^2 < 11.07$)

	0 inactive cycle		200 inactive cycles		400 inactive cycles	
	d_6^2	p-value	d_6^2	p-value	d_6^2	p-value
ANL / VIM	48.96	2.26E-09	35.02	1.49E-06	49.10	2.11E-09
EMS / KENO	49.15	2.07E-09	23.90	2.27E-04	17.09	4.33E-03
IPPE / KENO	33.46	3.05E-06	24.91	1.45E-04	23.26	3.01E-04
IRSN / MORET	11.42	4.37E-02	3.27	6.58E-01	1.93	8.59E-01
JNC / KENO	17.31	3.95E-03	22.83	3.65E-04	18.57	2.31E-03
LANL / MCNP	37.15	5.60E-07	36.60	7.22E-07	31.21	8.51E-06
ORNL / KENO	56.84	5.44E-11	62.18	4.30E-12	30.46	1.20E-05

The final k_{eff} values obtained after the automatic suppression of the transient with the replicas submitted by IRSN are the only ones which could be considered as being normally distributed around the reference k_{eff} value. This surprising difference should be investigated. The next section will show that that this difference cannot be attributed to a default of the automatic procedure used to suppress the transient.

Percentage of replicas with a mean value greater than the reference k_{eff} value versus the number of active cycles suppressed

In this section, the automatic suppression of the transient is not used, but an empirical and a global criterion to determine if the whole set of replicas are stationary after the suppression of the same number of initial active cycles in each replica. The mean values of the replicas should be equally distributed around the reference k_{eff}. For this, the observed frequency f of replicas with a mean value greater than the reference k_{eff} value is compared with the expected frequency of 50%. The following statistic d^2 is a measure of the distance between the observed distribution and the expected distribution:

$$d^2 = \frac{(f-50)^2}{50} + \frac{(100-f-50)^2}{50} = \frac{(f-50)^2}{25}$$

If the mean values of the replicas are equally distributed around the reference k_{eff}, the statistic d^2 tends to be distributed as a chi-square with 1 degree of freedom.

The hypothesis (the mean values of the replicas are equally distributed around the reference k_{eff}) is rejected if the probability of getting a value more extreme than d^2, under the hypothesis of a chi-squared distribution with 1 degree of freedom for d^2, is lower than 0.05, i.e. if $d^2 < 3.84$, i.e. if $f < 40.2$ or $f > 59.8$. If the frequency of replicas with a mean value greater than the reference k_{eff} value is comprised between 40.2% and 59.8%, the whole set of replicas can be considered as stationary.

Figures 5.2 to 5.8 (see P. 96) represent, for each contribution, the percentage of replicas with a mean value greater than the reference k_{eff} value versus the number of active cycles suppressed. These figures show that the minimum number of cycles to suppress before getting a correct distribution around the reference k_{eff} is obtained by IRSN / MORET whereas the maximum number is obtained by LANL / MCNP.

The present conclusions confirm the results of the previous section: the final k_{eff} values obtained after the automatic suppression of the transient with the replicas submitted by IRSN were the only ones which could be considered as being normally distributed around the reference k_{eff} value. Such a difference between the various contributions deserves more attention because it cannot be attributed to a default of the automatic procedure used to suppress the transient. We propose two possible origins of that difference:

- different cycle k_{eff} estimators are used by the contributors; the "balance-track-length" estimator used in the MORET code is the best one in the framework of the test 4 configuration;

- different algorithms are used in the codes to estimate the new distribution of sources at each cycle; the conventional strategy used by MORET is very close to the stratified sampling because the proportion of sources in each fissile volume is equal to the proportion of fission productions in each fissile volume during the previous cycle.

Figure 5.2 ANL / VIM

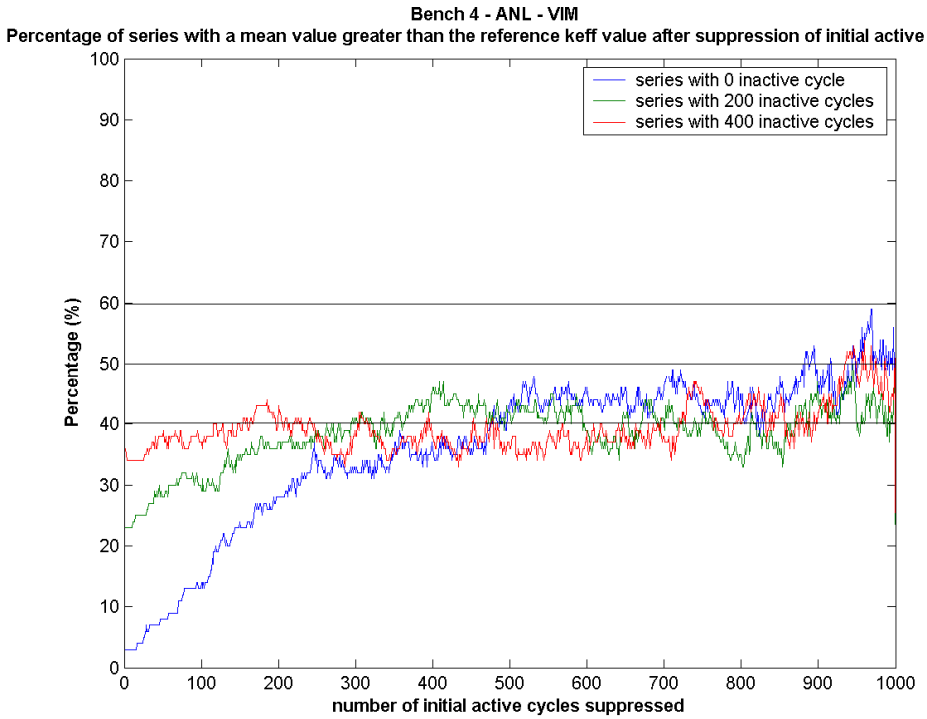

Figure 5.3 EMS / KENO

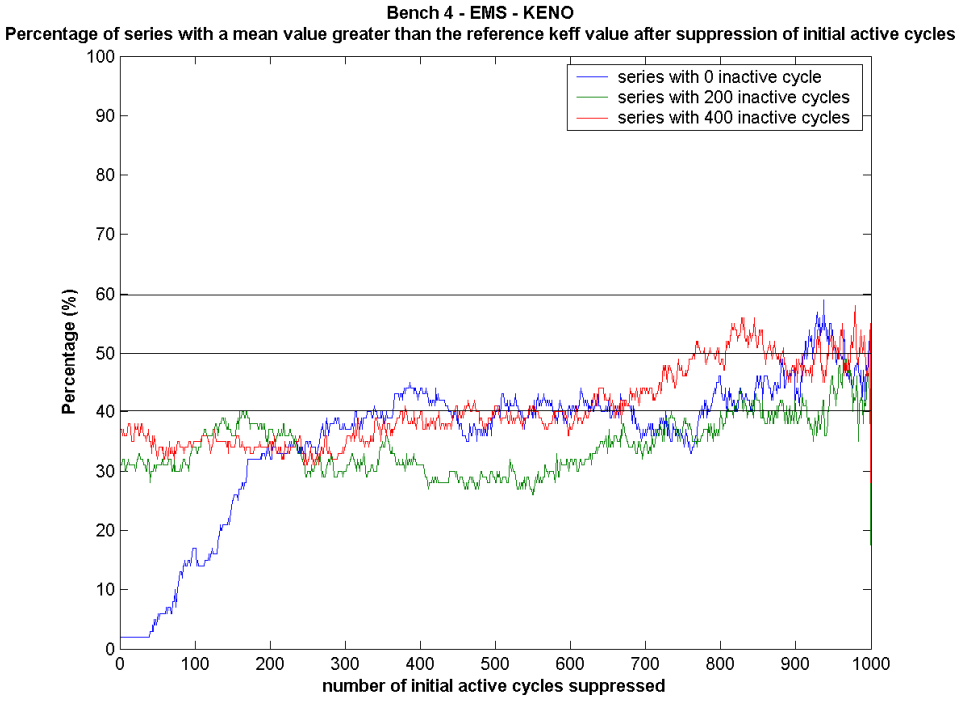

Figure 5.4 IPPE / KENO

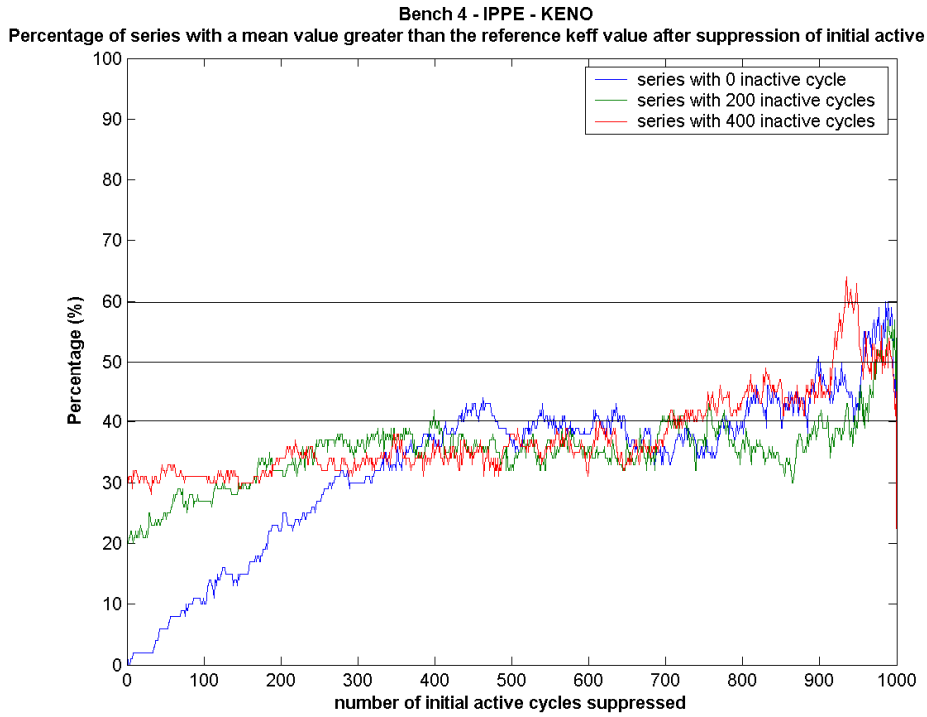

Figure 5.5 IRSN / MORET

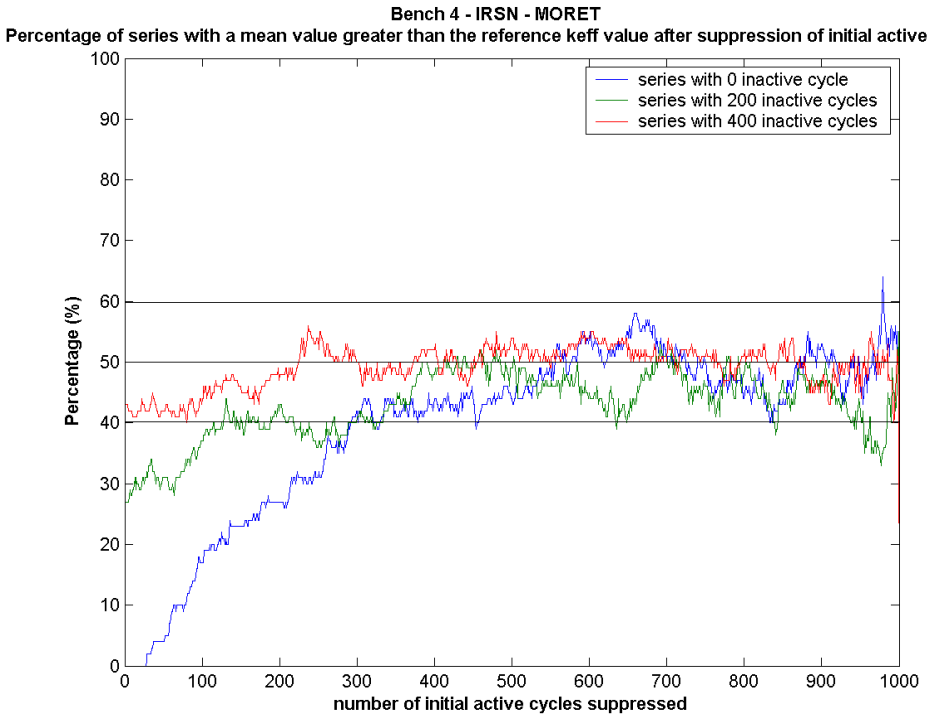

Figure 5.6 JNC / KENO

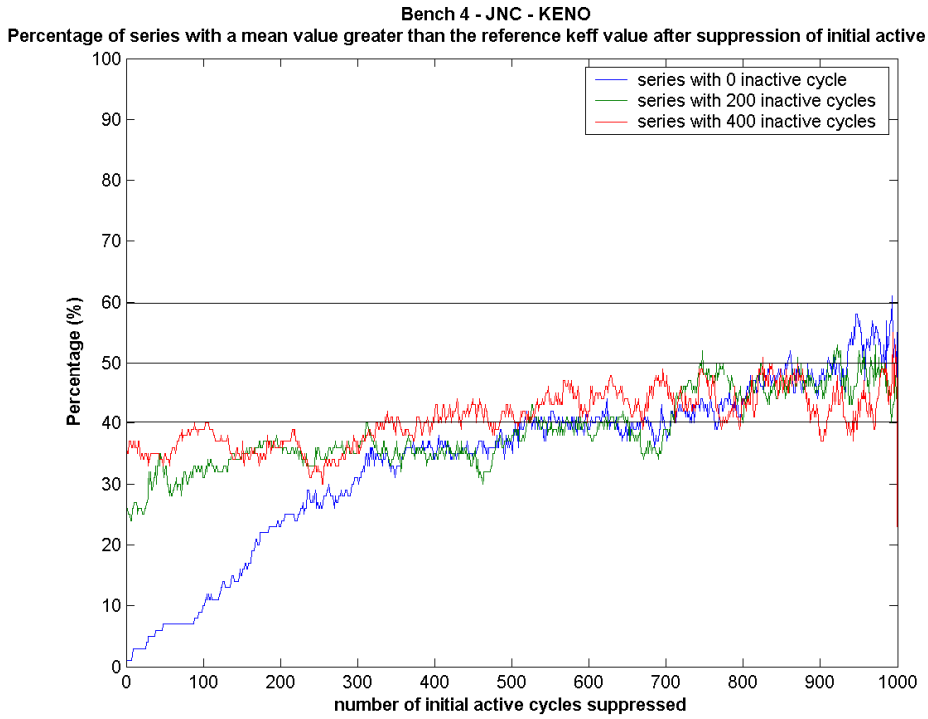

Figure 5.7 LANL / MCNP

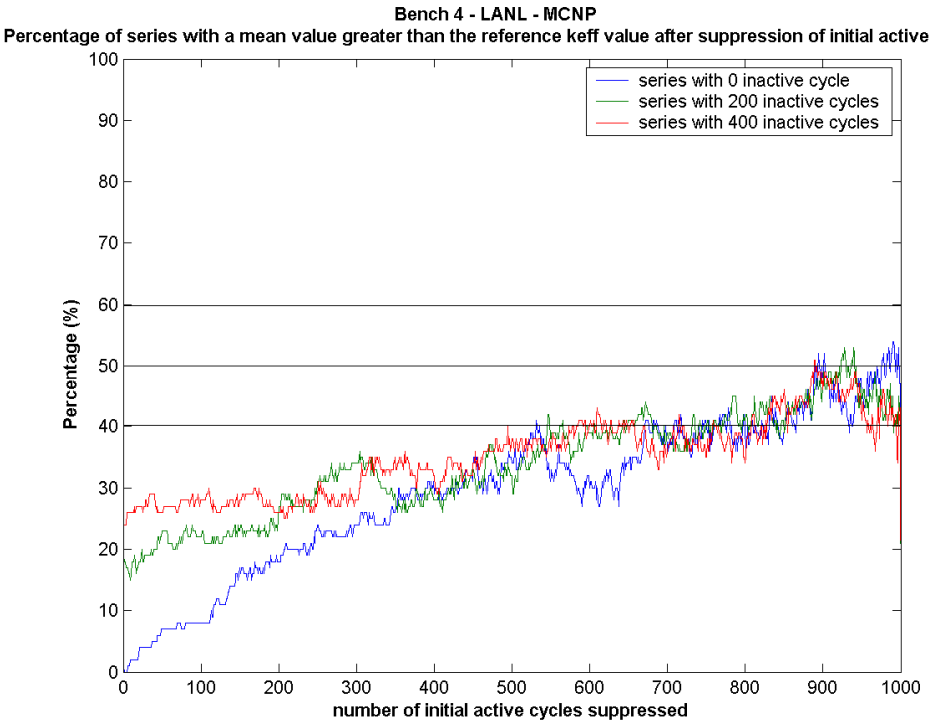

Figure 5.8 ORNL / KENO

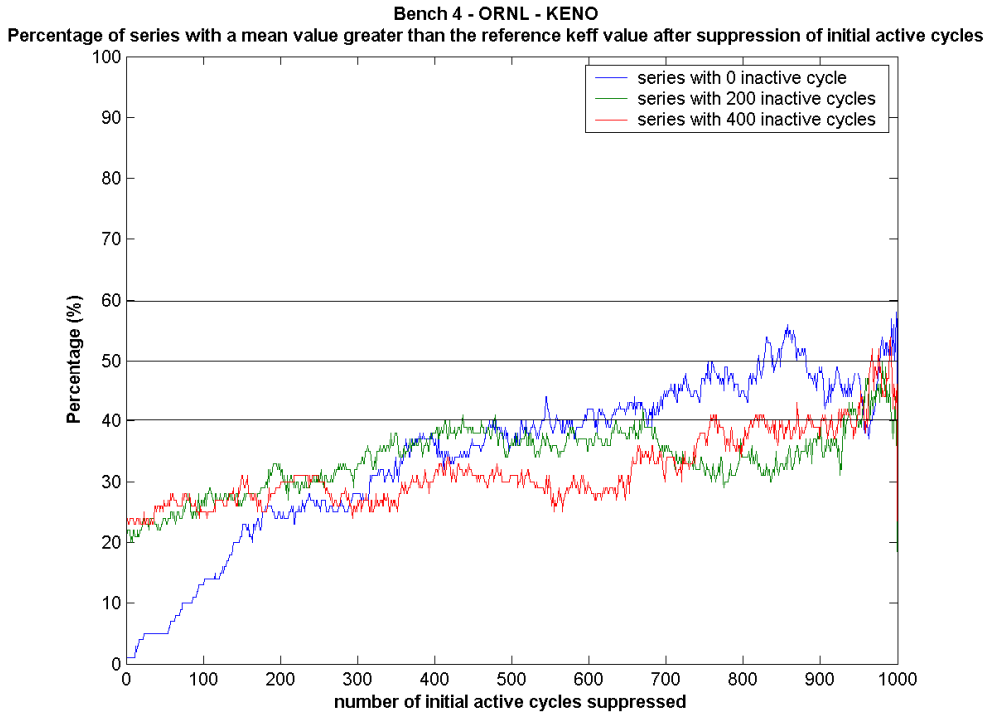

Final conclusions

Test problem 4 is a 5 x 5 x 1 array of metal spheres interacting in air with low coupling. The initial spatial distribution of neutrons was intentionally chosen to be far from the converged source. The greatest part of the initial source was placed in one of the least reactive units. Moreover the population of neutrons per generation was kept quite low (125 neutrons per cycle) in order to amplify the effects of undersampling. In those conditions, the source convergence process requires a large number of cycles before the most reactive unit is visited by a sufficient number of neutrons. As the number of active cycles was limited to 1000 with a maximum number of 400 inactive cycles, the final k_{eff} (cumulative over the active cycles) may be underestimated for two reasons:

1) Either the source convergence has not been achieved, i.e. the most reactive unit is still under-sampled at the end of the simulation; in the worst case, the most reactive unit may be unsampled and may remain so at the end of the simulation, leading to non-convergence.

2) Or source convergence has been achieved, but the number of skipped cycles is not sufficient.

In order to test the robustness of the criticality codes to converge to the correct distribution of sources when the initial guess is not realistic, each contributor ran one hundred replicas of the same configuration using different random seeds.

Despite the difficult conditions of test problem 4, the hundreds of replica calculations made with a variety of codes did not exhibit a single situation where the central, most reactive sphere remained undersampled during more than 1 000 cycles. Of course, if more replicas had been run, or if less than 1 000 active cycles had been run, some replicas would have probably have been unconverged. The

1000-cycle calculations suggest that the convergence properties of the Monte Carlo powering algorithm lead to a source distribution sufficiently close to the true solution to avoid the risk of large under-estimation of k_{eff}. If a sufficient number of cycles is run, the main problem seems to be more in the detection of this convergence and the use of reliable algorithms to truncate the transient.

The cumulative final values of k_{eff} and fission fraction of central sphere are underestimated only because the number of skipped cycles is insufficient: the initial transient during which the distribution of sources is not converged (most reactive sphere undersampled) is not entirely removed. The greater the number of inactive cycles (i.e. the smaller the size of transient in the active cycles):

- the greater the cumulative final values of k_{eff} and fission fraction of central sphere;
- the lower the standard deviation values.

400 inactive cycles seem to be insufficient for the configuration studied in this test and especially for the bad initial source guess considered.

The results obtained with MCNP highlight the smallest dispersion of the final values of k_{eff} and fission fraction of central sphere. A plausible explanation, but maybe not the only one, is the fact that neutrons can survive absorption in MCNP as in KENO. The threshold of the Russian roulette is 0.25 in MCNP and 0.333 in KENO. As a consequence the histories of neutrons are longer in MCNP than in KENO and histories in KENO are longer than in VIM or MORET since neutrons do not survive absorption in those two codes. Nevertheless, the dispersions of the results differ among KENO users. It should be noted that the scatter of the results obtained by ORNL tends to be significantly lower but an additional analysis has shown that this difference could be due not only to the different cross-sections libraries but also, in great part, to the anisotropic scattering treatment. Further investigation is needed to explain the origins of the differences. Another plausible explanation of the smallest dispersion of the results with MCNP is the fact that all fission sites obtained during a cycle are used as starters of the following cycle. In fact, a great variety of parameters (like the anisotropic scattering treatment) should be studied independently to identify their impact on the dispersion of the results.

More reliable estimations of uncertainties are obtained when correlations between generations are taken into account in the calculation of k_{eff} standard deviation. In this respect, the methods implemented in KENO (use of correlation coefficients) and VIM (batching method) lead to improved results compared to the standard method where inter-generation correlation are ignored.

The initial transient observed in the k_{eff} series is obviously a consequence of the source distribution (or eigenvector) convergence process from the initial guess to the fundamental mode. Since it is much easier to study the convergence in a series of scalar values than in a series of vectors, and because the cycle k_{eff} series is used for the estimation of the k_{eff} eigenvalue, a first approach to suppress the initial transient – using the Brownian bridge theory – focused on the stationarity detection of the cycle k_{eff} series.

An algorithm, based on the Brownian bridge theory, to automatically suppress the initial transient of cycle k_{eff} series was successfully applied to the results of the test problem 4. However the apparent convergence of k_{eff} series does not strictly imply the convergence of the source distribution. Recently, a stationarity diagnostic based on the Shannon entropy of source distribution, using the two-sample F test, was proposed [9]. An advantage of this method lies in the use of the Shannon entropy of source distribution which is a scalar value more representative of the source distribution than k_{eff}. The algorithm based on the Brownian bridge theory to automatically suppress the initial transient, which was tested here on cycle k_{eff} series, could also apply on cycle series of the Shannon entropy.

The number of cycles that should be skipped in order to get a correct distribution of the final k_{eff} around the reference k_{eff} varies from one code to the other. This number is the lowest for the results obtained with the IRSN / MORET code and the highest when the LANL / MCNP code is used. No obvious explanation for that was found. The cumulative final k_{eff} values obtained after the automatic suppression of the transient with the replicas submitted by IRSN are the only ones which could be considered as being normally distributed around the reference k_{eff} value. Such a difference between the various contributions deserves a great attention. Here are given two possible origins of that difference:

- different cycle k_{eff} estimators are used by the contributors; the "balance-track-length" estimator used in the MORET code is the best one in the framework of the test 4 configuration;

- different algorithms are used in the codes to estimate the new distribution of sources at each cycle; the conventional strategy used by MORET is very close to the stratified sampling because the proportion of sources in each fissile volume is equal to the proportion of fission productions in each fissile volume during the previous cycle.

References

[1] Kadotani *et al.* (Proc. ICNC'91, Oxford, 1991)

[2] RSICC DLC-182 "ABBN-90: Multigroup Constant Set for Calculation of Neutron and Photon Radiation Fields and Functionals, Including the CONSYST2 Program."

[3] A. Nouri *et al.*, "Further Investigations on the Comparison and the Combination of Monte Carlo k_{eff} Estimators", Proc. Int. Conf. On the Phys. of Nucl. Sci. and Tech., Long Island NY, Oct. 98

[4] E.M. Gelbard and R. Prael, "Computation of Standard Deviations in Eigenvalue Calculations", Progress in Nuclear Energy, Vol. 24, pp.237-241, 1990.

[5] Gelbard and Prael ("Computation of Standard Deviations in Eigenvalue Calculations", Progress in Nuclear Energy, Vol. 24, pp.237-241, 1990),

[6] "Automated Suppression of the Initial Transient in Monte Carlo Calculations based on Stationarity Detection using the Brownian Bridge Theory", Yann Richet et al., ICNC 2003)

[7] P. Heidelberger, P Welch, "Simulation Run Length Control in the Presence of an Initial Transient", Operations Research, vol. 31 (Nov-Dec 1983)

[8] Ueki *et al.* in "Error Estimations and Their Biases in Monte Carlo Eigenvalue Calculations", Nucl. Sci. Eng., 125, 1(1997).

[9] Ueki, *et al.*, "Stationarity Diagnostics Using Shannon Entropy in Monte Carlo Criticality Calculations I: F test," ANS Transactions, Washington, DC (2002).

Acknowledgements

We express our thanks to:

- Roger Blomquist (ANL, USA) as leader of the Expert Group on Source Convergence and for his contribution to this test,
- Ali Nouri (OECD) for his inspiring work in the field of Monte Carlo and source convergence and his help,
- Xavier Bay (EMSE, France) for his help in the field of statistics and stationarity detection,
- Dennis Mennerdahl (EMS, Sweden), Alexander Blyskavka and Tatiana Ivanova (IPPE, Russia), Nobutoshi Shirai (JNC, Japan), Robert Little and Forrest Brown (LANL, USA) and John Wagner (ORNL, USA) for their contribution to this test.

Appendix 5.a

SAMPLE INPUT FILES

ANL / VIM

```
000111001 Kadotani, Skip 400, one replica, batches=10
1000   1        0        400
1250   20       0
1  1
4  2    26       1          51
0.00001          1.0          1.E-05        2.E+7
1.11   0.0
0  0   0        0          0
30300 40300260300420300


0       0       52
SPH     1        0.0       0.0       0.0       8.71
SPH     2       80.0       0.0       0.0       8.71
SPH     3      160.0       0.0       0.0       8.71
SPH     4      240.0       0.0       0.0       8.71
SPH     5      320.0       0.0       0.0       8.71
SPH     6        0.0      80.0       0.0       8.71
SPH     7       80.0      80.0       0.0       8.71
SPH     8      160.0      80.0       0.0       8.71
SPH     9      240.0      80.0       0.0       8.71
SPH     10     320.0      80.0       0.0       8.71
SPH     11       0.0     160.0       0.0       8.71
SPH     12      80.0     160.0       0.0       8.71
SPH     13     160.0     160.0       0.0      10.00
SPH     14     240.0     160.0       0.0       8.71
SPH     15     320.0     160.0       0.0       8.71
SPH     16       0.0     240.0       0.0       8.71
SPH     17      80.0     240.0       0.0       8.71
SPH     18     160.0     240.0       0.0       8.71
SPH     19     240.0     240.0       0.0       8.71
SPH     20     320.0     240.0       0.0       8.71
SPH     21       0.0     320.0       0.0       8.71
SPH     22      80.0     320.0       0.0       8.71
SPH     23     160.0     320.0       0.0       8.71
SPH     24     240.0     320.0       0.0       8.71
SPH     25     320.0     320.0       0.0       8.71
RPP     26     -40.0      40.0001   -40.0      40.0001   -40.0001   40.0001
RPP     27      40.0     120.0001   -40.0      40.0001   -40.0001   40.0001
RPP     28     120.0     200.0001   -40.0      40.0001   -40.0001   40.0001
RPP     29     200.0     280.0001   -40.0      40.0001   -40.0001   40.0001
RPP     30     280.0     360.0001   -40.0      40.0001   -40.0001   40.0001
RPP     31     -40.0      40.0001    40.0     120.0001   -40.0001   40.0001
RPP     32      40.0     120.0001    40.0     120.0001   -40.0001   40.0001
```

```
RPP   33   120.0     200.0001    40.0     120.0001   -40.0001   40.0001
RPP   34   200.0     280.0001    40.0     120.0001   -40.0001   40.0001
RPP   35   280.0     360.0001    40.0     120.0001   -40.0001   40.0001
RPP   36   -40.0      40.0001   120.0     200.0001   -40.0001   40.0001
RPP   37    40.0     120.0001   120.0     200.0001   -40.0001   40.0001
RPP   38   120.0     200.0001   120.0     200.0001   -40.0001   40.0001
RPP   39   200.0     280.0001   120.0     200.0001   -40.0001   40.0001
RPP   40   280.0     360.0001   120.0     200.0001   -40.0001   40.0001
RPP   41   -40.0      40.0001   200.0     280.0001   -40.0001   40.0001
RPP   42    40.0     120.0001   200.0     280.0001   -40.0001   40.0001
RPP   43   120.0     200.0001   200.0     280.0001   -40.0001   40.0001
RPP   44   200.0     280.0001   200.0     280.0001   -40.0001   40.0001
RPP   45   280.0     360.0001   200.0     280.0001   -40.0001   40.0001
RPP   46   -40.0      40.0001   280.0     360.0001   -40.0001   40.0001
RPP   47    40.0     120.0001   280.0     360.0001   -40.0001   40.0001
RPP   48   120.0     200.0001   280.0     360.0001   -40.0001   40.0001
RPP   49   200.0     280.0001   280.0     360.0001   -40.0001   40.0001
RPP   50   280.0     360.0001   280.0     360.0001   -40.0001   40.0001
RPP   51   -39.9999  360.0000   -39.9999  360.0000   -40.0      40.0
RPP   52   -10.0     330.0      -10.0     330.0      -10.0      10.0
END
S11   1     1
V11   8    26     -1
S21   1     2
V21   8    27     -2
S31   1     3
V31   8    28     -3
S41   1     4
V41   8    29     -4
S51   1     5
V51   8    30     -5
S12   1     6
V12   8    31     -6
S22   1     7
V22   8    32     -7
S32   1     8
V32   8    33     -8
S42   1     9
V42   8    34     -9
S52   1    10
V52   8    35    -10
S13   1    11
V13   8    36    -11
S23   1    12
V23   8    37    -12
S33   1    13
V33   8    38    -13
S43   1    14
V43   8    39    -14
S53   1    15
```

```
        V53     8       40      -15
        S14     1       16
        V14     8       41      -16
        S24     1       17
        V24     8       42      -17
        S34     1       18
        V34     8       43      -18
        S44     1       19
        V44     8       44      -19
        S54     1       20
        V54     8       45      -20
        S15     1       21
        V15     8       46      -21
        S25     1       22
        V25     8       47      -22
        S35     1       23
        V35     8       48      -23
        S45     1       24
        V45     8       49      -24
        S55     1       25
        V55     8       50      -25
LEAK            8      -51
        END

        1       101     1       2       2600    2       3       201     1
        4       2600    2       5       301     1       6       2600    2
        7       401     1       8       2600    2       9       501     1
        10      2600    2       11      601     1       12      2600    2
        13      701     1       14      2600    2       15      801     1
        16      2600    2       17      901     1       18      2600    2
        19      1001    1       20      2600    2       21      1101    1
        22      2600    2       23      1201    1       24      2600    2
        25      1301    1       26      2600    2       27      1401    1
        28      2600    2       29      1501    1       30      2600    2
        31      1601    1       32      2600    2       33      1701    1
        34      2600    2       35      1801    1       36      2600    2
        37      1901    1       38      2600    2       39      2001    1
        40      2600    2       41      2101    1       42      2600    2
        43      2201    1       44      2600    2       45      2301    1
        46      2600    2       47      2401    1       48      2600    2
        49      2501    1       50      2600    2       51      000     -1
 30300 40300
260300420300
 4.549 E-02 2.560 E-03
 4.3250 E-05 1.0810 E-05
 1.0    E-05
      125
        0.0     0.0     0.0     1.00    1000000.0       1
        0.0     0.0     0.0     1.00    1000000.0       1
```

0.0	0.0	0.0	1.00	1000000.0	1
0.0	0.0	0.0	1.00	1000000.0	1
0.0	0.0	0.0	1.00	1000000.0	1
0.0	0.0	0.0	1.00	1000000.0	1
0.0	0.0	0.0	1.00	1000000.0	1
0.0	0.0	0.0	1.00	1000000.0	1
0.0	0.0	0.0	1.00	1000000.0	1
0.0	0.0	0.0	1.00	1000000.0	1
0.0	0.0	0.0	1.00	1000000.0	1
0.0	0.0	0.0	1.00	1000000.0	1
0.0	0.0	0.0	1.00	1000000.0	1
0.0	0.0	0.0	1.00	1000000.0	1
0.0	0.0	0.0	1.00	1000000.0	1
0.0	0.0	0.0	1.00	1000000.0	1
0.0	0.0	0.0	1.00	1000000.0	1
0.0	0.0	0.0	1.00	1000000.0	1
0.0	0.0	0.0	1.00	1000000.0	1
0.0	0.0	0.0	1.00	1000000.0	1
0.0	0.0	0.0	1.00	1000000.0	1
0.0	0.0	0.0	1.00	1000000.0	1
0.0	0.0	0.0	1.00	1000000.0	1
0.0	0.0	0.0	1.00	1000000.0	1
0.0	0.0	0.0	1.00	1000000.0	1
0.0	0.0	0.0	1.00	1000000.0	1
0.0	0.0	0.0	1.00	1000000.0	1
0.0	0.0	0.0	1.00	1000000.0	1
0.0	0.0	0.0	1.00	1000000.0	1
0.0	0.0	0.0	1.00	1000000.0	1
0.0	0.0	0.0	1.00	1000000.0	1
0.0	0.0	0.0	1.00	1000000.0	1
0.0	0.0	0.0	1.00	1000000.0	1
0.0	0.0	0.0	1.00	1000000.0	1
0.0	0.0	0.0	1.00	1000000.0	1
0.0	0.0	0.0	1.00	1000000.0	1
0.0	0.0	0.0	1.00	1000000.0	1
0.0	0.0	0.0	1.00	1000000.0	1
0.0	0.0	0.0	1.00	1000000.0	1
0.0	0.0	0.0	1.00	1000000.0	1
0.0	0.0	0.0	1.00	1000000.0	1
0.0	0.0	0.0	1.00	1000000.0	1
0.0	0.0	0.0	1.00	1000000.0	1
0.0	0.0	0.0	1.00	1000000.0	1
0.0	0.0	0.0	1.00	1000000.0	1
0.0	0.0	0.0	1.00	1000000.0	1
0.0	0.0	0.0	1.00	1000000.0	1
0.0	0.0	0.0	1.00	1000000.0	1
0.0	0.0	0.0	1.00	1000000.0	1
0.0	0.0	0.0	1.00	1000000.0	1
0.0	0.0	0.0	1.00	1000000.0	1
0.0	0.0	0.0	1.00	1000000.0	1

0.0	0.0	0.0	1.00	1000000.0	1
0.0	0.0	0.0	1.00	1000000.0	1
0.0	0.0	0.0	1.00	1000000.0	1
0.0	0.0	0.0	1.00	1000000.0	1
0.0	0.0	0.0	1.00	1000000.0	1
0.0	0.0	0.0	1.00	1000000.0	1
0.0	0.0	0.0	1.00	1000000.0	1
0.0	0.0	0.0	1.00	1000000.0	1
0.0	0.0	0.0	1.00	1000000.0	1
0.0	0.0	0.0	1.00	1000000.0	1
0.0	0.0	0.0	1.00	1000000.0	1
0.0	0.0	0.0	1.00	1000000.0	1
0.0	0.0	0.0	1.00	1000000.0	1
0.0	0.0	0.0	1.00	1000000.0	1
0.0	0.0	0.0	1.00	1000000.0	1
0.0	0.0	0.0	1.00	1000000.0	1
0.0	0.0	0.0	1.00	1000000.0	1
0.0	0.0	0.0	1.00	1000000.0	1
0.0	0.0	0.0	1.00	1000000.0	1
0.0	0.0	0.0	1.00	1000000.0	1
0.0	0.0	0.0	1.00	1000000.0	1
0.0	0.0	0.0	1.00	1000000.0	1
0.0	0.0	0.0	1.00	1000000.0	1
0.0	0.0	0.0	1.00	1000000.0	1
0.0	0.0	0.0	1.00	1000000.0	1
0.0	0.0	0.0	1.00	1000000.0	1
0.0	0.0	0.0	1.00	1000000.0	1
0.0	0.0	0.0	1.00	1000000.0	1
0.0	0.0	0.0	1.00	1000000.0	1
0.0	0.0	0.0	1.00	1000000.0	1
0.0	0.0	0.0	1.00	1000000.0	1
0.0	0.0	0.0	1.00	1000000.0	1
0.0	0.0	0.0	1.00	1000000.0	1
0.0	0.0	0.0	1.00	1000000.0	1
0.0	0.0	0.0	1.00	1000000.0	1
0.0	0.0	0.0	1.00	1000000.0	1
0.0	0.0	0.0	1.00	1000000.0	1
0.0	0.0	0.0	1.00	1000000.0	1
0.0	0.0	0.0	1.00	1000000.0	1
0.0	0.0	0.0	1.00	1000000.0	1
0.0	0.0	0.0	1.00	1000000.0	1
0.0	0.0	0.0	1.00	1000000.0	1
0.0	0.0	0.0	1.00	1000000.0	1
0.0	0.0	0.0	1.00	1000000.0	1
0.0	0.0	0.0	1.00	1000000.0	1
0.0	0.0	0.0	1.00	1000000.0	1
0.0	0.0	0.0	1.00	1000000.0	1
0.0	0.0	0.0	1.00	1000000.0	1
0.0	0.0	0.0	1.00	1000000.0	1
80.0	0.0	0.0	1.00	1000000.0	1

160.0	0.0	0.0	1.00	1000000.0	1
240.0	0.0	0.0	1.00	1000000.0	1
320.0	0.0	0.0	1.00	1000000.0	1
0.0	80.0	0.0	1.00	1000000.0	1
80.0	80.0	0.0	1.00	1000000.0	1
160.0	80.0	0.0	1.00	1000000.0	1
240.0	80.0	0.0	1.00	1000000.0	1
320.0	80.0	0.0	1.00	1000000.0	1
0.0	160.0	0.0	1.00	1000000.0	1
80.0	160.0	0.0	1.00	1000000.0	1
160.0	160.0	0.0	1.00	1000000.0	1
240.0	160.0	0.0	1.00	1000000.0	1
320.0	160.0	0.0	1.00	1000000.0	1
0.0	240.0	0.0	1.00	1000000.0	1
80.0	240.0	0.0	1.00	1000000.0	1
160.0	240.0	0.0	1.00	1000000.0	1
240.0	240.0	0.0	1.00	1000000.0	1
320.0	240.0	0.0	1.00	1000000.0	1
0.0	320.0	0.0	1.00	1000000.0	1
80.0	320.0	0.0	1.00	1000000.0	1
160.0	320.0	0.0	1.00	1000000.0	1
240.0	320.0	0.0	1.00	1000000.0	1
320.0	320.0	0.0	1.00	1000000.0	1

EMS / KENO

The KENOVa input file for the calculation of case 1 is given below. The input file of Cases 2 and 3 only differ by the parameters gen and nsk which are increased by 200 for each case. In Case 2 this means gen=1200 and nsk=200 while in case 3 gen=1400 and nsk=400. This preserves the number of active cycles to 1000 for all cases. The input for the other 297 cases only involves a change of the parameter rnd. Some of the rnd numbers chosen had to be rejected by the user since they were interpreted by the KENOVa code as identical to previous numbers.

```
=csasi parm=size=3000000
SOURCE COINVERGENCE SERIES 4
238groupndf5 infhommedium
u-235 1 0 4.549E-2 293.0 end
u-238 1 0 2.56E-3 293.0 end
n 2 0 4.325E-5 293.0 end
o 2 0 1.081E-5 293.0 end
end comp
cellmix 1
end
kenova parm=size=1000000
Source convergence series 4 - Case 1
read param gen=1000 npg=125 nsk=0 fdn=yes xsc=14
res=200 wrs=94 lng=1000000 rnd=000000000000
end param
read geom
unit 1
com='Position (1,1) - R=8.71 cm'
sphere 1 1 8.71
cuboid 2 1 40 -40 40 -40 40 -40
unit 2
com='Pos (1,2) R=8.71 cm'
sphere 1 1 8.71
cuboid 2 1 40 -40 40 -40 40 -40
unit 3
com='Pos (1,3) R=8.71 cm'
sphere 1 1 8.71
cuboid 2 1 40 -40 40 -40 40 -40
unit 4
com='Pos (1,4) R=8.71 cm'
sphere 1 1 8.71
cuboid 2 1 40 -40 40 -40 40 -40
unit 5
com='Pos (1,5) R=8.71 cm'
sphere 1 1 8.71
cuboid 2 1 40 -40 40 -40 40 -40
unit 6
com='Pos (2,1) R=8.71 cm'
sphere 1 1 8.71
cuboid 2 1 40 -40 40 -40 40 -40
```

```
unit 7
com='Pos (2,2) R=8.71 cm'
sphere 1 1 8.71
cuboid 2 1 40 -40 40 -40 40 -40
unit 8
com='Pos (2,3) R=8.71 cm'
sphere 1 1 8.71
cuboid 2 1 40 -40 40 -40 40 -40
unit 9
com='Pos (2,4) R=8.71 cm'
sphere 1 1 8.71
cuboid 2 1 40 -40 40 -40 40 -40
unit 10
com='Pos (2,5) R=8.71 cm'
sphere 1 1 8.71
cuboid 2 1 40 -40 40 -40 40 -40
unit 11
com='Pos (3,1) R=8.71 cm'
sphere 1 1 8.71
cuboid 2 1 40 -40 40 -40 40 -40
unit 12
com='Pos (3,2) R=8.71 cm'
sphere 1 1 8.71
cuboid 2 1 40 -40 40 -40 40 -40
unit 13
com='Pos (3,3) R=10.0 cm'
sphere 1 1 10
cuboid 2 1 40 -40 40 -40 40 -40
unit 14
com='Pos (3,4) R=8.71 cm'
sphere 1 1 8.71
cuboid 2 1 40 -40 40 -40 40 -40
unit 15
com='Pos (3,5) R=8.71 cm'
sphere 1 1 8.71
cuboid 2 1 40 -40 40 -40 40 -40
unit 16
com='Pos (4,1) R=8.71 cm'
sphere 1 1 8.71
cuboid 2 1 40 -40 40 -40 40 -40
unit 17
com='Pos (4,2) R=8.71 cm'
sphere 1 1 8.71
cuboid 2 1 40 -40 40 -40 40 -40
unit 18
com='Pos (4,3) R=8.71 cm'
sphere 1 1 8.71
cuboid 2 1 40 -40 40 -40 40 -40
unit 19
com='Pos (4,4) R=8.71 cm'
```

```
sphere 1 1 8.71
cuboid 2 1 40 -40 40 -40 40 -40
unit 20
com='Pos (4,5) R=8.71 cm'
sphere 1 1 8.71
cuboid 2 1 40 -40 40 -40 40 -40
unit 21
com='Pos (5,1) R=8.71 cm'
sphere 1 1 8.71
cuboid 2 1 40 -40 40 -40 40 -40
unit 22
com='Pos (5,2) R=8.71 cm'
sphere 1 1 8.71
cuboid 2 1 40 -40 40 -40 40 -40
unit 23
com='Pos (5,3) R=8.71 cm'
sphere 1 1 8.71
cuboid 2 1 40 -40 40 -40 40 -40
unit 24
com='Pos (5,4) R=8.71 cm'
sphere 1 1 8.71
cuboid 2 1 40 -40 40 -40 40 -40
unit 25
com='Pos (5,5) R=8.71 cm'
sphere 1 1 8.71
cuboid 2 1 40 -40 40 -40 40 -40
global unit 26
com='5x5x1'
array 1 0 0 0
end geom
read array
ara=1 nux=5 nuy=5 nuz=1
com='5x5x1 array'
fill 1 2 3 4 5 6 7 8 9 10 11 12 13 14 15 16 17 18 19 20 21 22 23 24 25
end fill
end array
read start
nst=6
NXS=1 NYS=1 NZS=1 LNU=101
NXS=2 NYS=1 NZS=1 LNU=102
NXS=3 NYS=1 NZS=1 LNU=103
NXS=4 NYS=1 NZS=1 LNU=104
NXS=5 NYS=1 NZS=1 LNU=105
NXS=1 NYS=2 NZS=1 LNU=106
NXS=2 NYS=2 NZS=1 LNU=107
NXS=3 NYS=2 NZS=1 LNU=108
NXS=4 NYS=2 NZS=1 LNU=109
NXS=5 NYS=2 NZS=1 LNU=110
NXS=1 NYS=3 NZS=1 LNU=111
NXS=2 NYS=3 NZS=1 LNU=112
```

NXS=3 NYS=3 NZS=1 LNU=113
NXS=4 NYS=3 NZS=1 LNU=114
NXS=5 NYS=3 NZS=1 LNU=115
NXS=1 NYS=4 NZS=1 LNU=116
NXS=2 NYS=4 NZS=1 LNU=117
NXS=3 NYS=4 NZS=1 LNU=118
NXS=4 NYS=4 NZS=1 LNU=119
NXS=5 NYS=4 NZS=1 LNU=120
NXS=1 NYS=5 NZS=1 LNU=121
NXS=2 NYS=5 NZS=1 LNU=122
NXS=3 NYS=5 NZS=1 LNU=123
NXS=4 NYS=5 NZS=1 LNU=124
NXS=5 NYS=5 NZS=1 LNU=125
end start
end data
end

IPPE / KENO

```
=cons9901
TASK:
*
* benchm4-01
*
 MULTIC = 1
 NOUT  = 2
 IHT   = 4
 IHS   = 77
 NG    = 299
 IPRIB = 0
 IDELTA= 0
 THERM = 1
 NMOM  = 5
 IZT   = 2
 INZ   = 4
 NRZT  = 2
 ICOR  = 1 2
 MAT   = 1000 2000
 NAME  = 'U235' 'U238' 'N' 'O'
 RO    =
*FUEL
 4.549E-02   2.560E-03  0. 0.
*AIR
 0. 0. 4.325E-05  1.081E-05
 END
end
=lava
-1$$  170000
 0$$  30 50 18 19
 1$$  2 299 4 77 375 227 0 -1 1 t
 2$$  1000 2000
 3$$  f5
 4$$  1000 2000
 5$$  1 1452 27 1018
 7**
  2.00000E+07  1.86182E+07  1.73318E+07  1.61343E+07  1.50195E+07  1.39818E+07
  1.30158E+07  1.21165E+07  1.12793E+07  1.05000E+07  9.69341E+06  8.94878E+06
  8.26136E+06  7.62674E+06  7.04087E+06  6.50000E+06  5.99475E+06  5.52878E+06
  5.09902E+06  4.70267E+06  4.33713E+06  4.00000E+06  3.69862E+06  3.41995E+06
  3.16228E+06  2.92402E+06  2.70371E+06  2.50000E+06  2.32522E+06  2.16265E+06
  2.01146E+06  1.87083E+06  1.74003E+06  1.61838E+06  1.50524E+06  1.40000E+06
  1.30541E+06  1.21722E+06  1.13498E+06  1.05830E+06  9.86800E+05  9.20131E+05
  8.57965E+05  8.00000E+05  7.40700E+05  6.85795E+05  6.34961E+05  5.87894E+05
  5.44316E+05  5.03968E+05  4.66612E+05  4.32024E+05  4.00000E+05  3.70350E+05
  3.42898E+05  3.17480E+05  2.93947E+05  2.72158E+05  2.51984E+05  2.33306E+05
  2.16012E+05  2.00000E+05  1.85175E+05  1.71449E+05  1.58740E+05  1.46974E+05
  1.36079E+05  1.25992E+05  1.16653E+05  1.08006E+05  1.00000E+05  9.38042E+04
  8.79923E+04  8.25404E+04  7.74264E+04  7.26292E+04  6.81292E+04  6.39081E+04
```

5.99484E+04 5.62341E+04 5.27500E+04 4.94817E+04 4.64159E+04 4.35401E+04
4.08424E+04 3.83119E+04 3.59381E+04 3.37115E+04 3.16228E+04 2.96635E+04
2.78256E+04 2.61016E+04 2.44844E+04 2.29674E+04 2.15443E+04 2.02095E+04
1.89574E+04 1.77828E+04 1.66810E+04 1.56475E+04 1.46780E+04 1.37686E+04
1.29155E+04 1.21153E+04 1.13646E+04 1.06605E+04 1.00000E+04 9.38042E+03
8.79923E+03 8.25404E+03 7.74264E+03 7.26292E+03 6.81292E+03 6.39081E+0
5.99484E+03 5.62341E+03 5.27500E+03 4.94817E+03 4.64159E+03 4.35400E+03
4.08424E+03 3.83119E+03 3.59381E+03 3.37115E+03 3.16228E+03 2.96635E+03
2.78256E+03 2.61016E+03 2.44844E+03 2.29674E+03 2.15444E+03 2.02095E+03
1.89574E+03 1.77828E+03 1.66810E+03 1.56475E+03 1.46780E+03 1.37686E+03
1.29155E+03 1.21153E+03 1.13646E+03 1.06605E+03 1.00000E+03 9.38042E+02
8.79923E+02 8.25404E+02 7.74264E+02 7.26292E+02 6.81292E+02 6.39081E+02
5.99484E+02 5.62341E+02 5.27500E+02 4.94817E+02 4.64159E+02 4.35400E+02
4.08424E+02 3.83119E+02 3.59381E+02 3.37115E+02 3.16228E+02 2.96635E+02
2.78256E+02 2.61016E+02 2.44844E+02 2.29674E+02 2.15443E+02 2.02095E+02
1.89574E+02 1.77828E+02 1.66810E+02 1.56475E+02 1.46780E+02 1.37686E+02
1.29155E+02 1.21153E+02 1.13646E+02 1.06605E+02 1.00000E+02 9.38042E+01
8.79923E+01 8.25404E+01 7.74264E+01 7.26292E+01 6.81292E+01 6.39081E+01
5.99484E+01 5.62341E+01 5.27500E+01 4.94817E+01 4.64159E+01 4.35401E+01
4.08424E+01 3.83119E+01 3.59381E+01 3.37115E+01 3.16228E+01 2.96635E+01
2.78256E+01 2.61016E+01 2.44844E+01 2.29674E+01 2.15443E+01 2.02095E+01
1.89574E+01 1.77828E+01 1.66810E+01 1.56475E+01 1.46780E+01 1.37686E+01
1.29155E+01 1.21153E+01 1.13646E+01 1.06605E+01 1.00000E+01 9.38042E+00
8.79923E+00 8.25404E+00 7.74264E+00 7.26292E+00 6.81292E+00 6.39080E+00
5.99484E+00 5.62341E+00 5.27500E+00 4.94817E+00 4.64159E+00 4.35400E+00
4.08424E+00 3.83119E+00 3.59381E+00 3.37115E+00 3.16228E+00 2.96635E+00
2.78256E+00 2.61016E+00 2.44844E+00 2.29674E+00 2.15443E+00 2.02095E+00
1.89574E+00 1.77828E+00 1.66810E+00 1.56475E+00 1.46780E+00 1.37686E+00
1.29155E+00 1.21153E+00 1.13646E+00 1.06605E+00 1.00000E+00 9.38042E-01
8.79922E-01 8.25404E-01 7.74263E-01 7.26291E-01 6.81292E-01 6.39080E-01
5.99484E-01 5.62341E-01 5.27499E-01 4.94816E-01 4.64158E-01 4.35400E-01
4.08423E-01 3.83118E-01 3.59381E-01 3.37114E-01 3.16227E-01 2.96634E-01
2.78255E-01 2.61015E-01 2.44843E-01 2.29673E-01 2.15443E-01 1.89573E-01
1.66810E-01 1.46780E-01 1.29155E-01 1.13646E-01 1.00000E-01 8.25404E-02
6.81292E-02 5.62341E-02 4.64159E-02 3.83119E-02 3.16228E-02 2.61016E-02
2.15444E-02 1.77828E-02 1.46780E-02 1.21153E-02 1.00000E-02 6.81292E-03
4.64158E-03 3.16227E-03 2.15443E-03 1.00000E-03 1.00000E-04 1.00000E-05
9$$ f0 t
end
#sc_bin
50
51
end
=kenova
benchm4-01.
read param
tme=3000
lib=51
gen=1000
npg=125

```
nsk=0
lng=2000000
nb8=4000
rnd=100010001
fdn=yes
mkp=yes
run=yes
plt=no
end param
read mixt
sct=3
eps=1.
mix= 1  1000 1.
mix= 2  2000 1.
end mixt
read geometry
unit 1
sphere 1 1 8.71
cuboid 2 1 6p40.
unit 2
sphere 1 1 10.
cuboid 2 1 6p40.
unit 3
sphere 1 1 8.71
cuboid 2 1 6p40.
unit 4
sphere 1 1 8.71
cuboid 2 1 6p40.
end geometry
read array
 gbl=1 ara=1 nux=5 nuy=5 nuz=1
 fill 1 11R4 2 11R4 3 end fill
end array
read start
 nst=6
 nxs=1 nys=1 nzs=1 tfx=0. tfy=0. tfz=0. lnu=101
 nxs=2 nys=1 nzs=1 tfx=0. tfy=0. tfz=0. lnu=102
 nxs=3 nys=1 nzs=1 tfx=0. tfy=0. tfz=0. lnu=103
 nxs=4 nys=1 nzs=1 tfx=0. tfy=0. tfz=0. lnu=104
 nxs=5 nys=1 nzs=1 tfx=0. tfy=0. tfz=0. lnu=105
 nxs=1 nys=2 nzs=1 tfx=0. tfy=0. tfz=0. lnu=106
 nxs=2 nys=2 nzs=1 tfx=0. tfy=0. tfz=0. lnu=107
 nxs=3 nys=2 nzs=1 tfx=0. tfy=0. tfz=0. lnu=108
 nxs=4 nys=2 nzs=1 tfx=0. tfy=0. tfz=0. lnu=109
 nxs=5 nys=2 nzs=1 tfx=0. tfy=0. tfz=0. lnu=110
 nxs=1 nys=3 nzs=1 tfx=0. tfy=0. tfz=0. lnu=111
 nxs=2 nys=3 nzs=1 tfx=0. tfy=0. tfz=0. lnu=112
 nxs=3 nys=3 nzs=1 tfx=0. tfy=0. tfz=0. lnu=113
 nxs=4 nys=3 nzs=1 tfx=0. tfy=0. tfz=0. lnu=114
 nxs=5 nys=3 nzs=1 tfx=0. tfy=0. tfz=0. lnu=115
```

```
 nxs=1 nys=4 nzs=1 tfx=0. tfy=0. tfz=0. lnu=116
 nxs=2 nys=4 nzs=1 tfx=0. tfy=0. tfz=0. lnu=117
 nxs=3 nys=4 nzs=1 tfx=0. tfy=0. tfz=0. lnu=118
 nxs=4 nys=4 nzs=1 tfx=0. tfy=0. tfz=0. lnu=119
 nxs=5 nys=4 nzs=1 tfx=0. tfy=0. tfz=0. lnu=120
 nxs=1 nys=5 nzs=1 tfx=0. tfy=0. tfz=0. lnu=121
 nxs=2 nys=5 nzs=1 tfx=0. tfy=0. tfz=0. lnu=122
 nxs=3 nys=5 nzs=1 tfx=0. tfy=0. tfz=0. lnu=123
 nxs=4 nys=5 nzs=1 tfx=0. tfy=0. tfz=0. lnu=124
 nxs=5 nys=5 nzs=1 tfx=0. tfy=0. tfz=0. lnu=125
end start
read plot
scr=yes
lpi=10
ttl='x-y plot'
pic=mix
xul= -40.  yul= 40.    zul=0.
xlr= 40.  ylr=-40.    zlr=0.
uax=1.0 vdn=-1.0
nax=800 end
end plot
end data
end
```

IRSN / MORET

```
Reseau de 5x5x1 spheres d'uranium tres enrichi, distance de 80 cm
*          5 x 5 x 1 spheres
MINI 1000 SIGI 0.1 SIGE 0.1 PAS 1
NOBIL
GEOM
*     BOITE EXTERIEUR    AIR
TYPE 1 BOIT 180. 180. 20. VOLU   26   0    1    1    0.0   0.0  0.0
RBOIT   0. 0. 0. 0. 0. 0.
* sphere  rayon 8.71 cm
TYPE 2 SPHE 8.71
                    VOLU   1    26   2    2    -160.0    160.0     0.
                    VOLU   2    26   2    2    -160.0     80.0     0.
                    VOLU   3    26   2    2    -160.0      0.0     0.
                    VOLU   4    26   2    2    -160.0    -80.0     0.
                    VOLU   5    26   2    2    -160.0   -160.0     0.
                    VOLU   6    26   2    2     -80.0    160.0     0.
                    VOLU   7    26   2    2     -80.0     80.0     0.
                    VOLU   8    26   2    2     -80.0      0.0     0.
                    VOLU   9    26   2    2     -80.0    -80.0     0.
                    VOLU   10   26   2    2     -80.0   -160.0     0.
                    VOLU   11   26   2    2       0.0    160.0     0.
                    VOLU   12   26   2    2       0.0     80.0     0.
*
* sphere centrale rayon 10 cm
TYPE 3 SPHE 10.         VOLU   13   26   3    2    0.0      0.0  0.
```

```
*
                VOLU  14   26   2    2      0.0    -80.0     0.
                VOLU  15   26   2    2      0.0   -160.0     0.
                VOLU  16   26   2    2     80.0    160.0     0.
                VOLU  17   26   2    2     80.0     80.0     0.
                VOLU  18   26   2    2     80.0      0.0     0.
                VOLU  19   26   2    2     80.0    -80.0     0.
                VOLU  20   26   2    2     80.0   -160.0     0.
                VOLU  21   26   2    2    160.0    160.0     0.
                VOLU  22   26   2    2    160.0     80.0     0.
                VOLU  23   26   2    2    160.0      0.0     0.
                VOLU  24   26   2    2    160.0    -80.0     0.
                VOLU  25   26   2    2    160.0   -160.0     0.
FING
CHIMIE MACRO 1 1 AIR 1
      MICRO 1 2       U235      U238
            CONC   0.04549   0.00256
FINC
SOURCE  NRES  POINT 100 5 -160. -160. 0.
           SUNI   25
FINS
ALEA 1
SIMU
  NATU
  DEBU 0
  *   matrice
  MATR 4
    1  13
    4  8  12  14  18
    4  7   9  17  19
    16 1   2   3   4  5  6  10 11 15  16  20 21 22 23 24 25
FSIM
FIND
```

JNC / KENO

```
=csas25   parm=size=1000000
source convergence test 4 (case1)
27groupndf4  infhommedium
'High enriched uranium metal
u-235    1  0  4.549-2  end
u-238    1  0  2.560-3  end
'Air
n        2  0  4.3250-5  end
o        2  0  1.0810-5  end
end comp
test 4 (case1) geometry
read parm  rnd=94b119fb92c3   tme=300
```

```
 gen=11000  npg=10000 nsk=1000 plt=no far=yes gas=no
end parm
read geometry
unit 1
com='position(1,1)'
sphere    1 1  8.71
cuboid    2 1  40.0  -80.0   40.0  -80.0   80.0  -80.0
unit 2
com='position(1,2)'
sphere    1 1  8.71
cuboid    2 1  40.0  -40.0   40.0  -80.0   80.0  -80.0
unit 3
com='position(1,3)'
sphere    1 1  8.71
cuboid    2 1  40.0  -40.0   40.0  -80.0   80.0  -80.0
unit 4
com='position(1,4)'
sphere    1 1  8.71
cuboid    2 1  40.0  -40.0   40.0  -80.0   80.0  -80.0
unit 5
com='position(1,5)'
sphere    1 1  8.71
cuboid    2 1  80.0  -40.0   40.0  -80.0   80.0  -80.0
unit 6
com='position(2,1)'
sphere    1 1  8.71
cuboid    2 1  40.0  -80.0   40.0  -40.0   80.0  -80.0
unit 7
com='position(2,2)'
sphere    1 1  8.71
cuboid    2 1  40.0  -40.0   40.0  -40.0   80.0  -80.0
unit 8
com='position(2,3)'
sphere    1 1  8.71
cuboid    2 1  40.0  -40.0   40.0  -40.0   80.0  -80.0
unit 9
com='position(2,4)'
sphere    1 1  8.71
cuboid    2 1  40.0  -40.0   40.0  -40.0   80.0  -80.0
unit 10
com='position(2,5)'
sphere    1 1  8.71
cuboid    2 1  80.0  -40.0   40.0  -40.0   80.0  -80.0
unit 11
com='position(3,1)'
sphere    1 1  8.71
cuboid    2 1  40.0  -80.0   40.0  -40.0   80.0  -80.0
unit 12
com='position(3,2)'
sphere    1 1  8.71
```

```
cuboid    2 1  40.0  -40.0   40.0  -40.0   80.0  -80.0
unit 13
com='position(3,3)'
sphere    1 1  10.0
cuboid    2 1  40.0  -40.0   40.0  -40.0   80.0  -80.0
unit 14
com='position(3,4)'
sphere    1 1  8.71
cuboid    2 1  40.0  -40.0   40.0  -40.0   80.0  -80.0
unit 15
com='position(3,5)'
sphere    1 1  8.71
cuboid    2 1  80.0  -40.0   40.0  -40.0   80.0  -80.0
unit 16
com='position(4,1)'
sphere    1 1  8.71
cuboid    2 1  40.0  -80.0   40.0  -40.0   80.0  -80.0
unit 17
com='position(4,2)'
sphere    1 1  8.71
cuboid    2 1  40.0  -40.0   40.0  -40.0   80.0  -80.0
unit 18
com='position(4,3)'
sphere    1 1  8.71
cuboid    2 1  40.0  -40.0   40.0  -40.0   80.0  -80.0
unit 19
com='position(4,4)'
sphere    1 1  8.71
cuboid    2 1  40.0  -40.0   40.0  -40.0   80.0  -80.0
unit 20
com='position(4,5)'
sphere    1 1  8.71
cuboid    2 1  80.0  -40.0   40.0  -40.0   80.0  -80.0
unit 21
com='position(5,1)'
sphere    1 1  8.71
cuboid    2 1  40.0  -80.0   80.0  -40.0   80.0  -80.0
unit 22
com='position(5,2)'
sphere    1 1  8.71
cuboid    2 1  40.0  -40.0   80.0  -40.0   80.0  -80.0
unit 23
com='position(5,3)'
sphere    1 1  8.71
cuboid    2 1  40.0  -40.0   80.0  -40.0   80.0  -80.0
unit 24
com='position(5,4)'
sphere    1 1  8.71
cuboid    2 1  40.0  -40.0   80.0  -40.0   80.0  -80.0
unit 25
```

```
com='position(5,5)'
sphere    1 1  8.71
cuboid    2 1  80.0  -40.0   80.0  -40.0   80.0  -80.0
global unit 30
array 1  0.0  0.0  0.0
cuboid    0 1  480.0  0.0   480.0  0.0   160.0  0.0
end geometry
read array
gbl=1 ara=1 nux=5 nuy=5 nuz=1 fill
  1  2  3  4  5
  6  7  8  9 10
 11 12 13 14 15
 16 17 18 19 20
 21 22 23 24 25 end fill
end array
read start
nst=2
nxs=3 nys=3 nzs=1 fct=0.90
psp=yes
end start
end data
end
```

LANL / MCNP

```
OECD/NEA Source Convergence Test 4:Array of Interacting Spheres
c         case = 1
c
c         Test defined by Jacquet (IPSN/DPEA/SEC)
c         Implemented for MCNP by R.C.Little (June 2001)
c
c         Case 1,4,7,...298: 0 skipped generations
c         Case 2,5,8,...299: 200 skipped generations
c         Case 3,6,9,...300: 400 skipped generations
c
c         There are 100 replicas for each number of skipped generations
c         The initial random number is chosen to be (N*1000)+1
c
c         Case:    1
c         Skipped Generations:    0
c         Total Generations:        1000
c         Initial Random Number:           1001
c
c         Cell Cards
c
c         cells 1-25 are the spheres of uranium metal
c         1-12 and 14-25 are radius 8.71 cm
c         13 has radius of 10.0 cm
1         1 .04805 -1
2         1 .04805 -2
```

```
3       1 .04805 -3
4       1 .04805 -4
5       1 .04805 -5
6       1 .04805 -6
7       1 .04805 -7
8       1 .04805 -8
9       1 .04805 -9
10      1 .04805 -10
11      1 .04805 -11
12      1 .04805 -12
13      1 .04805 -13
14      1 .04805 -14
15      1 .04805 -15
16      1 .04805 -16
17      1 .04805 -17
18      1 .04805 -18
19      1 .04805 -19
20      1 .04805 -20
21      1 .04805 -21
22      1 .04805 -22
23      1 .04805 -23
24      1 .04805 -24
25      1 .04805 -25
c
c       Air -- Inside Box; Outside Spheres
26      2 5.406e-05 26 -27 28 -29 30 -31 1 2 3 4 5 6 7 8 9 10
        11 12 13 14 15 16 17 18 19 20 21 22 23 24 25
c
c       External World (void)
27      0 -26:27:-28:29:-30:31

c
c       Surface Cards
c
c       24 Small Spheres (surfaces 1-12; 14-25)
c       1 Large Sphere (surface 13)
1       s       80      80 0 8.71
2       s 160   80 0 8.71
3       s 240   80 0 8.71
4       s 320   80 0 8.71
5       s 400   80 0 8.71
6       s       80 160 0 8.71
7       s 160 160 0 8.71
8       s 240 160 0 8.71
9       s 320 160 0 8.71
10      s 400 160 0 8.71
11      s       80 240 0 8.71
12      s 160 240 0 8.71
13      s 240 240 0 10.0
14      s 320 240 0 8.71
```

```
15        s 400 240 0 8.71
16        s         80 320 0 8.71
17        s 160 320 0 8.71
18        s 240 320 0 8.71
19        s 320 320 0 8.71
20        s 400 320 0 8.71
21        s         80 400 0 8.71
22        s 160 400 0 8.71
23        s 240 400 0 8.71
24        s 320 400 0 8.71
25        s 400 400 0 8.71
c
c         6 Planes to Bound Box of Air
26        px 0
27        px 480
28        py 0
29        py 480
30        pz -80
31        pz 80

c
c         Material Cards
c
c         M1 - Highly Enriched Uranium Metal
m1        92235 .04549 92238 2.56e-03
c
c         M2 - Air
m2        7014 4.325e-05 8016 1.081e-05
c
c         Miscellaneous Cards
c
mode n
imp:n 1 25r 0
print 130
dbcn 1001
c
c         I chose *not* to print out cumulative source distribution at each cycle
c         prdmp 1
c
c         KCODE Cards
c
c         125 neutrons per cycle
c         initial distribution:
c         101 neutrons in center of sphere # 1
c         1 neutron in center of each of the other 24 spheres
c         initial k_eff estimate of 1.11 is from preliminary calculations
kcode 125 1.11 0 1000
ksrc  80 80 0       80 80 0       80 80 0       80 80 0       80 80 0       80 80 0
      80 80 0       80 80 0       80 80 0       80 80 0       80 80 0       80 80 0
      80 80 0       80 80 0       80 80 0       80 80 0       80 80 0       80 80 0
```

```
          80 80 0      80 80 0      80 80 0      80 80 0      80 80 0      80 80 0
          80 80 0      80 80 0      80 80 0      80 80 0      80 80 0      80 80 0
          80 80 0      80 80 0      80 80 0      80 80 0      80 80 0      80 80 0
          80 80 0      80 80 0      80 80 0      80 80 0      80 80 0      80 80 0
          80 80 0      80 80 0      80 80 0      80 80 0      80 80 0      80 80 0
          80 80 0      80 80 0      80 80 0      80 80 0      80 80 0      80 80 0
          80 80 0      80 80 0      80 80 0      80 80 0      80 80 0      80 80 0
          80 80 0      80 80 0      80 80 0      80 80 0      80 80 0      80 80 0
          80 80 0      80 80 0      80 80 0      80 80 0      80 80 0      80 80 0
          80 80 0      80 80 0      80 80 0      80 80 0      80 80 0      80 80 0
          80 80 0      80 80 0      80 80 0      80 80 0      80 80 0      80 80 0
          80 80 0      80 80 0      80 80 0      80 80 0      80 80 0      80 80 0
          80 80 0      80 80 0      80 80 0      80 80 0      80 80 0      80 80 0
          80 80 0      80 80 0      80 80 0      80 80 0      80 80 0
          80 160 0     80 240 0     80 320 0     80 400 0
          160 80 0     160 160 0    160 240 0    160 320 0    160 400 0
          240 80 0     240 160 0    240 240 0    240 320 0    240 400 0
          320 80 0     320 160 0    320 240 0    320 320 0    320 400 0
          400 80 0     400 160 0    400 240 0    400 320 0    400 400 0
c
c      tally cards
c
c      f4:n neutron flux tally in each of the 25 spheres
c      multiply the flux tally by the fission cross section (fm -6)
c      to get fission fractions in each sphere
c
f4:n 1 23i 25
fm4 -1 1 -
```

ORNL / KENO

```
=csas25     parm=(size=1000000)
test 4 - case 1
238group   infhommedium
u-235    1 0 4.549-2 300 end u-235
u-238    1 0 2.560-3 300 end u-238
n        2 0 4.325-5 300 end n
o        2 0 1.081-5 300 end o
end comp
test 4 - case 1
read parm nb8=500 nsk=000 gen=1000 fdn=yes
  rnd=100010001 npg=125 wrs=31 end parm
read geom
  unit 1
  sphere  1 1 8.71
  cuboid  2 1 6p40
  unit 2
  sphere  1 1 8.71
```

```
cuboid  2 1 6p40
unit 3
sphere  1 1 8.71
cuboid  2 1 6p40
unit 4
sphere  1 1 8.71
cuboid  2 1 6p40
unit 5
sphere  1 1 8.71
cuboid  2 1 6p40
unit 6
sphere  1 1 8.71
cuboid  2 1 6p40
unit 7
sphere  1 1 8.71
cuboid  2 1 6p40
unit 8
sphere  1 1 8.71
cuboid  2 1 6p40
unit 9
sphere  1 1 8.71
cuboid  2 1 6p40
unit 10
sphere  1 1 8.71
cuboid  2 1 6p40
unit 11
sphere  1 1 8.71
cuboid  2 1 6p40
unit 12
sphere  1 1 8.71
cuboid  2 1 6p40
unit 13
sphere  1 1 10
cuboid  2 1 6p40
unit 14
sphere  1 1 8.71
cuboid  2 1 6p40
unit 15
sphere  1 1 8.71
cuboid  2 1 6p40
unit 16
sphere  1 1 8.71
cuboid  2 1 6p40
unit 17
sphere  1 1 8.71
cuboid  2 1 6p40
unit 18
sphere  1 1 8.71
cuboid  2 1 6p40
unit 19
```

```
  sphere  1 1 8.71
  cuboid  2 1 6p40
  unit 20
  sphere  1 1 8.71
  cuboid  2 1 6p40
  unit 21
  sphere  1 1 8.71
  cuboid  2 1 6p40
  unit 22
  sphere  1 1 8.71
  cuboid  2 1 6p40
  unit 23
  sphere  1 1 8.71
  cuboid  2 1 6p40
  unit 24
  sphere  1 1 8.71
  cuboid  2 1 6p40
  unit 25
  sphere  1 1 8.71
  cuboid  2 1 6p40
end geom
read array
  gbl=1 ara=1 nux=5 nuy=5 nuz=1 fill 23i1 25 end fill
end array
read start
  nst=6  ps6=no
  nxs=1 nys=1 nzs=1 tfx=0 tfy=0 tfz=0 lnu=101
  nxs=2 nys=1 nzs=1 tfx=0 tfy=0 tfz=0 lnu=102
  nxs=3 nys=1 nzs=1 tfx=0 tfy=0 tfz=0 lnu=103
  nxs=4 nys=1 nzs=1 tfx=0 tfy=0 tfz=0 lnu=104
  nxs=5 nys=1 nzs=1 tfx=0 tfy=0 tfz=0 lnu=105
  nxs=1 nys=2 nzs=1 tfx=0 tfy=0 tfz=0 lnu=106
  nxs=2 nys=2 nzs=1 tfx=0 tfy=0 tfz=0 lnu=107
  nxs=3 nys=2 nzs=1 tfx=0 tfy=0 tfz=0 lnu=108
  nxs=4 nys=2 nzs=1 tfx=0 tfy=0 tfz=0 lnu=109
  nxs=5 nys=2 nzs=1 tfx=0 tfy=0 tfz=0 lnu=110
  nxs=1 nys=3 nzs=1 tfx=0 tfy=0 tfz=0 lnu=111
  nxs=2 nys=3 nzs=1 tfx=0 tfy=0 tfz=0 lnu=112
  nxs=3 nys=3 nzs=1 tfx=0 tfy=0 tfz=0 lnu=113
  nxs=4 nys=3 nzs=1 tfx=0 tfy=0 tfz=0 lnu=114
  nxs=5 nys=3 nzs=1 tfx=0 tfy=0 tfz=0 lnu=115
  nxs=1 nys=4 nzs=1 tfx=0 tfy=0 tfz=0 lnu=116
  nxs=2 nys=4 nzs=1 tfx=0 tfy=0 tfz=0 lnu=117
  nxs=3 nys=4 nzs=1 tfx=0 tfy=0 tfz=0 lnu=118
  nxs=4 nys=4 nzs=1 tfx=0 tfy=0 tfz=0 lnu=119
  nxs=5 nys=4 nzs=1 tfx=0 tfy=0 tfz=0 lnu=120
  nxs=1 nys=5 nzs=1 tfx=0 tfy=0 tfz=0 lnu=121
  nxs=2 nys=5 nzs=1 tfx=0 tfy=0 tfz=0 lnu=122
  nxs=3 nys=5 nzs=1 tfx=0 tfy=0 tfz=0 lnu=123
  nxs=4 nys=5 nzs=1 tfx=0 tfy=0 tfz=0 lnu=124
```

```
  nxs=5 nys=5 nzs=1 tfx=0 tfy=0 tfz=0 lnu=125
end start
read mixt   sct=3 eps=1    end mixt
end data
end
```

Appendix 5.b
COMMENTS

EMS (Dennis Mennerdahl)

Convergence of fission fractions in all units is not necessarily required for convergence of k_{eff}. However, convergence of fission fractions in the larger unit in the center is vital in this problem.

The system includes unmoderated and unreflected fissionable material. The number of collisions of an average neutron after fission is very low compared with a moderated and reflected system. To get acceptable statistics, it is well known to criticality safety specialists that more neutron histories are required than for moderated and reflected systems. The extra calculation time needed for more neutron histories is compensated with the reduced number of collisions.

The statistics obtained from the postulated input for this test series are not very good. A poor initial neutron source distribution slows convergence. In most cases, after skipping the first 50 000 neutrons, the following 125 000 "active" neutrons result in reasonable values of k_{eff} and fission fraction for the central unit. In a typical validation of a method, it is likely that a good value would be reported. However, as can be seen in several cases, some of the values are significantly in error, much more than what the standard deviation indicates. A bad start (a specific random number together with the chosen start distribution) takes a long time to recover. This can be seen from results using the same random number seed but with different numbers of neutrons skipped.

The statistical uncertainties for the fission fractions are very large for the locations (1,1) and (5,5). KENOVa gives the uncertainty as a percentage. Since the fission rates include many generations before the fission distribution has converged, the uncertainties are even more unreliable than the fission rates. For the smaller units in locations (1,1) and (5,5), the uncertainties given by KENOVa grow considerably when the number of skipped generations is increased. For the large unit in location (3,3) the reverse is noted.

For the best model (400 generations skipped) the uncertainties vary between 9 and 100 percent for location (1,1). When no generations are skipped, while keeping the active generations to 1 000, the variation is reduced to between 3 and 22 per cent. This is clearly misleading. For the location (5,5) the trend is not so clear. The uncertainties are always large for this location. For the large central unit in location (3,3), the cases when 400 generations are skipped result in the smallest uncertainties. A few calculations resulted in an uncertainty larger than 1 (maximum 1.75) per cent, but most gave less than 0.5 per cent uncertainty. Not surprisingly, the cases with the largest fission rate uncertainties in the central unit correspond to those giving the lowest values of k_{eff}.

Source convergence related to fission fractions could be defined as a fixed limit below which the fission fraction deviation is acceptable. It is clear that source convergence related to k_{eff} and to criticality safety does not necessarily require source convergence related to fission rates in every part of the fissionable material. Source convergence related to k_{eff} is difficult to define without knowing the correct result. The correct result can be estimated using a combination of good understanding of the physics of the problem, understanding of the causes of slow convergence, results from calculations using simplified models, etc.

Selection of random number seeds

The input random seed is a 12 digit hexadecimal number. An initial seed of 000000000000 was selected (not a random choice). To get 100 different seeds, the previous seed was modified by changing

one or a few figures in various positions. The random number seeds are given in the previous tables. It turned out that several of the first selection of seeds generated identical random number sequences. New seeds were selected to replace those duplicated sequences. Later, Lester Petrie from ORNL informed me how the random number seed works on a PC. The 12-figure input seed is actually divided into three 4-figure seeds added together. A 1 in the last position of each 4-figure number is changed into a 0. This is something that I had already observed, but I was pleased to hear that it was a known design "feature".

Another observation is that a random number seed given in the KENOVa input gives different random number sequences depending on the SCALE sequence in which KENOVa is run. If CSAS25 is used with a random number given in the parameter input for KENOVa, the result will be different than if the same code modules were run separately, ending with a KENOVa run. I only generated the cross sections once and saved them in an ICE-format for later KENOVa use. The memory use of KENOVa is smaller in this case since the cross section mixing requires more direct access data blocks. The major purpose is however to save time. Three hundred cases can use the same cross section subset instead of preparing new (but identical) cross sections for each case.

*LANL (**Robert C. Little**)*

Description of Calculations

All calculations were performed with MCNP4C2 (load date 01/20/01) on a SUN Ultra 80. Cross sections are all from the ENDF60 library, which is based on ENDF/B-VI Release 2. MCNP ZAID identifiers are 7014.60c, 8016.60c, 92235.60c and 92238.60c.

Bounding planes were specified in each dimension at 80 cm perpendicular from the center of the exterior spheres. Neutrons crossing these surfaces were killed. For replica N (N=1,100), the starting random number was chosen to be 1000 * N + 1. The quantity neutron flux times fission cross section times material number density was tallied in each of the 25 spheres. The tally is calculated over all active cycles, not for each individual cycle.

Required Output

The required output for each case is part of the test specification. For each of the 300 cases we produced a simple text file with this output. The text files were combined to form one continuous text file and were transmitted electronically to Olivier Jacquet.

The first 12 lines of results for each case include the case number, some summary description, and contact information. The next 4 lines provide the number of skipped generations, the number of active generations, the number of histories per generation, and the number of generations per superhistory. For MCNP this latter quantity is always 1. The next two lines contain the final k_{eff} estimate and the one standard deviation absolute (not relative) uncertainty. The values reported here are from the MCNP combined collision / absorption / track-length estimator. For readability we then skip a line. Then we report the individual k_{eff} estimate for each cycle. For these results we use the MCNP collision estimator. Results are reported for each cycle (inactive or active). We then include another blank line. Finally we report the cumulative fission fraction in each of the 25 uranium spheres. The fractions are derived from the tallies described above multiplied by the cell volumes. The first entry is for sphere 1 (the sphere that dominates the original source distribution), the 13^{th} entry is for the central sphere, etc. These values are cumulative over all active generations and are normalised to 1.

Reference Calculations

To provide a reference result for comparison purposes, an extended calculation was performed. In this case, the initial source was specified to be equal in each of the 25 spheres. 10 000 histories per cycle were simulated. We skipped 1 000 cycles and calculated a total of 6 000 cycles. Therefore we had 50 million active histories in this run. The final combined collision / absorption / track-length estimate of k_{eff} was 1.11294 with a one sigma absolute standard deviation of 0.00009.

We also have performed eigenvalue calculations for isolated spheres, with radii of 10.0 cm and 8.71 cm. For these runs, all neutrons leaking from the sphere were terminated. We ran 5 000 histories per cycle, skipped 500 cycles, and calculated a total of 2 500 cycles (10 M active histories). The initial source was simply a point in the center of the sphere. For the 10.0-cm sphere, the k_{eff} was 1.11233 with a one-sigma absolute standard deviation of 0.00019, and for the 8.71-cm sphere, the k_{eff} was 0.99519 with a one-sigma absolute standard deviation of 0.00019.

Eigenvalue Results

The table below provides some summary information for the eigenvalues for each of the 3 cases. Typical standard deviations reported by MCNP for the individual runs were ~ 0.002. The mean and standard deviation of the mean were calculated from the 100 replica results using the standard formulas that weight the contributions based on the individual uncertainties. The population estimated standard deviation of the mean is calculated from the observed scatter of the population of replica eigenvalues. The ratio of the two standard deviations gives some indication of the Monte Carlo underestimation of the individual eigenvalue uncertainties (assuming, of course, unbiased results).

Case	Skipped Cycles	Minimum k_{eff}	Maximum k_{eff}	Mean k_{eff}	Standard Deviation of the Mean	Population Estimated Standard Deviation of the Mean	Ratio
1	0	1.05756	1.11291	1.09399	0.000218	0.001433	6.6
2	200	1.07862	1.11667	1.10738	0.000195	0.000909	4.7
3	400	1.09798	1.11779	1.11094	0.000188	0.000317	1.7

We have also analyzed the eigenvalue results for each case with respect to the reference value provided above. The deleterious impact of skipping too few cycles is particularly clear in the following table where we provide the percent of replicas for each case that lie within various multiples of a standard deviation from the reference result.

Case	Skipped Cycles	> 5 SD	4-5 SD	3-4 SD	2-3 SD	1-2 SD	< 1 SD
1	0	74	9	3	8	4	2
2	200	24	4	6	12	24	30
3	400	3	2	3	14	36	42

If we compare the magnitude of the replica eigenvalues to the reference result, we find that even when skipping 400 cycles, there is clearly an underestimation of the eigenvalue. It has not been determined from this work how many cycles would need to be skipped for unbiased results (given the unrealistically poor initial source guess).

Case	Skipped Cycles	Percent of Replicas with k_{eff}< Reference Value	Percent of Replicas with k_{eff}> Reference Value
1	0	100	0
2	200	88	12
3	400	80	20

MCNP performs several statistical checks on the eigenvalue results and warns the user if the statistical checks fail in some manner. In these calculations, 3 main warning messages arose. The first is "The cycle values do not appear normally distributed at the 99% confidence level." This check is performed for each of the 3 estimators: collision, absorption, and track length. The second warning was "The first and second half values of the combined estimator appear to be different at the 99% confidence level." The third is a warning that "There appears to be an {increasing / decreasing} trend in the combined estimator over the last 10 cycles." The percent of the replica runs for each case flagging these warning messages is indicated in the next Table.

Case	Skipped Cycles	Cycle Values Not Normally Distributed	First Half / Second Half Different	Trend in Last 10 Cycles	At Least One Warning Message
1	0	21	81	6	85
2	200	5	35	1	37
3	400	3	13	0	16

For Case 1, three of the replicas flagged the warning about "cycle values not normally distributed" for each of the three individual estimators. When this happens, MCNP draws attention to the fact by not printing "boxed" results for the final k_{eff}. The combined estimators for these 3 runs were 1.06226, 1.07231, and 1.07909. These are some of the worst, but certainly not the absolute worst, k_{eff} estimates. On the other hand, for the 15 replicas of case 1 with no MCNP eigenvalue warnings, the average k_{eff} is 1.10704, not great compared to the reference calculation, but much closer than the typical Case 1 replica.

Fission Fractions

We will first present fission fraction results from the reference calculation described above. It should be noted, however, that an even longer run is likely necessary to provide true reference fission fractions. Nevertheless, results are given in the following table.

Symmetric Cell ID	Number of Cells	Cells	Average Fission Fraction Per Cell
1	1	13	0.910624
2	4	8, 12, 14, 18	0.011157
3	4	7, 9, 17, 19	0.005783
4	8	2, 4, 6, 10, 16, 20, 22, 24	0.002344
5	4	3, 11, 15, 23	0.000463
6	4	1, 5, 21, 25	0.000254

MCNP errors reported for the number of fissions in each cell are clearly underestimated, likely by a factor of up to several for the outer spheres. We have not as yet analyzed these data however.

The next table provides the average fission fraction over all replicas for each case in 3 specific cells: cell 1, with the artificially high initial source; cell 13, the central sphere; and cell 25, the cell symmetric to cell 1 but all the way on the other side of the array (note that cell 25 also has an artificially high initial source representation, although not nearly as high as cell 1). The reference values from the above table are included for comparison purposes. Once more, we are able to conclude that, using the source specified, skipping 400 cycles is not enough for this problem to be converged. It is also noted that MCNP's statistical checks flagged a trend problem in the fission tallies for each of the 100 replicas in Case 1.

Case	Skipped Cycles	Cell 1 Average Fission Fraction	Cell 13 Average Fission Fraction	Cell 25 Average Fission Fraction
1	0	0.089250	0.739715	0.001633
2	200	0.012845	0.862278	0.000655
3	400	0.004325	0.900642	0.000377
Ref		0.000254	0.910624	0.000254

Appendix 5.c

FINAL K_{EFF}

On each figure, the horizontal line corresponds to the reference k_{eff} determined by the contributor. The k_{eff} value for each replica is given with one standard deviation uncertainty, computed by the code.

ANL / VIM

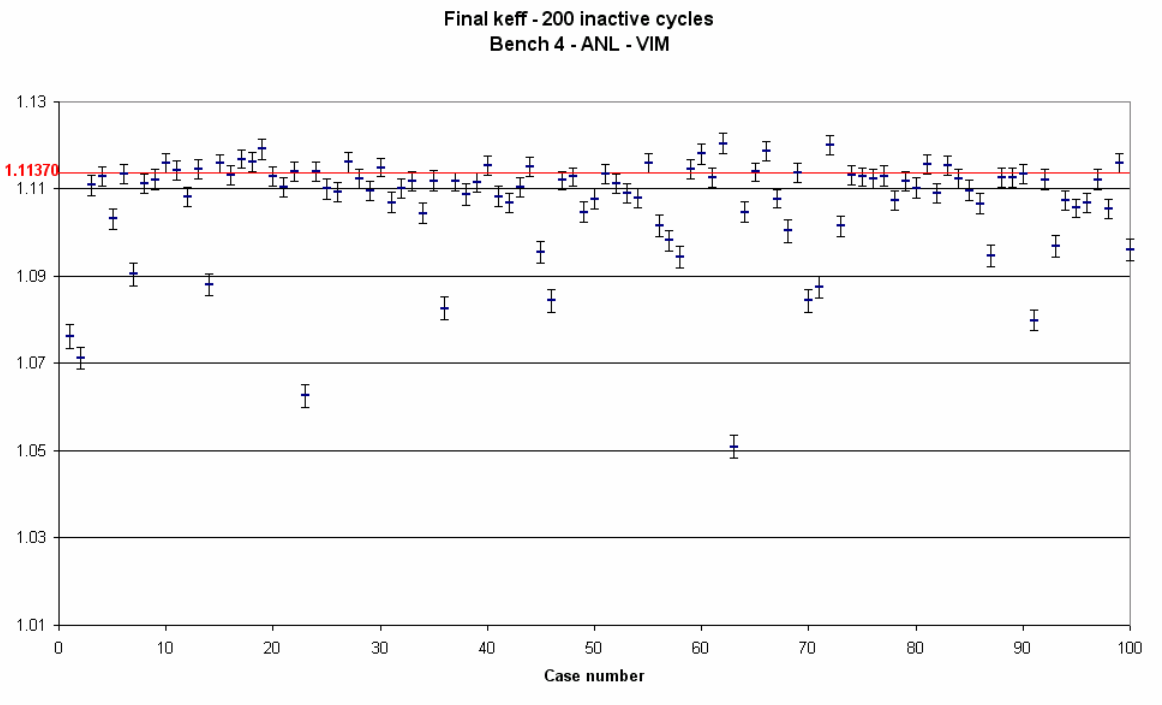

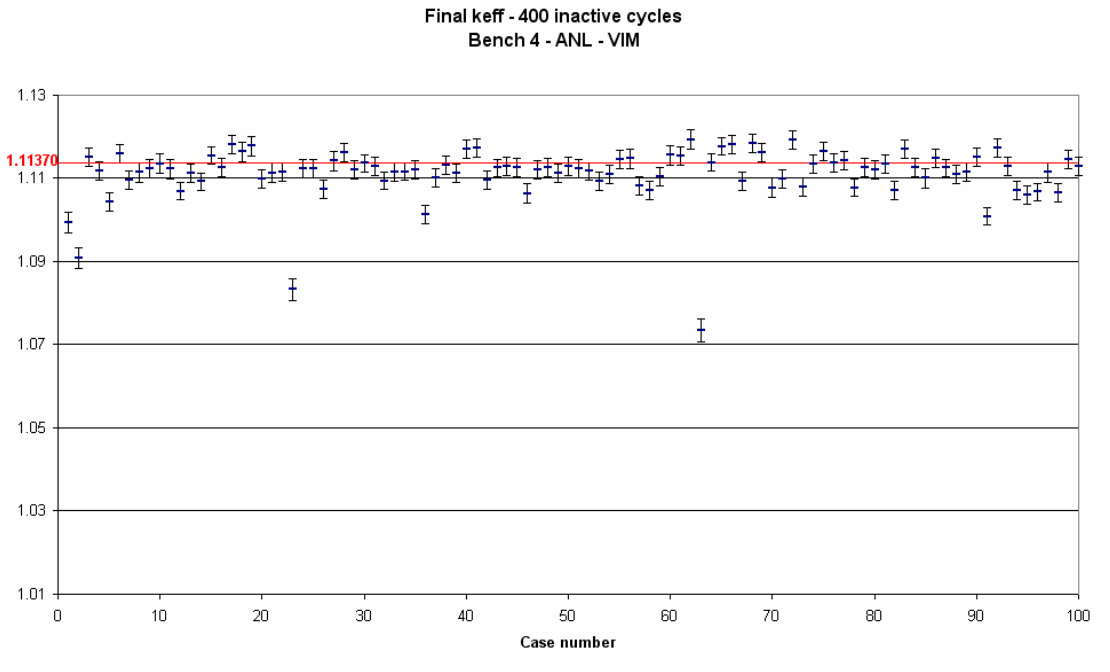

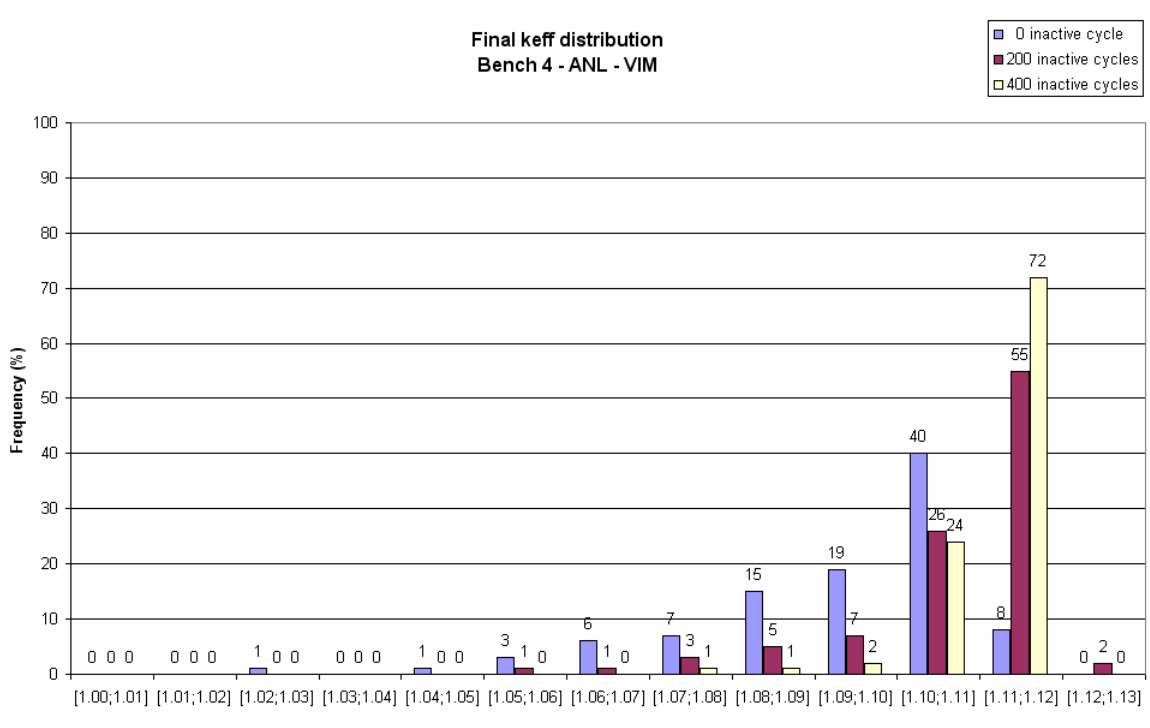
Final keff distribution
Bench 4 - ANL - VIM
0 inactive cycle
200 inactive cycles
400 inactive cycles
Frequency (%)
[1.00;1.01] [1.01;1.02] [1.02;1.03] [1.03;1.04] [1.04;1.05] [1.05;1.06] [1.06;1.07] [1.07;1.08] [1.08;1.09] [1.09;1.10] [1.10;1.11] [1.11;1.12] [1.12;1.13]

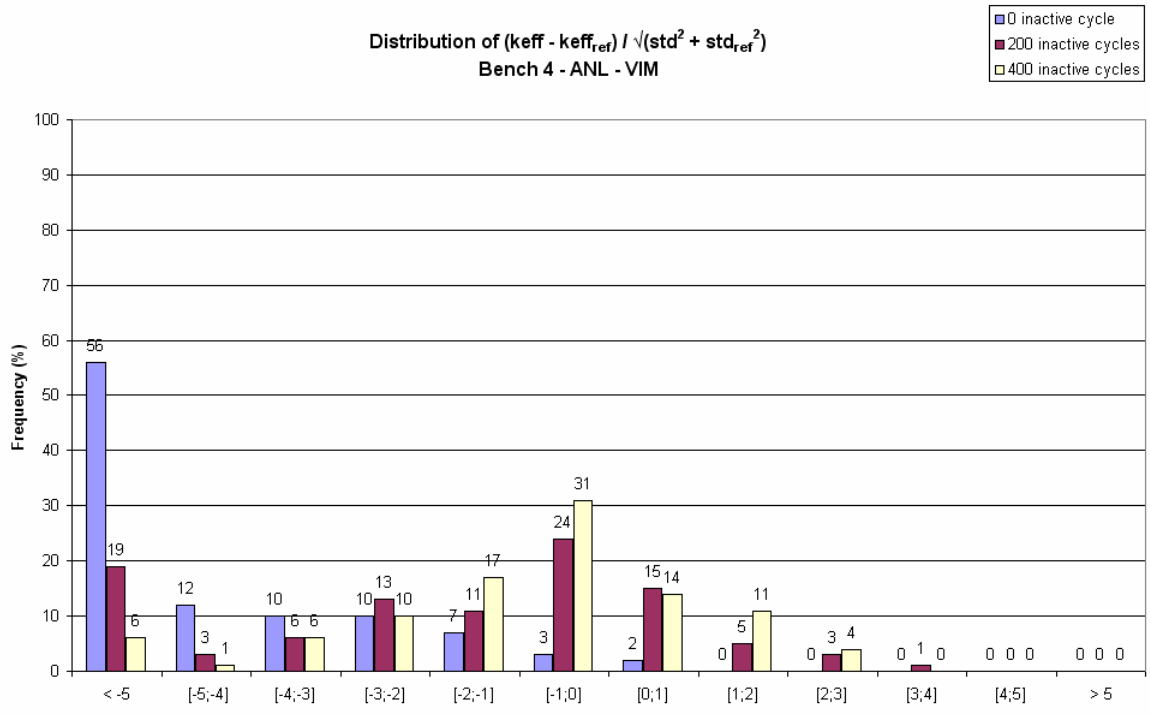
Distribution of (keff - keff$_{ref}$) / √(std^2 + std$_{ref}^2$)
Bench 4 - ANL - VIM
0 inactive cycle
200 inactive cycles
400 inactive cycles
Frequency (%)
< -5 [-5;-4] [-4;-3] [-3;-2] [-2;-1] [-1;0] [0;1] [1;2] [2;3] [3;4] [4;5] > 5

EMS / KENO

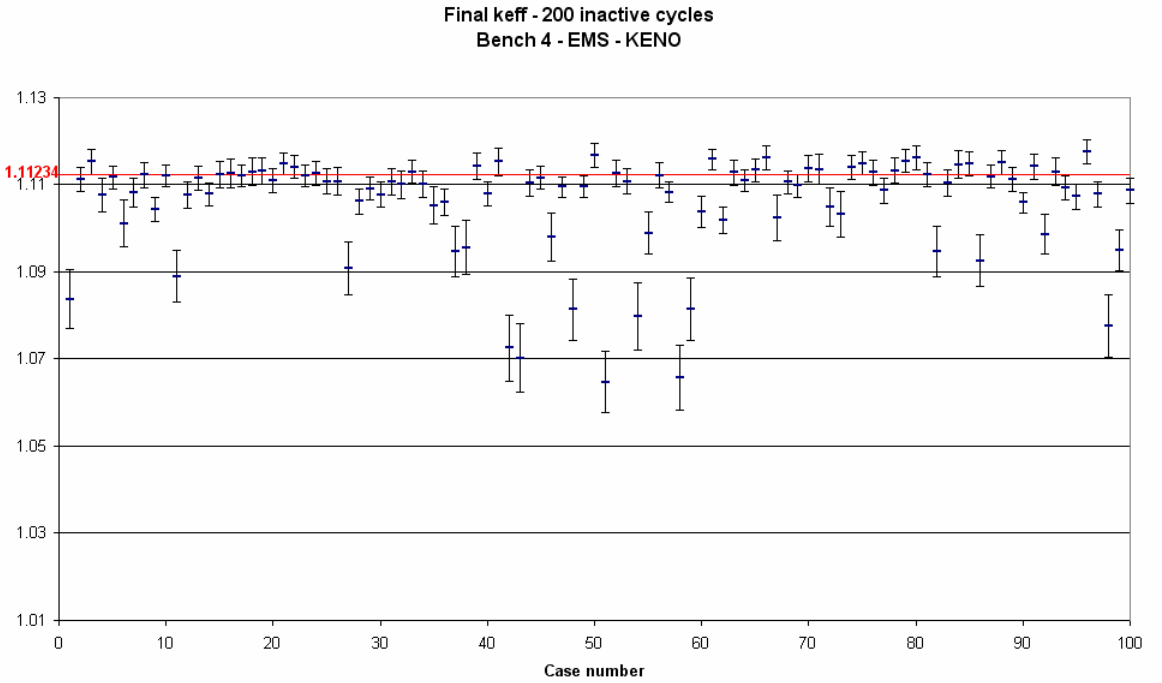
Final keff - 200 inactive cycles
Bench 4 - EMS - KENO
1.13
1.11234
1.11
1.09
1.07
1.05
1.03
1.01
0
10
20
30
40
50
60
70
80
90
100
Case number

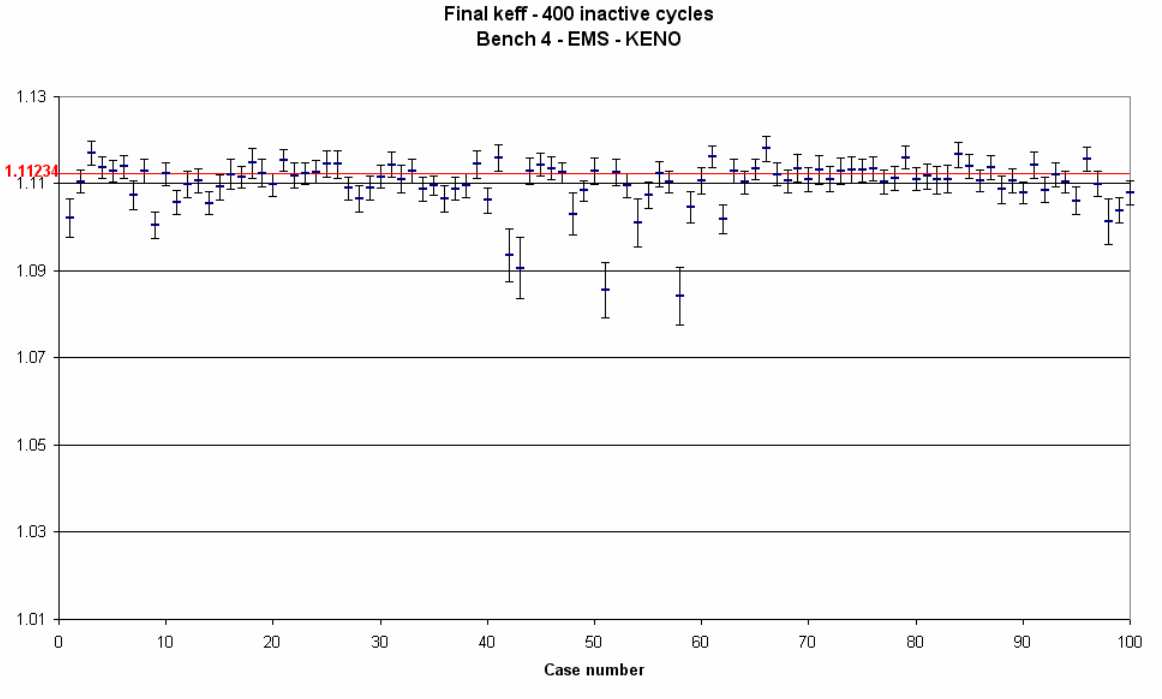
Final keff - 400 inactive cycles
Bench 4 - EMS - KENO
1.13
1.11234
1.11
1.09
1.07
1.05
1.03
1.01
0
10
20
30
40
50
60
70
80
90
100
Case number

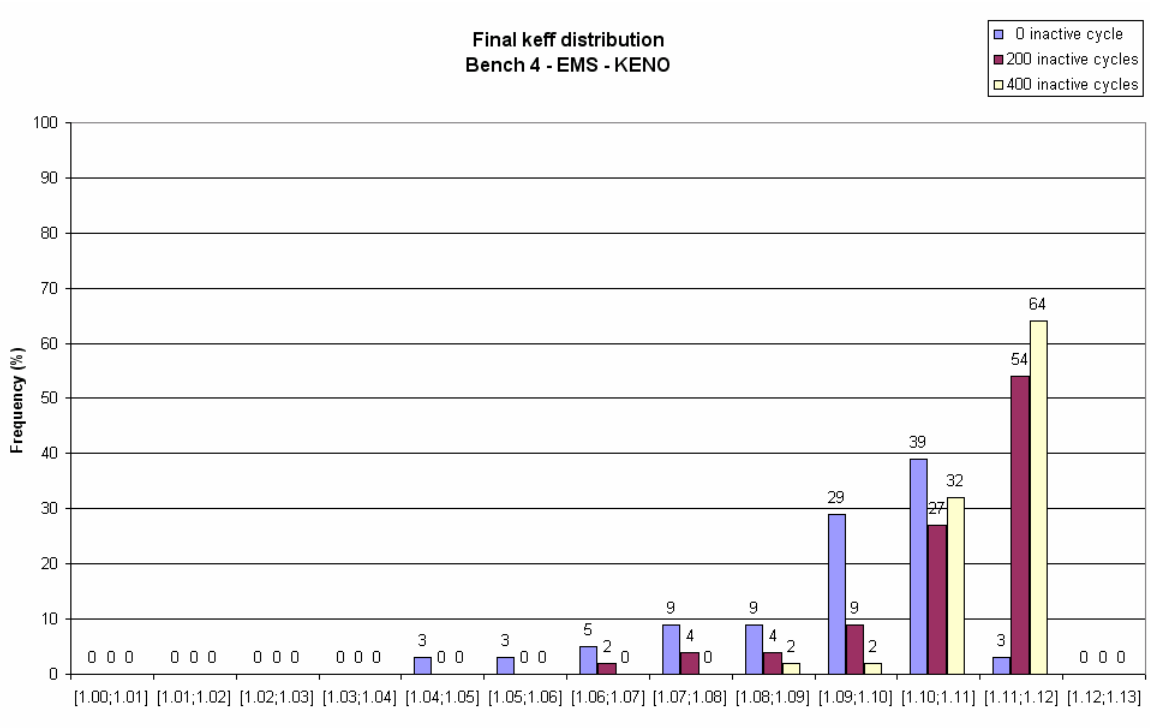
Final keff distribution
Bench 4 - EMS - KENO
0 inactive cycle
200 inactive cycles
400 inactive cycles
Frequency (%)
100
90
80
70
60
50
40
30
20
10
0
0 0 0
0 0 0
0 0 0
0 0 0
3 0 0
3 0 0
5 2 0
9 4 0
9 4 2
29 9 2
39 27 32
3 54 64
0 0 0
[1.00;1.01]
[1.01;1.02]
[1.02;1.03]
[1.03;1.04]
[1.04;1.05]
[1.05;1.06]
[1.06;1.07]
[1.07;1.08]
[1.08;1.09]
[1.09;1.10]
[1.10;1.11]
[1.11;1.12]
[1.12;1.13]

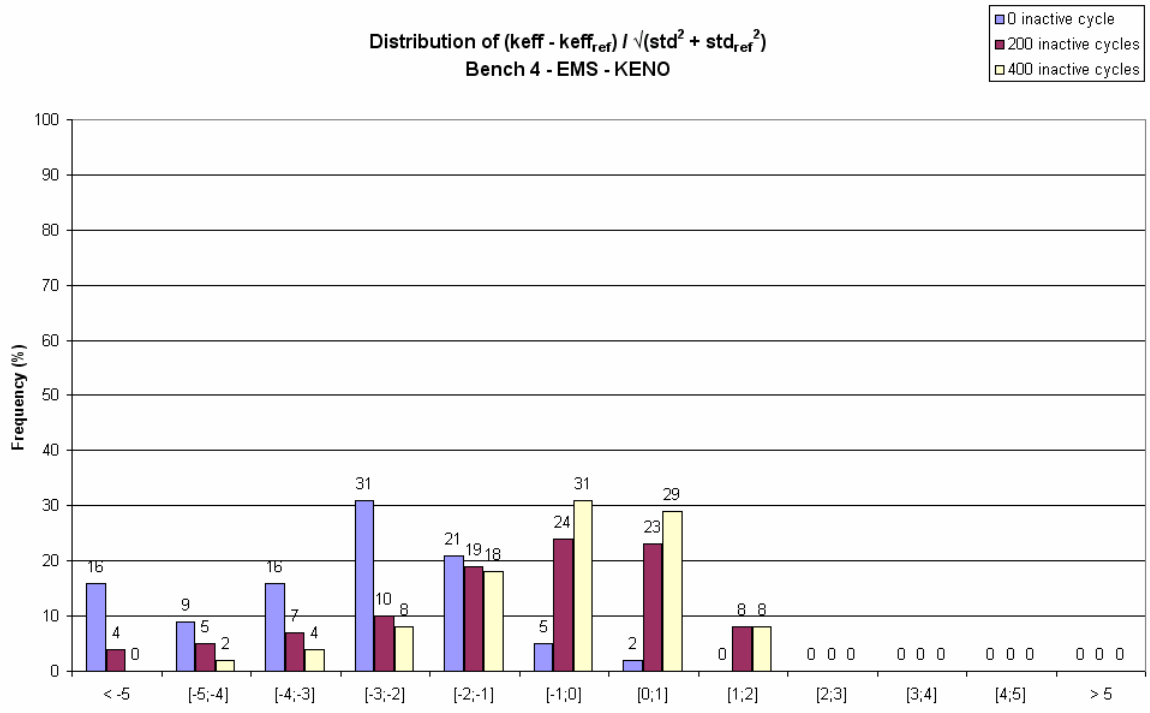
Distribution of (keff - keff$_{ref}$) / √(std^2 + std$_{ref}^2$)
Bench 4 - EMS - KENO
0 inactive cycle
200 inactive cycles
400 inactive cycles
Frequency (%)
100
90
80
70
60
50
40
30
20
10
0
16 4 0
9 5 2
16 7 4
31 10 8
21 19 18
5 24 31
2 23 29
0 8 8
0 0 0
0 0 0
0 0 0
0 0 0
< -5
[-5;-4]
[-4;-3]
[-3;-2]
[-2;-1]
[-1;0]
[0;1]
[1;2]
[2;3]
[3;4]
[4;5]
> 5

IPPE / KENO

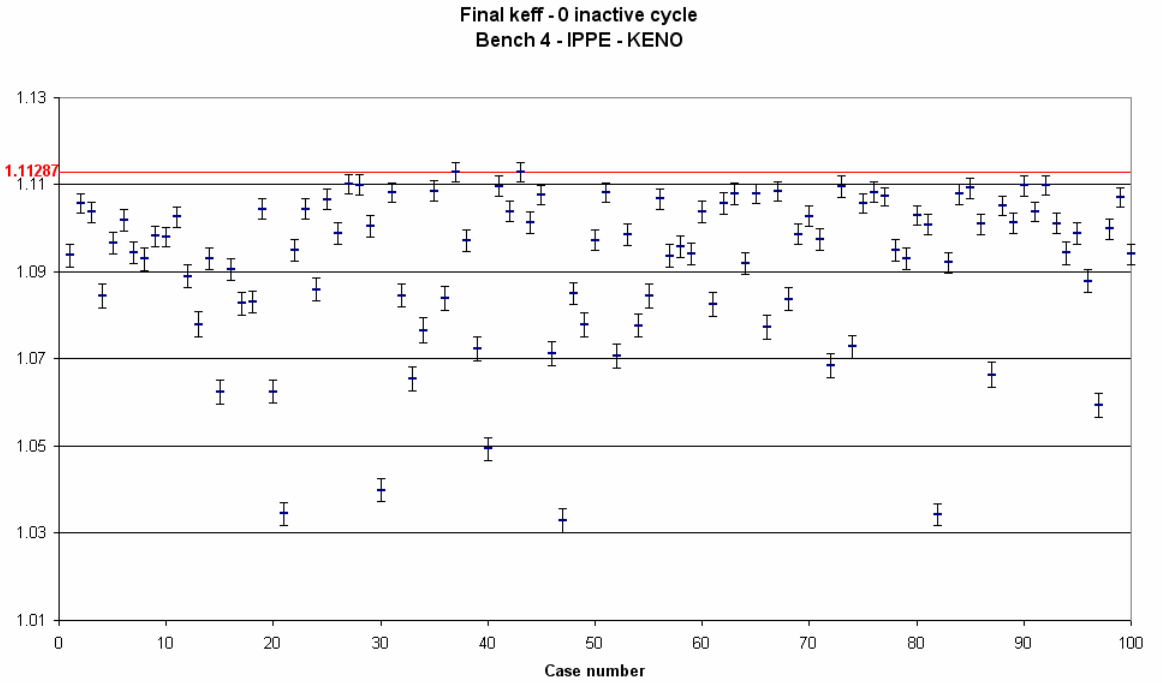
Final keff - 0 inactive cycle
Bench 4 - IPPE - KENO
1.13
1.11287
1.11
1.09
1.07
1.05
1.03
1.01
0
10
20
30
40
50
60
70
80
90
100
Case number

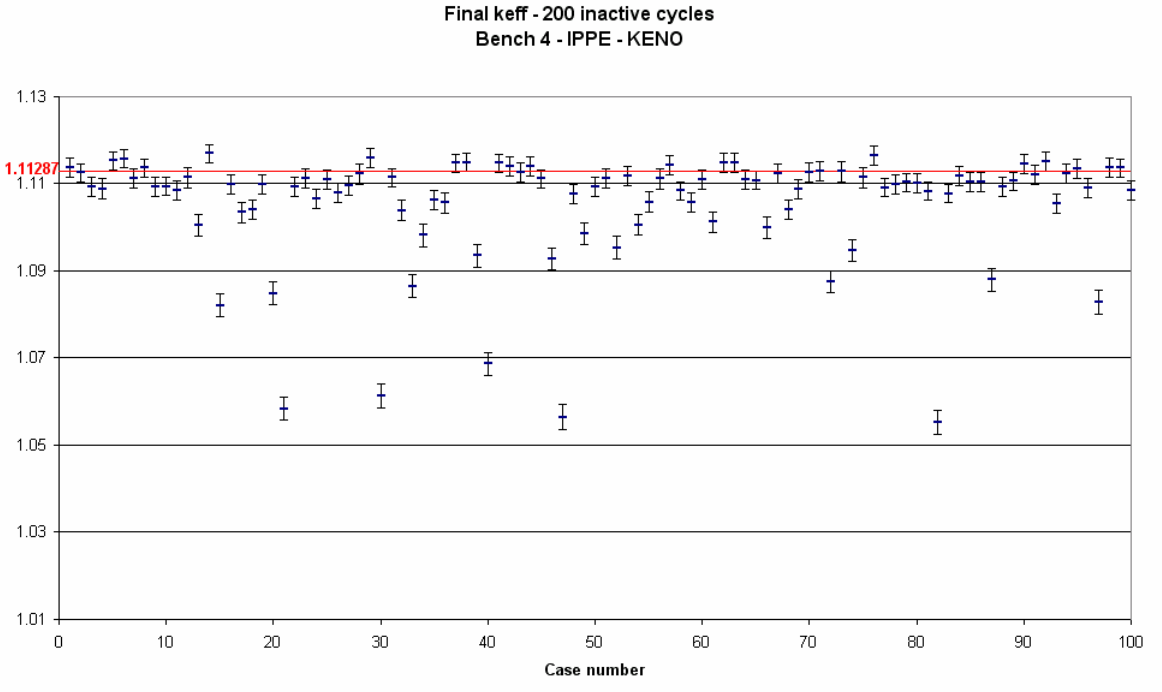
Final keff - 200 inactive cycles
Bench 4 - IPPE - KENO
1.13
1.11287
1.11
1.09
1.07
1.05
1.03
1.01
0
10
20
30
40
50
60
70
80
90
100
Case number

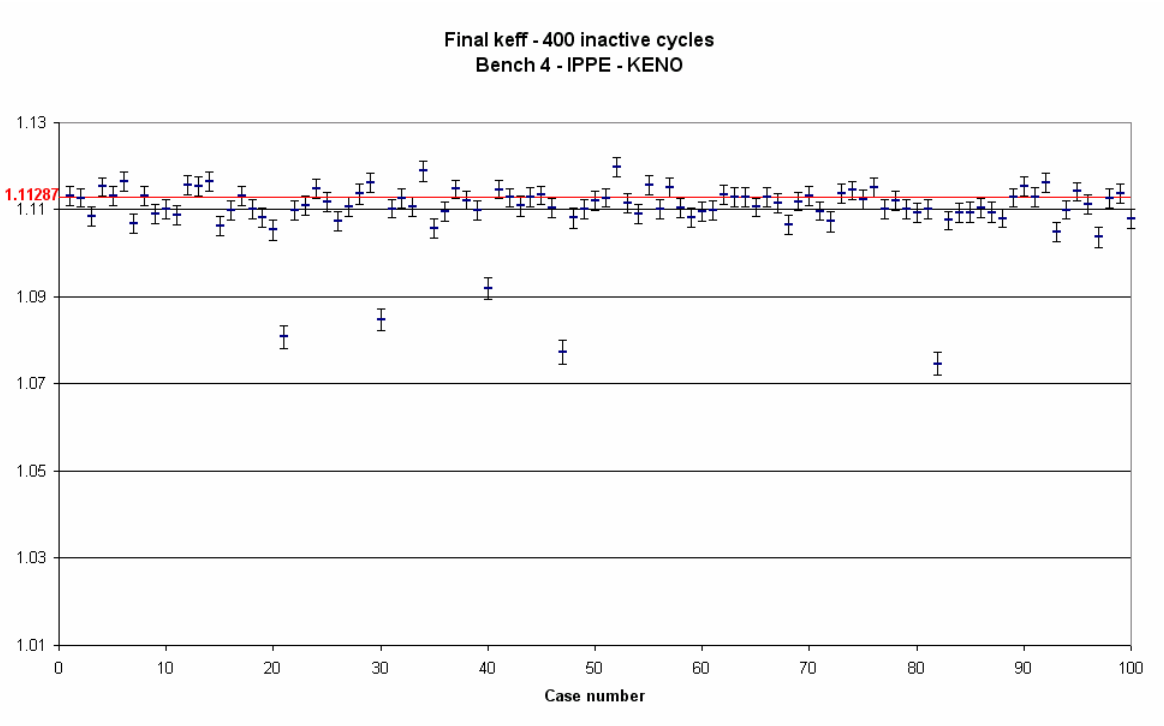
Final keff - 400 inactive cycles
Bench 4 - IPPE - KENO
1.13
1.11287
1.11
1.09
1.07
1.05
1.03
1.01
0
10
20
30
40
50
60
70
80
90
100
Case number

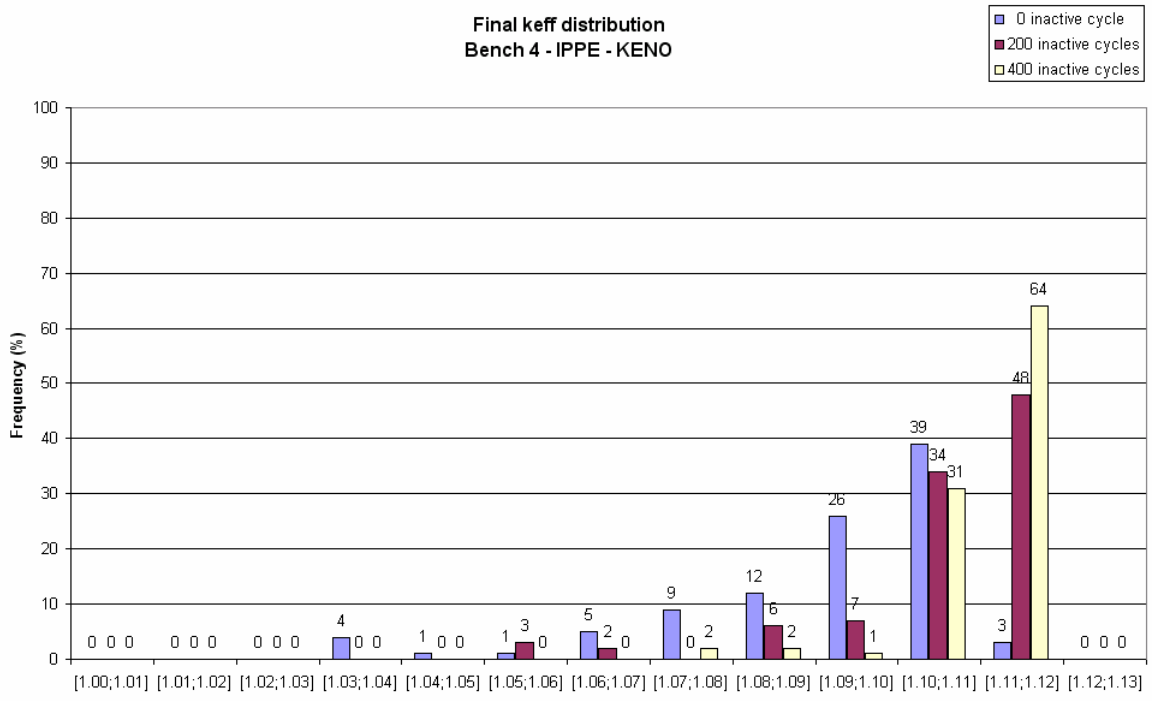
Final keff distribution
Bench 4 - IPPE - KENO
0 inactive cycle
200 inactive cycles
400 inactive cycles
Frequency (%)
100
90
80
70
60
50
40
30
20
10
0
0 0 0
0 0 0
0 0 0
4 0 0
1 0 0
1 3 0
5 2 0
9 0 2
12 6 2
26 7 1
39 34 31
3 48 64
0 0 0
[1.00;1.01]
[1.01;1.02]
[1.02;1.03]
[1.03;1.04]
[1.04;1.05]
[1.05;1.06]
[1.06;1.07]
[1.07;1.08]
[1.08;1.09]
[1.09;1.10]
[1.10;1.11]
[1.11;1.12]
[1.12;1.13]

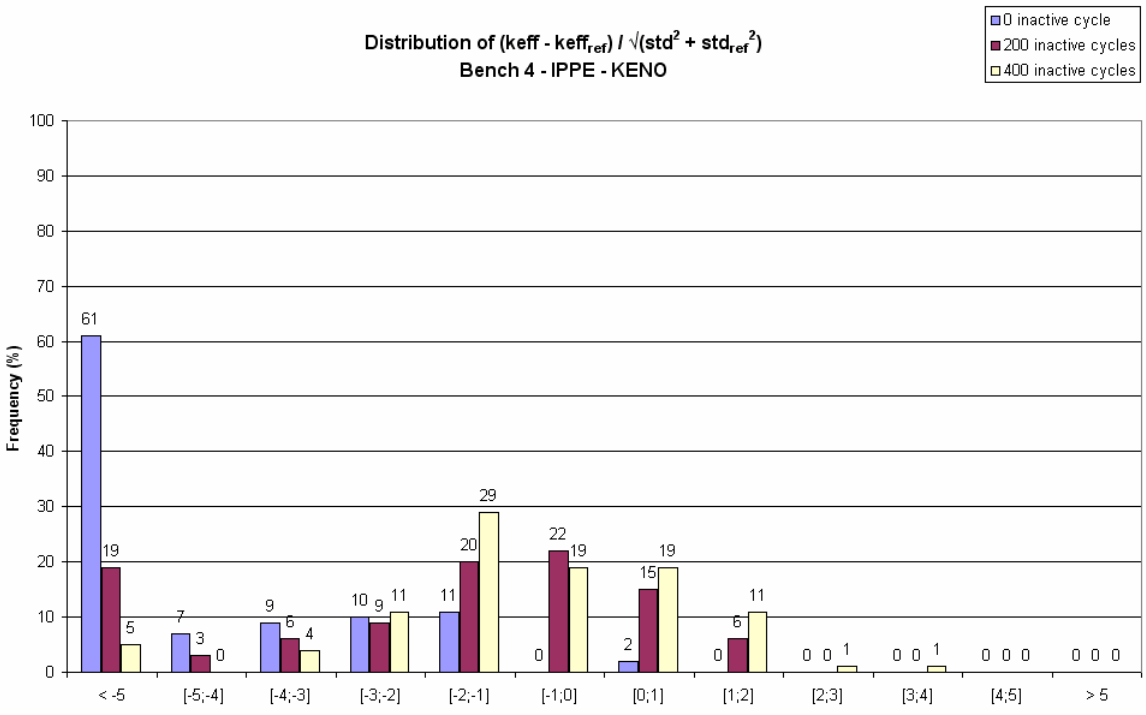
Distribution of (keff - keff$_{ref}$) / √(std^2 + std$_{ref}^2$)
Bench 4 - IPPE - KENO
0 inactive cycle
200 inactive cycles
400 inactive cycles
Frequency (%)
100
90
80
70
60
50
40
30
20
10
0
61
19
5
7
3
0
9
6
4
10
9
11
11
20
29
0
22
19
2
15
19
0
6
11
0 0 1
0 0 1
0 0 0
0 0 0
< -5
[-5;-4]
[-4;-3]
[-3;-2]
[-2;-1]
[-1;0]
[0;1]
[1;2]
[2;3]
[3;4]
[4;5]
> 5

IPPE / KENO

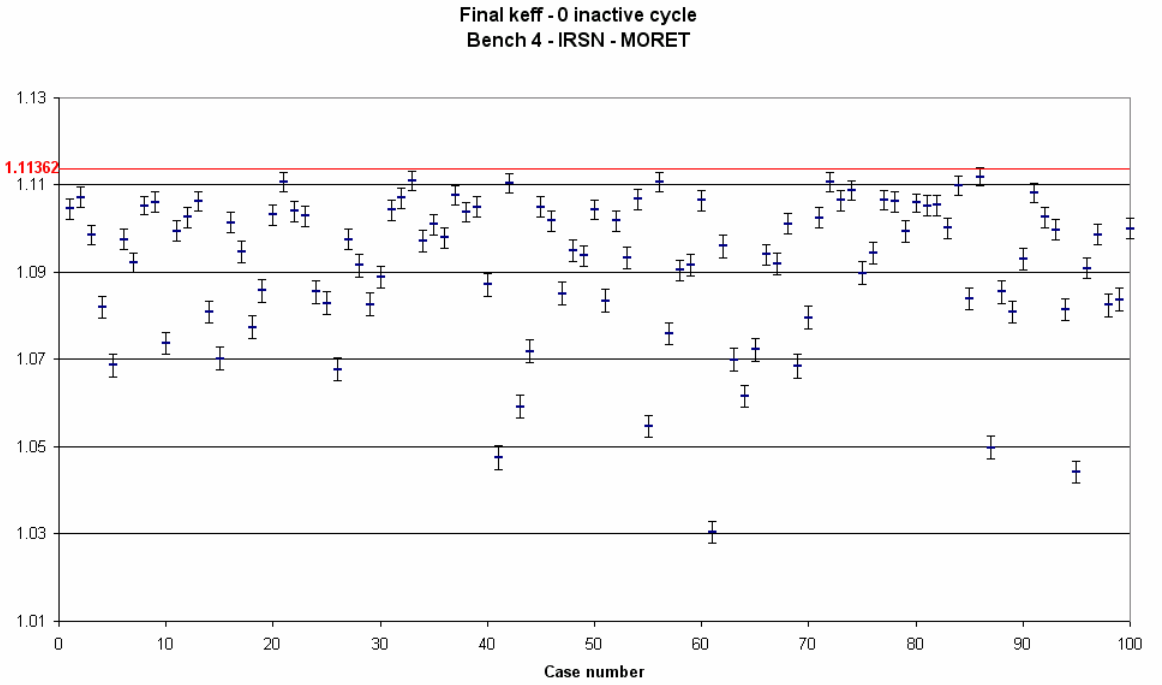
Final keff - 0 inactive cycle
Bench 4 - IRSN - MORET
1.13
1.11362
1.11
1.09
1.07
1.05
1.03
1.01
0
10
20
30
40
50
60
70
80
90
100
Case number

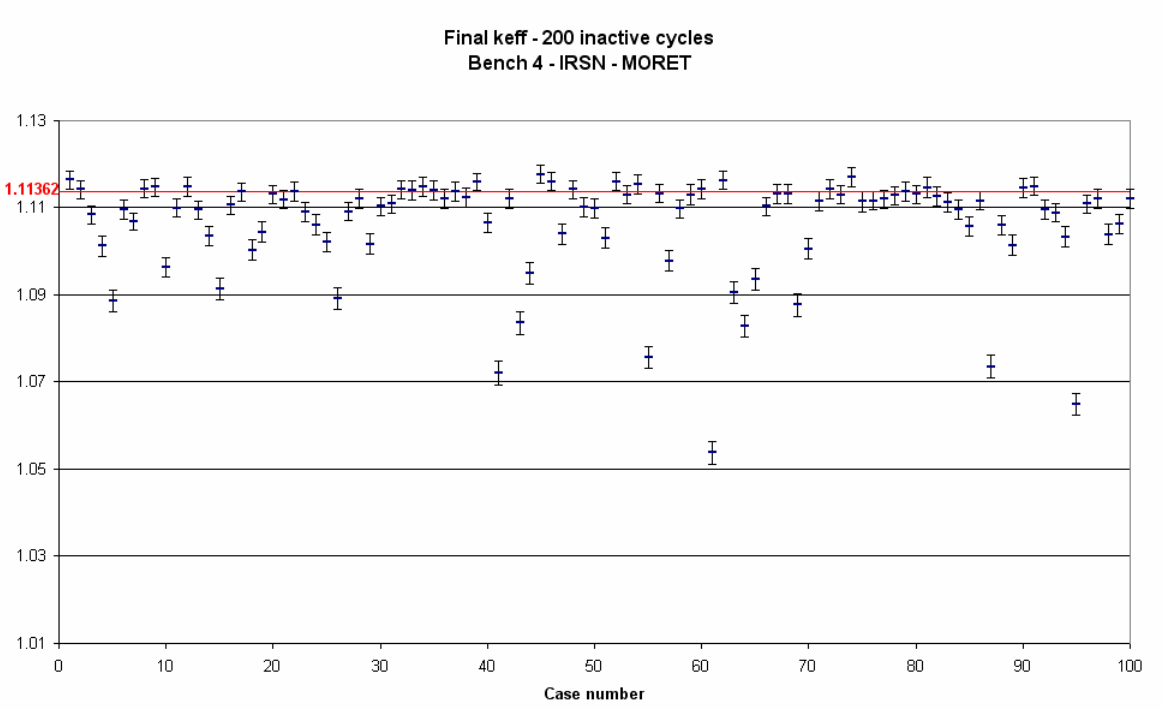
Final keff - 200 inactive cycles
Bench 4 - IRSN - MORET
1.13
1.11362
1.11
1.09
1.07
1.05
1.03
1.01
0
10
20
30
40
50
60
70
80
90
100
Case number

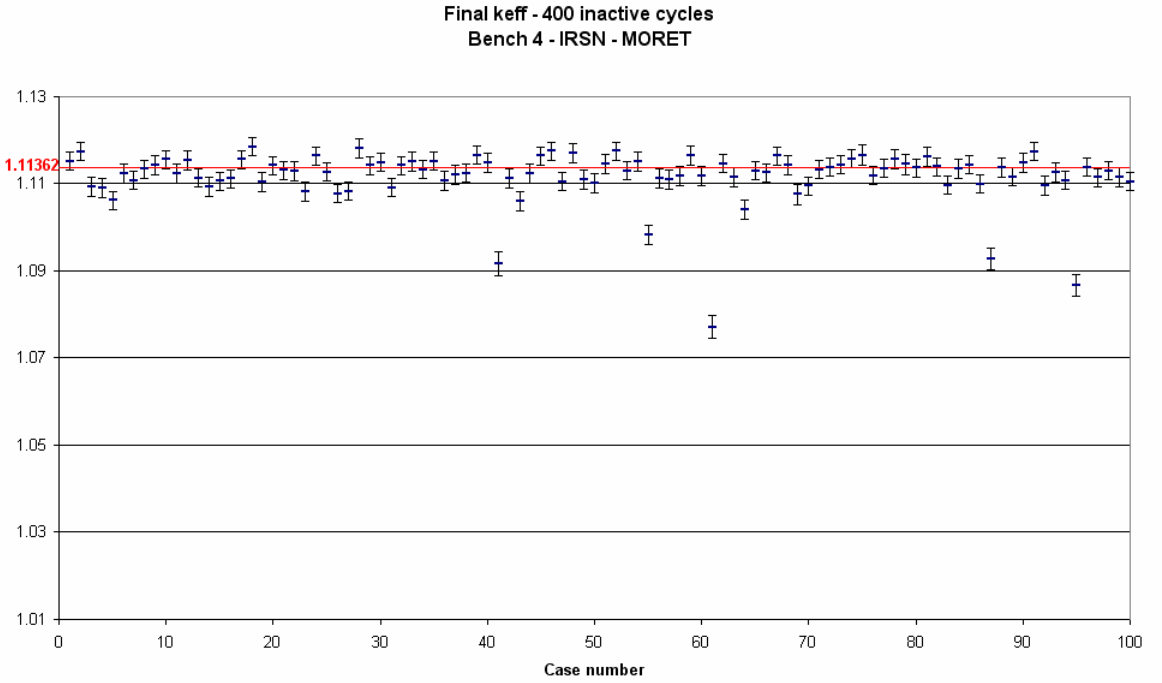
Final keff - 400 inactive cycles
Bench 4 - IRSN - MORET
1.13
1.11362
1.11
1.09
1.07
1.05
1.03
1.01
0
10
20
30
40
50
60
70
80
90
100
Case number

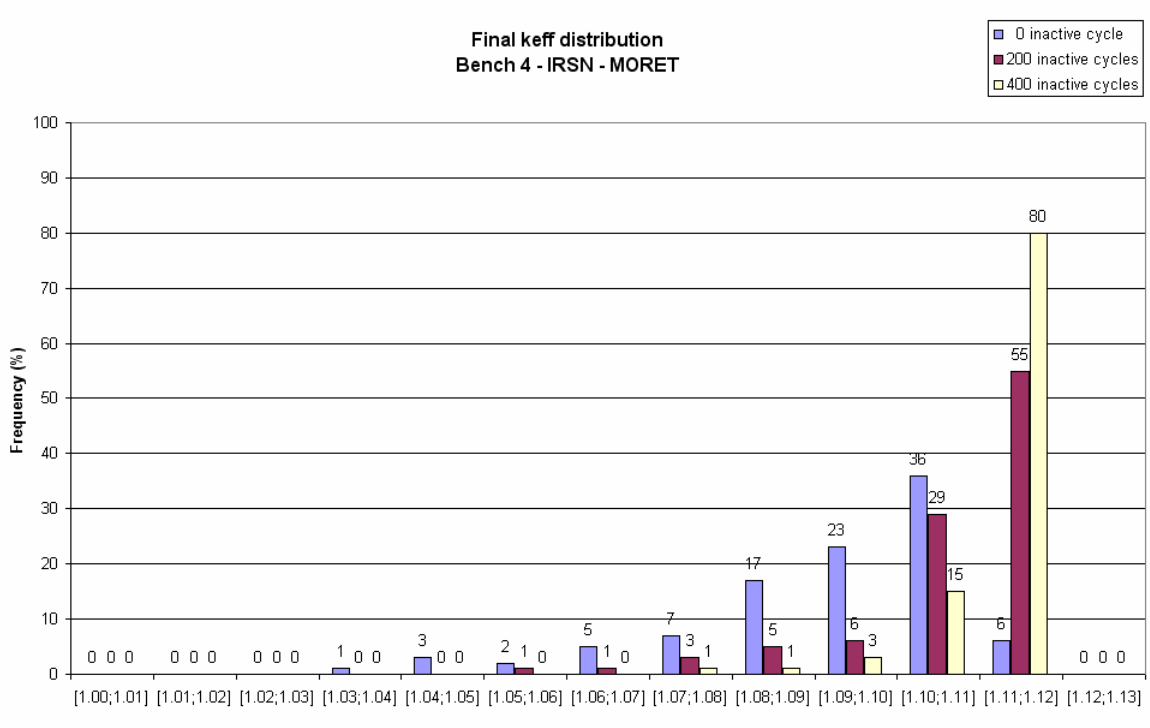
Final keff distribution
Bench 4 - IRSN - MORET
0 inactive cycle
200 inactive cycles
400 inactive cycles
Frequency (%)
[1.00;1.01] [1.01;1.02] [1.02;1.03] [1.03;1.04] [1.04;1.05] [1.05;1.06] [1.06;1.07] [1.07;1.08] [1.08;1.09] [1.09;1.10] [1.10;1.11] [1.11;1.12] [1.12;1.13]

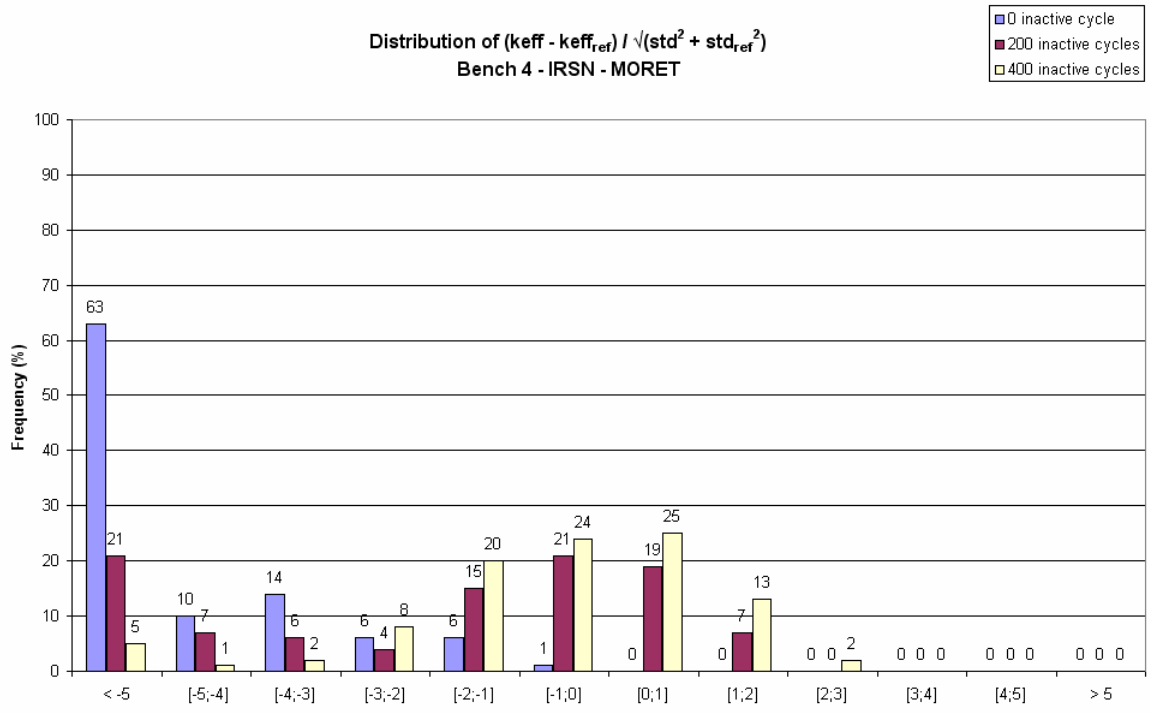
Distribution of (keff - keff$_{ref}$) / √(std^2 + std$_{ref}^2$)
Bench 4 - IRSN - MORET
0 inactive cycle
200 inactive cycles
400 inactive cycles
Frequency (%)
< -5 [-5;-4] [-4;-3] [-3;-2] [-2;-1] [-1;0] [0;1] [1;2] [2;3] [3;4] [4;5] > 5

JNC / KENO

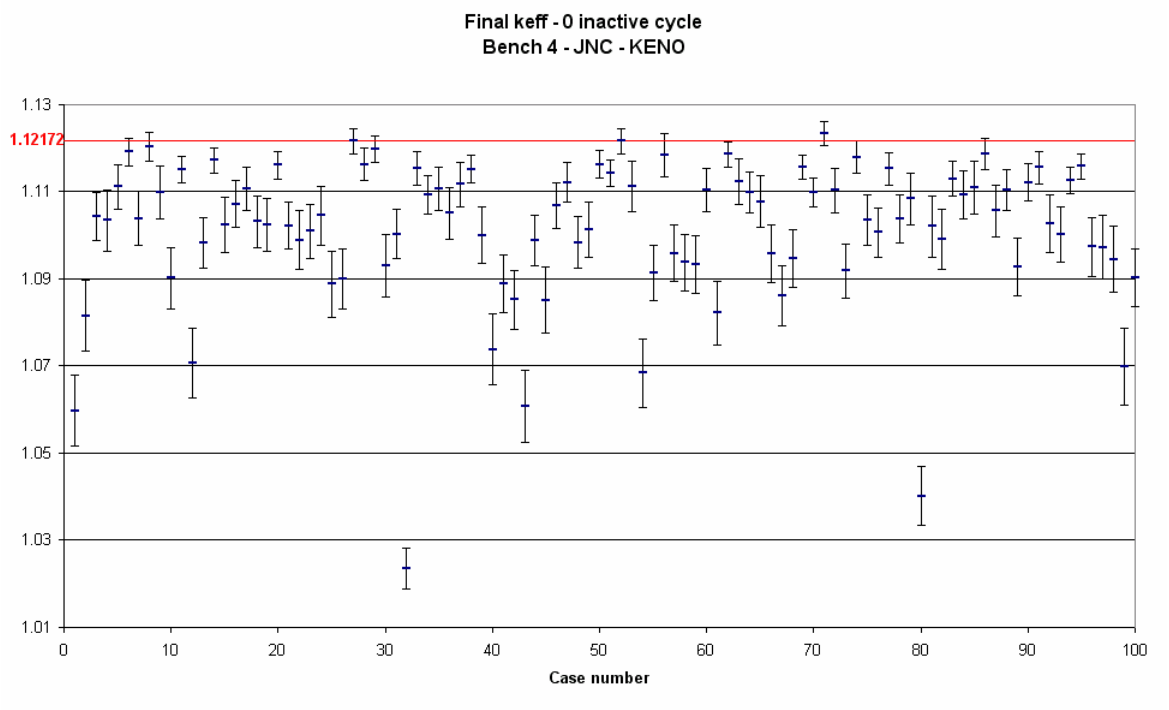
Final keff - 0 inactive cycle
Bench 4 - JNC - KENO
1.13
1.12172
1.11
1.09
1.07
1.05
1.03
1.01
0
10
20
30
40
50
60
70
80
90
100
Case number

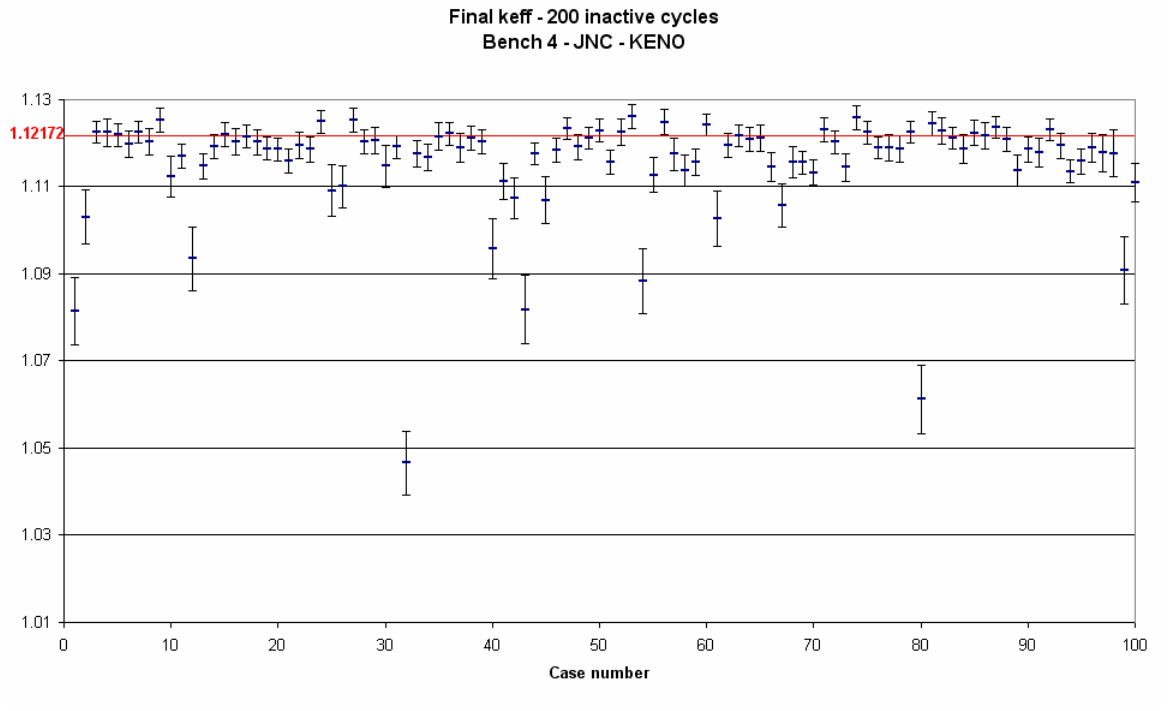
Final keff - 200 inactive cycles
Bench 4 - JNC - KENO
1.13
1.12172
1.11
1.09
1.07
1.05
1.03
1.01
0
10
20
30
40
50
60
70
80
90
100
Case number

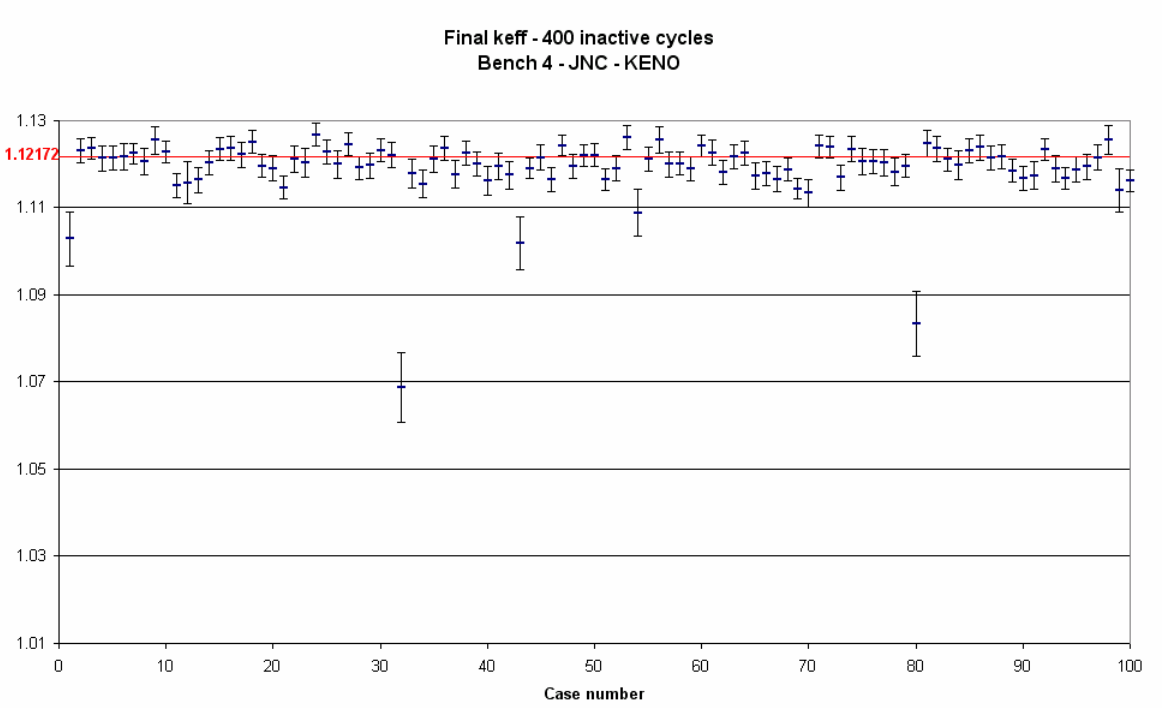
Final keff - 400 inactive cycles
Bench 4 - JNC - KENO
1.12172
1.13
1.11
1.09
1.07
1.05
1.03
1.01
0
10
20
30
40
50
60
70
80
90
100
Case number

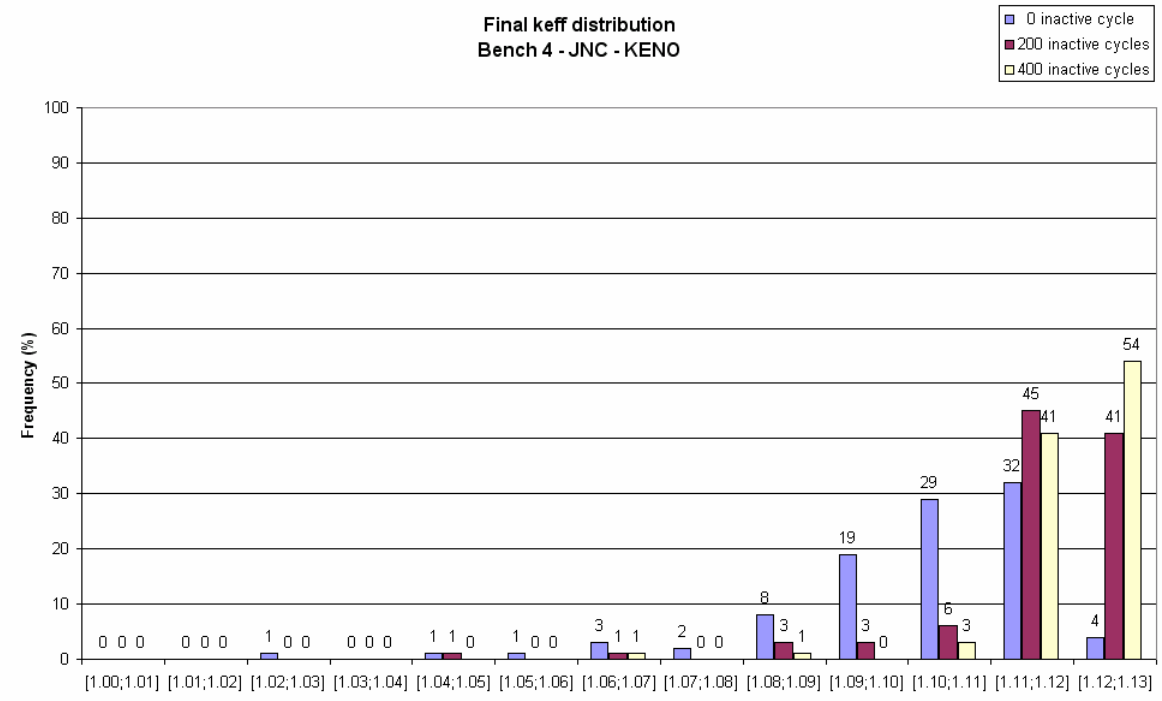
Final keff distribution
Bench 4 - JNC - KENO
0 inactive cycle
200 inactive cycles
400 inactive cycles
Frequency (%)
100
90
80
70
60
50
40
30
20
10
0
0 0 0
0 0 0
1 0 0
0 0 0
1 1 0
1 0 0
3 1 1
2 0 0
8 3 1
19 3 0
29 6 3
32 45 41
4 41 54
[1.00;1.01]
[1.01;1.02]
[1.02;1.03]
[1.03;1.04]
[1.04;1.05]
[1.05;1.06]
[1.06;1.07]
[1.07;1.08]
[1.08;1.09]
[1.09;1.10]
[1.10;1.11]
[1.11;1.12]
[1.12;1.13]

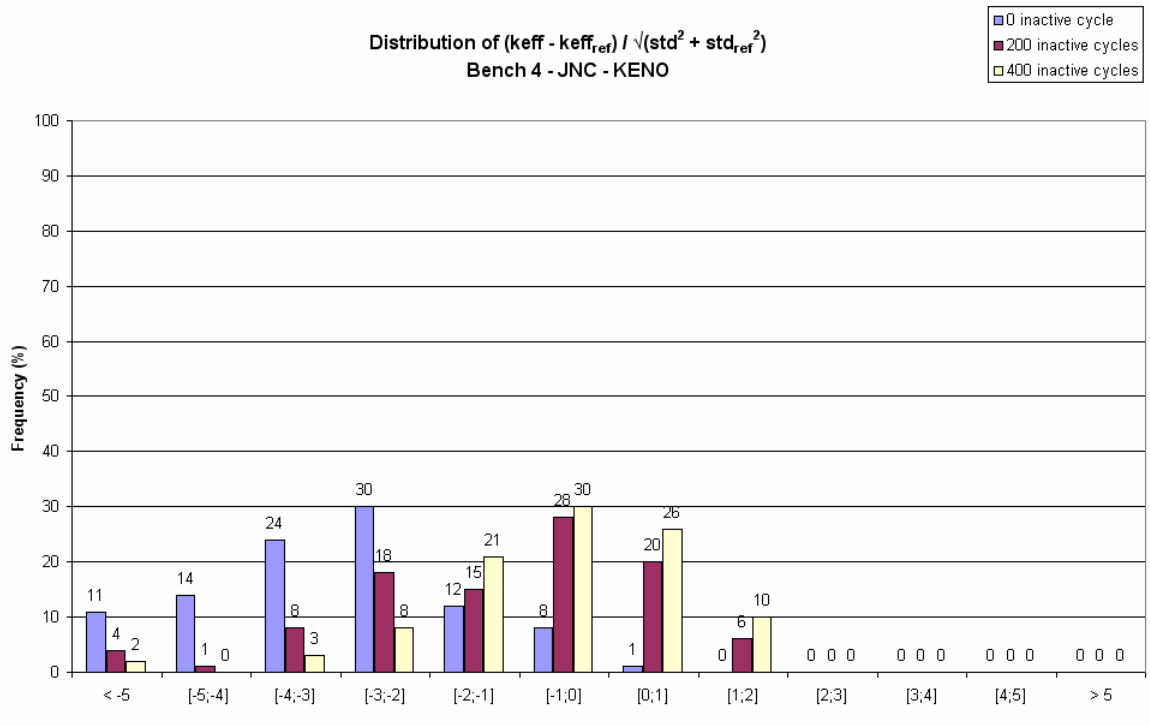
Distribution of (keff - keff$_{ref}$) / √(std^2 + std$_{ref}^2$)
Bench 4 - JNC - KENO
0 inactive cycle
200 inactive cycles
400 inactive cycles
Frequency (%)
100
90
80
70
60
50
40
30
20
10
0
11
4
2
14
1
0
24
8
3
30
18
8
12
15
21
8
28
30
1
20
26
0
6
10
0 0 0
0 0 0
0 0 0
0 0 0
< -5
[-5;-4]
[-4;-3]
[-3;-2]
[-2;-1]
[-1;0]
[0;1]
[1;2]
[2;3]
[3;4]
[4;5]
> 5

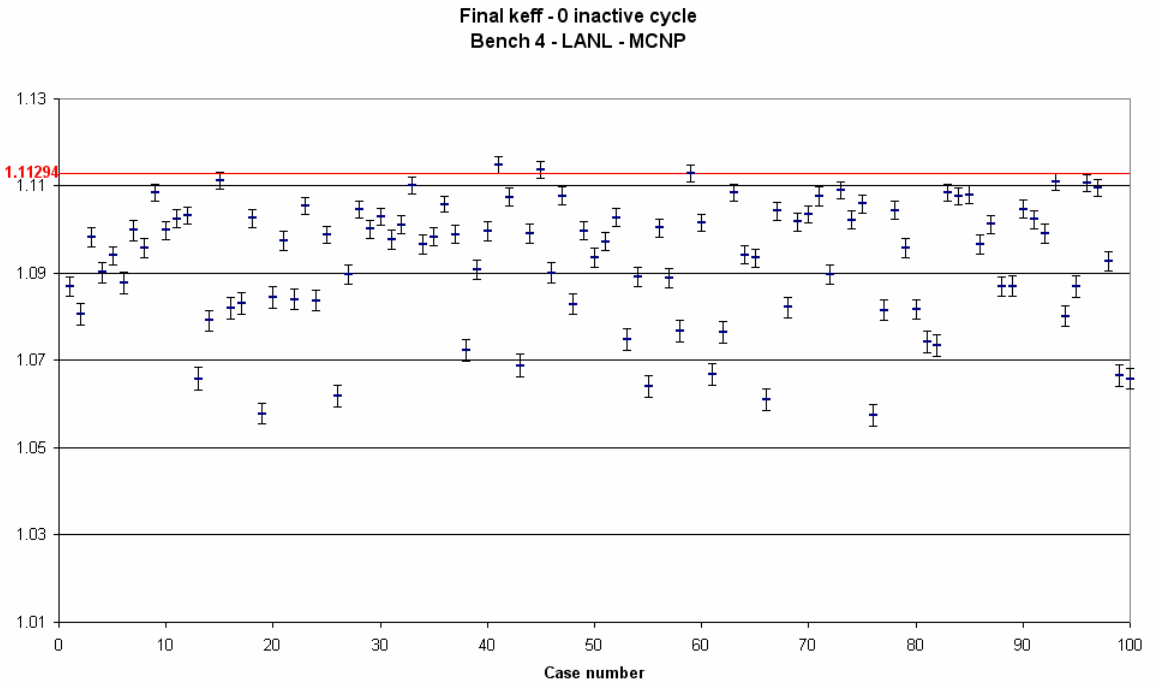
Final keff - 0 inactive cycle
Bench 4 - LANL - MCNP
1.13
1.11294
1.11
1.09
1.07
1.05
1.03
1.01
0
10
20
30
40
50
60
70
80
90
100
Case number

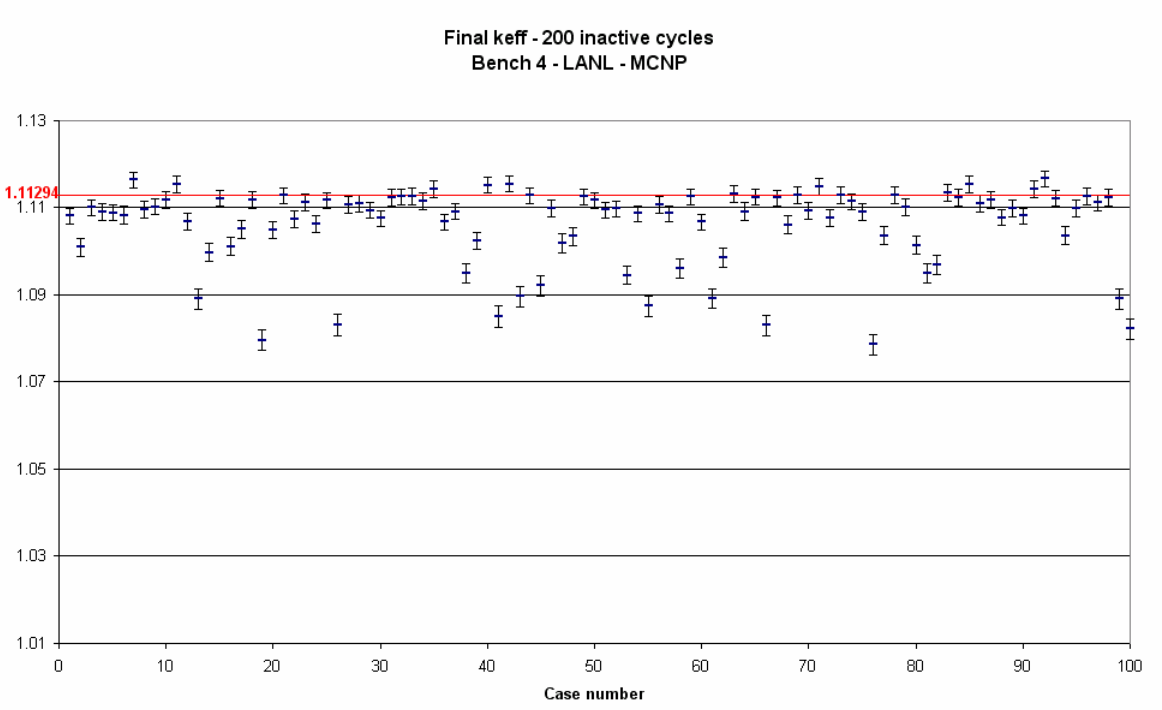
Final keff - 200 inactive cycles
Bench 4 - LANL - MCNP
1.13
1.11294
1.11
1.09
1.07
1.05
1.03
1.01
0
10
20
30
40
50
60
70
80
90
100
Case number

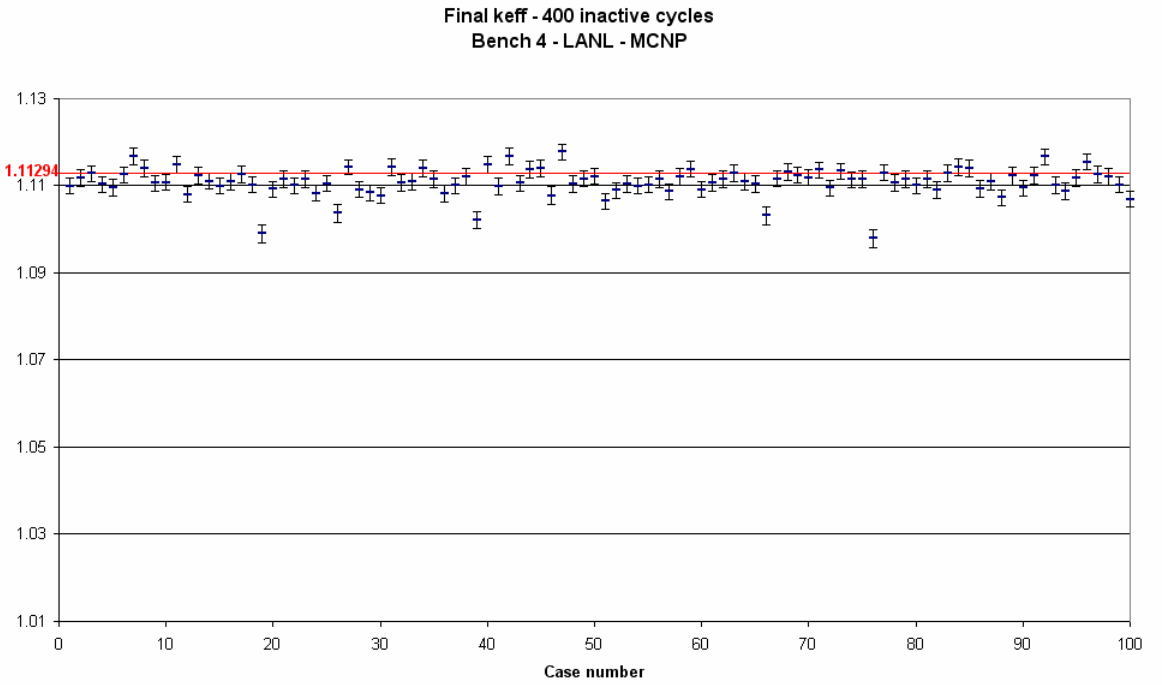
Final keff - 400 inactive cycles
Bench 4 - LANL - MCNP
1.13
1.11294
1.11
1.09
1.07
1.05
1.03
1.01
0
10
20
30
40
50
60
70
80
90
100
Case number

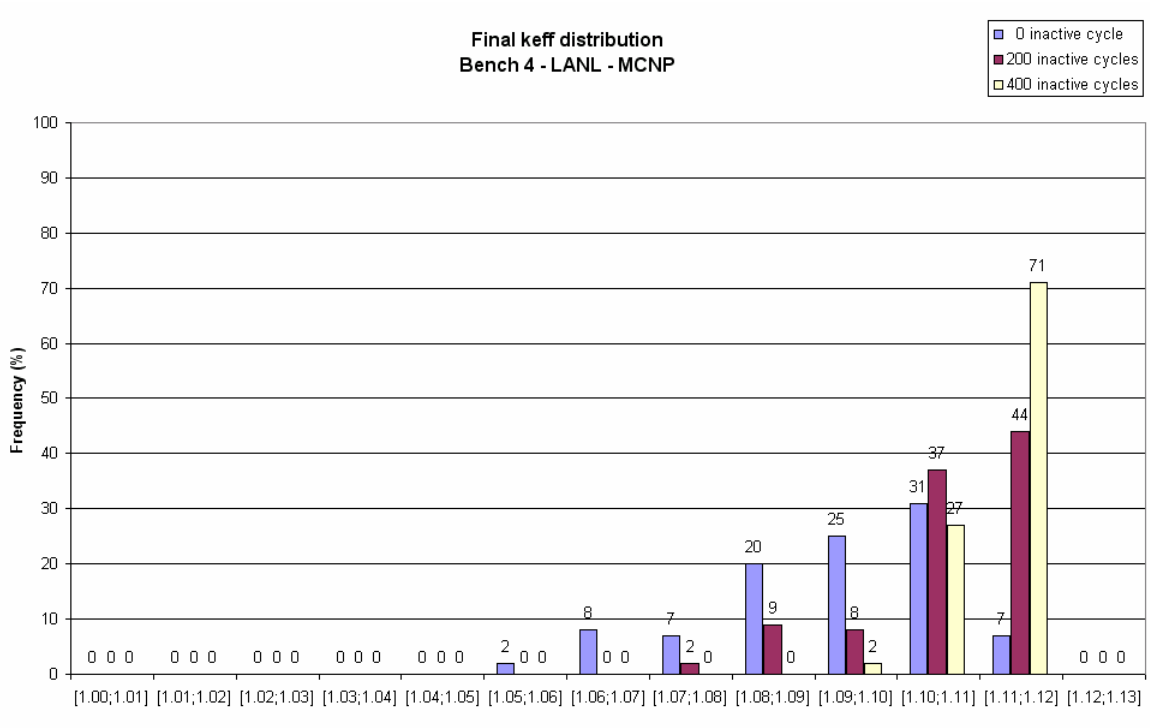
Final keff distribution
Bench 4 - LANL - MCNP
0 inactive cycle
200 inactive cycles
400 inactive cycles
Frequency (%)
[1.00;1.01] [1.01;1.02] [1.02;1.03] [1.03;1.04] [1.04;1.05] [1.05;1.06] [1.06;1.07] [1.07;1.08] [1.08;1.09] [1.09;1.10] [1.10;1.11] [1.11;1.12] [1.12;1.13]

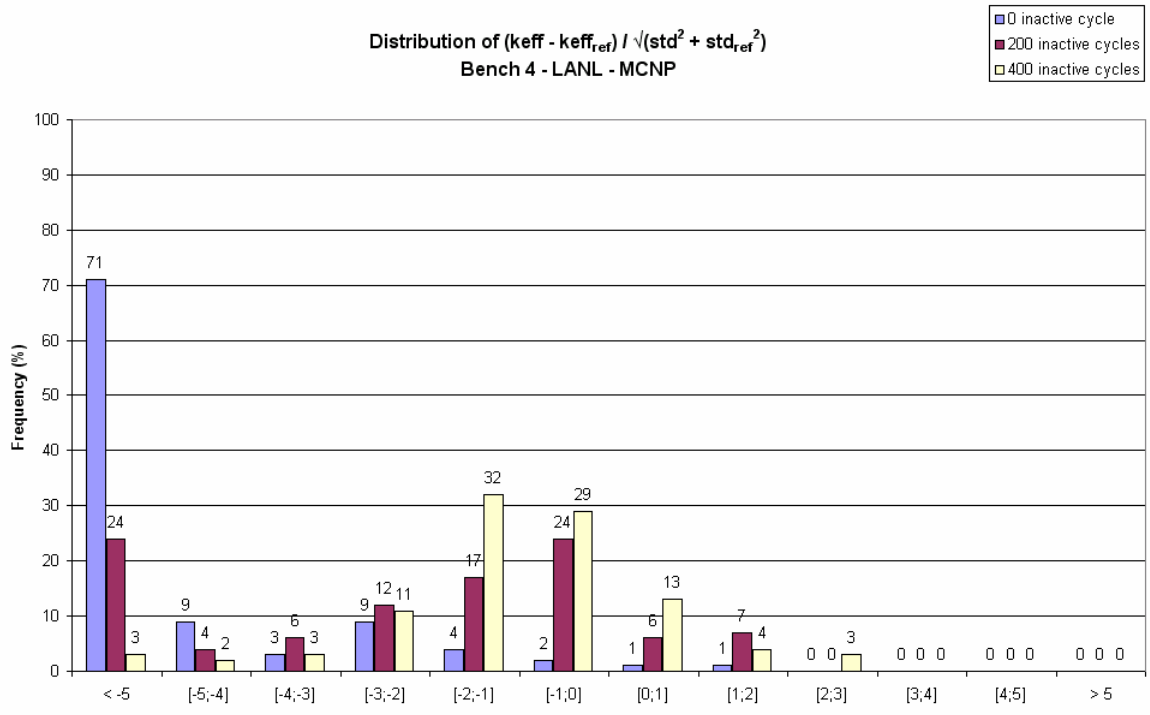
Distribution of (keff - keff$_{ref}$) / √(std^2 + std$_{ref}^2$)
Bench 4 - LANL - MCNP
0 inactive cycle
200 inactive cycles
400 inactive cycles
Frequency (%)
< -5 [-5;-4] [-4;-3] [-3;-2] [-2;-1] [-1;0] [0;1] [1;2] [2;3] [3;4] [4;5] > 5

ORNL / KENO

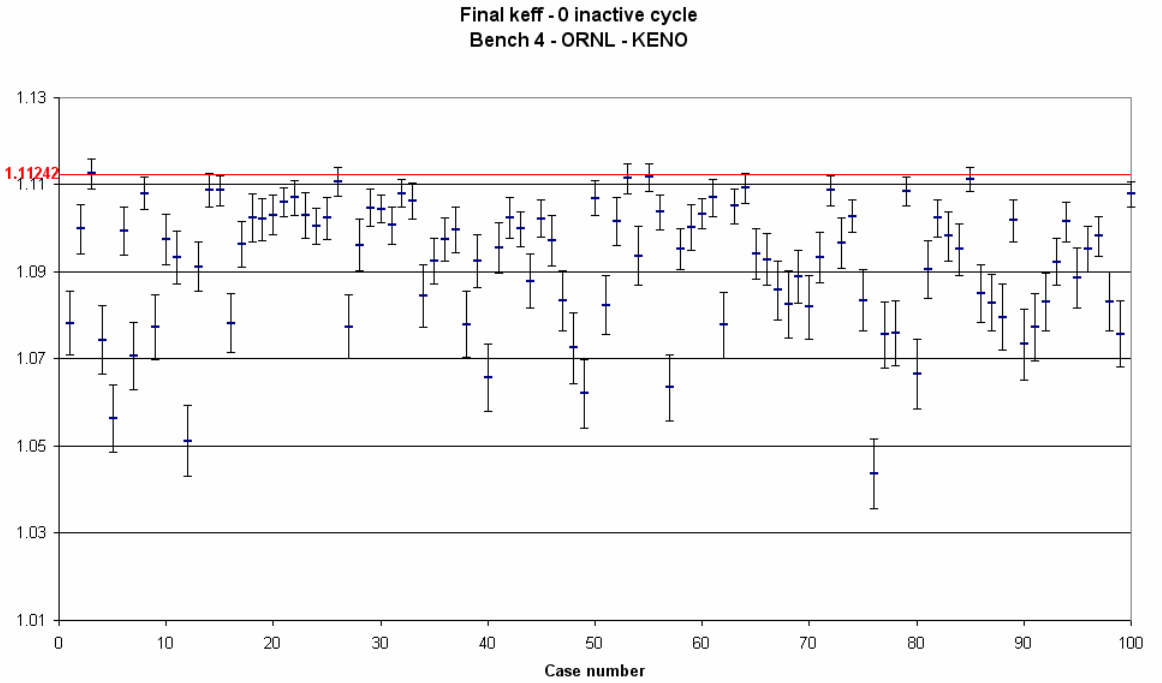
Final keff - 0 inactive cycle
Bench 4 - ORNL - KENO
1.13
1.11242
1.11
1.09
1.07
1.05
1.03
1.01
0
10
20
30
40
50
60
70
80
90
100
Case number

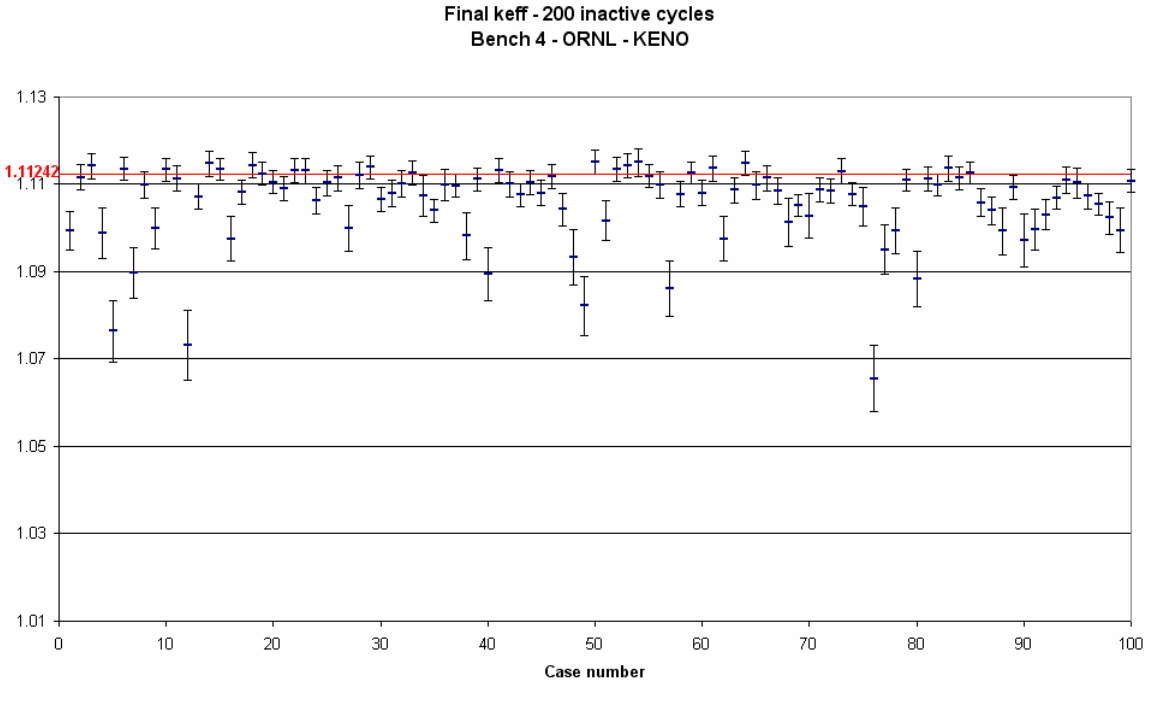
Final keff - 200 inactive cycles
Bench 4 - ORNL - KENO
1.13
1.11242
1.11
1.09
1.07
1.05
1.03
1.01
0
10
20
30
40
50
60
70
80
90
100
Case number

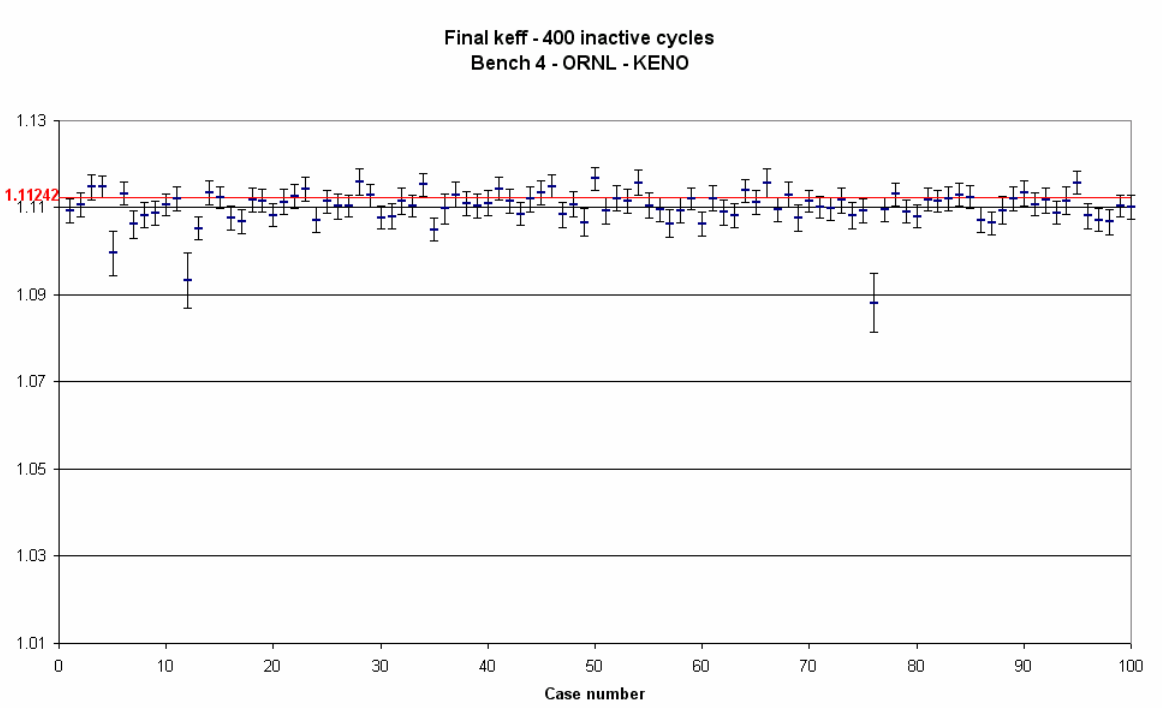
Final keff - 400 inactive cycles
Bench 4 - ORNL - KENO
1.13
1.11242
1.11
1.09
1.07
1.05
1.03
1.01
0
10
20
30
40
50
60
70
80
90
100
Case number

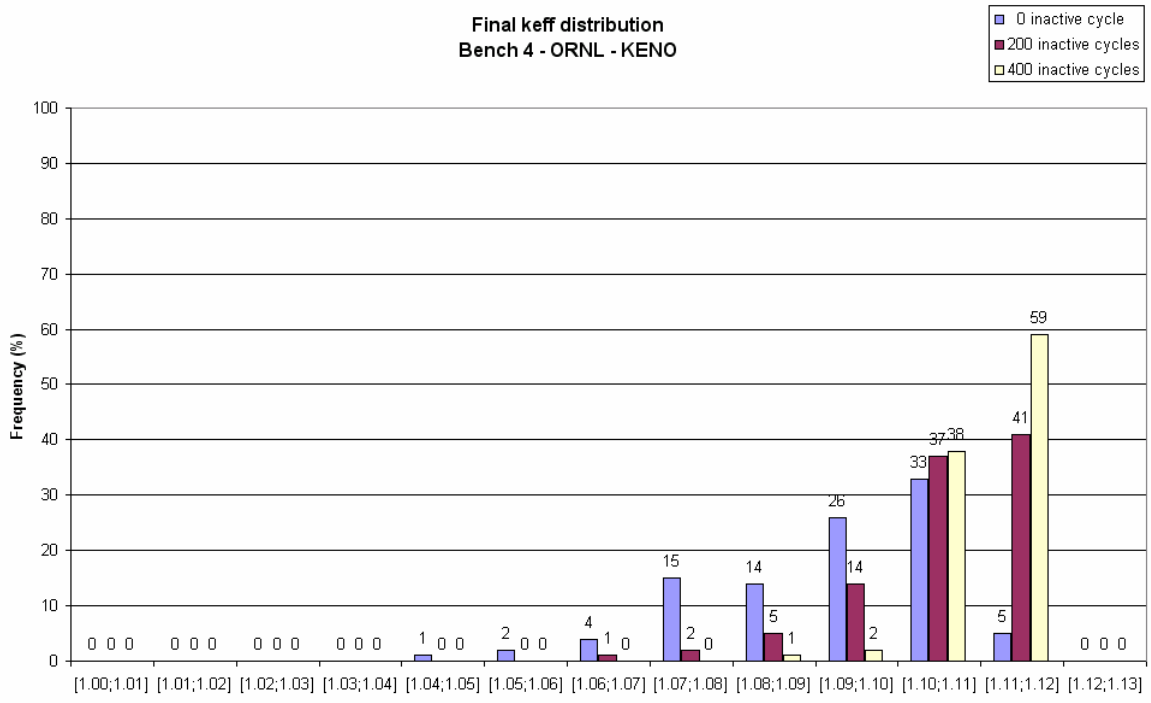
Final keff distribution
Bench 4 - ORNL - KENO
0 inactive cycle
200 inactive cycles
400 inactive cycles
Frequency (%)
100
90
80
70
60
50
40
30
20
10
0
0 0 0
0 0 0
0 0 0
0 0 0
1 0 0
2 0 0
4 1 0
15 2 0
14 5 1
26 14 2
33 37 38
5 41 59
0 0 0
[1.00;1.01]
[1.01;1.02]
[1.02;1.03]
[1.03;1.04]
[1.04;1.05]
[1.05;1.06]
[1.06;1.07]
[1.07;1.08]
[1.08;1.09]
[1.09;1.10]
[1.10;1.11]
[1.11;1.12]
[1.12;1.13]

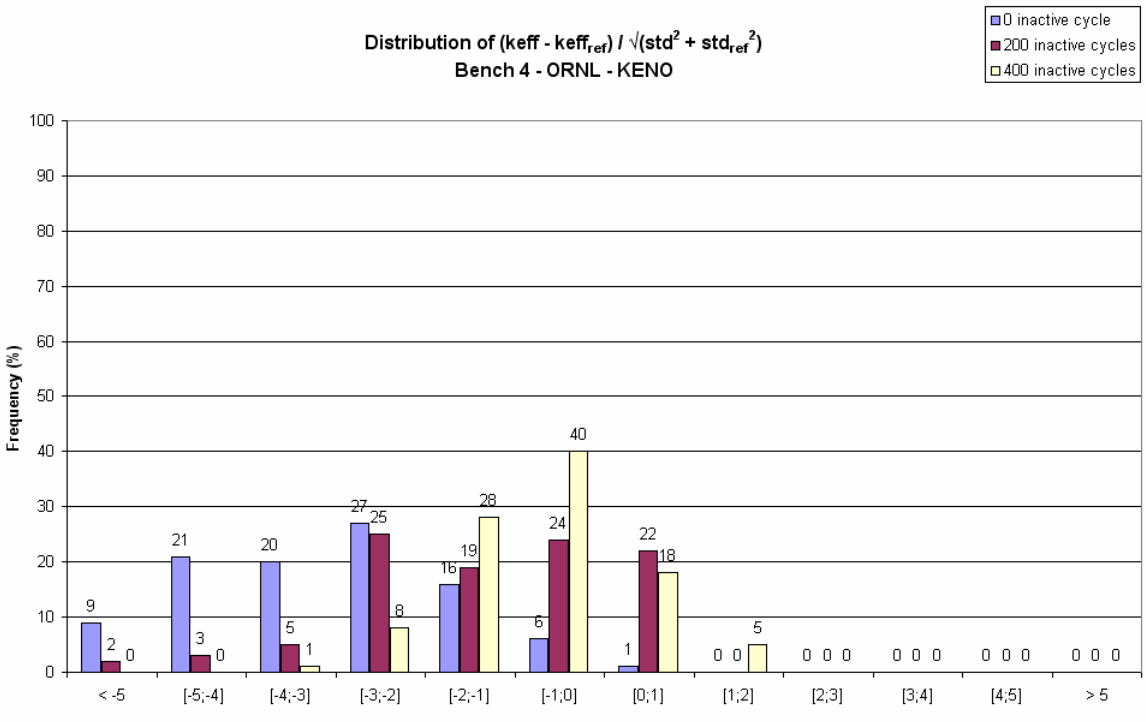
Distribution of (keff - keff$_{ref}$) / √(std^2 + std$_{ref}^2$)
Bench 4 - ORNL - KENO
0 inactive cycle
200 inactive cycles
400 inactive cycles
Frequency (%)
100
90
80
70
60
50
40
30
20
10
0
9 2 0
21 3 0
20 5 1
27 25 8
16 19 28
6 24 40
1 22 18
0 0 5
0 0 0
0 0 0
0 0 0
0 0 0
< -5
[-5;-4]
[-4;-3]
[-3;-2]
[-2;-1]
[-1;0]
[0;1]
[1;2]
[2;3]
[3;4]
[4;5]
> 5

Appendix 5.d

FINAL FISSION FRACTION OF CENTRAL SPHERE

On each figure, the horizontal line corresponds to the reference fission fraction of the central sphere determined by the contributor. The fission fractions are given with one standard deviation uncertainty, computed by the code, when this information is available.

ANL / VIM

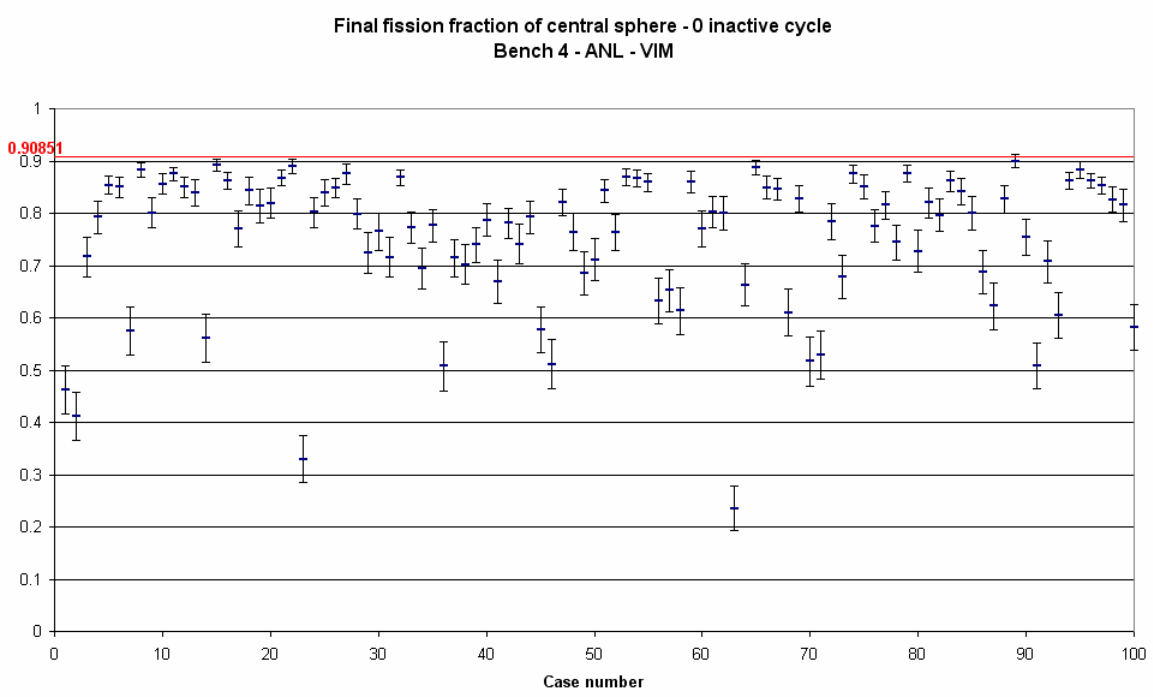

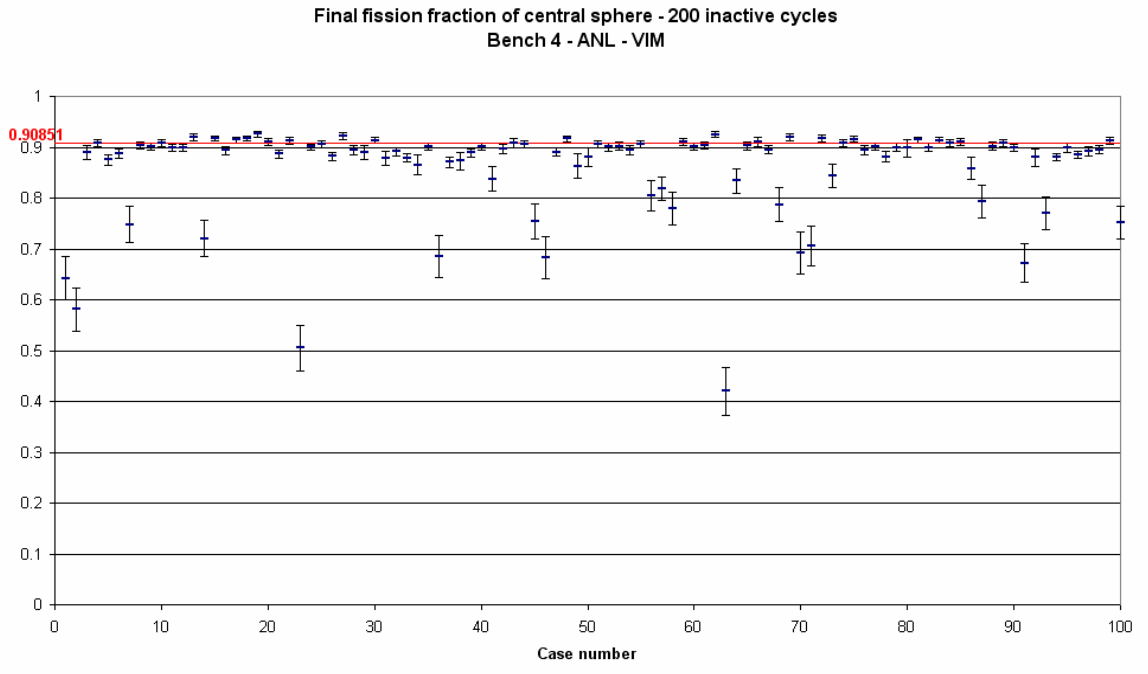

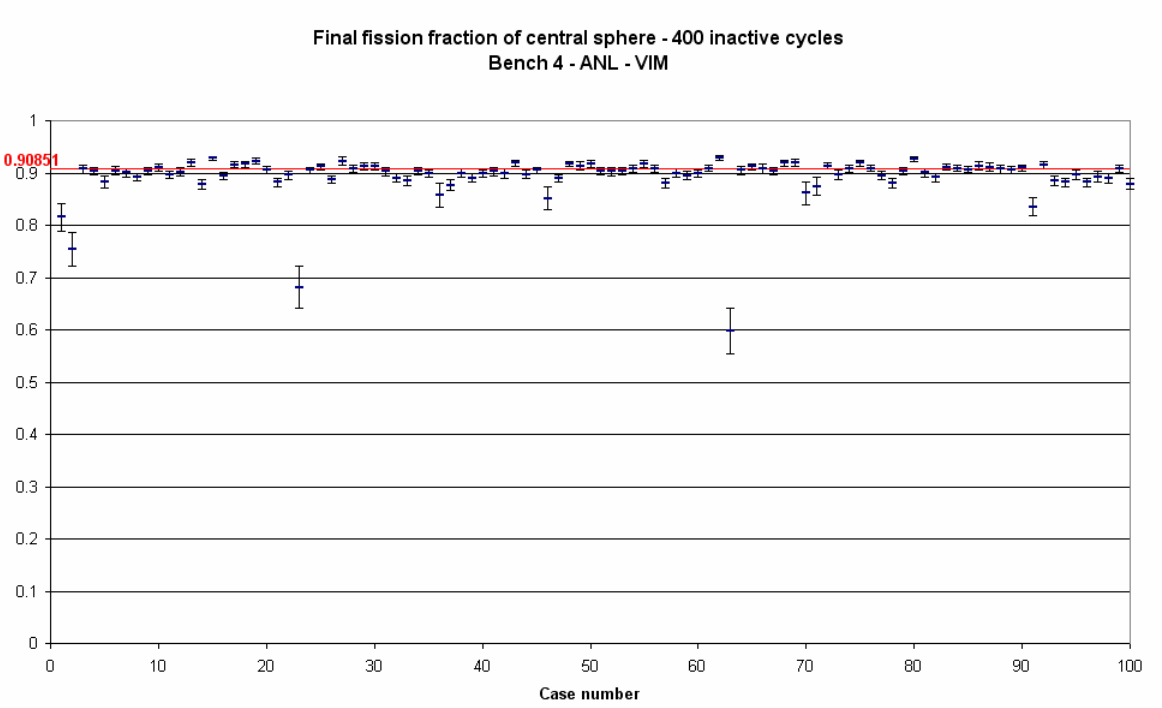
Final fission fraction of central sphere - 400 inactive cycles
Bench 4 - ANL - VIM
0.90851
Case number

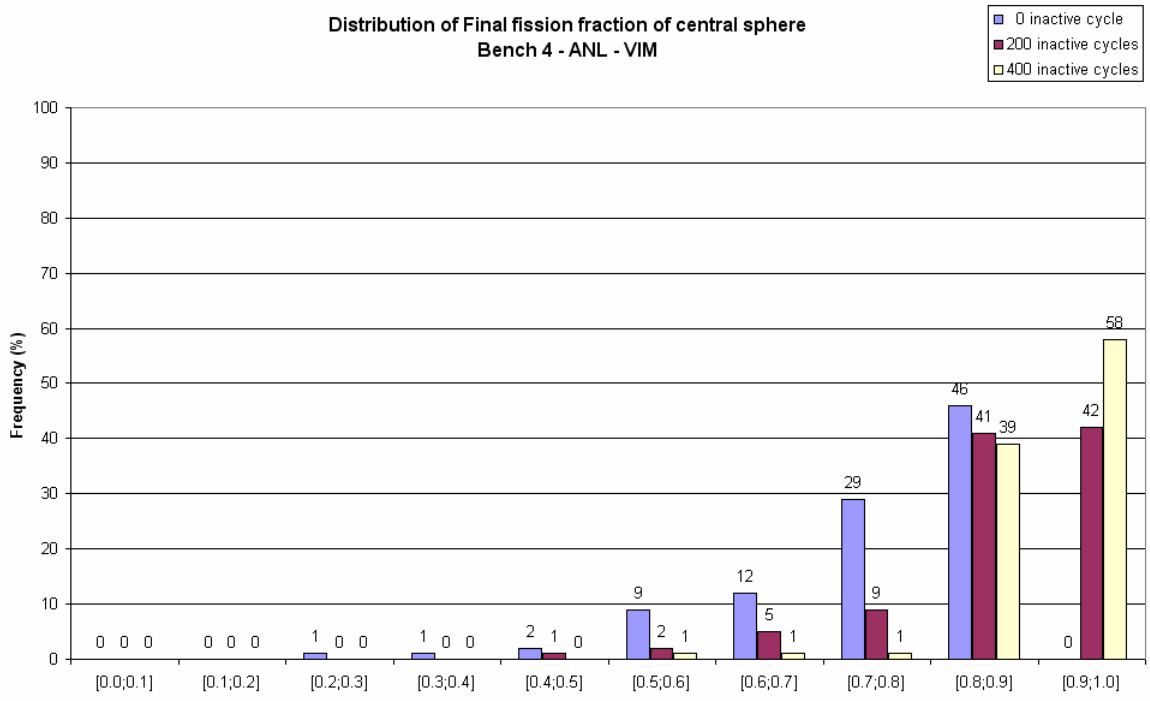
Distribution of Final fission fraction of central sphere
Bench 4 - ANL - VIM
0 inactive cycle
200 inactive cycles
400 inactive cycles
Frequency (%)
[0.0;0.1]
[0.1;0.2]
[0.2;0.3]
[0.3;0.4]
[0.4;0.5]
[0.5;0.6]
[0.6;0.7]
[0.7;0.8]
[0.8;0.9]
[0.9;1.0]

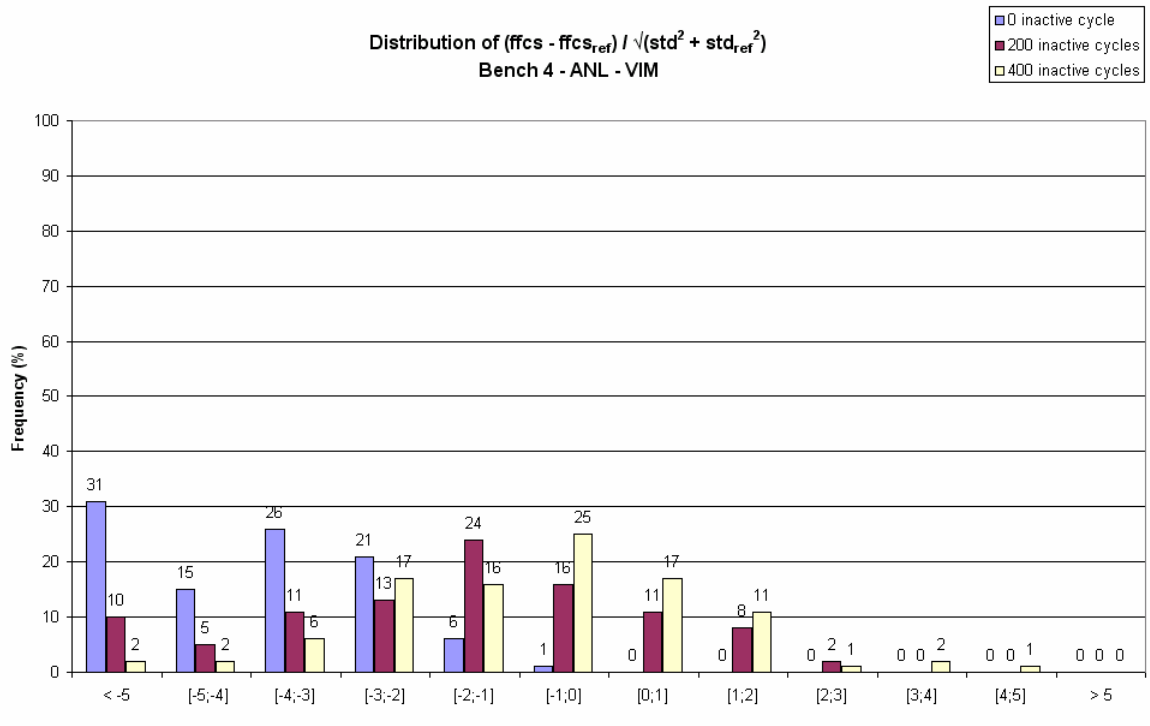
Distribution of (ffcs - ffcs$_{ref}$) / √(std^2 + std$_{ref}^2$)
Bench 4 - ANL - VIM
0 inactive cycle
200 inactive cycles
400 inactive cycles
Frequency (%)
< -5
[-5;-4]
[-4;-3]
[-3;-2]
[-2;-1]
[-1;0]
[0;1]
[1;2]
[2;3]
[3;4]
[4;5]
> 5

EMS / KENO

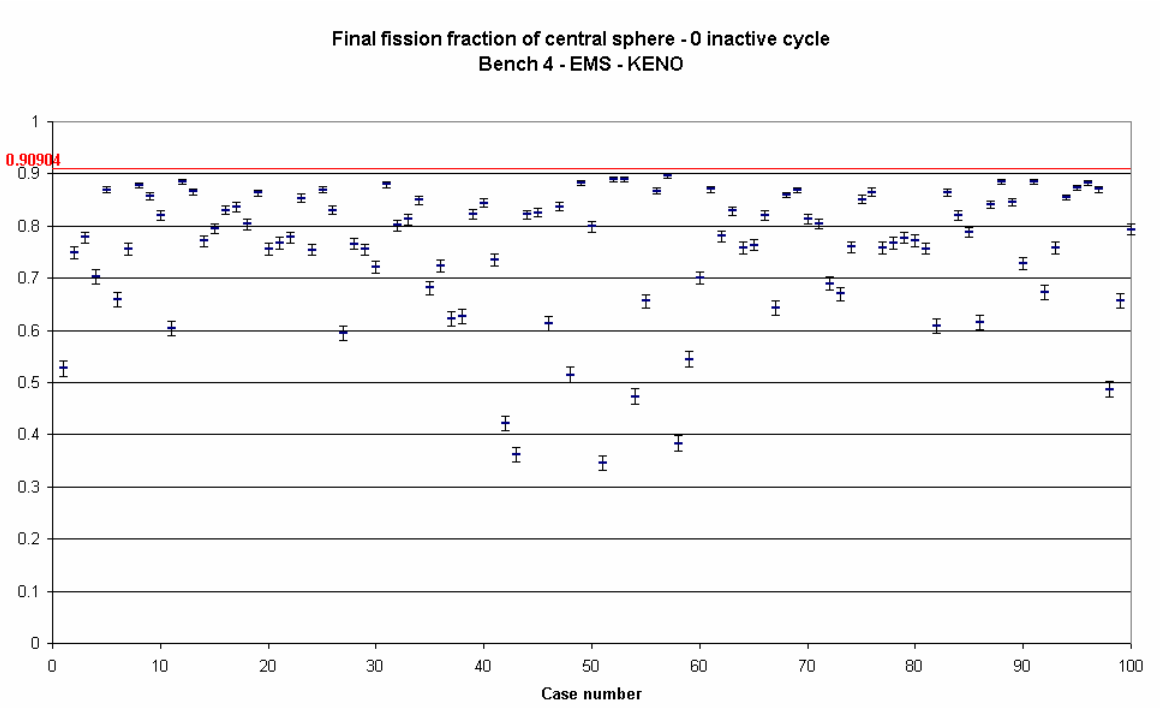
Final fission fraction of central sphere - 0 inactive cycle
Bench 4 - EMS - KENO
0.90904
Case number

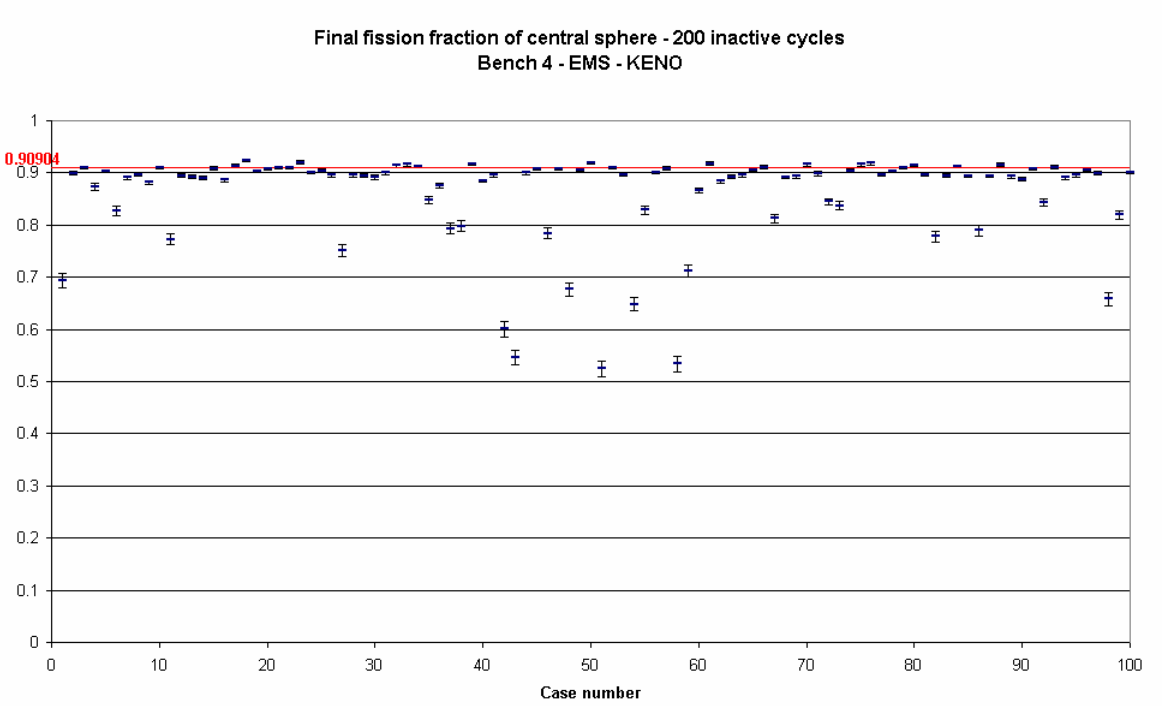
Final fission fraction of central sphere - 200 inactive cycles
Bench 4 - EMS - KENO
0.90904
1
0.9
0.8
0.7
0.6
0.5
0.4
0.3
0.2
0.1
0
0
10
20
30
40
50
60
70
80
90
100
Case number

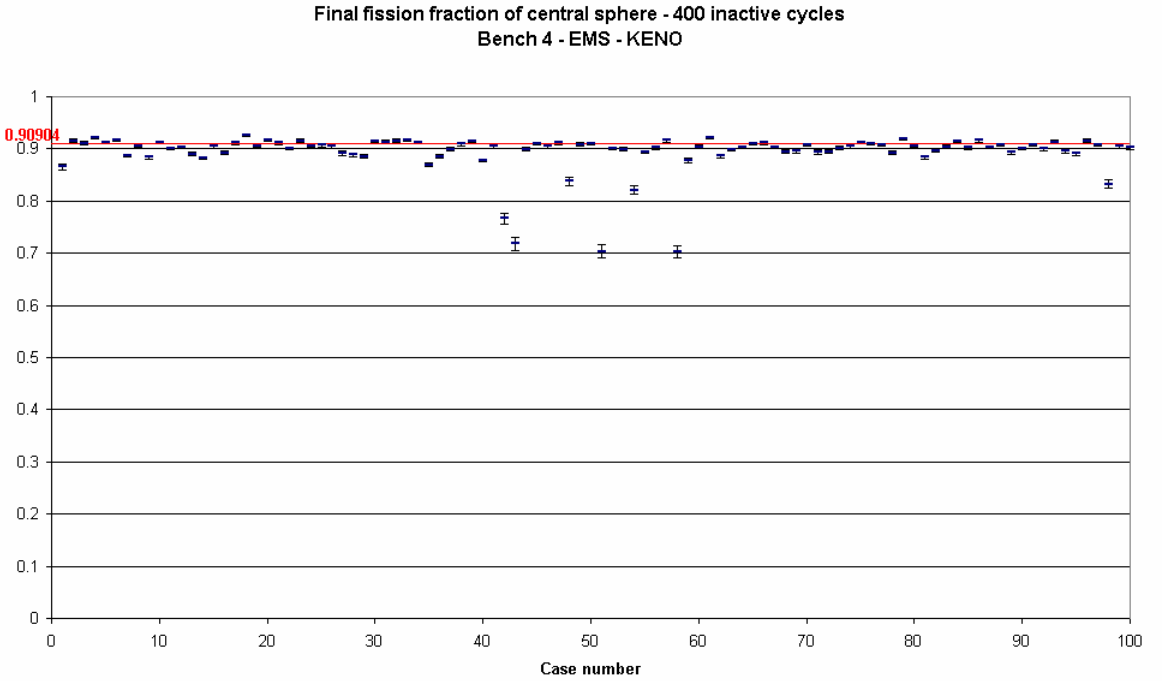
Final fission fraction of central sphere - 400 inactive cycles
Bench 4 - EMS - KENO
0.90904
1
0.9
0.8
0.7
0.6
0.5
0.4
0.3
0.2
0.1
0
0
10
20
30
40
50
60
70
80
90
100
Case number

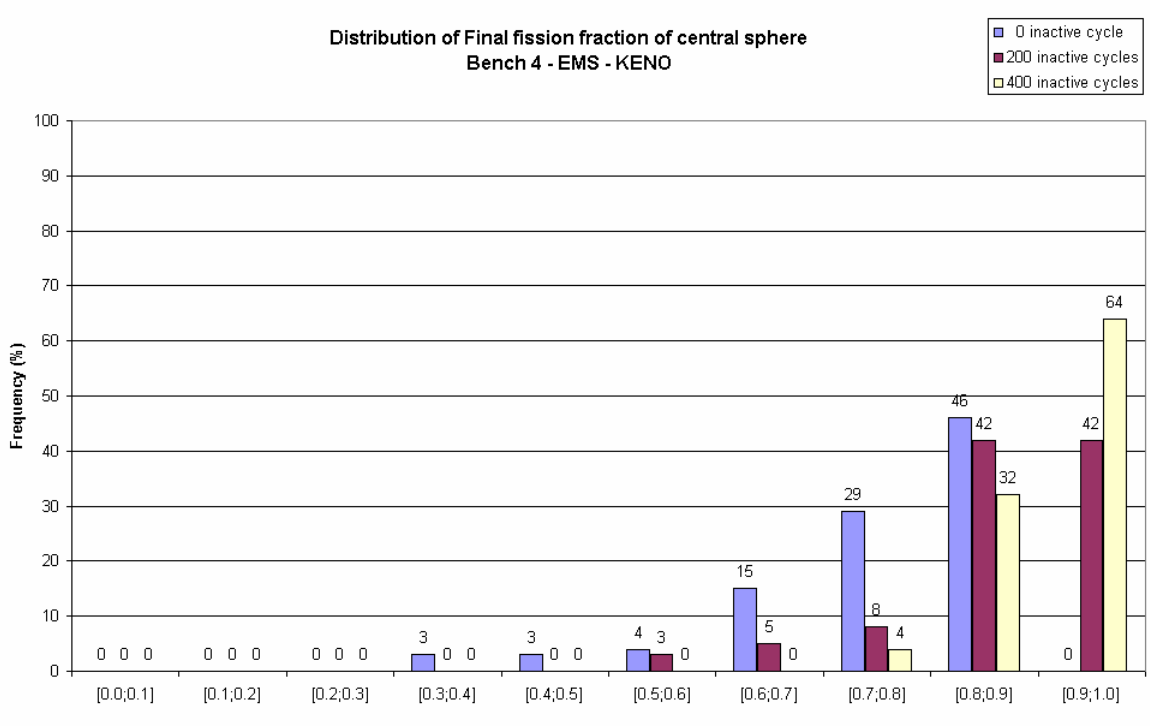
Distribution of Final fission fraction of central sphere
Bench 4 - EMS - KENO
0 inactive cycle
200 inactive cycles
400 inactive cycles
Frequency (%)
100
90
80
70
60
50
40
30
20
10
0
0 0 0
0 0 0
0 0 0
3 0 0
3 0 0
4 3 0
15 5 0
29 8 4
46 42 32
0 42 64
[0.0;0.1]
[0.1;0.2]
[0.2;0.3]
[0.3;0.4]
[0.4;0.5]
[0.5;0.6]
[0.6;0.7]
[0.7;0.8]
[0.8;0.9]
[0.9;1.0]

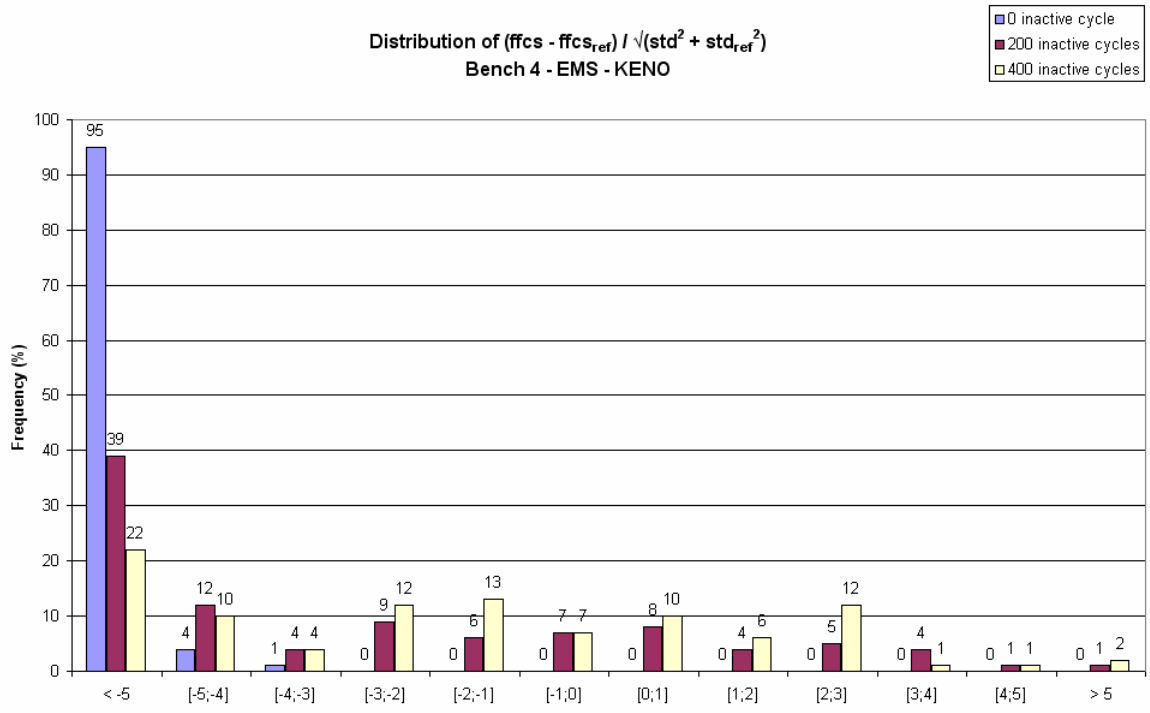
Distribution of (ffcs - ffcs$_{ref}$) / √(std^2 + std$_{ref}^2$)
Bench 4 - EMS - KENO
0 inactive cycle
200 inactive cycles
400 inactive cycles
Frequency (%)
100
90
80
70
60
50
40
30
20
10
0
95 39 22
4 12 10
1 4 4
0 9 12
0 6 13
0 7 7
0 8 10
0 4 6
0 5 12
0 4 1
0 1 1
0 1 2
< -5
[-5;-4]
[-4;-3]
[-3;-2]
[-2;-1]
[-1;0]
[0;1]
[1;2]
[2;3]
[3;4]
[4;5]
> 5

IPPE / KENO

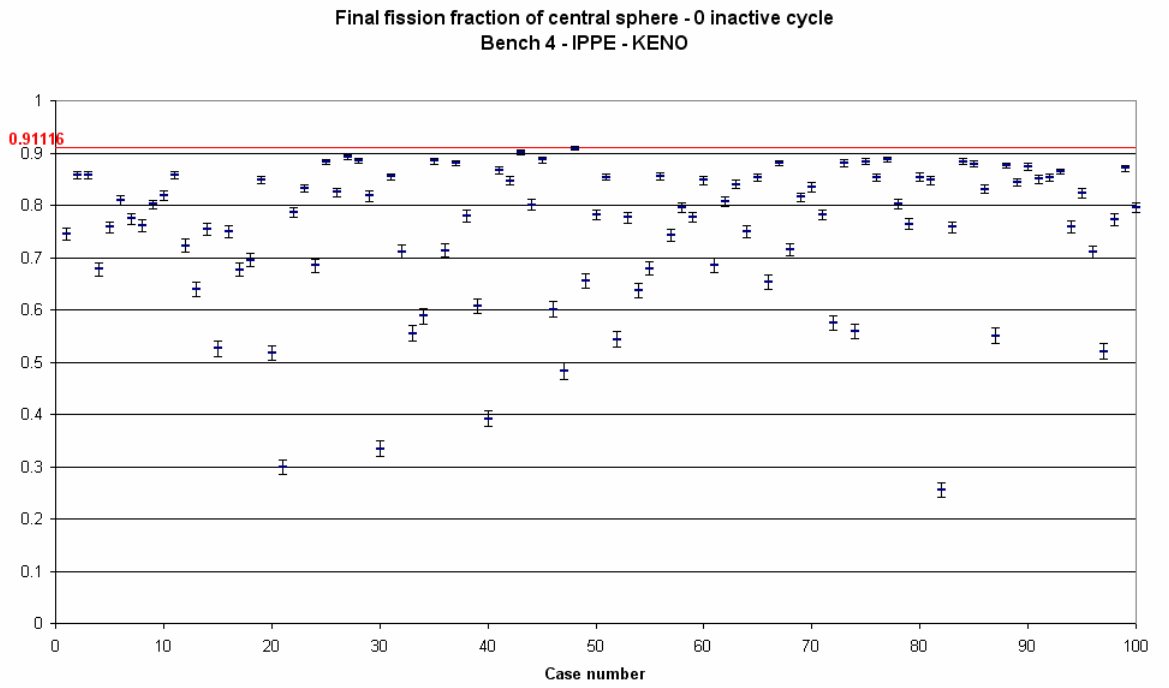
Final fission fraction of central sphere - 0 inactive cycle
Bench 4 - IPPE - KENO
0.91116
Case number

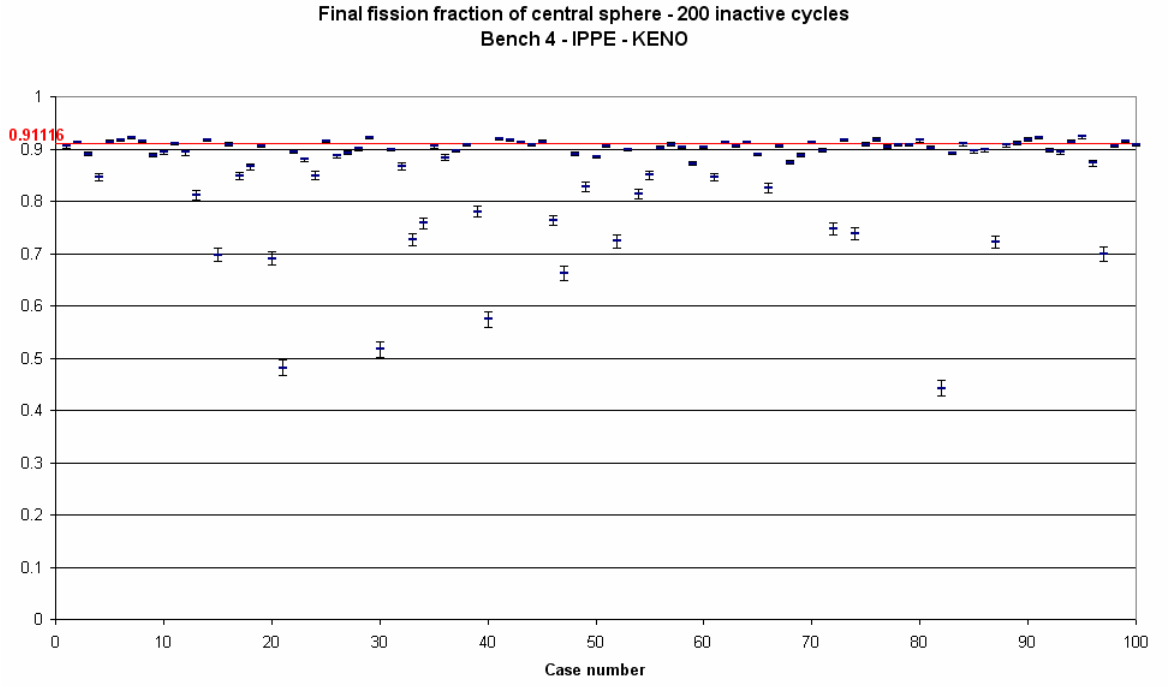
Final fission fraction of central sphere - 200 inactive cycles
Bench 4 - IPPE - KENO
0.91116
Case number

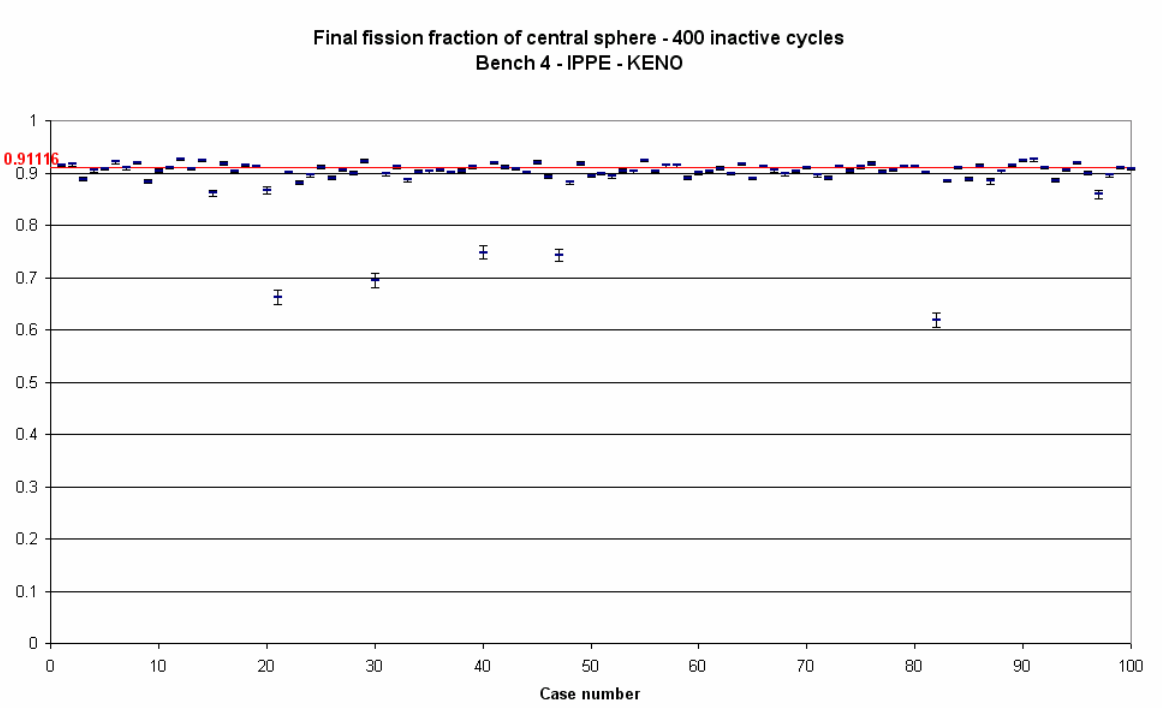
Final fission fraction of central sphere - 400 inactive cycles
Bench 4 - IPPE - KENO
0.91116
1
0.9
0.8
0.7
0.6
0.5
0.4
0.3
0.2
0.1
0
0
10
20
30
40
50
60
70
80
90
100
Case number

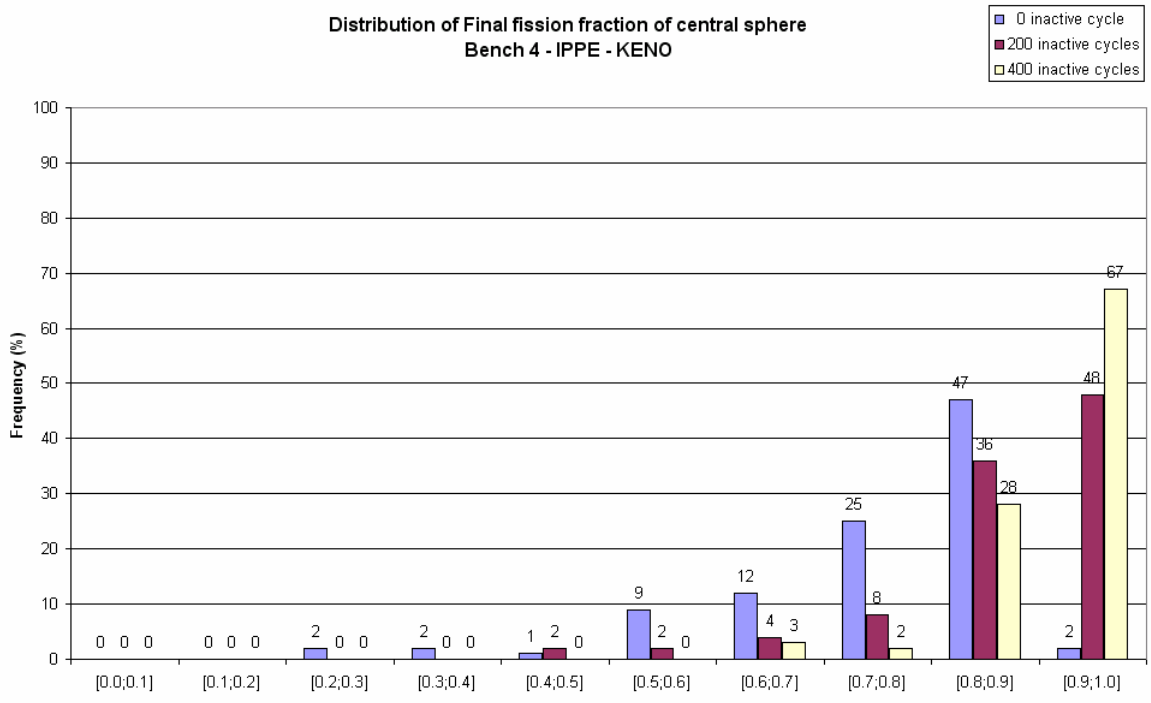
Distribution of Final fission fraction of central sphere
Bench 4 - IPPE - KENO
0 inactive cycle
200 inactive cycles
400 inactive cycles
Frequency (%)
100
90
80
70
60
50
40
30
20
10
0
0 0 0
0 0 0
2 0 0
2 0 0
1 2 0
9 2 0
12 4 3
25 8 2
47 36 28
2 48 67
[0.0;0.1]
[0.1;0.2]
[0.2;0.3]
[0.3;0.4]
[0.4;0.5]
[0.5;0.6]
[0.6;0.7]
[0.7;0.8]
[0.8;0.9]
[0.9;1.0]

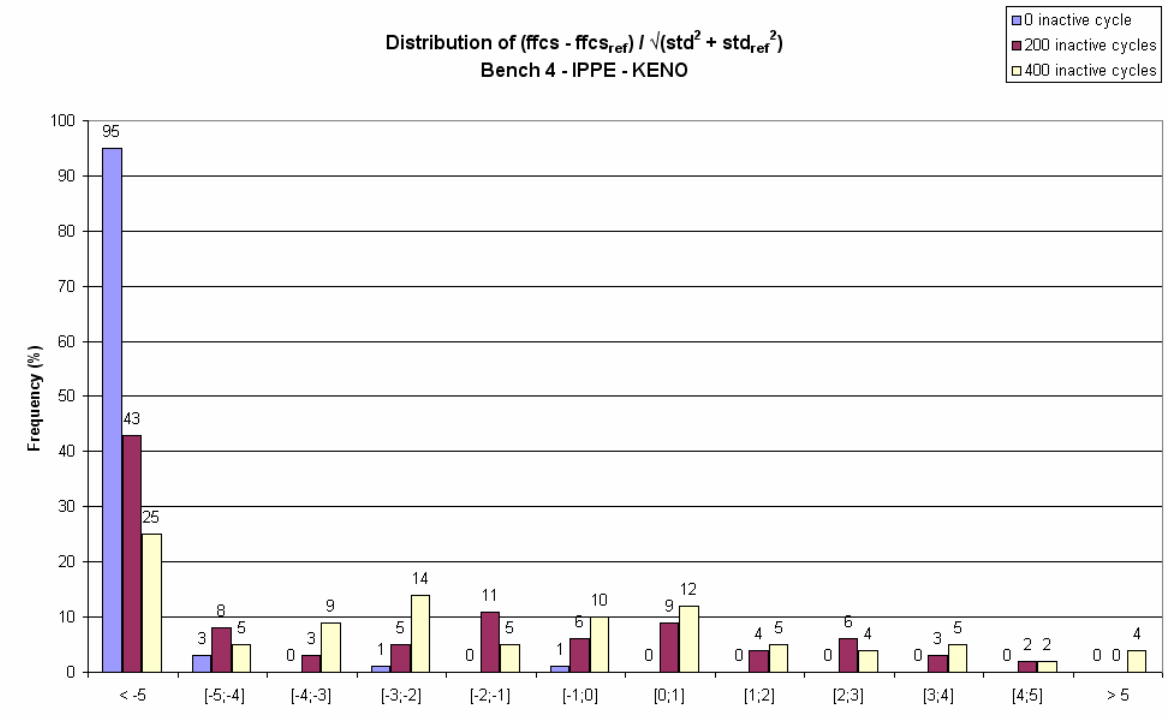
Distribution of (ffcs - ffcs$_{ref}$) / √(std^2 + std$_{ref}^2$)
Bench 4 - IPPE - KENO
0 inactive cycle
200 inactive cycles
400 inactive cycles
Frequency (%)
< -5
[-5;-4]
[-4;-3]
[-3;-2]
[-2;-1]
[-1;0]
[0;1]
[1;2]
[2;3]
[3;4]
[4;5]
> 5

IRSN / MORET

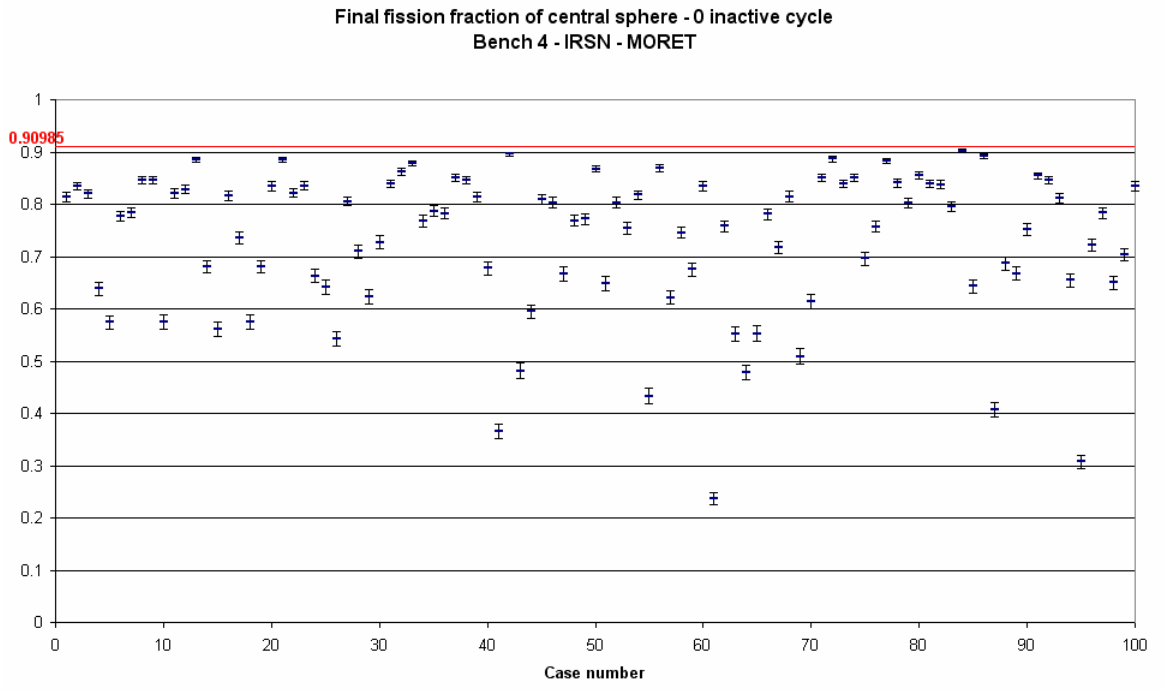
Final fission fraction of central sphere - 0 inactive cycle
Bench 4 - IRSN - MORET
0.90985
Case number

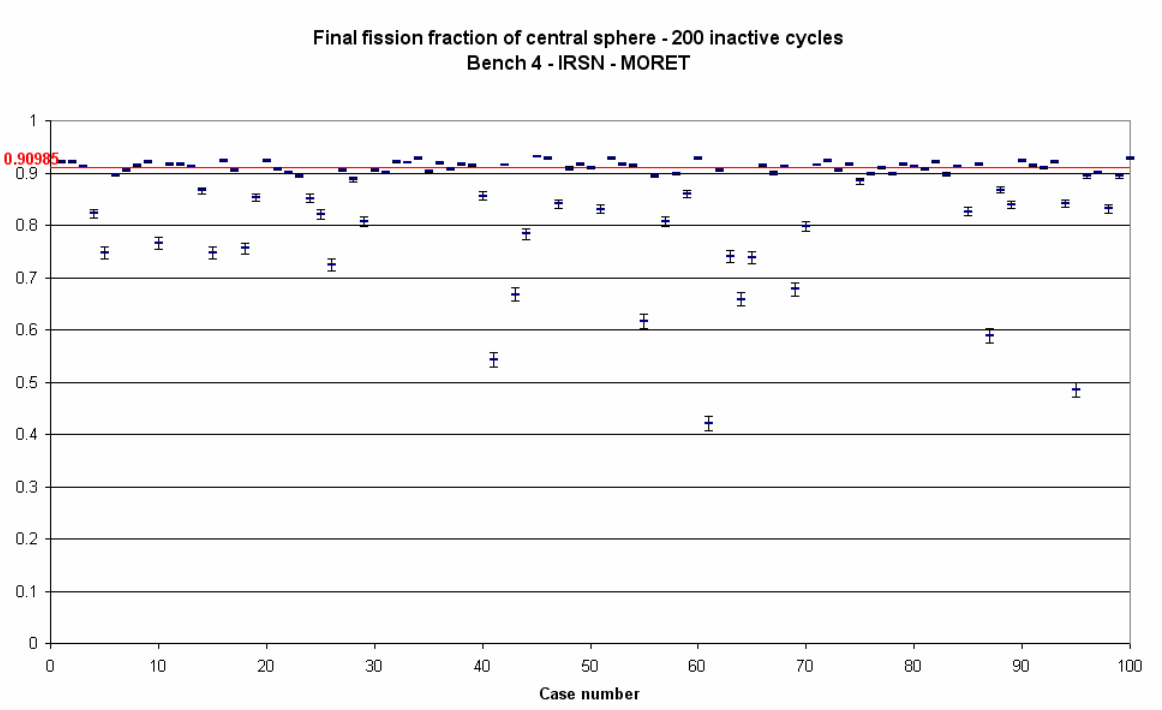
Final fission fraction of central sphere - 200 inactive cycles
Bench 4 - IRSN - MORET
0.90985
Case number

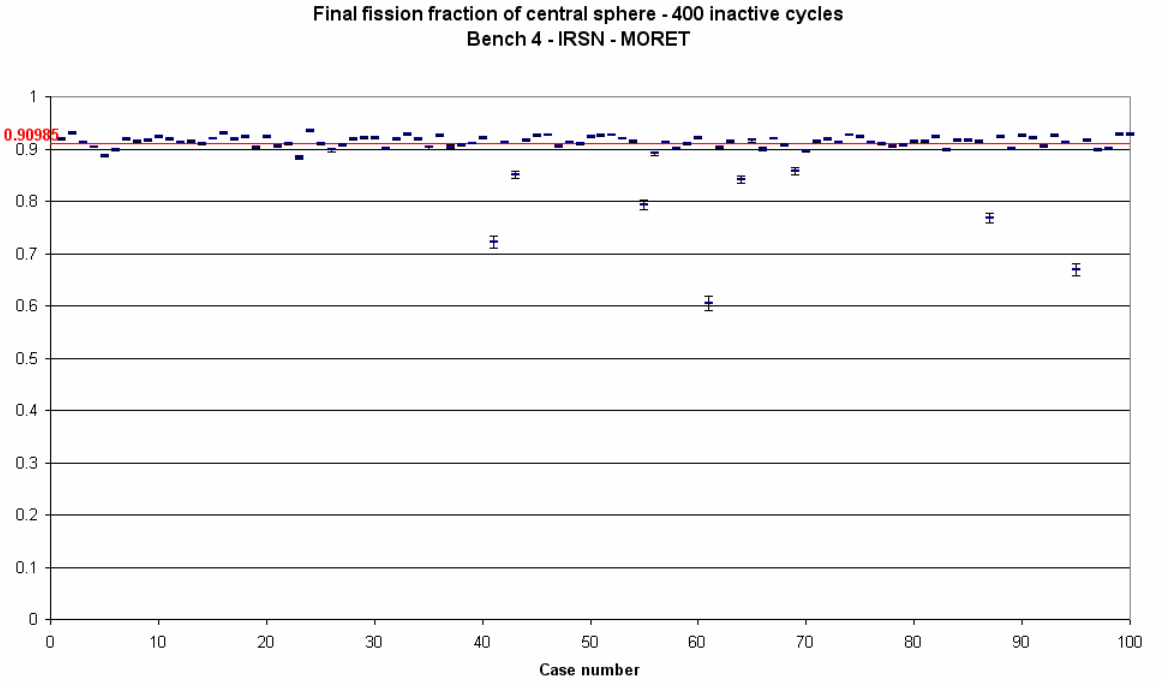
Final fission fraction of central sphere - 400 inactive cycles
Bench 4 - IRSN - MORET
0.90985
Case number

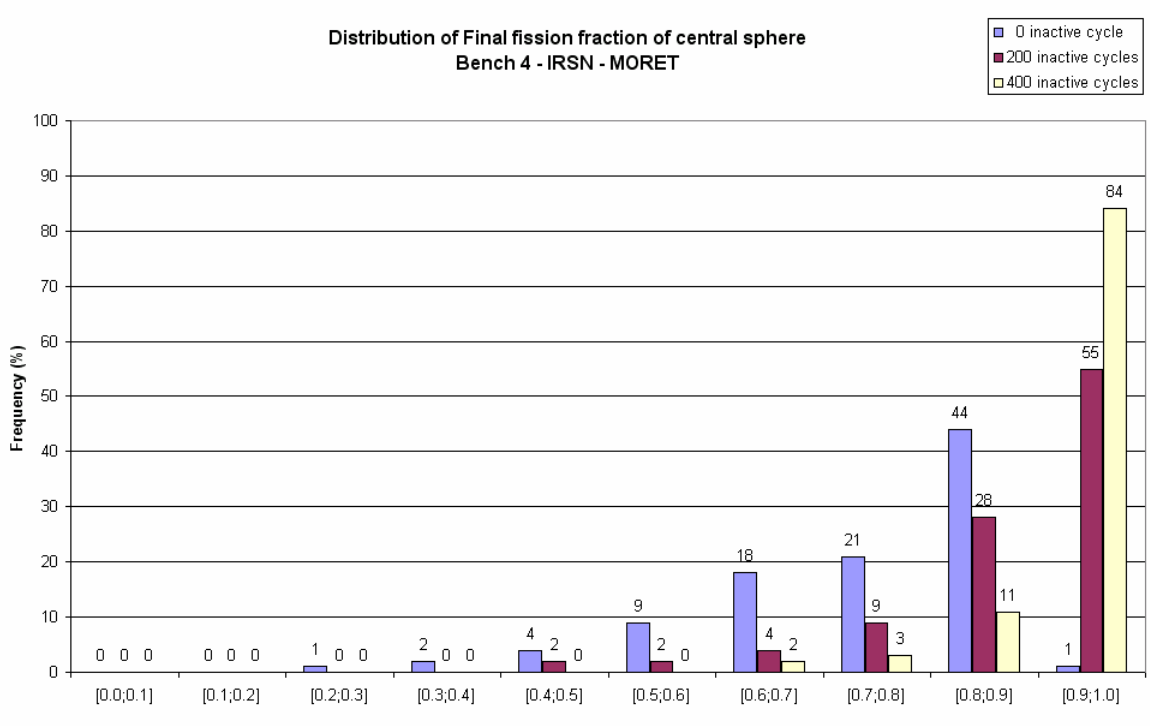
Distribution of Final fission fraction of central sphere
Bench 4 - IRSN - MORET
0 inactive cycle
200 inactive cycles
400 inactive cycles
Frequency (%)
[0.0;0.1]
[0.1;0.2]
[0.2;0.3]
[0.3;0.4]
[0.4;0.5]
[0.5;0.6]
[0.6;0.7]
[0.7;0.8]
[0.8;0.9]
[0.9;1.0]

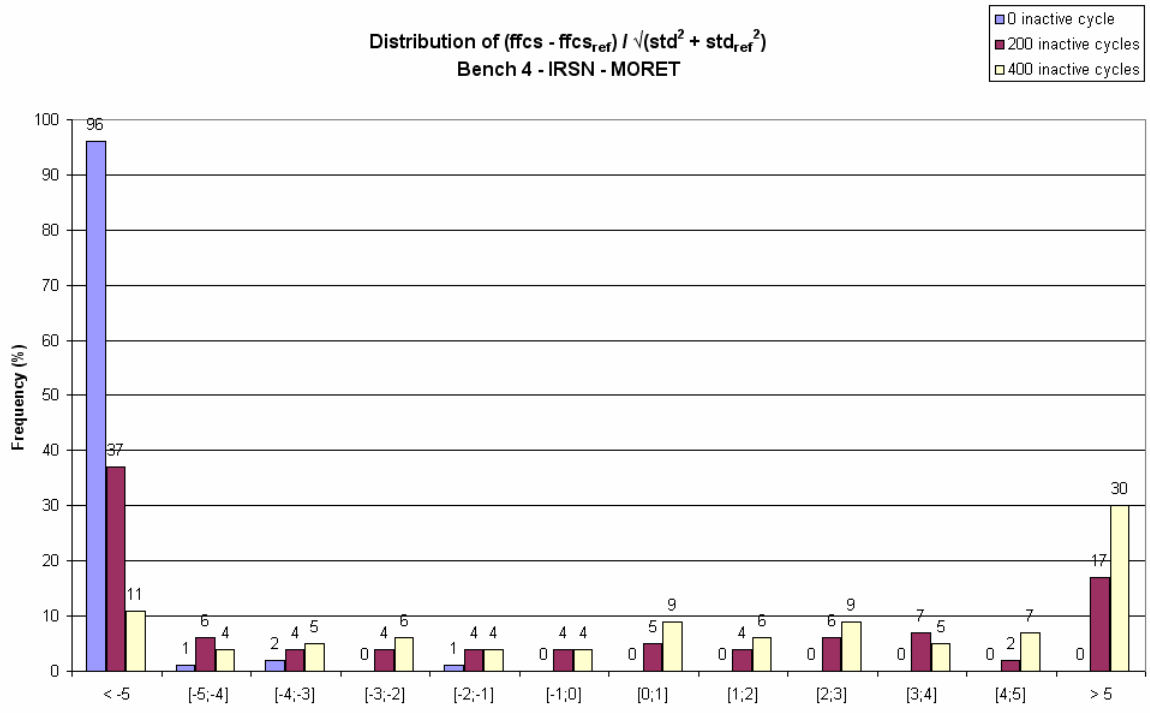
Distribution of (ffcs - ffcs$_{ref}$) / √(std^2 + std$_{ref}^2$)
Bench 4 - IRSN - MORET
0 inactive cycle
200 inactive cycles
400 inactive cycles
Frequency (%)
< -5
[-5;-4]
[-4;-3]
[-3;-2]
[-2;-1]
[-1;0]
[0;1]
[1;2]
[2;3]
[3;4]
[4;5]
> 5

JNC / KENO

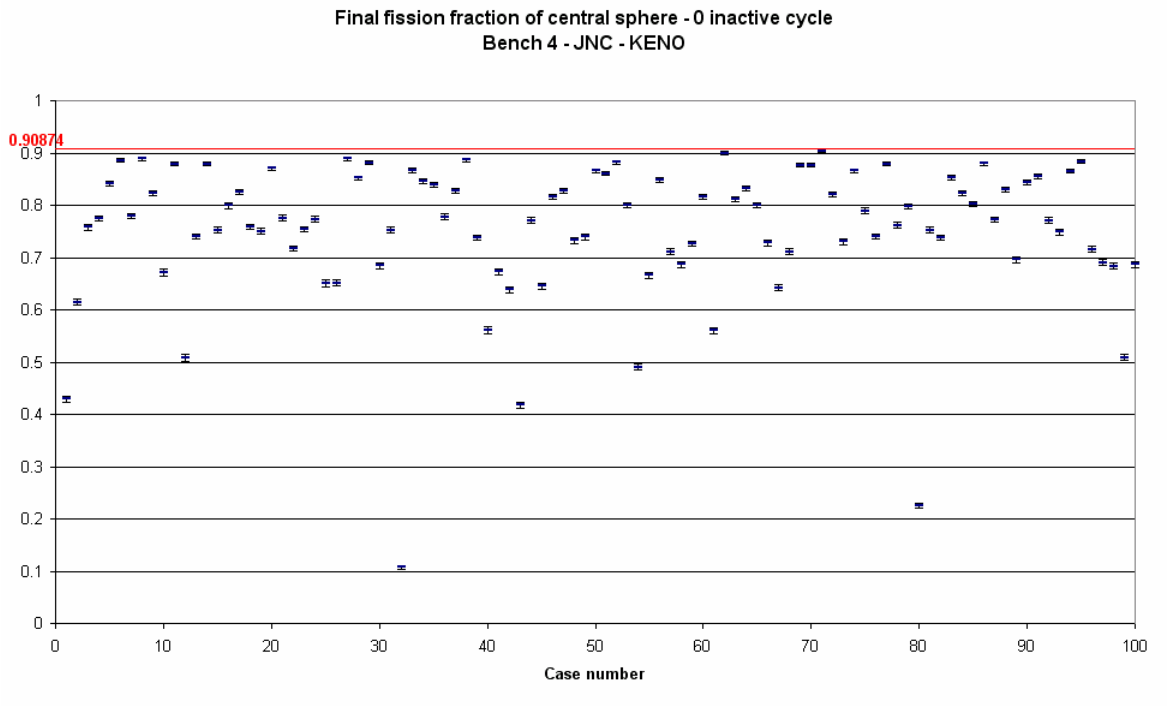
Final fission fraction of central sphere - 0 inactive cycle
Bench 4 - JNC - KENO
0.90874
1
0.9
0.8
0.7
0.6
0.5
0.4
0.3
0.2
0.1
0
0
10
20
30
40
50
60
70
80
90
100
Case number

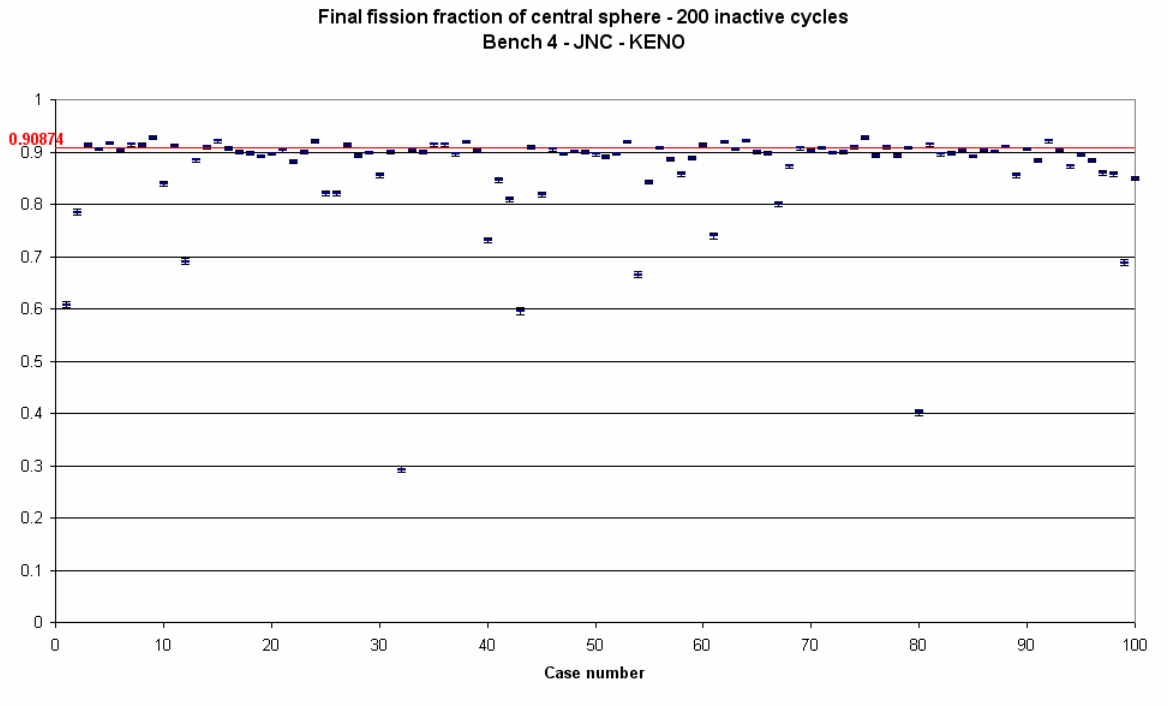
Final fission fraction of central sphere - 200 inactive cycles
Bench 4 - JNC - KENO
0.90874
1
0.9
0.8
0.7
0.6
0.5
0.4
0.3
0.2
0.1
0
0
10
20
30
40
50
60
70
80
90
100
Case number

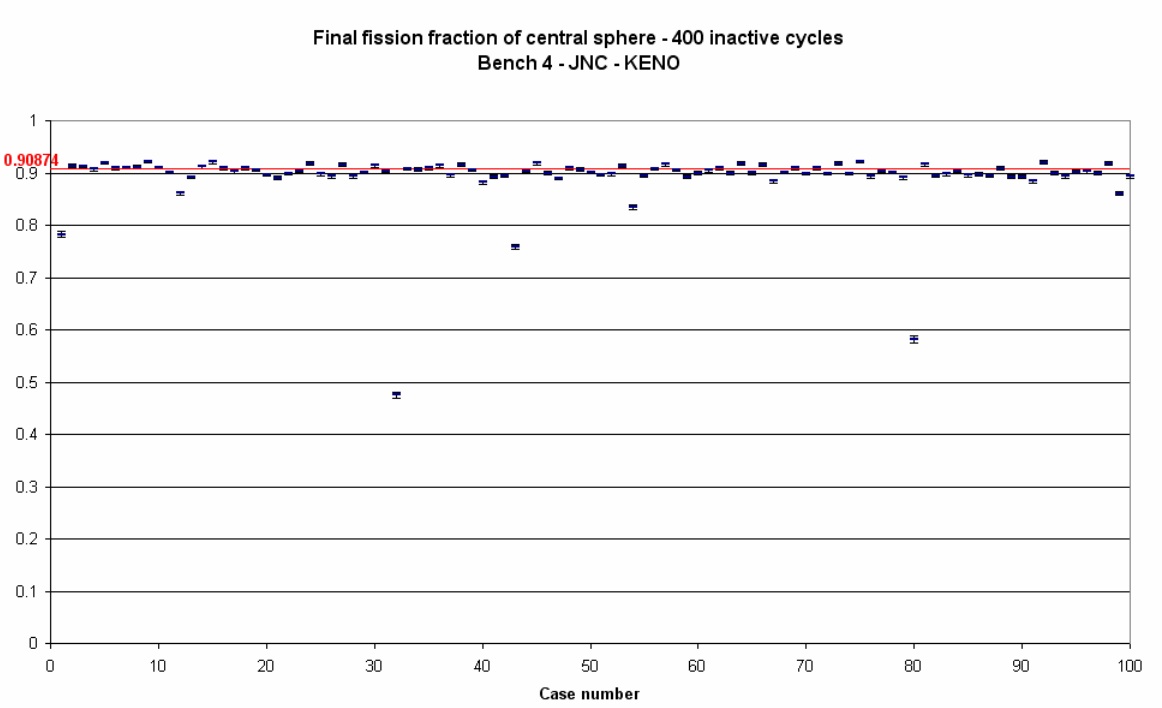
Final fission fraction of central sphere - 400 inactive cycles
Bench 4 - JNC - KENO
0.90874
Case number

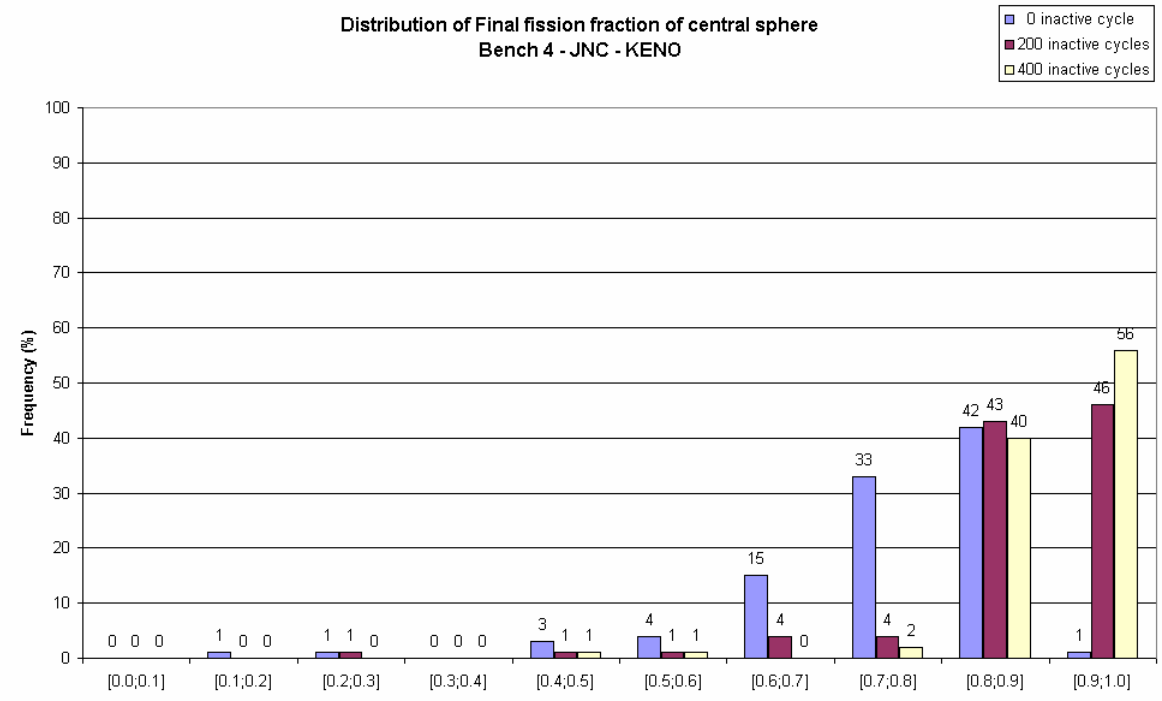
Distribution of Final fission fraction of central sphere
Bench 4 - JNC - KENO
0 inactive cycle
200 inactive cycles
400 inactive cycles
Frequency (%)
[0.0;0.1]
[0.1;0.2]
[0.2;0.3]
[0.3;0.4]
[0.4;0.5]
[0.5;0.6]
[0.6;0.7]
[0.7;0.8]
[0.8;0.9]
[0.9;1.0]

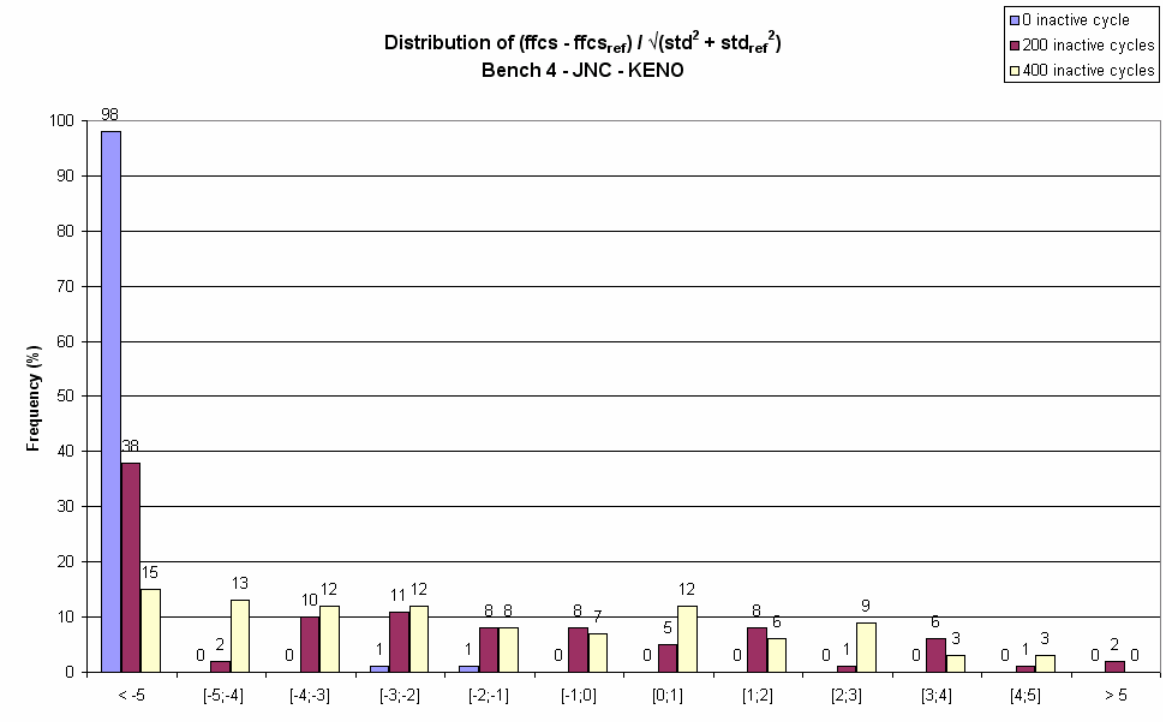
Distribution of (ffcs - ffcs$_{ref}$) / √(std^2 + std$_{ref}^2$)
Bench 4 - JNC - KENO
0 inactive cycle
200 inactive cycles
400 inactive cycles
Frequency (%)
< -5
[-5;-4]
[-4;-3]
[-3;-2]
[-2;-1]
[-1;0]
[0;1]
[1;2]
[2;3]
[3;4]
[4;5]
> 5

LANL / MCNP

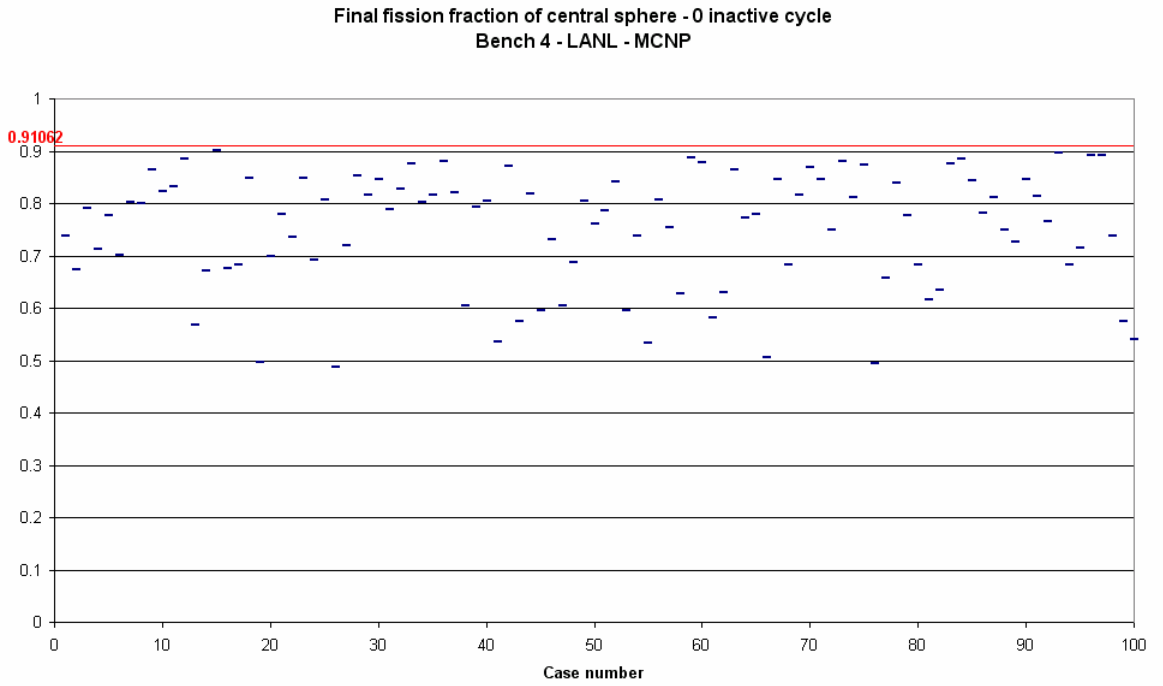
Final fission fraction of central sphere - 0 inactive cycle
Bench 4 - LANL - MCNP
0.91062
Case number

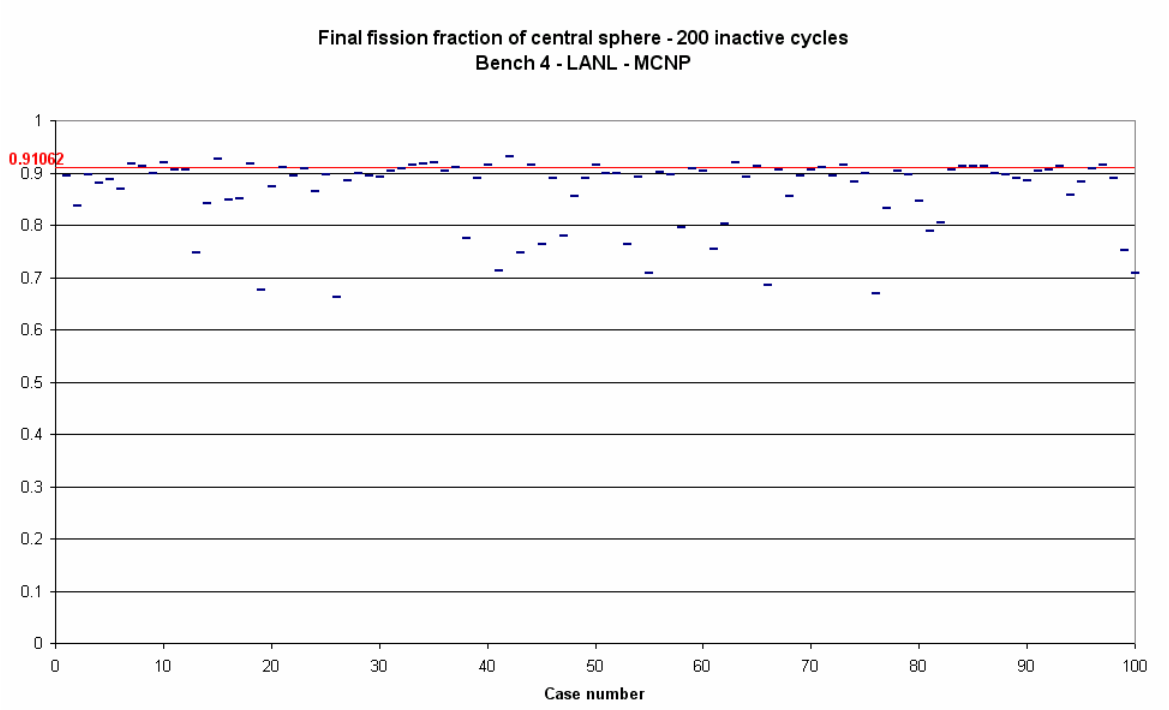
Final fission fraction of central sphere - 200 inactive cycles
Bench 4 - LANL - MCNP
0.91062
1
0.9
0.8
0.7
0.6
0.5
0.4
0.3
0.2
0.1
0
0
10
20
30
40
50
60
70
80
90
100
Case number

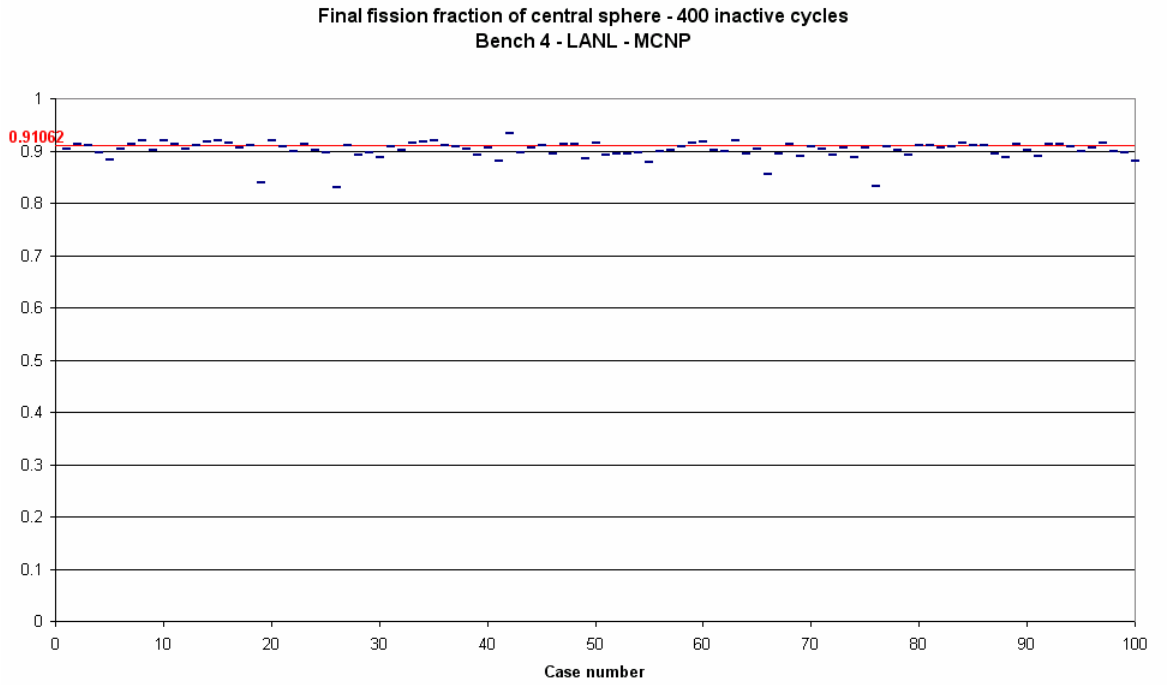
Final fission fraction of central sphere - 400 inactive cycles
Bench 4 - LANL - MCNP
0.91062
1
0.9
0.8
0.7
0.6
0.5
0.4
0.3
0.2
0.1
0
0
10
20
30
40
50
60
70
80
90
100
Case number

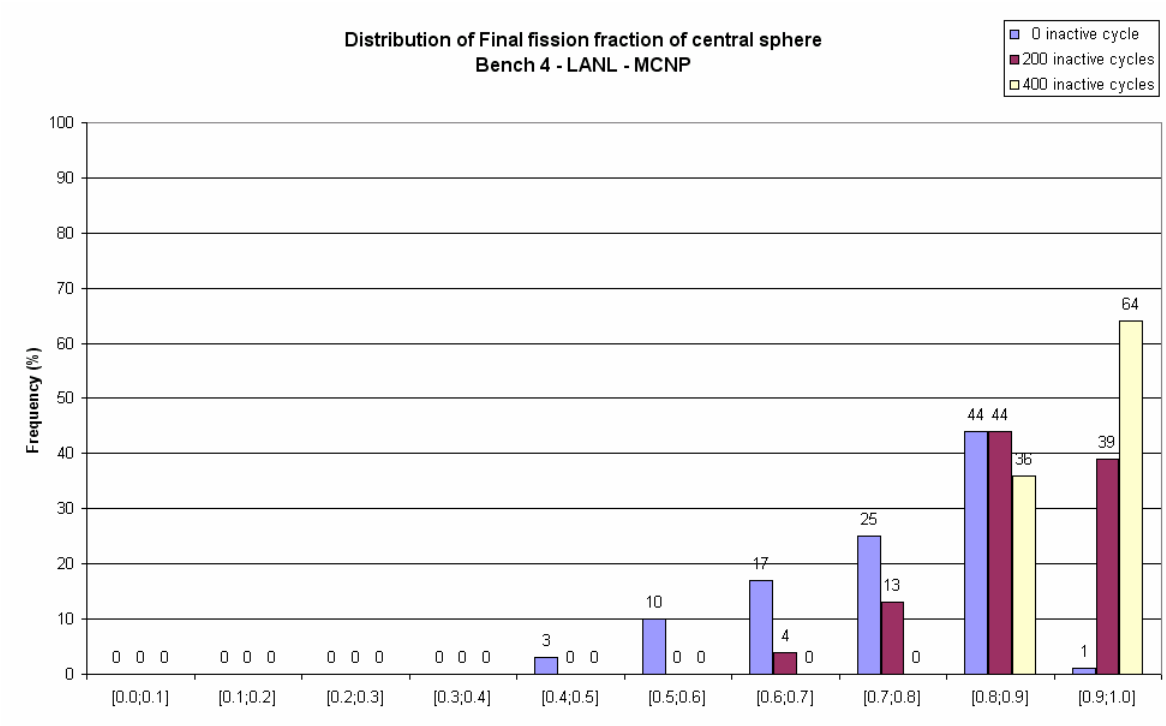
Distribution of Final fission fraction of central sphere
Bench 4 - LANL - MCNP
0 inactive cycle
200 inactive cycles
400 inactive cycles
Frequency (%)
[0.0;0.1]
[0.1;0.2]
[0.2;0.3]
[0.3;0.4]
[0.4;0.5]
[0.5;0.6]
[0.6;0.7]
[0.7;0.8]
[0.8;0.9]
[0.9;1.0]

ORNL / KENO

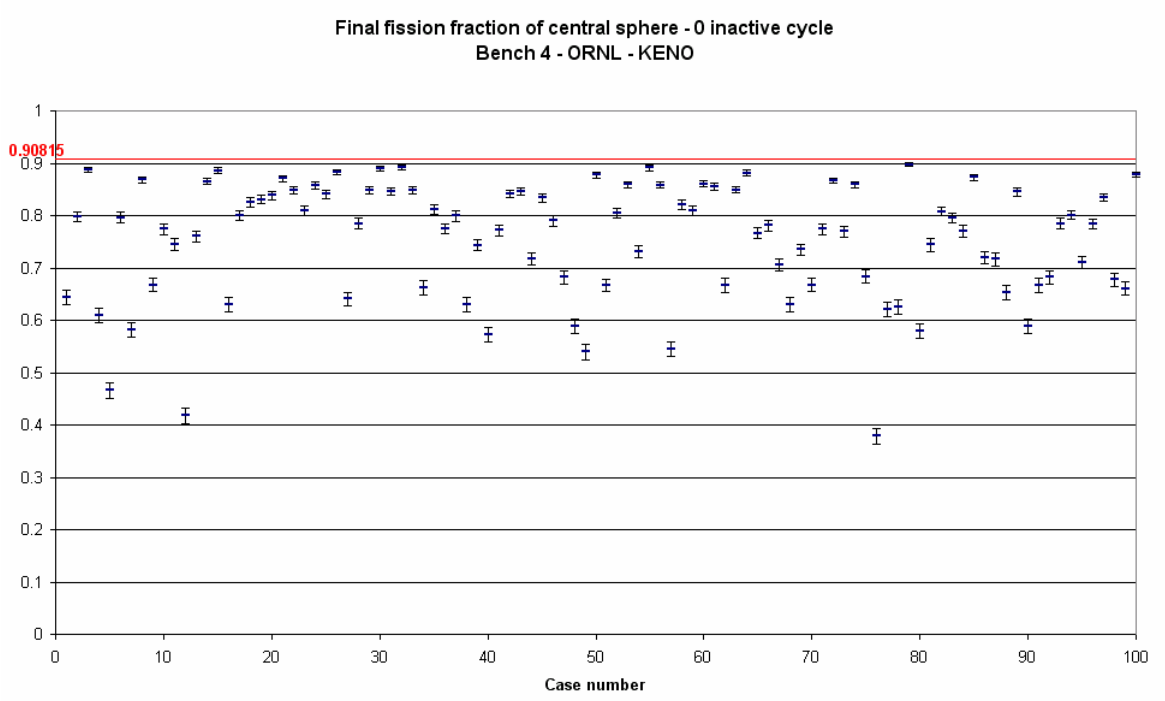
Final fission fraction of central sphere - 0 inactive cycle
Bench 4 - ORNL - KENO
0.90815
Case number

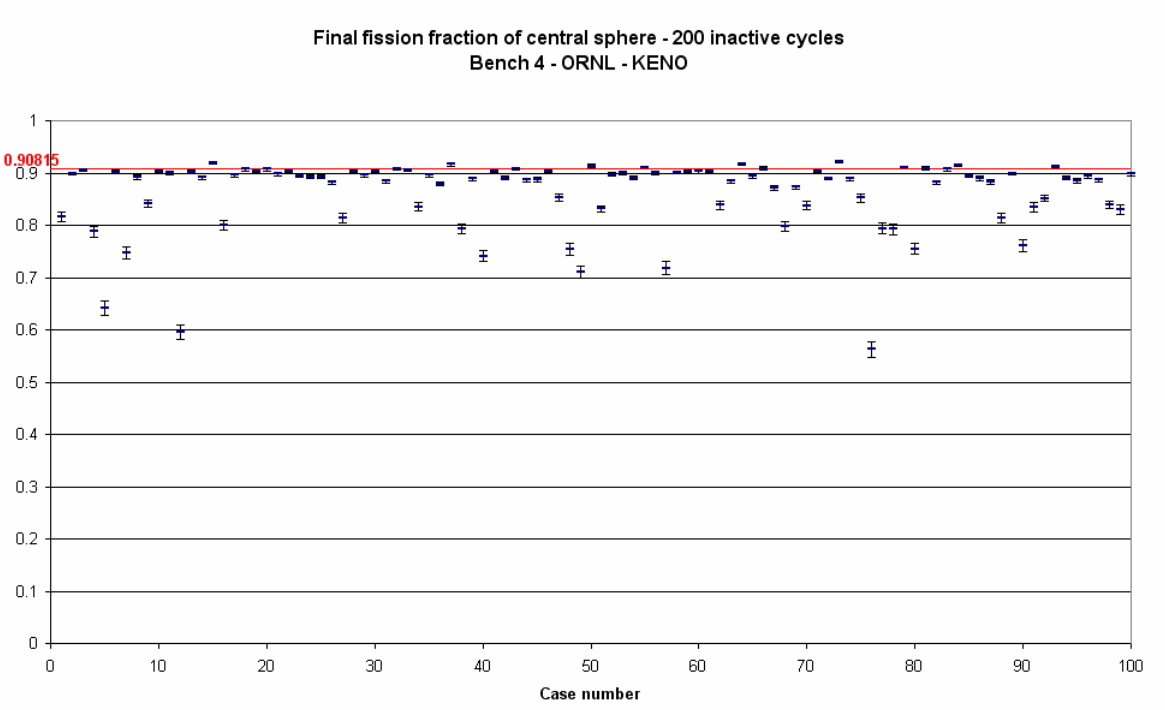
Final fission fraction of central sphere - 200 inactive cycles
Bench 4 - ORNL - KENO
0.90815
1
0.9
0.8
0.7
0.6
0.5
0.4
0.3
0.2
0.1
0
0
10
20
30
40
50
60
70
80
90
100
Case number

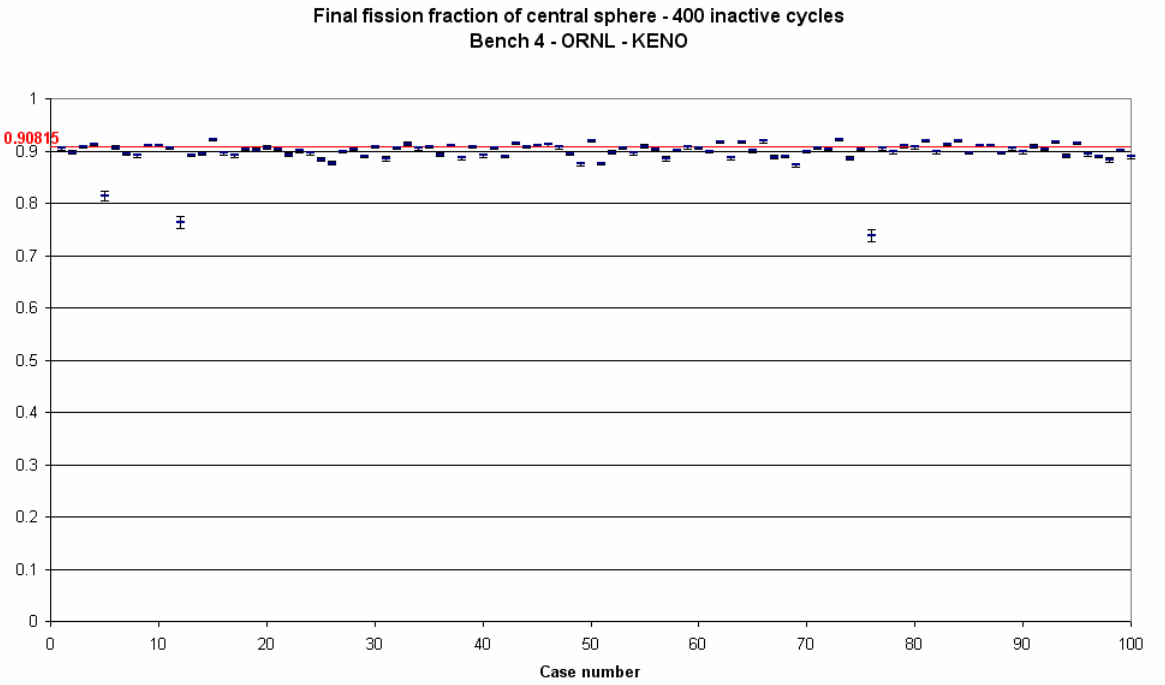
Final fission fraction of central sphere - 400 inactive cycles
Bench 4 - ORNL - KENO
0.90815
1
0.9
0.8
0.7
0.6
0.5
0.4
0.3
0.2
0.1
0
0
10
20
30
40
50
60
70
80
90
100
Case number

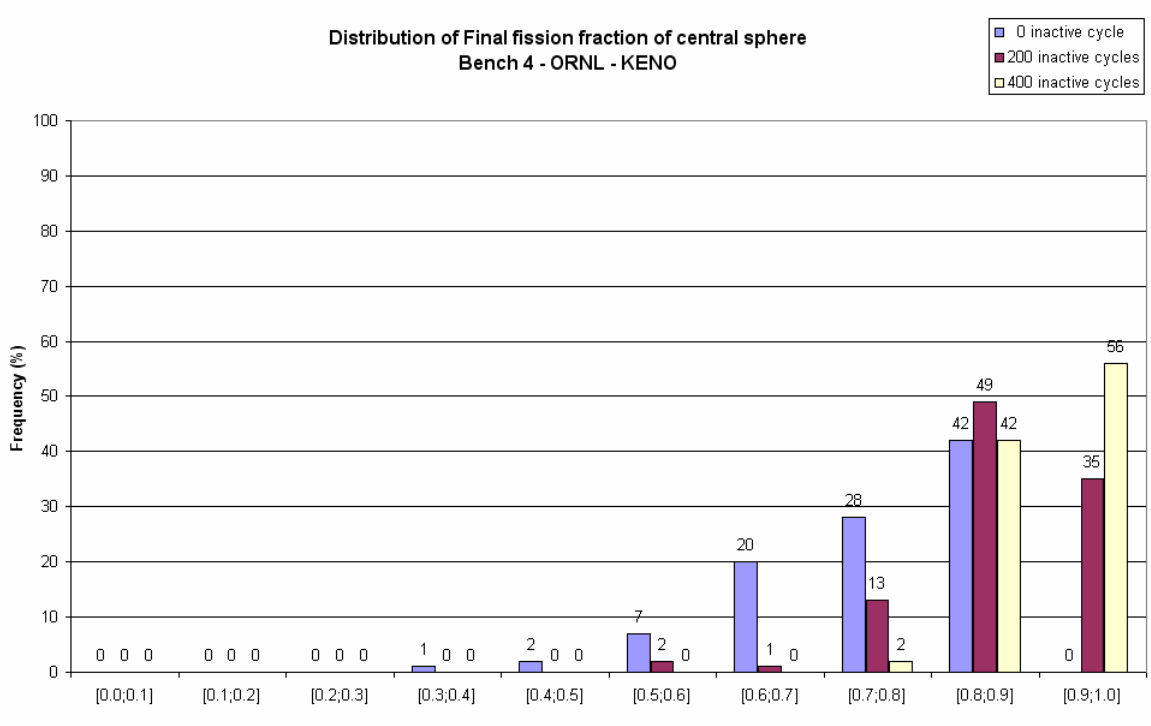
Distribution of Final fission fraction of central sphere
Bench 4 - ORNL - KENO
0 inactive cycle
200 inactive cycles
400 inactive cycles
Frequency (%)
100
90
80
70
60
50
40
30
20
10
0
0 0 0
0 0 0
0 0 0
1 0 0
2 0 0
7 2 0
20 1 0
28 13 2
42 49 42
0 35 56
[0.0;0.1]
[0.1;0.2]
[0.2;0.3]
[0.3;0.4]
[0.4;0.5]
[0.5;0.6]
[0.6;0.7]
[0.7;0.8]
[0.8;0.9]
[0.9;1.0]

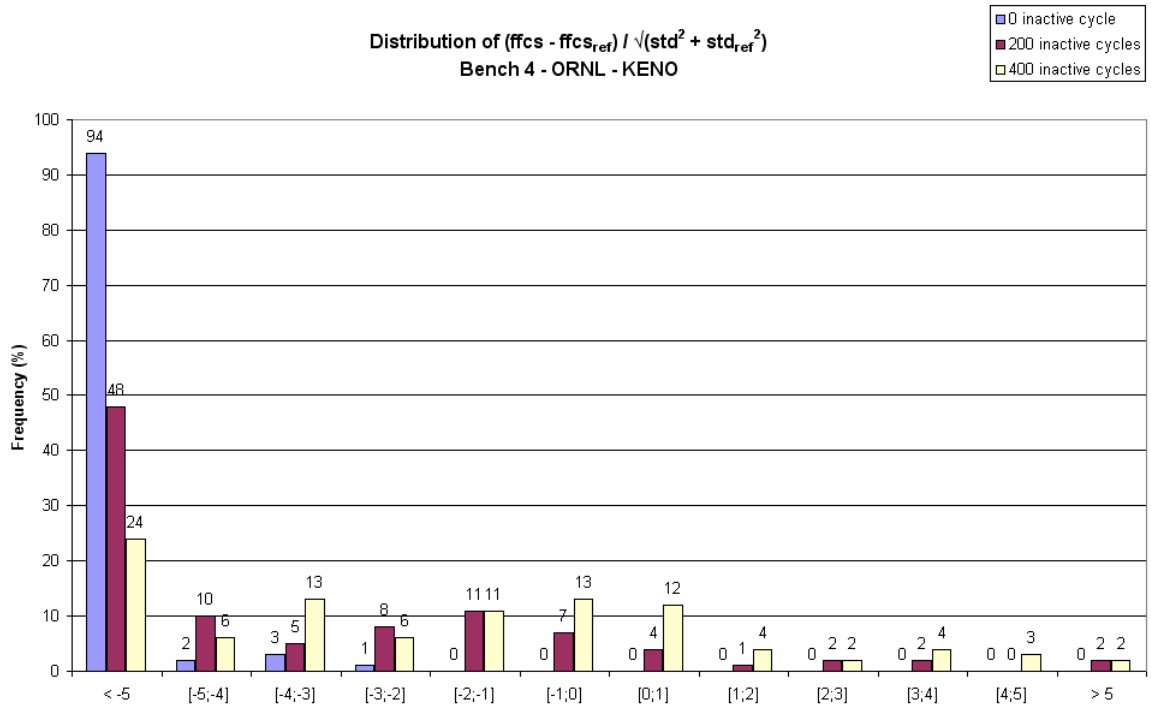
Distribution of (ffcs - ffcs$_{ref}$) / √(std^2 + std$_{ref}^2$)
Bench 4 - ORNL - KENO
0 inactive cycle
200 inactive cycles
400 inactive cycles
Frequency (%)
100
90
80
70
60
50
40
30
20
10
0
94 48 24
2 10 6
3 5 13
1 8 6
0 11 11
0 7 13
0 4 12
0 1 4
0 2 2
0 2 4
0 0 3
0 2 2
< -5
[-5;-4]
[-4;-3]
[-3;-2]
[-2;-1]
[-1;0]
[0;1]
[1;2]
[2;3]
[3;4]
[4;5]
> 5

Appendix 5.e

STATIONARITY DETECTION

Basic idea about stationarity

(ki) : a cycle k_{eff} series of length N

$$\overline{k}_j = \frac{1}{j}\sum_{i=1}^{j} k_i \qquad 1 \le j \le N$$

What is the behaviour of $\overline{k}_j - \overline{k}_N$ when j varies between 1 and N?

If (k_i) is stationary, this variable should take "small" values around 0.

Brownian bridge

A Brownian bridge is a centered gaussian process verifying the following properties:

- $B_N(0) = B_N(1) = 0$
- $E\left(B_N(t)\right) = 0 \qquad (0 \le t \le 1)$
- $\mathrm{var}\left(B_N(t)\right) = t(1-t) \qquad (0 \le t \le 1)$

The probability that it takes high values is low.

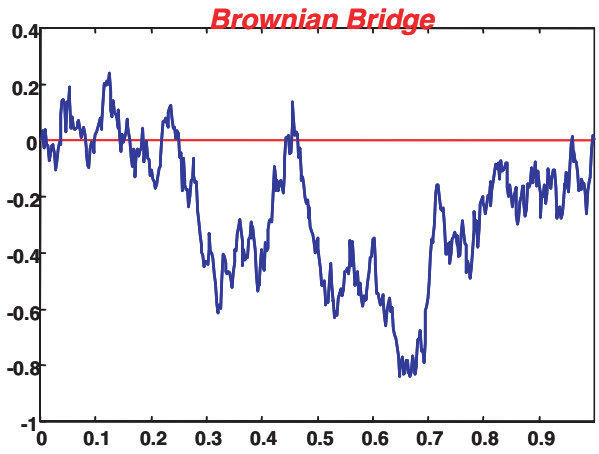

Link between stationarity and Brownian bridge

Let introduce:

- the autocorrelations of a stationary series (k_i):

$$\gamma(h) = \mathrm{cov}\left(k_i, k_{i+h}\right)$$

- the variance of the mean:

$$\mathrm{var}\left(\overline{k}_j\right) = \frac{1}{j}\sum_{h=-(j-1)}^{j-1}\left(1 - \frac{|h|}{j}\right)\gamma(h)$$

- the parameter τ :

$$\tau^2 = \lim_{j\to\infty}\left[j \cdot \mathrm{var}\left(\overline{k}_j\right)\right] = \sum_{h=-\infty}^{+\infty}\gamma(h)$$

Let define the following process:

$$B_N : \frac{j}{N} \rightarrow \frac{j}{\tau\sqrt{N}}\left(\bar{K}_j - \bar{K}_N\right) \quad (0 \le j \le N)$$

If (ki) is a stationary series, BN verifies the two following properties:

- $B_N(0) = B_N(1) = 0$
- $E\left(B_N(t)\right) = 0 \qquad (0 \le t \le 1)$

If N is high enough, for most j values (j sufficiently high): $\mathrm{var}\left(\bar{K}_j\right) \sim \tau^2/j$ Then, for most j values, BN verifies the third property of a Brownian bridge:

$$\mathrm{var}\left(B_N\left(\frac{j}{N}\right)\right) = \frac{j}{N}\left(1 - \frac{j}{N}\right)$$

As a conclusion, if (ki) is stationary and if N is high enough, BN tends to a Brownian bridge.

Example of a stationary series

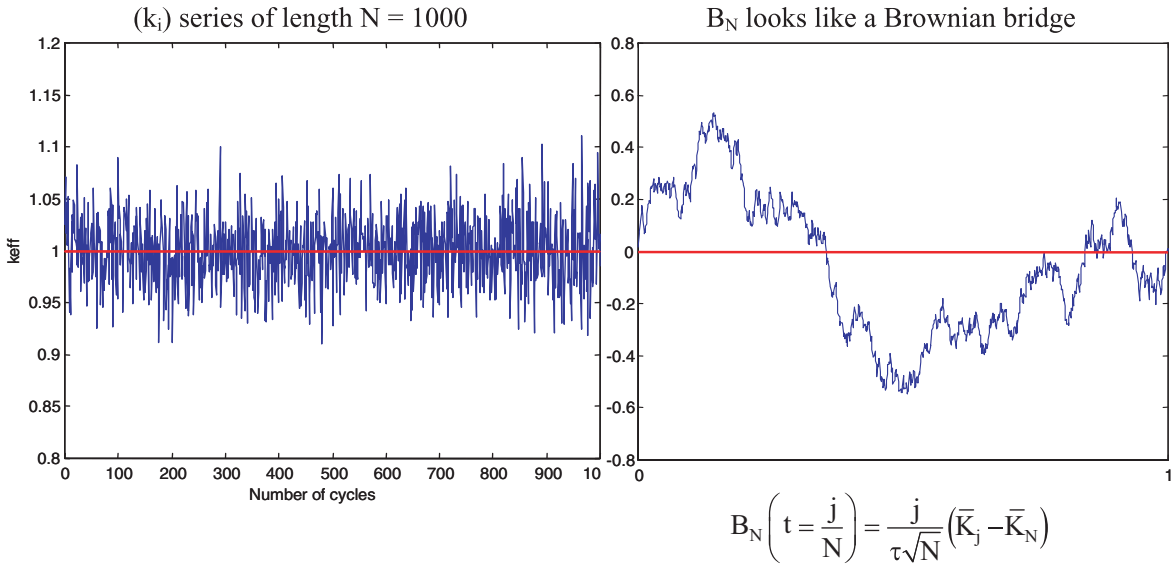

$$B_N\left(t = \frac{j}{N}\right) = \frac{j}{\tau\sqrt{N}}\left(\bar{K}_j - \bar{K}_N\right)$$

Example of a non-stationary series (negative transient, i.e. initial underestimation)

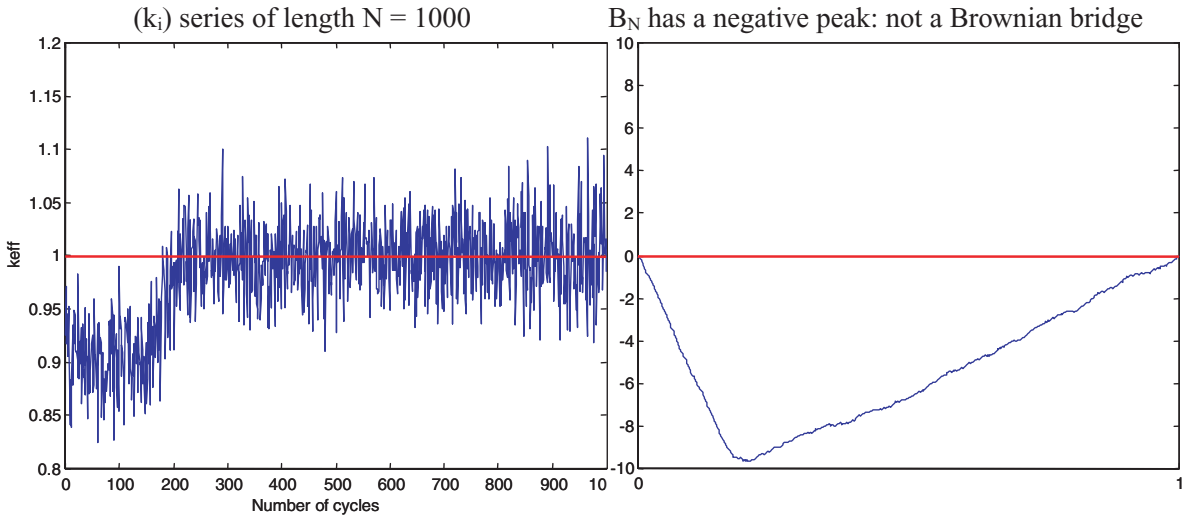

$$B_N\left(t=\frac{j}{N}\right)=\frac{j}{\tau\sqrt{N}}\left(\bar{K}_j-\bar{K}_N\right)$$

Example of a parametric test to detect stationarity

The tests proposed by Schruben [1] to detect a negative transient (i.e. an initial underestimation) or a positive transient (i.e. an initial overestimation) are based respectively on the statistics:

$$S_*=\frac{B_N^{\,2}\left(t_*\right)}{t_*\left(1-t_*\right)}\ \text{and}\ S^*=\frac{B_N^{\,2}\left(t^*\right)}{t^*\left(1-t^*\right)}$$

where t_* and t^* are respectively the values at which the negative and positive peaks of B_N occur.

If B_N is a Brownian bridge, S_* and S^* are distributed as a chi-square with 3 degrees of freedom. The p-value of these tests (i.e. the probability of getting a value more extreme than the statistic under the H0 hypothesis of stationarity) is:

$$p=P\left(\chi^2>S\right)$$

with S being S_* or S^*.

If α denotes the level of significance of the test (for instance α = 5%), the null hypothesis of the test (the cycle k_{eff} series is stationary) is rejected if $p<\alpha$.

The disadvantage of the Schruben test is the necessity to estimate the parameter τ ($\tau^2=\lim_{j\to\infty}\left[j\cdot\mathrm{var}\left(\bar{K}_j\right)\right]=\sum_{h=-\infty}^{+\infty}\gamma\left(h\right)$). A reliable estimate of this parameter is difficult to obtain in the presence of an initialisation bias!

Examples of non parametric tests to detect stationarity

Modification of the Schruben test

To avoid the estimation of the parameter τ , we can eliminate this parameter by using the statistic S:

$$S = \frac{S_*}{S^*} = \frac{B_N^{\,2}(t_*)}{B_N^{\,2}(t^*)} \frac{t^*(1-t^*)}{t_*(1-t_*)}$$

The distribution of S (and consequently the p-value of the test) is not analytically known but can be determined empirically (by simulating a large number of Brownian bridges and estimating the statistic S for each of them).

Vassilacopoulos test [1]

The sequence R_N of the signed ranks of the cycle k_{eff} series is defined as follows:

$$R_N(i) = \sum_{j=1}^{N} S(K_i - K_j),\ 1 \le i \le N$$

$$\text{with } S(x) = \begin{cases} -1, & x < 0 \\ 0, & x = 0 \\ 1, & x > 0 \end{cases}$$

The process U_N is the cumulative sums of the ranks R_N:

$$U_N(i) = \sum_{j=1}^{i} R_N(i)$$

The tests proposed by Vassilacopoulos to detect a negative transient or a positive transient are based respectively on the statistics:

$$C_{min} = \min_{1 \le i \le N} \{U_N(i)\} \text{ and } C_{max} = \max_{1 \le i \le N} \{U_N(i)\}$$

The p-value of these tests is (i.e. the probability to exceed the statistic of the test under the H0 hypothesis of stationarity):

$$p = \exp\left(-\frac{6C^2}{N^2(N+1)}\right)$$

with C being C_{min} or C_{max}.

If α denotes the level of significance of the test, the null hypothesis of the test (the cycle k_{eff} series is stationary) is rejected if $p < \alpha$.

References

[1] L.W. Schruben, “Detecting Initialization Bias in Simulation Output”, Operations Research, vol. 30 (May-June 1982)

[2] G. Vassilacopoulos, “Testing for Initialization Bias in Simulation Output”, Simulation Coucils (1989).

[3] P. Heidelberger, P. Welch, “Simulation Run Length Control in the Presence of an Initial Transient”, Operations Research, vol. 31 (Nov-Dec 1983).

Appendix 5.f

LENGTH OF THE TRANSIENT AUTOMATICALLY SUPPRESSED

Number of active cycles removed until detection of stationarity for the 300 replicas (100 with 0 inactive cycles, 100 with 200 inactive cycles, 100 with 400 inactive cycles).

Table 5.f.1 Length of the transient automatically suppressed – ANL / VIM

length of the transient automatically suppressed	Percentage of replicas with		
	0 inactive cycles	200 inactive cycles	400 inactive cycles
0	**13**	**62**	**81**
50	**14**	**10**	**7**
100	**13**	**5**	**6**
150	**16**	**6**	**2**
200	**11**	**4**	0
250	**10**	**5**	**1**
300	**3**	**2**	0
350	**6**	**3**	**1**
400	**3**	0	**1**
450	**2**	**2**	**1**
500	**5**	0	0
550	**2**	**1**	0
600	0	0	0
650	**1**	0	0
700	0	0	0
750	**1**	0	0
800	0	0	0
850	0	0	0
900	0	0	0
950	0	0	0
1000	0	0	0
	Total = 100	Total = 100	Total = 100

Table 5.f.2 Length of the transient automatically suppressed – EMS / KENO

length of the transient automatically suppressed	Percentage of replicas with		
	0 inactive cycles	200 inactive cycles	400 inactive cycles
0	**9**	**62**	**81**
50	**15**	**7**	**6**
100	**12**	**10**	**3**
150	**17**	**7**	**1**
200	**18**	**2**	0
250	**5**	**3**	**4**
300	**6**	**3**	0
350	**8**	**1**	**1**
400	**1**	0	**1**
450	**2**	**3**	0
500	**3**	0	**1**
550	0	0	**2**
600	**1**	0	0
650	**2**	**1**	0
700	0	**1**	0
750	**1**	0	0
800	0	0	0
850	0	0	0
900	0	0	0
950	0	0	0
1000	0	0	0
	Total = 100	Total = 100	Total = 100

Table 5.f.3 Length of the transient automatically suppressed – IPPE / KENO

length of the transient automatically suppressed	Percentage of replicas with		
	0 inactive cycles	200 inactive cycles	400 inactive cycles
0	**3**	**64**	**81**
50	**21**	**9**	**7**
100	**15**	**7**	**3**
150	**15**	**3**	**1**
200	**16**	**6**	**1**
250	**7**	**3**	**1**
300	**4**	**1**	**1**
350	**4**	**1**	**3**
400	**2**	**1**	0
450	**6**	0	**1**
500	**1**	**1**	**1**
550	0	**4**	0
600	**1**	0	0
650	**1**	0	0
700	**1**	0	0
750	**2**	0	0
800	**1**	0	0
850	0	0	0
900	0	0	0
950	0	0	0
1000	0	0	0
	Total = 100	Total = 100	Total = 100

Table 5.f.4 Length of the transient automatically suppressed – IRSN / MORET

length of the transient automatically suppressed	Percentage of replicas with		
	0 inactive cycles	200 inactive cycles	400 inactive cycles
0	**2**	**53**	**76**
50	**11**	**14**	**6**
100	**20**	**9**	**4**
150	**14**	**4**	**2**
200	**7**	**3**	**3**
250	**9**	**4**	**3**
300	**12**	**3**	**1**
350	**5**	**4**	**2**
400	**3**	**2**	0
450	**4**	**1**	0
500	**4**	0	**1**
550	**1**	**2**	0
600	**2**	0	**1**
650	**5**	0	0
700	0	0	0
750	**1**	0	0
800	0	0	0
850	0	**1**	**1**
900	0	0	0
950	0	0	0
1000	0	0	0
	Total = 100	Total = 100	Total = 100

Table 5.f.5 Length of the transient automatically suppressed – JNC / KENO

length of the transient automatically suppressed	Percentage of replicas with		
	0 inactive cycles	200 inactive cycles	400 inactive cycles
0	**10**	**62**	**80**
50	**13**	**9**	**4**
100	**12**	**10**	**4**
150	**7**	**4**	**4**
200	**20**	**1**	**1**
250	**13**	**2**	**1**
300	**11**	**3**	0
350	**3**	**3**	**3**
400	**1**	0	0
450	0	0	0
500	**2**	**1**	0
550	**2**	0	**1**
600	**2**	**1**	0
650	0	0	**1**
700	0	**1**	**1**
750	0	**2**	0
800	**1**	0	0
850	**1**	0	0
900	0	**1**	0
950	0	0	0
1000	**2**	0	0
	Total = 100	Total = 100	Total = 100

Table 5.f.6 Length of the transient automatically suppressed – LANL / MCNP

length of the transient automatically suppressed	Percentage of replicas with		
	0 inactive cycles	200 inactive cycles	400 inactive cycles
0	**6**	**57**	**89**
50	**9**	**13**	**3**
100	**16**	**7**	**5**
150	**15**	**7**	**1**
200	**14**	**4**	**1**
250	**8**	**3**	0
300	**10**	**5**	0
350	**3**	**2**	0
400	**7**	0	**1**
450	**3**	**1**	0
500	**4**	0	0
550	0	0	0
600	0	**1**	0
650	**2**	0	0
700	**1**	0	0
750	**1**	0	0
800	0	0	0
850	**1**	0	0
900	0	0	0
950	0	0	0
1000	0	0	0
	Total = 100	Total = 100	Total = 100

Table 5.f.7 Length of the transient automatically suppressed – ORNL / KENO

length of the transient automatically suppressed	Percentage of replicas with		
	0 inactive cycles	200 inactive cycles	400 inactive cycles
0	**4**	**56**	**83**
50	**14**	**8**	**7**
100	**16**	**13**	**1**
150	**16**	**10**	**2**
200	**8**	**6**	**1**
250	**9**	**3**	**1**
300	**10**	**1**	0
350	**4**	0	**1**
400	**8**	**2**	**2**
450	**3**	**1**	0
500	0	0	0
550	**3**	0	0
600	**2**	0	0
650	**2**	0	0
700	0	0	**2**
750	0	0	0
800	**1**	0	0
850	0	0	0
900	0	0	0
950	0	0	0
1000	0	0	0
	Total = 100	Total = 100	Total = 100

Appendix 5.g

STANDARD DEVIATION CALCULATION BASED ON THE METHOD PROPOSED BY UEKI ET AL.

Let consider a cycle k_{eff} series of length N.
Ueki et al. established the theoretical expression of the bias of the conventional estimation of the variance of the mean of the cycle k_{eff} series, denoted as $\hat{\sigma}^2$:

$$B\left(\hat{\sigma}^2\right) = -\frac{2}{N(N-1)}\sum_{i=1}^{N-1}(N-i)\,c\,(i),$$

c(i) being the true autocovariance coefficients of the cycle k_{eff} series.
Ueki et al. also established the theoretical expression of the bias of the conventional estimation of the autocovariance coefficients of the cycle k_{eff} series, denoted as $\hat{c}\,(i)$, for the small values of i:

$$B\left(\hat{c}\,(i)\right) = -\sigma^2$$

σ^2 being the true variance of the mean of the cycle k_{eff} series.
An approximation of the method of Ueki et al. is to consider only the first p (p = 10) autocovariance coefficients, assuming that the autocovariance function c(i) quickly decreases to 0 when the lag i increases.

The method of Ueki et al. consists in iterating the estimation of the variance of the mean σ_u^2 :

$$\hat{\sigma}_u^2 = \hat{\sigma}^2 + \frac{2}{N(N-1)}\sum_{i=1}^{p}(N-i)\,c\,(i)$$

with $c\,(i) = \hat{c}\,(i)$ for the first iteration and $c\,(i) = \hat{c}\,(i) + \hat{\sigma}_u^2$ for the next iterations.
So the successive estimates of the variance of the mean with the method of Ueki et al. define a linear recurring sequence of order 1:

$$\sigma_{u,k+1}^2 = a \cdot \sigma_{u,k}^2 + b$$

with

$$\sigma_{u,0}^2 = 0\ ,\ a = \frac{2p\left(N - \frac{p+1}{2}\right)}{N(N-1)} \approx \frac{2p}{N} \text{ and } b = \hat{\sigma}^2 + \frac{2}{N(N-1)}\sum_{i=1}^{p}(N-i)\,\hat{c}\,(i).$$

When the number of cycle N is about a few hundreds, a is very small and the number of iterations needed is very low: 1 or 2.

The limit l of this linear recurring sequence is determined by the equation $l = a \cdot l + b$ as illustrated in Figure 5.g.1.

Figure 5.g.1 Successive estimates of the variance of the mean with the iterative method of Ueki et al.

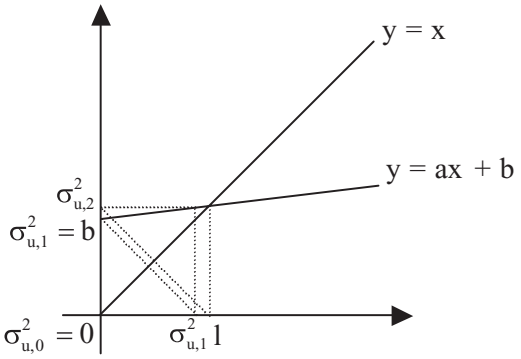

An improvement of the method of Ueki et al. consists in estimating directly the limit l of the sequence:

$$\sigma_u^2 = \frac{\hat{\sigma}^2 + \dfrac{2}{N(N-1)} \sum_{i=1}^{p} (N-i)\,\hat{c}(i)}{1 - \dfrac{2p\left(N - \dfrac{p+1}{2}\right)}{N(N-1)}}$$

One of the major difficulty of the method of Ueki et al. is the fact that σ_u^2 can be negative ! Indeed, due to the uncertainties on the estimates $\hat{c}(i)$ of the first p autocovariance coefficients, the corrective term $\dfrac{2}{N(N-1)} \sum_{i=1}^{p} (N-i)\,\hat{c}(i)$ can be negative and greater in absolute value than $\hat{\sigma}^2$.

A modification has been made to the method of Ueki et al. consisting in decreasing the number p of autocovariance coefficients taken into account while σ_u^2 is negative. The initial value of p is 10.

Appendix 5.h

FINAL K_{EFF} AFTER AUTOMATIC SUPPRESSION OF TRANSIENT ACTIVE CYCLES

On each figure, the horizontal line corresponds to the reference k_{eff} determined by the contributor. The k_{eff} values are given with one standard deviation uncertainty (calculation detailed in Appendix 5.g).

ANL / VIM

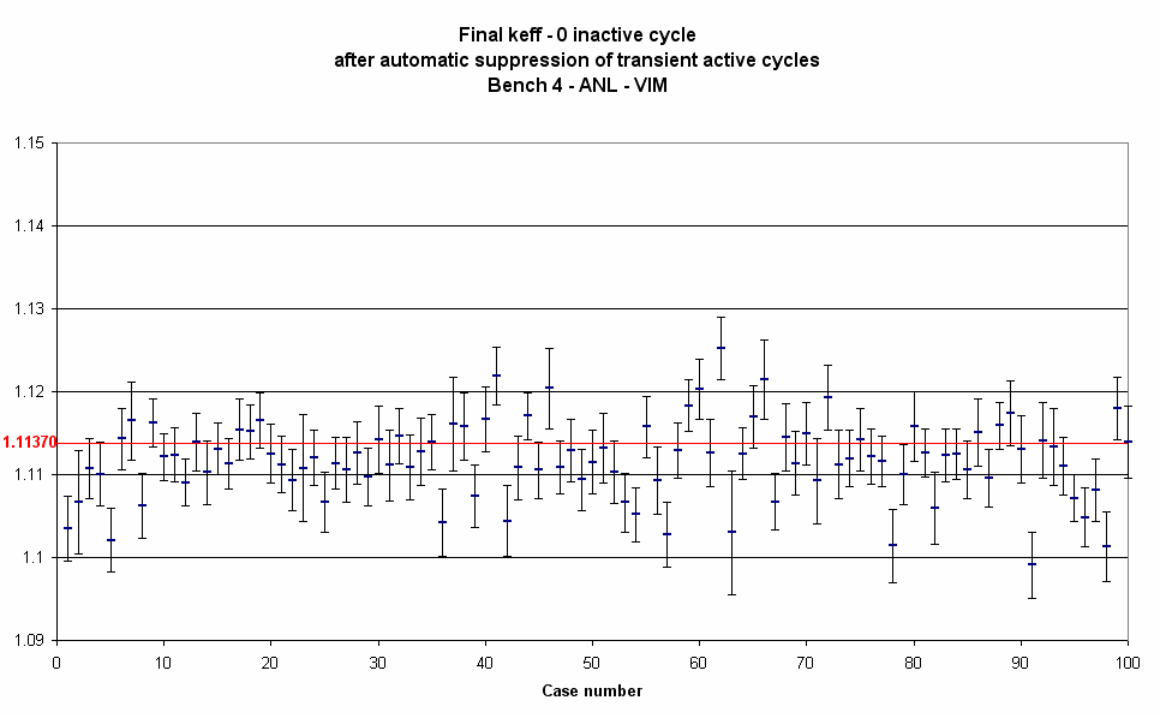

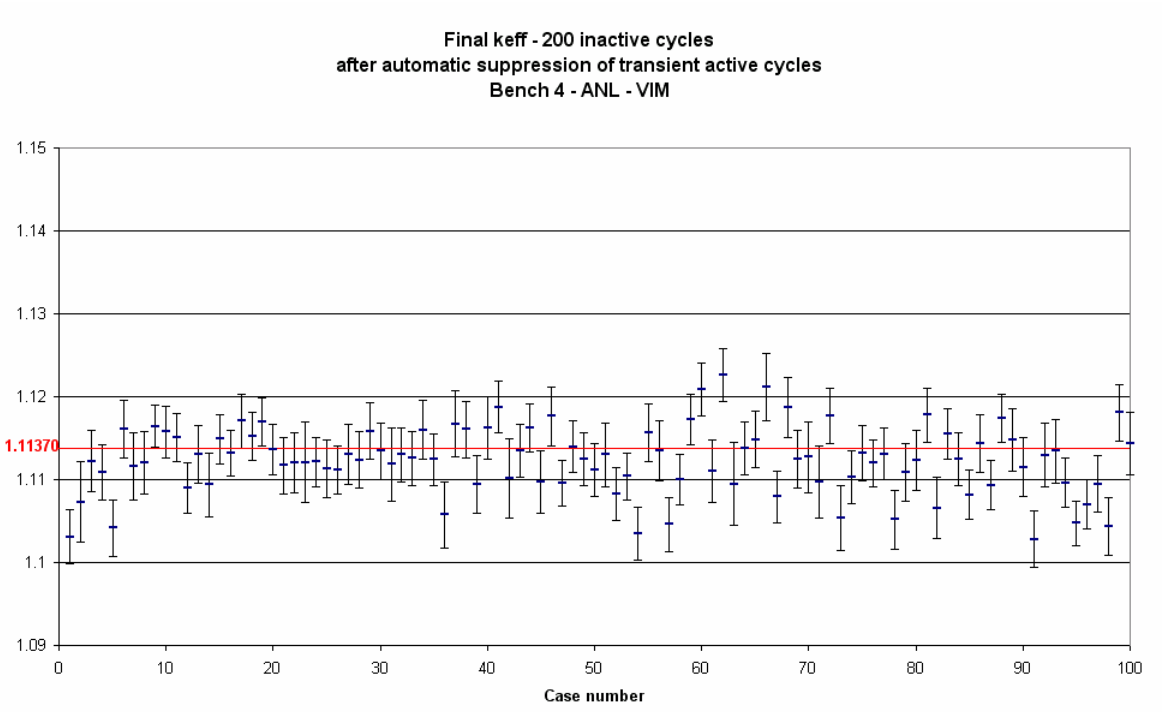
Final keff - 200 inactive cycles
after automatic suppression of transient active cycles
Bench 4 - ANL - VIM
1.15
1.14
1.13
1.12
1.11370
1.11
1.1
1.09
0
10
20
30
40
50
60
70
80
90
100
Case number

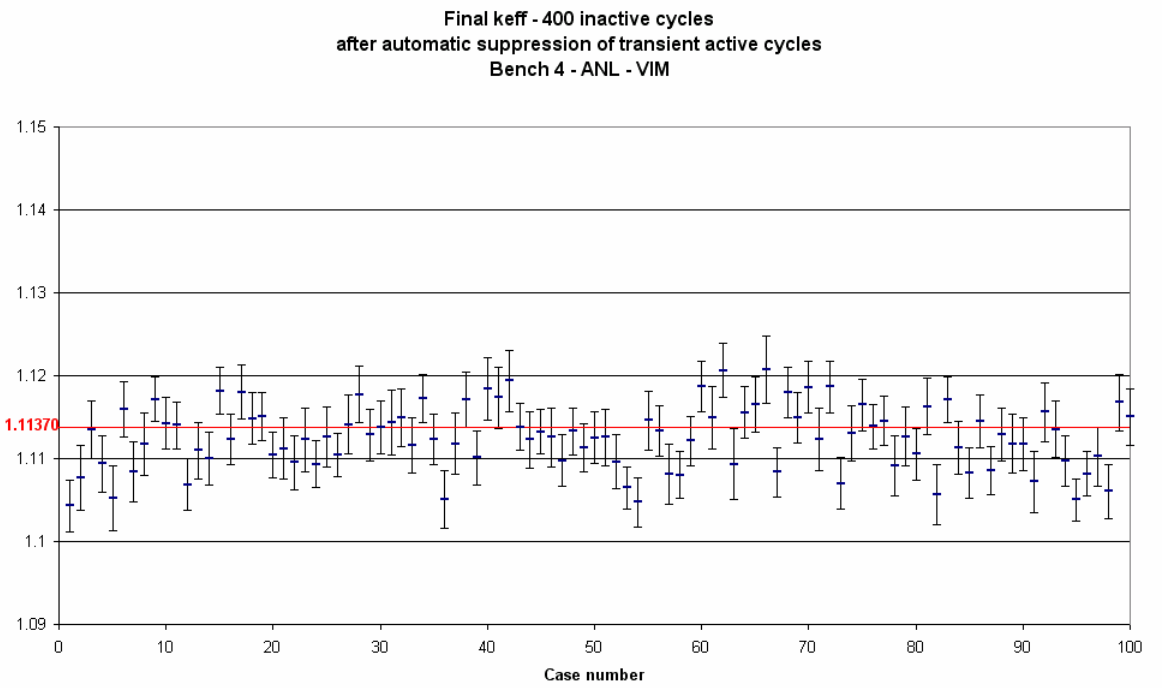
Final keff - 400 inactive cycles
after automatic suppression of transient active cycles
Bench 4 - ANL - VIM
1.15
1.14
1.13
1.12
1.11370
1.11
1.1
1.09
0
10
20
30
40
50
60
70
80
90
100
Case number

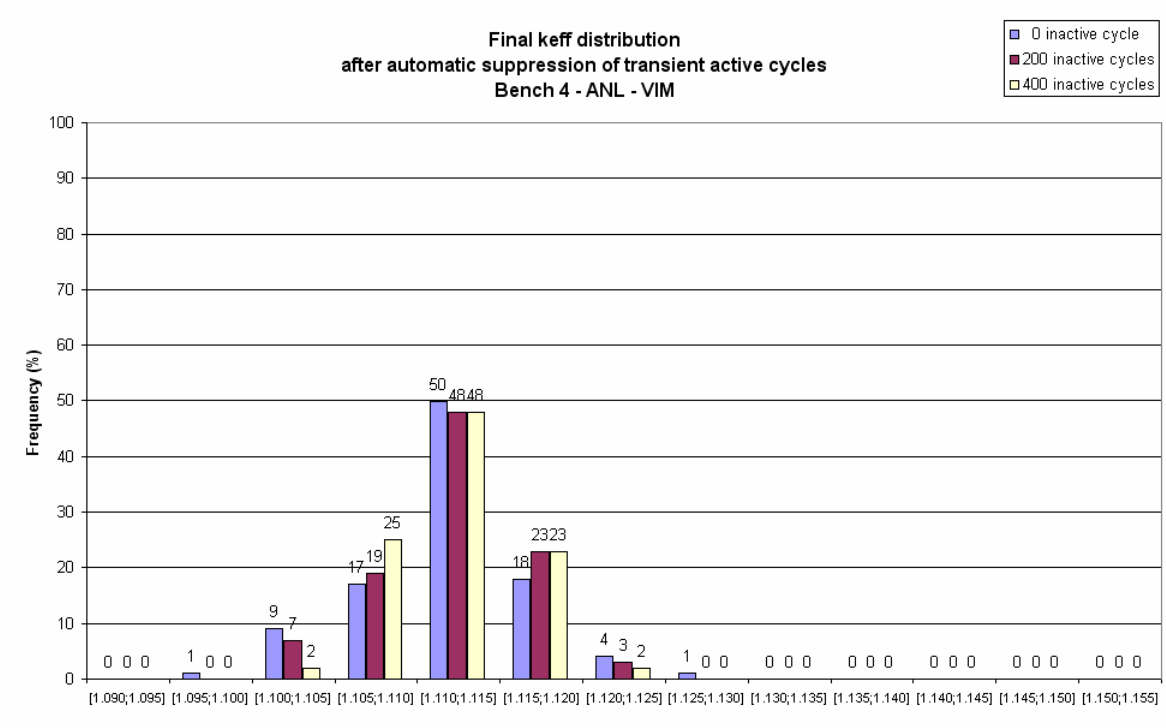
Final keff distribution
after automatic suppression of transient active cycles
Bench 4 - ANL - VIM
0 inactive cycle
200 inactive cycles
400 inactive cycles
Frequency (%)
[1.090;1.095]
[1.095;1.100]
[1.100;1.105]
[1.105;1.110]
[1.110;1.115]
[1.115;1.120]
[1.120;1.125]
[1.125;1.130]
[1.130;1.135]
[1.135;1.140]
[1.140;1.145]
[1.145;1.150]
[1.150;1.155]

EMS / KENO

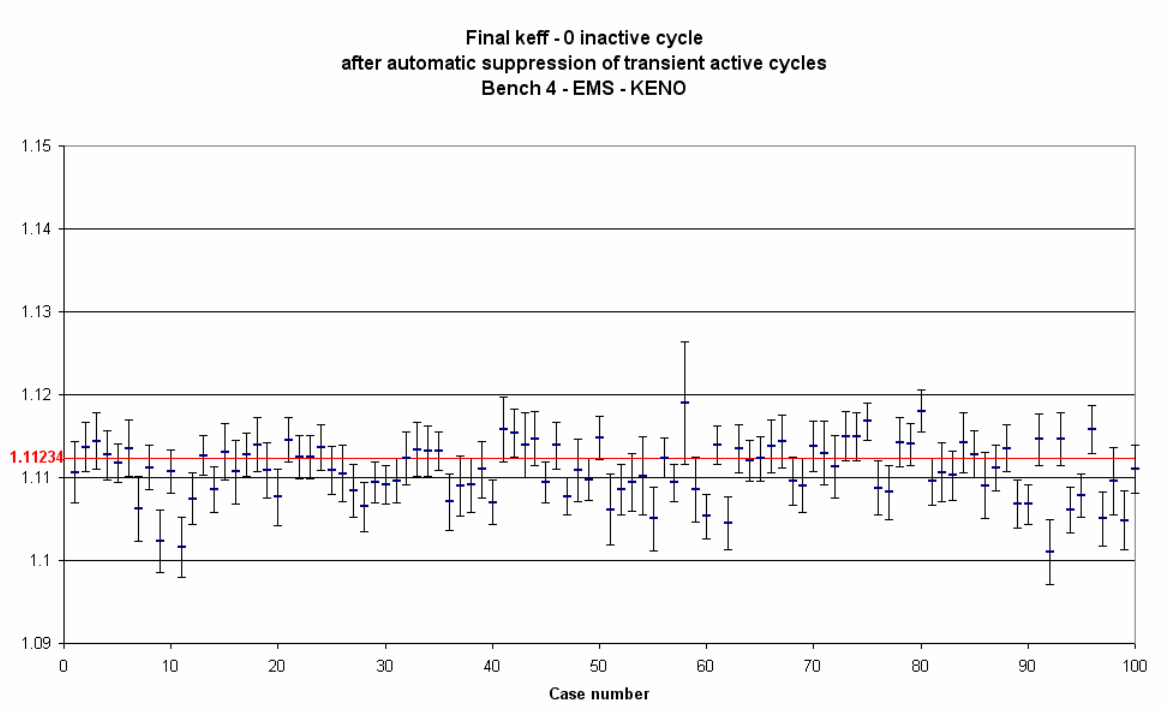
Final keff - 0 inactive cycle
after automatic suppression of transient active cycles
Bench 4 - EMS - KENO
1.11234
Case number

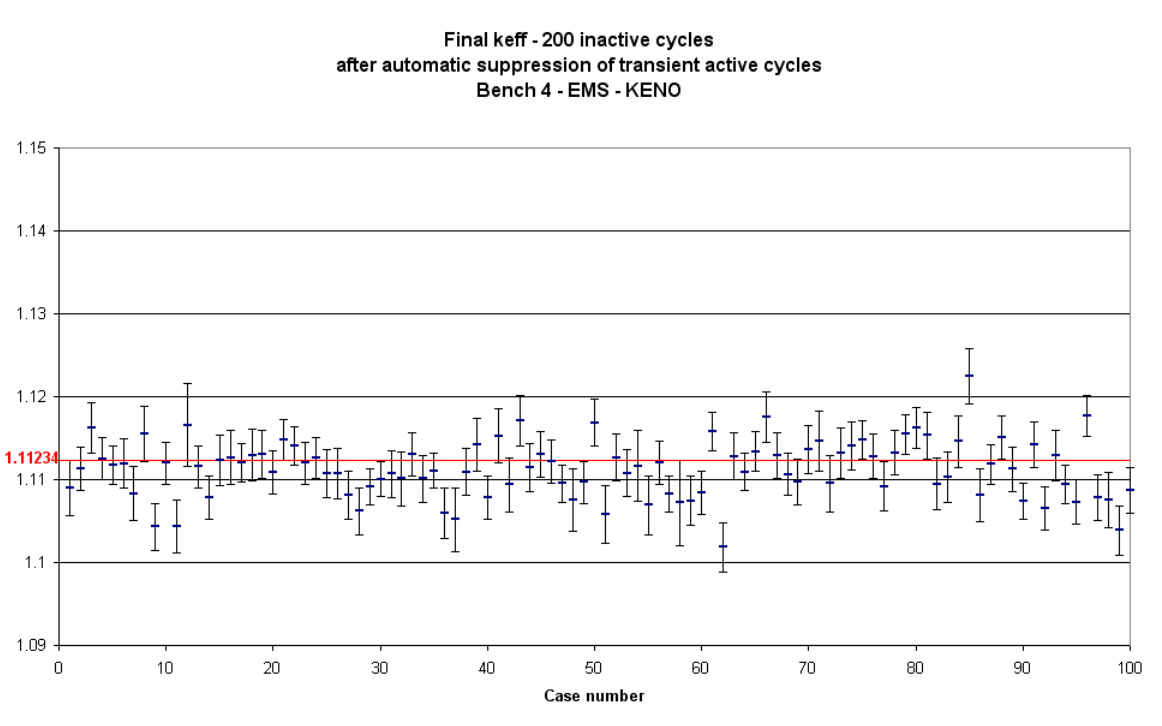
Final keff - 200 inactive cycles
after automatic suppression of transient active cycles
Bench 4 - EMS - KENO
1.15
1.14
1.13
1.12
1.11234
1.11
1.1
1.09
0
10
20
30
40
50
60
70
80
90
100
Case number

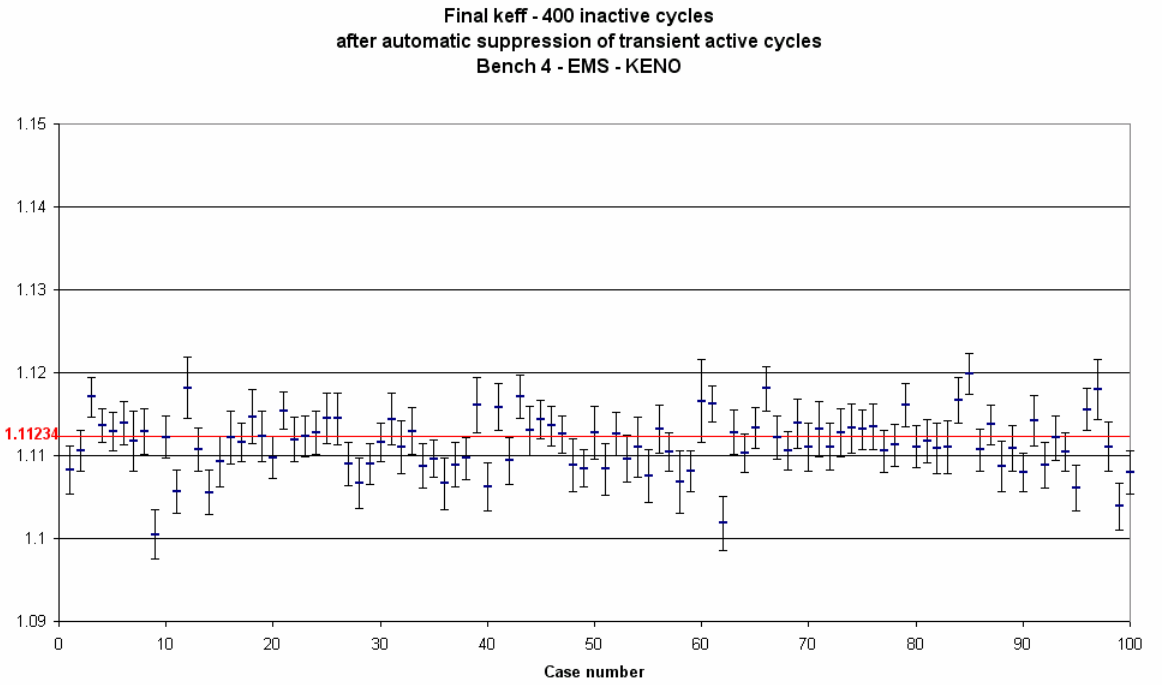
Final keff - 400 inactive cycles
after automatic suppression of transient active cycles
Bench 4 - EMS - KENO
1.15
1.14
1.13
1.12
1.11234
1.11
1.1
1.09
0
10
20
30
40
50
60
70
80
90
100
Case number

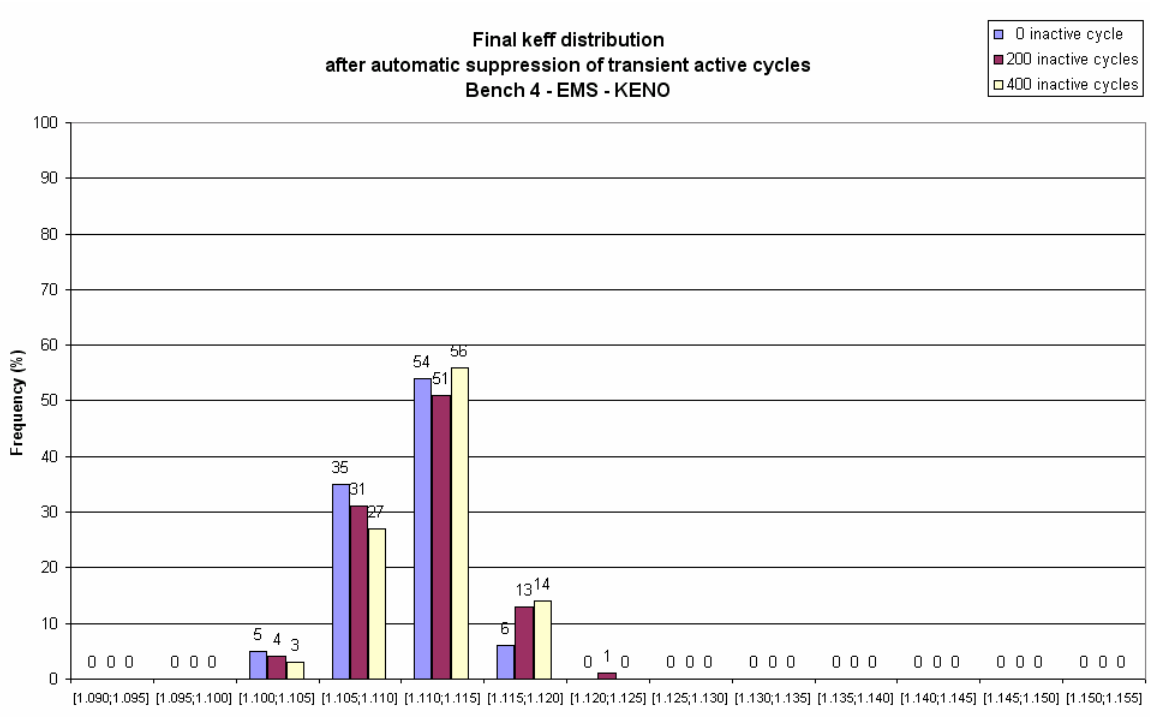
Final keff distribution
after automatic suppression of transient active cycles
Bench 4 - EMS - KENO
0 inactive cycle
200 inactive cycles
400 inactive cycles
Frequency (%)
[1.090;1.095]
[1.095;1.100]
[1.100;1.105]
[1.105;1.110]
[1.110;1.115]
[1.115;1.120]
[1.120;1.125]
[1.125;1.130]
[1.130;1.135]
[1.135;1.140]
[1.140;1.145]
[1.145;1.150]
[1.150;1.155]

IPPE / KENO

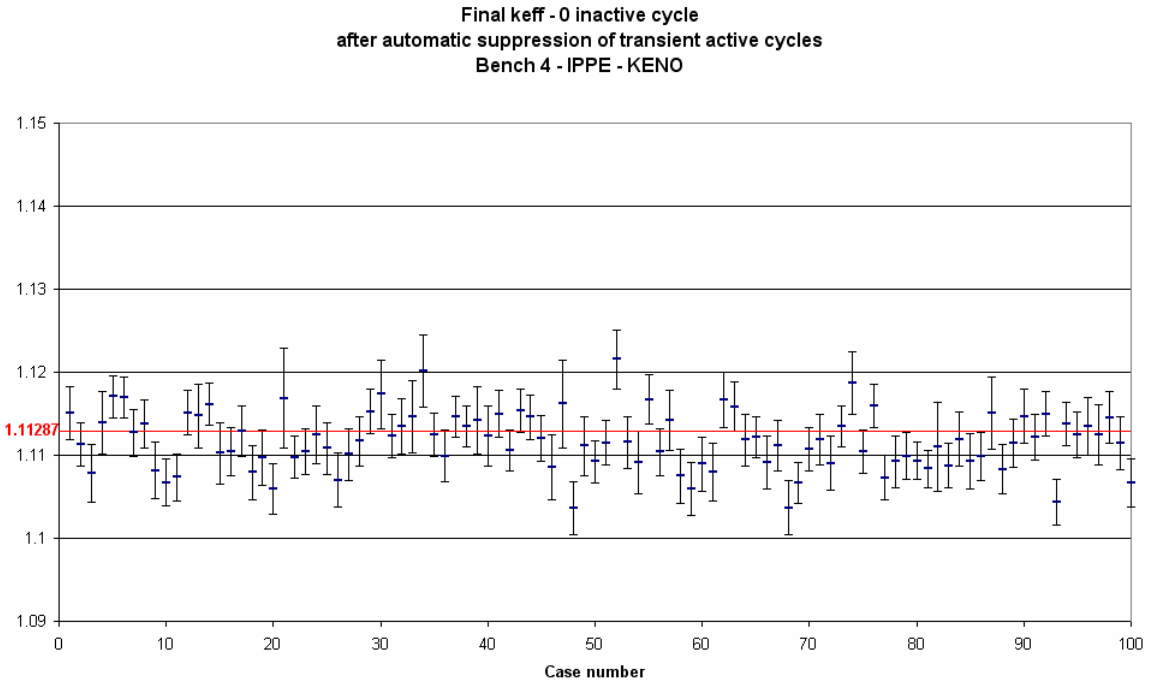
Final keff - 0 inactive cycle
after automatic suppression of transient active cycles
Bench 4 - IPPE - KENO
1.11287
Case number

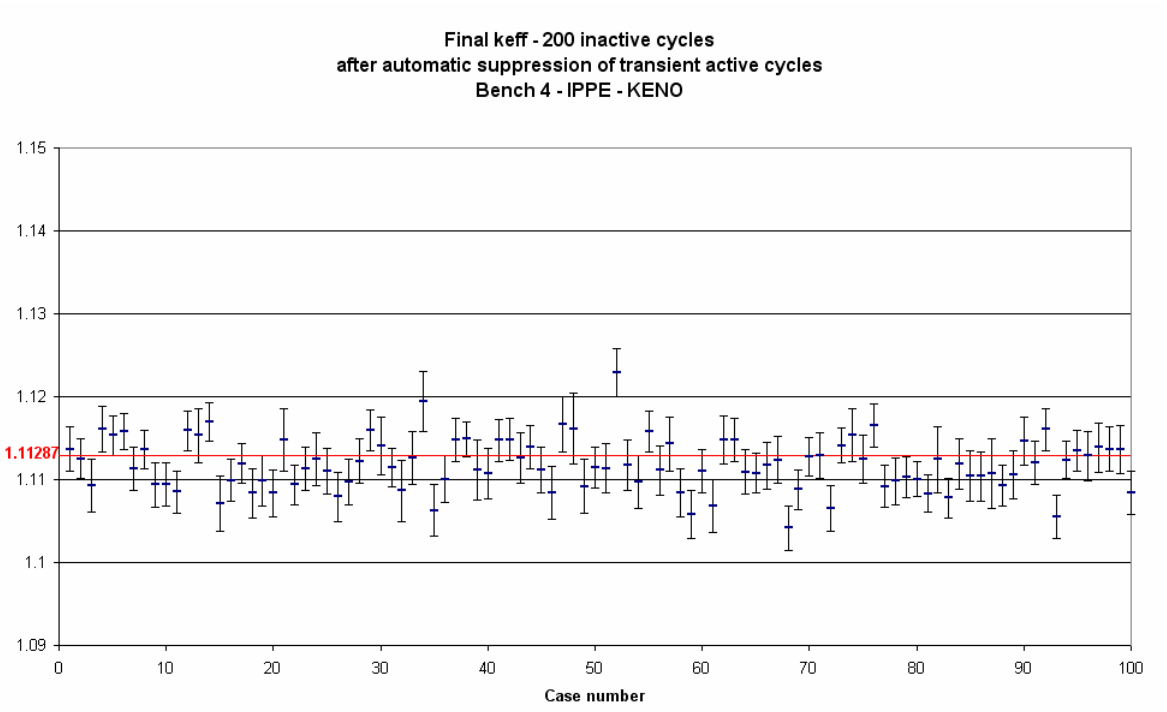
Final keff - 200 inactive cycles
after automatic suppression of transient active cycles
Bench 4 - IPPE - KENO
1.15
1.14
1.13
1.12
1.11287
1.11
1.1
1.09
0
10
20
30
40
50
60
70
80
90
100
Case number

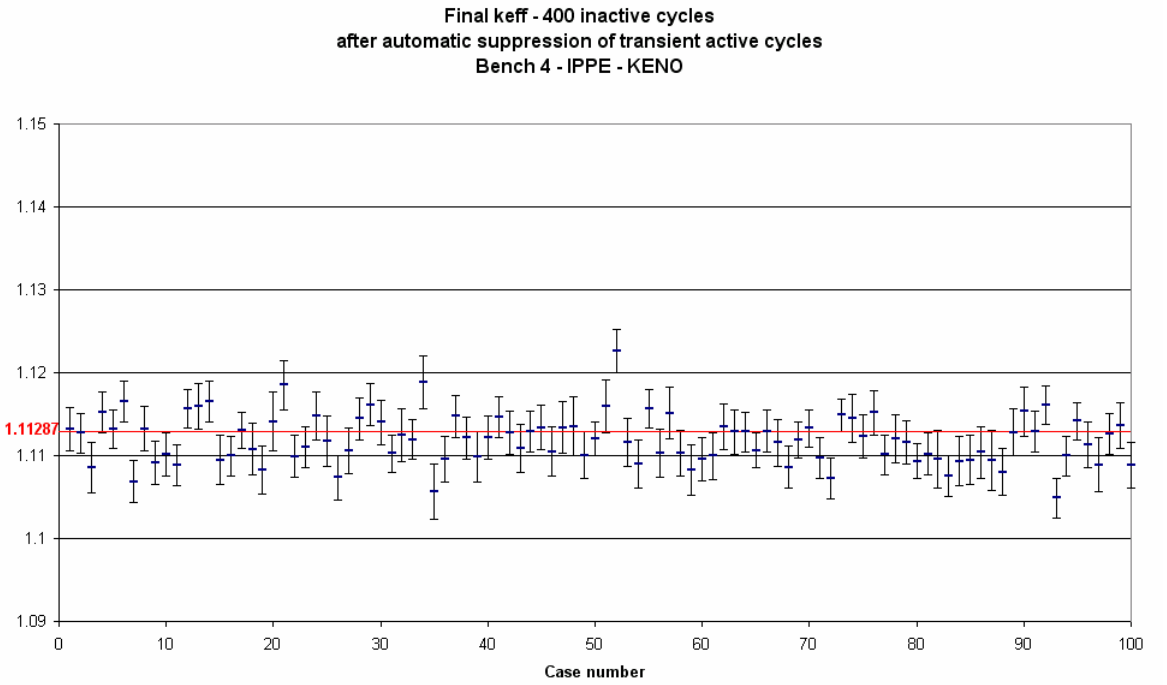
Final keff - 400 inactive cycles
after automatic suppression of transient active cycles
Bench 4 - IPPE - KENO
1.15
1.14
1.13
1.12
1.11287
1.11
1.1
1.09
0
10
20
30
40
50
60
70
80
90
100
Case number

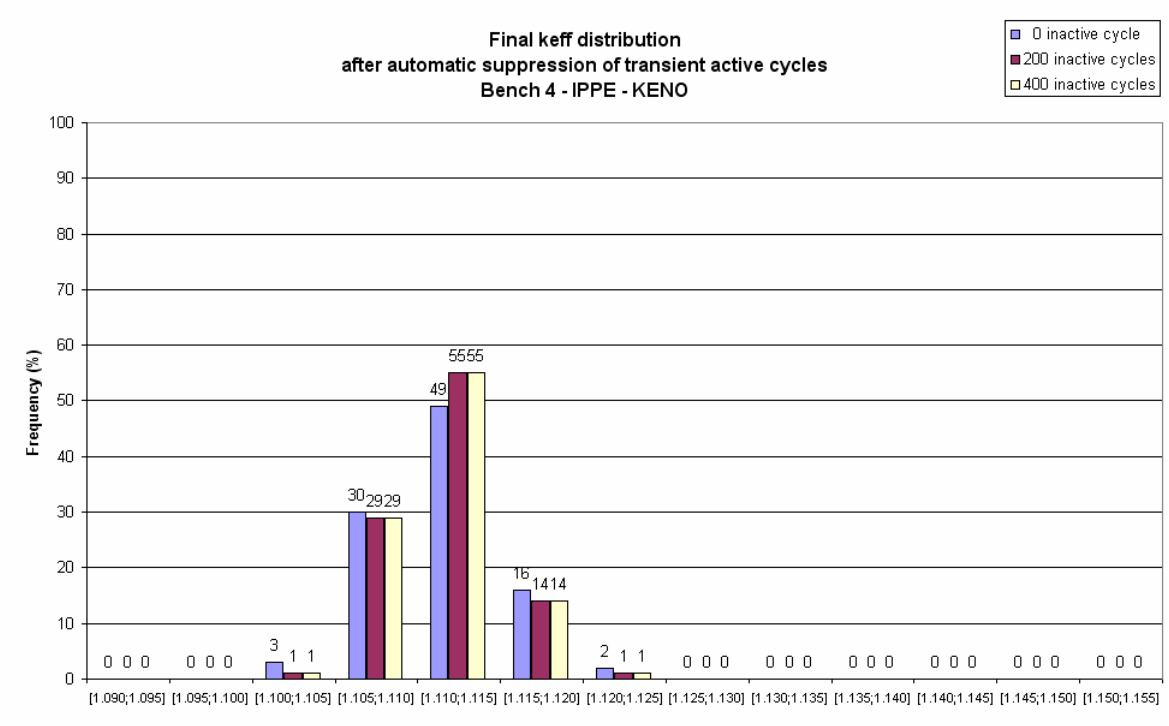
Final keff distribution
after automatic suppression of transient active cycles
Bench 4 - IPPE - KENO
0 inactive cycle
200 inactive cycles
400 inactive cycles
Frequency (%)
[1.090;1.095]
[1.095;1.100]
[1.100;1.105]
[1.105;1.110]
[1.110;1.115]
[1.115;1.120]
[1.120;1.125]
[1.125;1.130]
[1.130;1.135]
[1.135;1.140]
[1.140;1.145]
[1.145;1.150]
[1.150;1.155]

IRSN / MORET

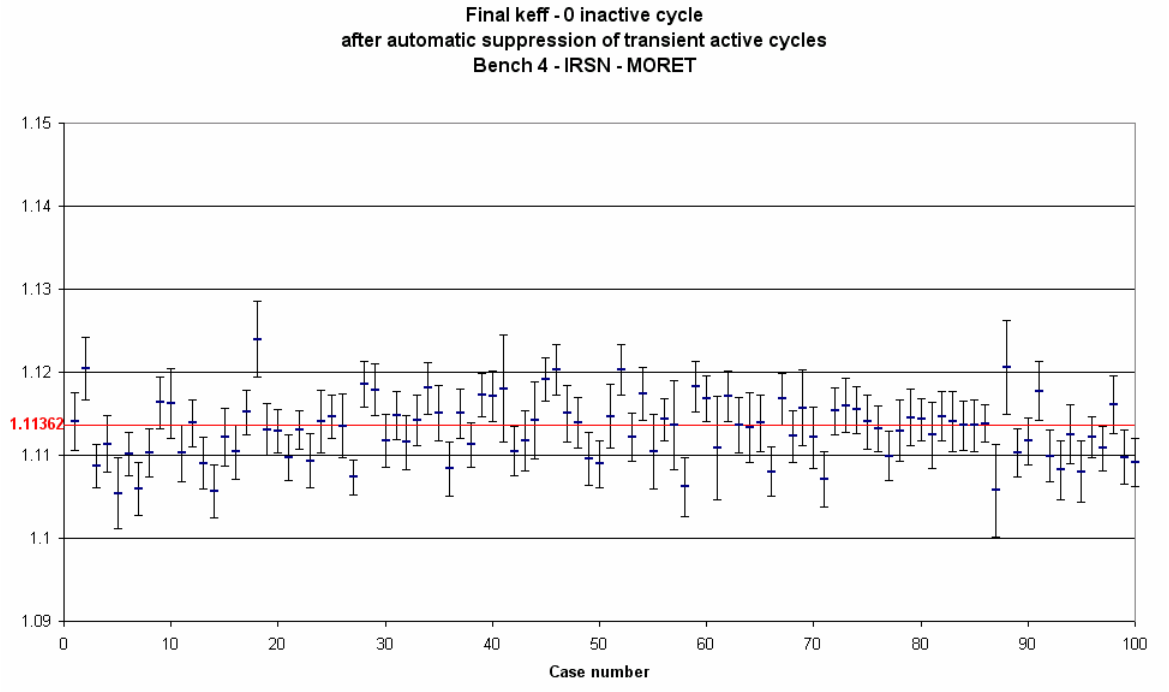
Final keff - 0 inactive cycle
after automatic suppression of transient active cycles
Bench 4 - IRSN - MORET
1.11362
Case number

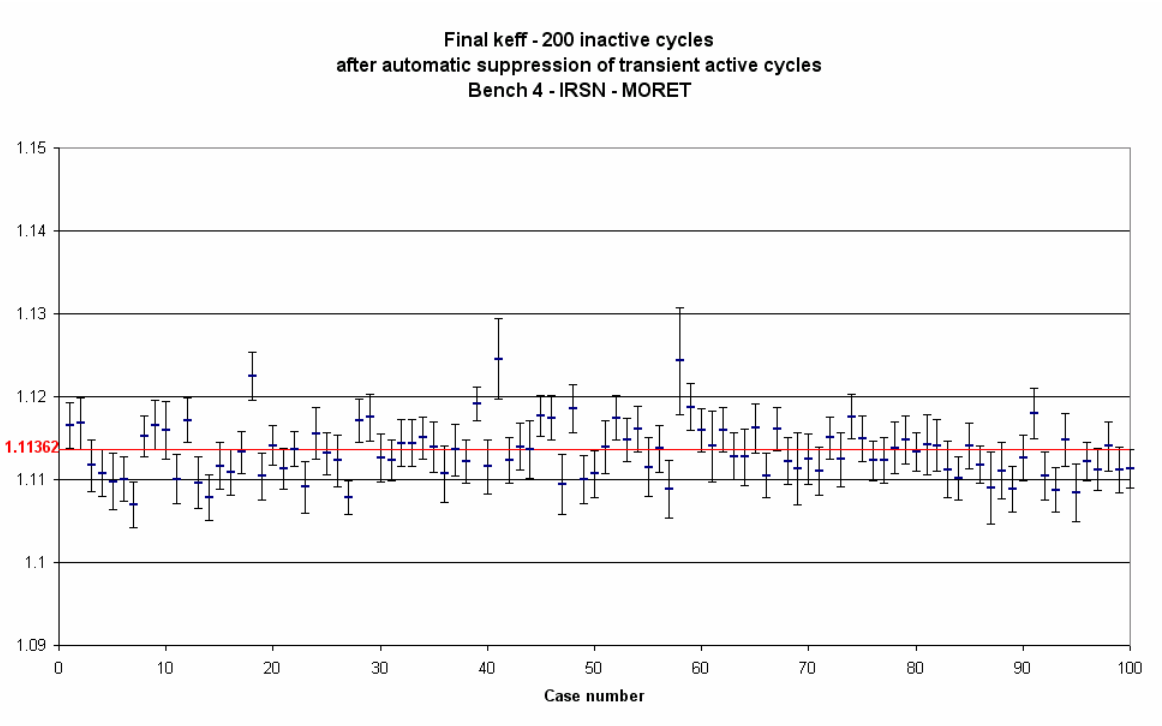
Final keff - 200 inactive cycles
after automatic suppression of transient active cycles
Bench 4 - IRSN - MORET
1.15
1.14
1.13
1.12
1.11362
1.11
1.1
1.09
0
10
20
30
40
50
60
70
80
90
100
Case number

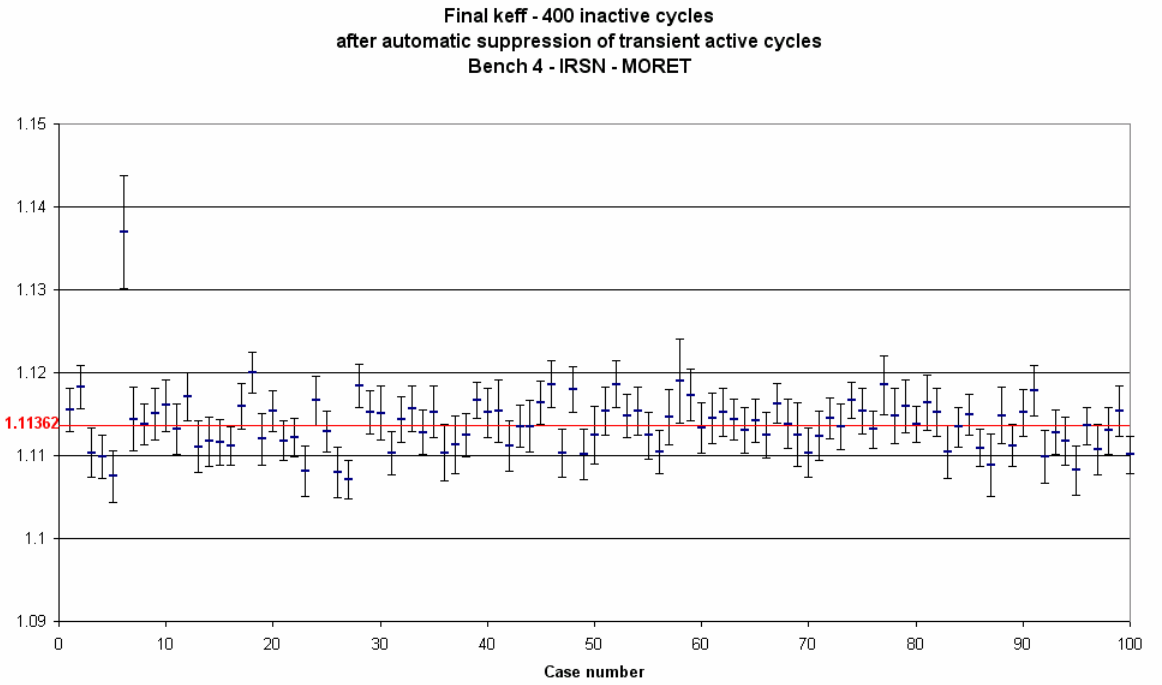
Final keff - 400 inactive cycles
after automatic suppression of transient active cycles
Bench 4 - IRSN - MORET
1.15
1.14
1.13
1.12
1.11362
1.11
1.1
1.09
0
10
20
30
40
50
60
70
80
90
100
Case number

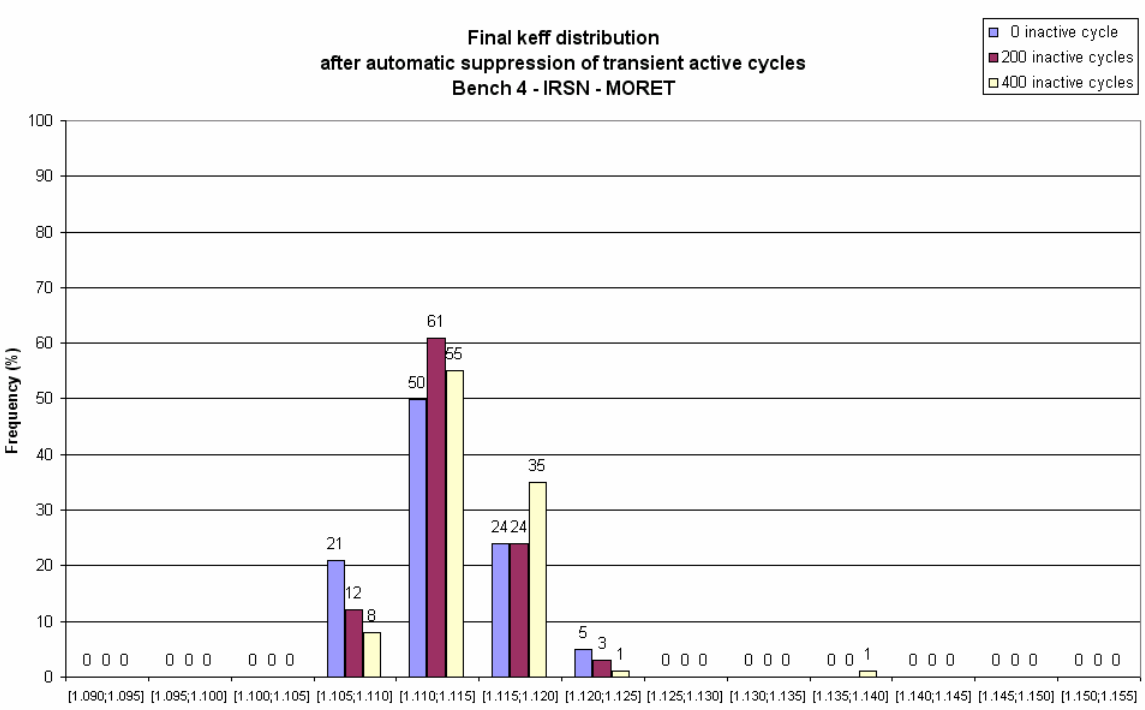
Final keff distribution
after automatic suppression of transient active cycles
Bench 4 - IRSN - MORET
0 inactive cycle
200 inactive cycles
400 inactive cycles
Frequency (%)
[1.090;1.095]
[1.095;1.100]
[1.100;1.105]
[1.105;1.110]
[1.110;1.115]
[1.115;1.120]
[1.120;1.125]
[1.125;1.130]
[1.130;1.135]
[1.135;1.140]
[1.140;1.145]
[1.145;1.150]
[1.150;1.155]

JNV / KENO

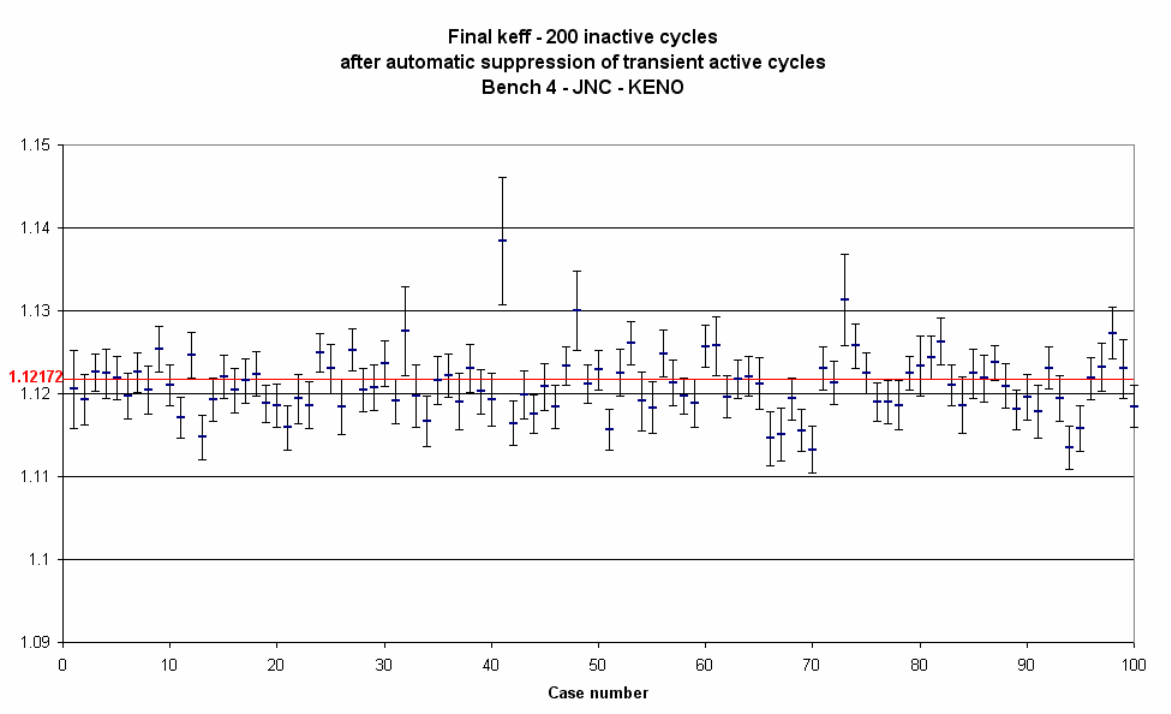
Final keff - 200 inactive cycles
after automatic suppression of transient active cycles
Bench 4 - JNC - KENO
1.12172
Case number

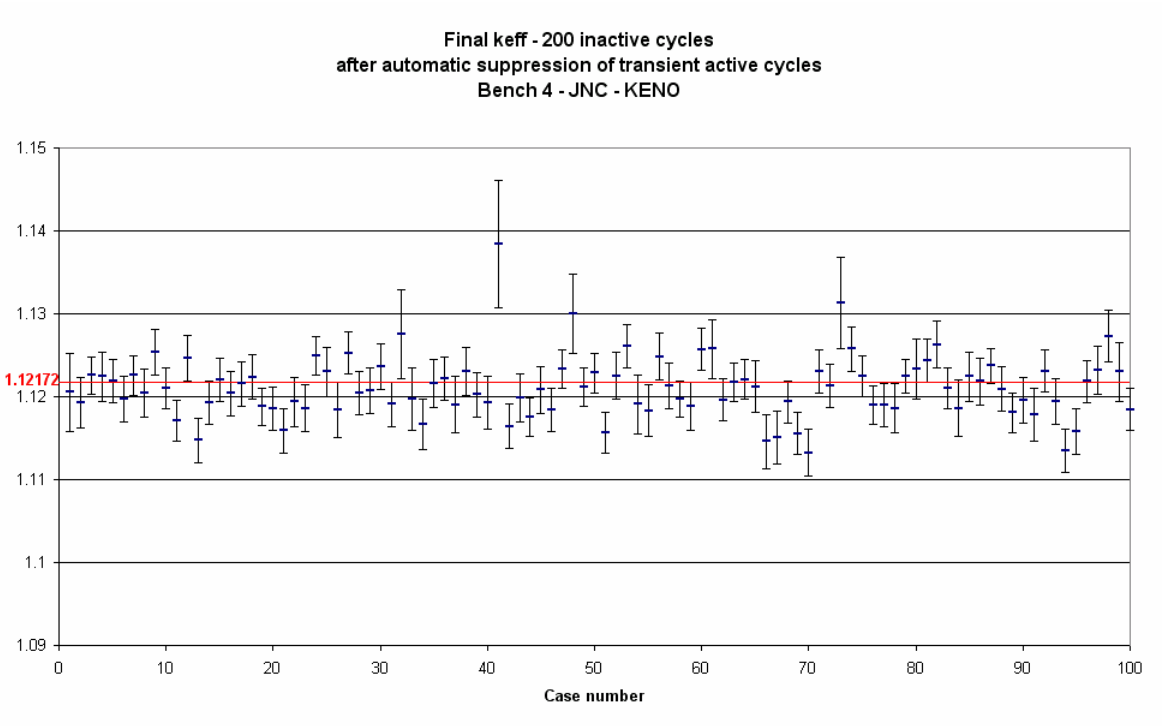
Final keff - 200 inactive cycles
after automatic suppression of transient active cycles
Bench 4 - JNC - KENO
1.15
1.14
1.13
1.12172
1.12
1.11
1.1
1.09
0
10
20
30
40
50
60
70
80
90
100
Case number

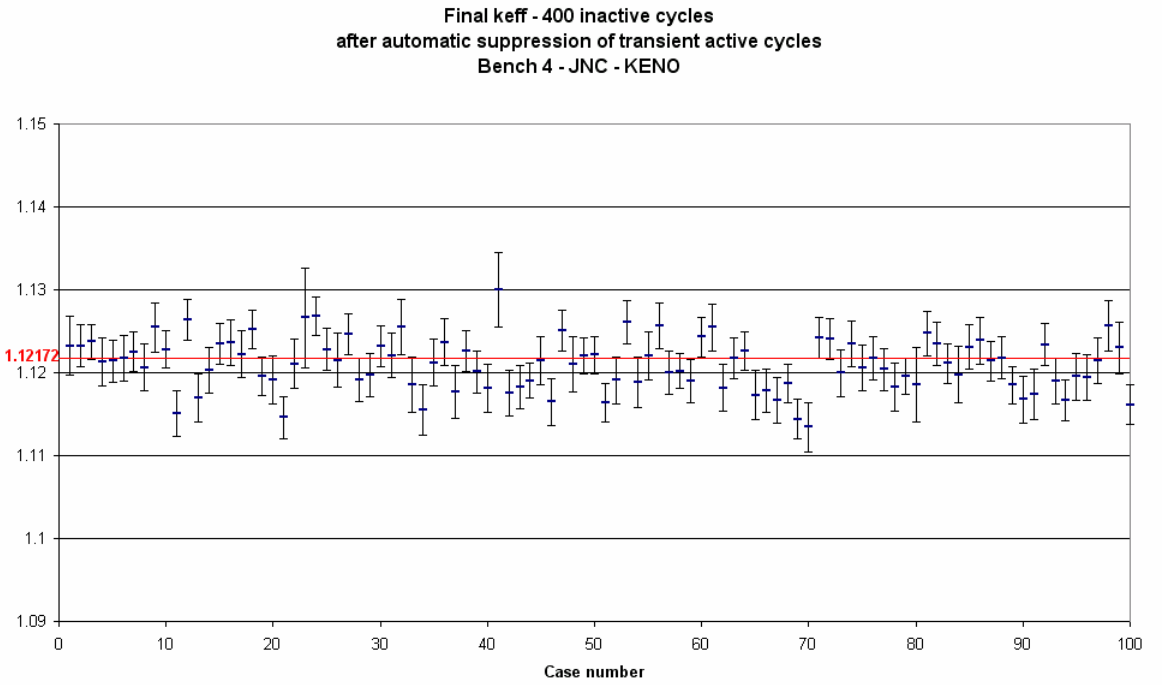
Final keff - 400 inactive cycles
after automatic suppression of transient active cycles
Bench 4 - JNC - KENO
1.15
1.14
1.13
1.12172
1.12
1.11
1.1
1.09
0
10
20
30
40
50
60
70
80
90
100
Case number

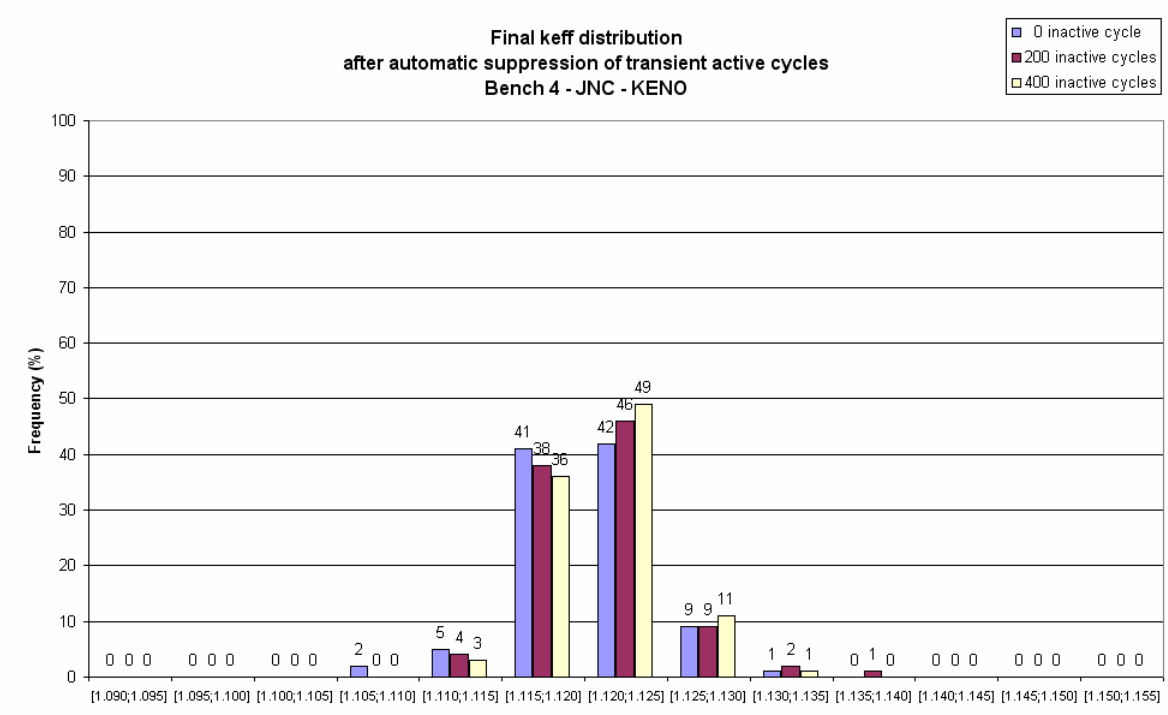
Final keff distribution
after automatic suppression of transient active cycles
Bench 4 - JNC - KENO
0 inactive cycle
200 inactive cycles
400 inactive cycles
Frequency (%)
[1.090;1.095]
[1.095;1.100]
[1.100;1.105]
[1.105;1.110]
[1.110;1.115]
[1.115;1.120]
[1.120;1.125]
[1.125;1.130]
[1.130;1.135]
[1.135;1.140]
[1.140;1.145]
[1.145;1.150]
[1.150;1.155]

LANL / MCNP

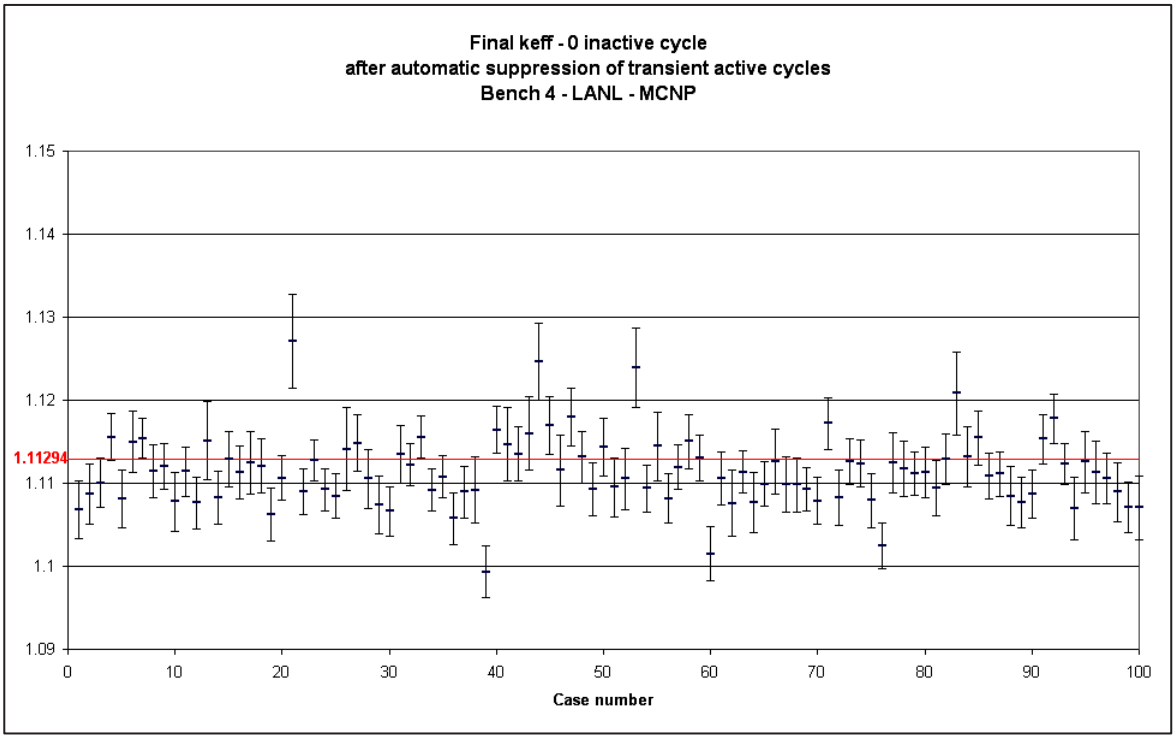
Final keff - 0 inactive cycle
after automatic suppression of transient active cycles
Bench 4 - LANL - MCNP
1.11294
Case number

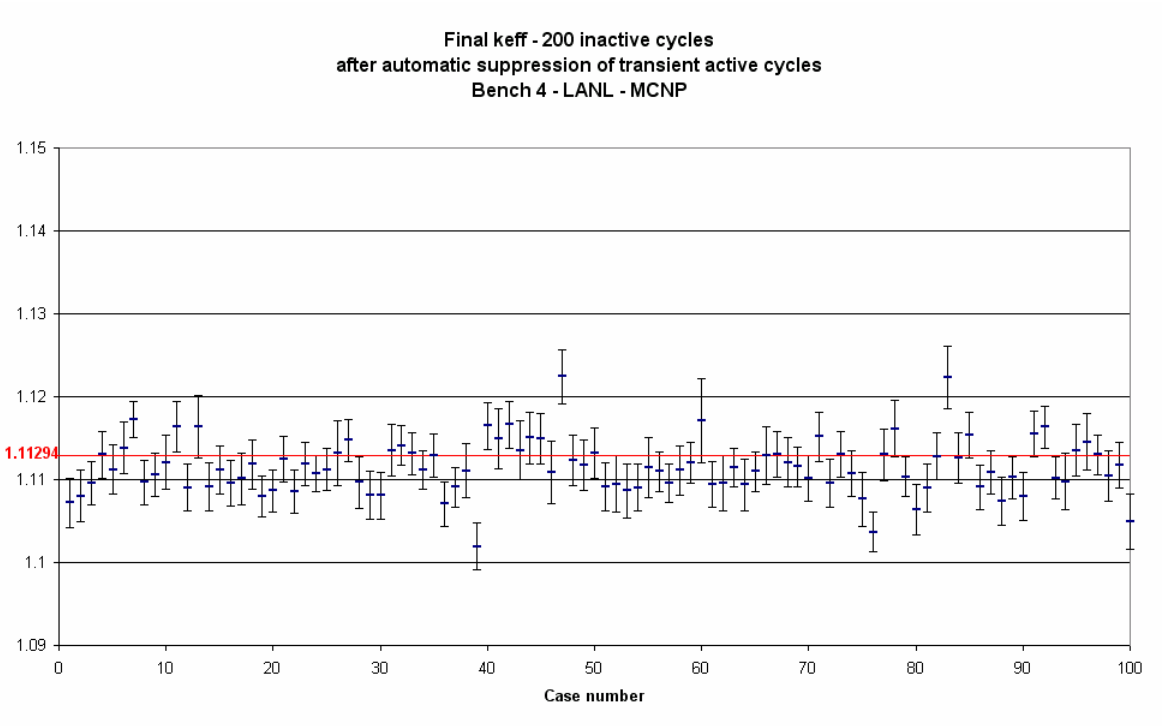
Final keff - 200 inactive cycles
after automatic suppression of transient active cycles
Bench 4 - LANL - MCNP
1.15
1.14
1.13
1.12
1.11294
1.11
1.1
1.09
0
10
20
30
40
50
60
70
80
90
100
Case number

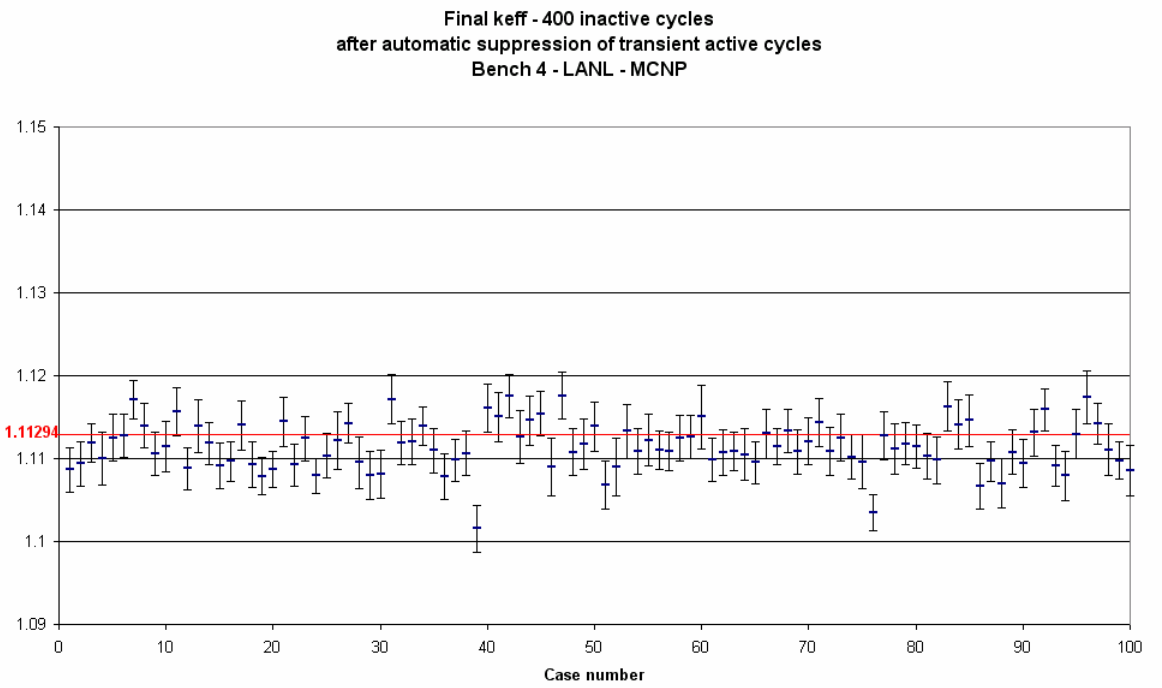
Final keff - 400 inactive cycles
after automatic suppression of transient active cycles
Bench 4 - LANL - MCNP
1.15
1.14
1.13
1.12
1.11294
1.11
1.1
1.09
0
10
20
30
40
50
60
70
80
90
100
Case number

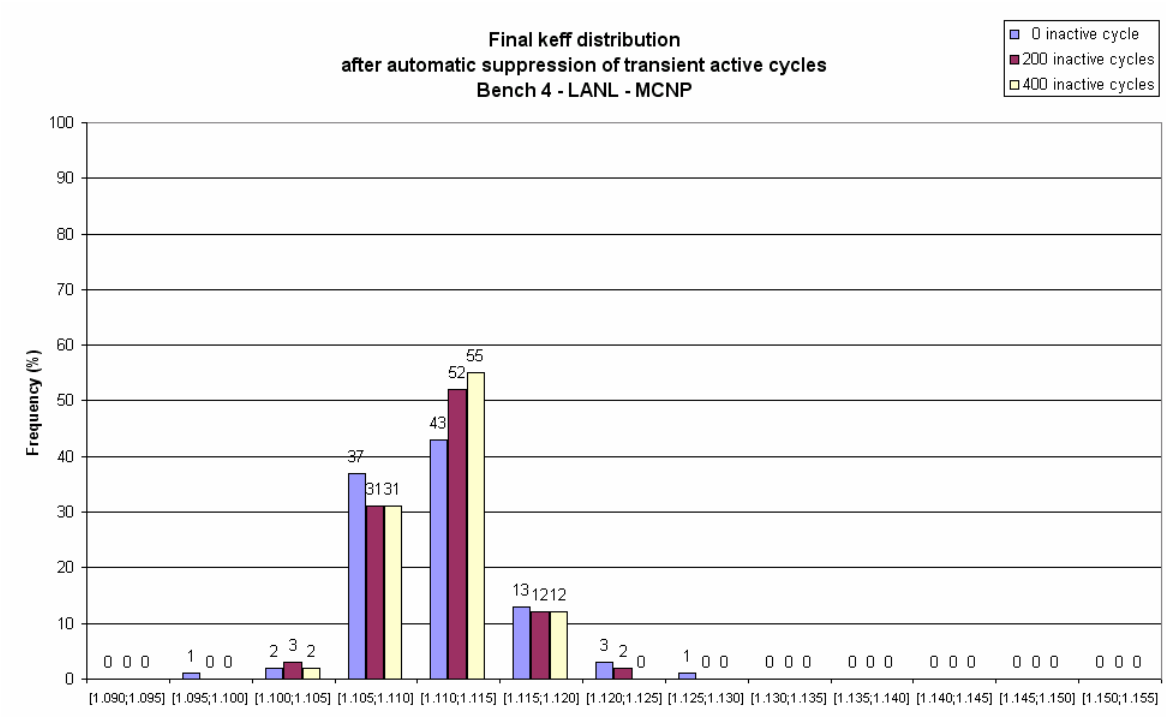
Final keff distribution
after automatic suppression of transient active cycles
Bench 4 - LANL - MCNP
0 inactive cycle
200 inactive cycles
400 inactive cycles
Frequency (%)
[1.090;1.095]
[1.095;1.100]
[1.100;1.105]
[1.105;1.110]
[1.110;1.115]
[1.115;1.120]
[1.120;1.125]
[1.125;1.130]
[1.130;1.135]
[1.135;1.140]
[1.140;1.145]
[1.145;1.150]
[1.150;1.155]

ORNL / KENO

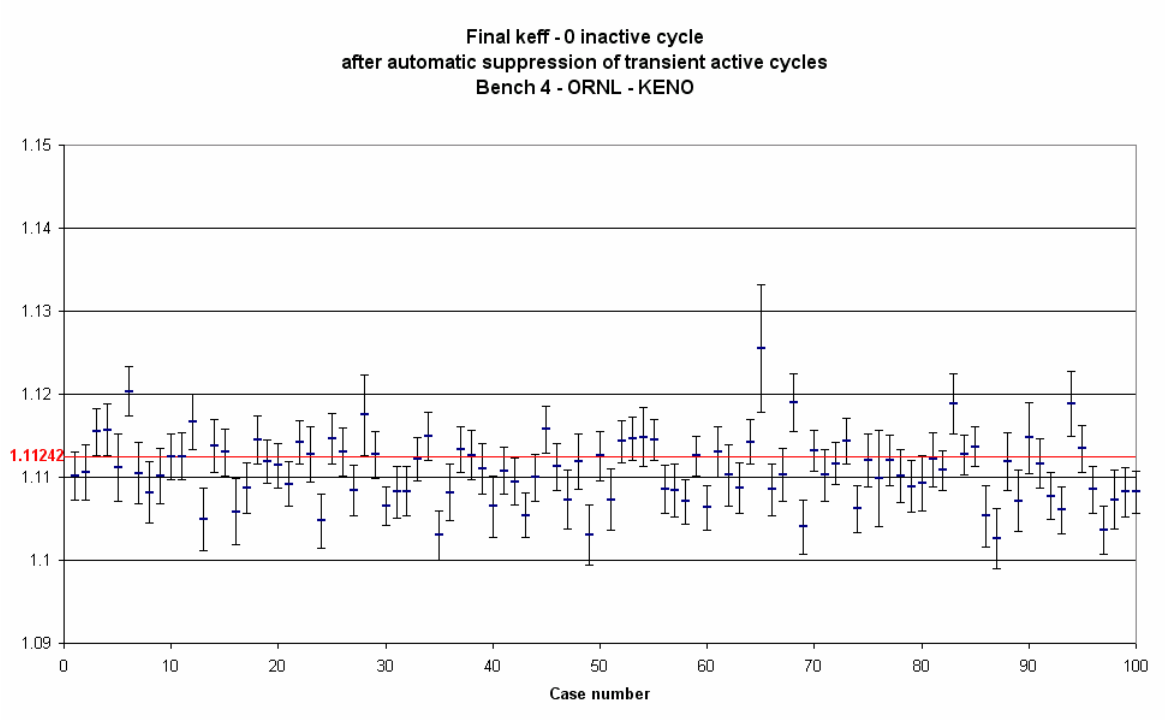
Final keff - 0 inactive cycle
after automatic suppression of transient active cycles
Bench 4 - ORNL - KENO
1.11242
Case number

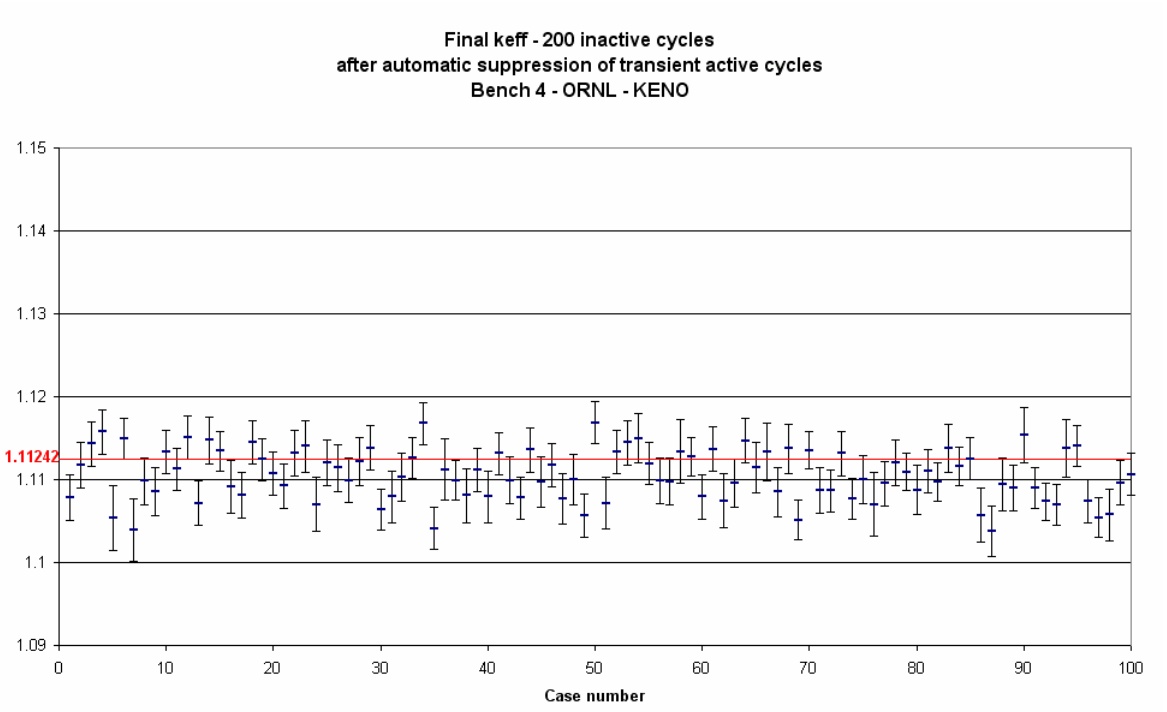
Final keff - 200 inactive cycles
after automatic suppression of transient active cycles
Bench 4 - ORNL - KENO
1.15
1.14
1.13
1.12
1.11242
1.11
1.1
1.09
0
10
20
30
40
50
60
70
80
90
100
Case number

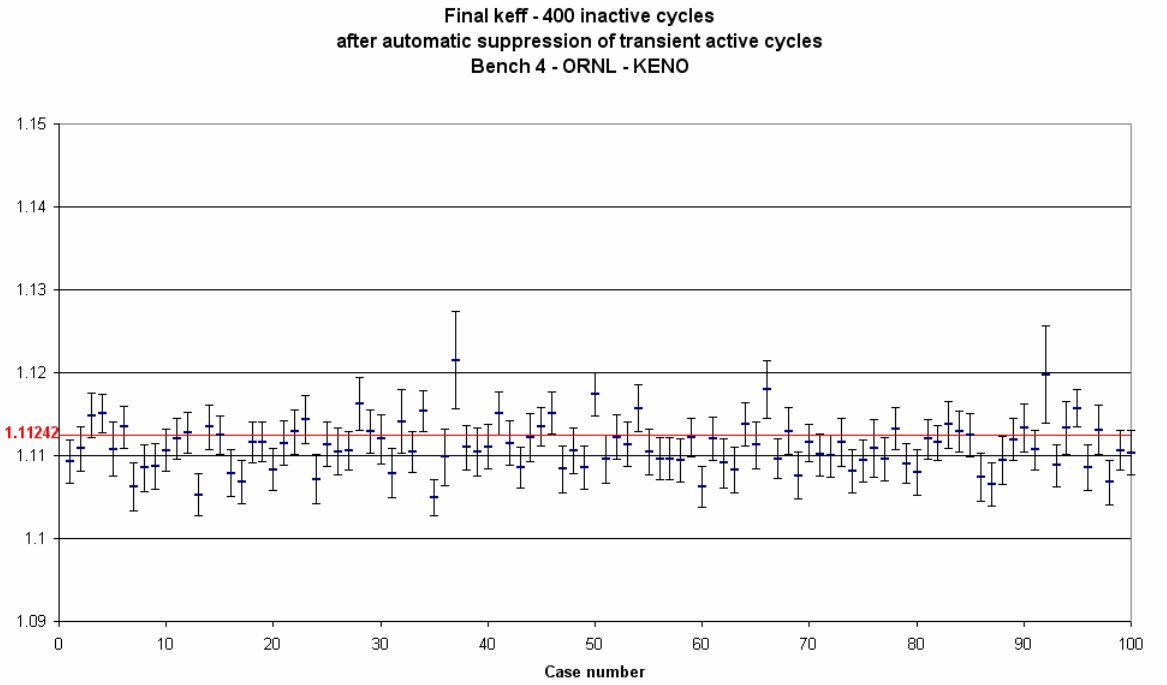
Final keff - 400 inactive cycles
after automatic suppression of transient active cycles
Bench 4 - ORNL - KENO
1.15
1.14
1.13
1.12
1.11242
1.11
1.1
1.09
0
10
20
30
40
50
60
70
80
90
100
Case number

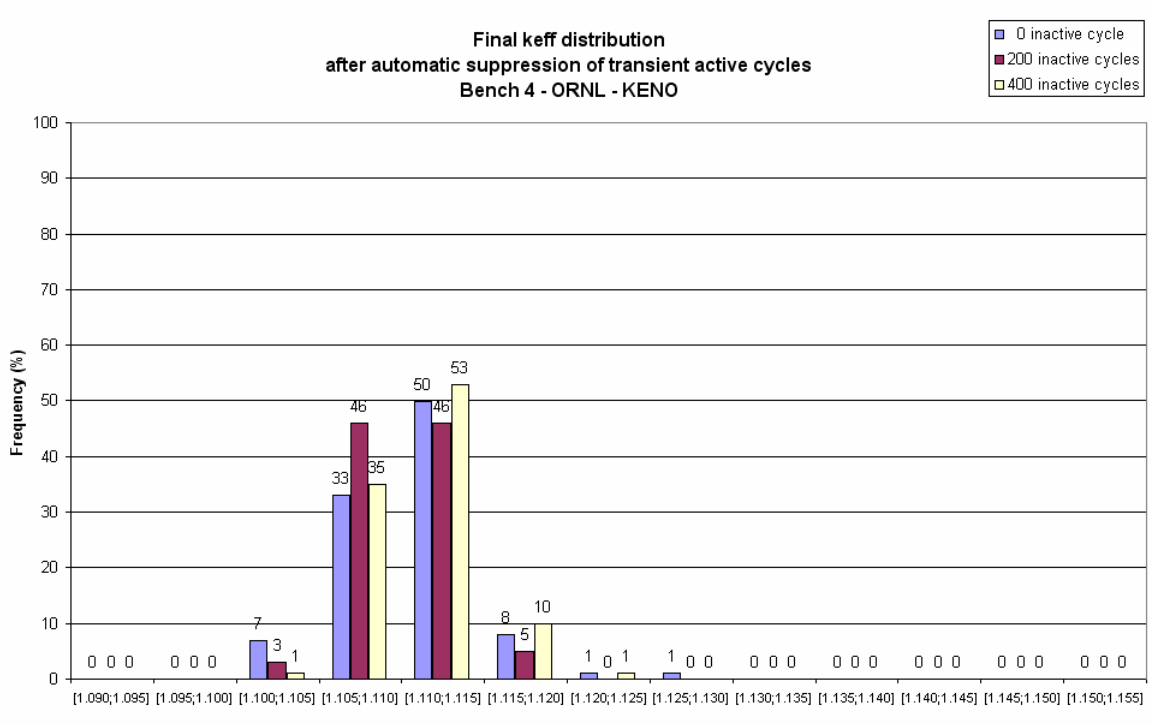
Final keff distribution
after automatic suppression of transient active cycles
Bench 4 - ORNL - KENO
0 inactive cycle
200 inactive cycles
400 inactive cycles
Frequency (%)
100
90
80
70
60
50
40
30
20
10
0
0 0 0
0 0 0
7
3
1
33
46
35
50
46
53
8
5
10
1
0
1
1
0 0
0 0 0
0 0 0
0 0 0
0 0 0
0 0 0
[1.090;1.095]
[1.095;1.100]
[1.100;1.105]
[1.105;1.110]
[1.110;1.115]
[1.115;1.120]
[1.120;1.125]
[1.125;1.130]
[1.130;1.135]
[1.135;1.140]
[1.140;1.145]
[1.145;1.150]
[1.150;1.155]

Appendix 5.i

DISTRIBUTION OF ($K_{EFF} - K_{EFF,REF}$) / $\sqrt{(STD^2 + STD_{REF}^2)}$ AFTER AUTOMATIC SUPPRESSION OF TRANSIENT ACTIVE CYCLES

ANL / VIM

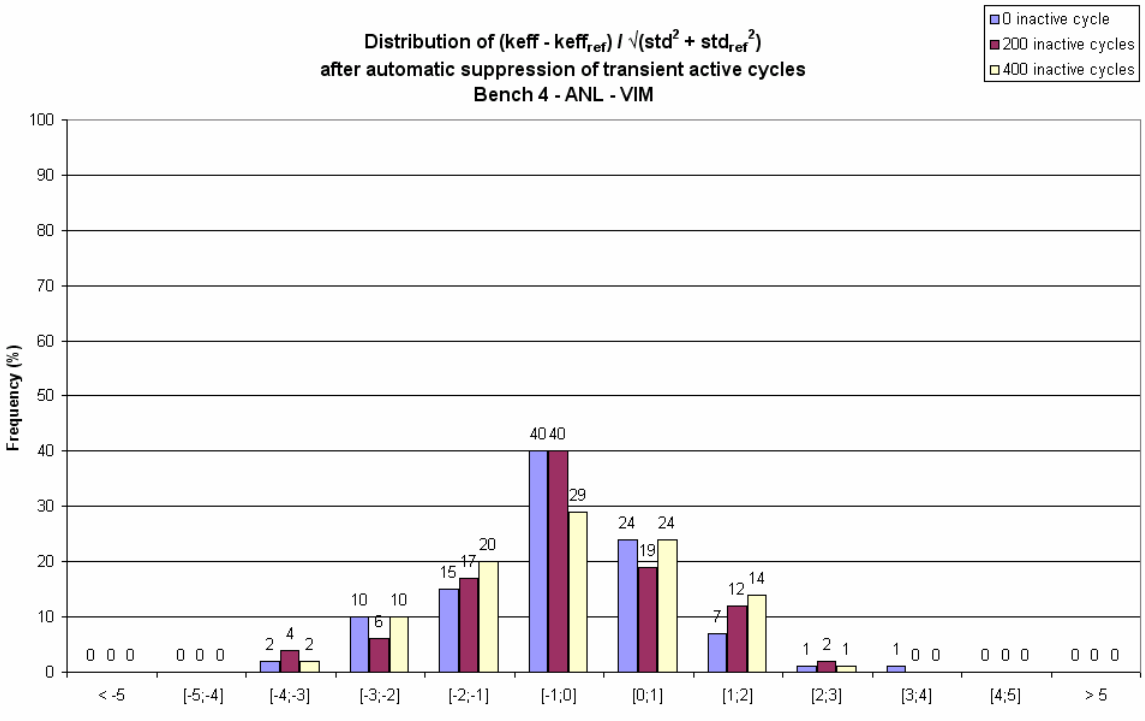

EMS / KENO

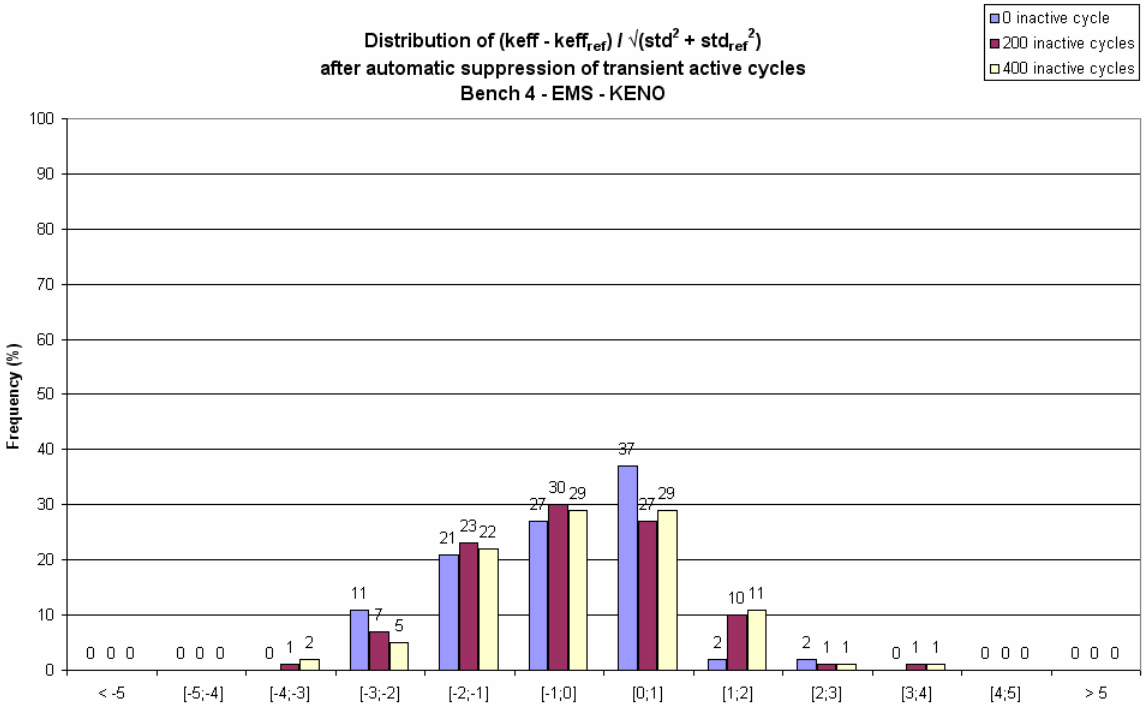

IPPE/ KENO

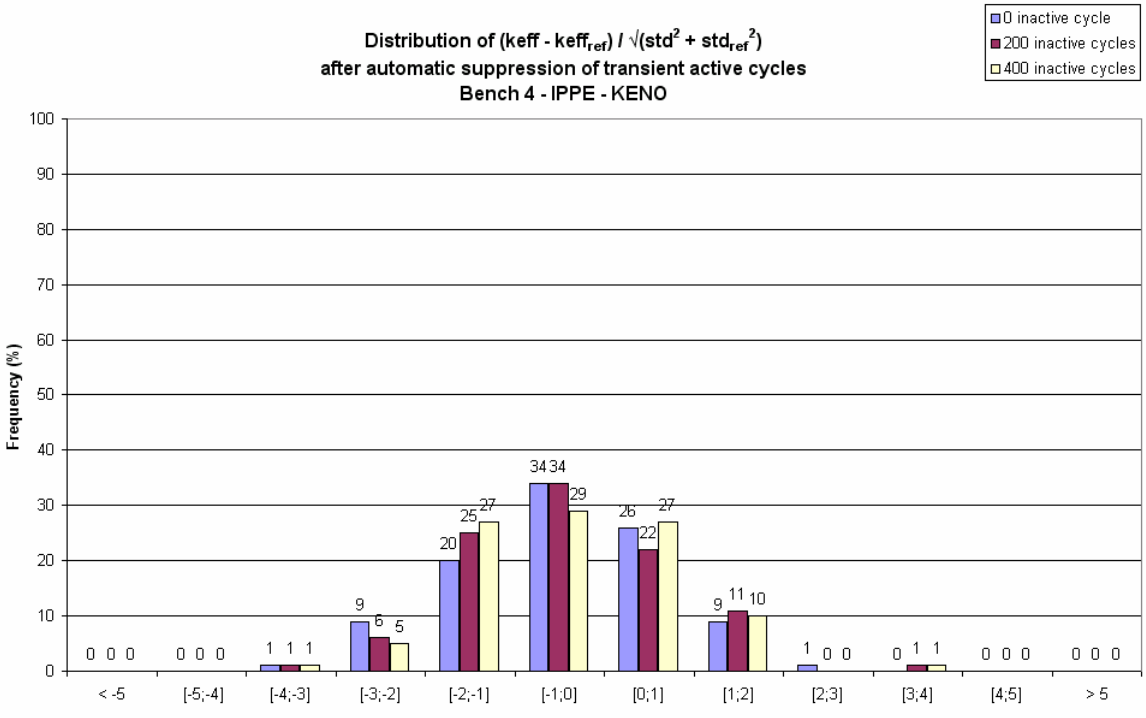

IRSN / MORET

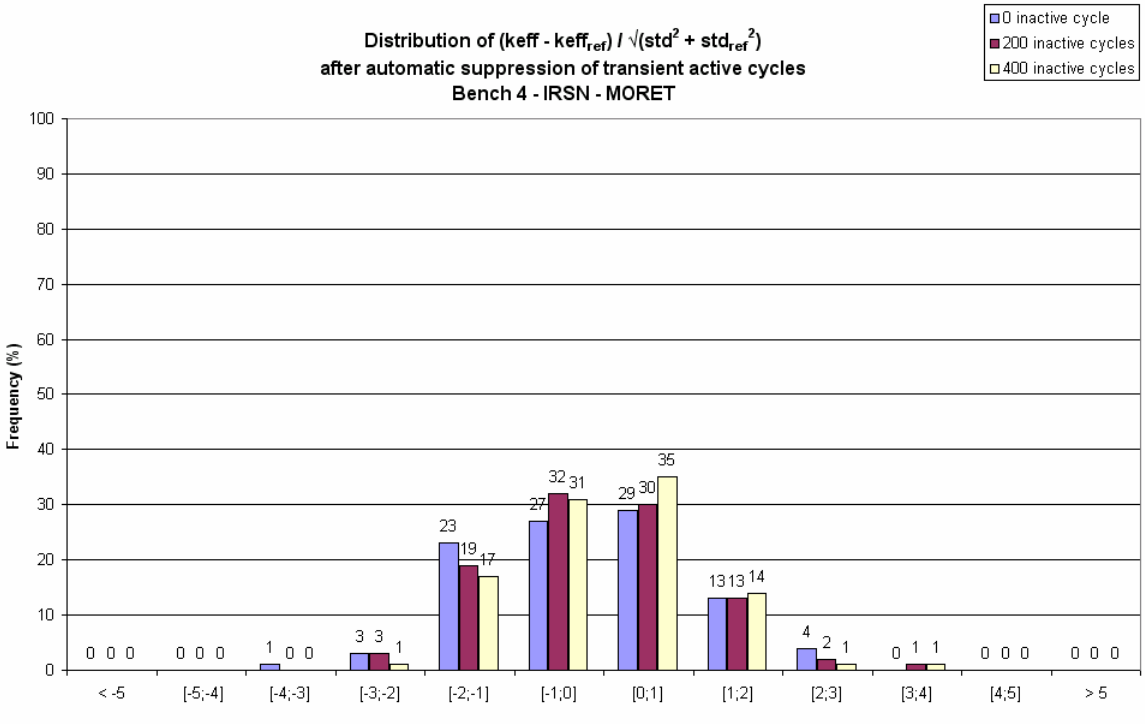

JNC / KENO

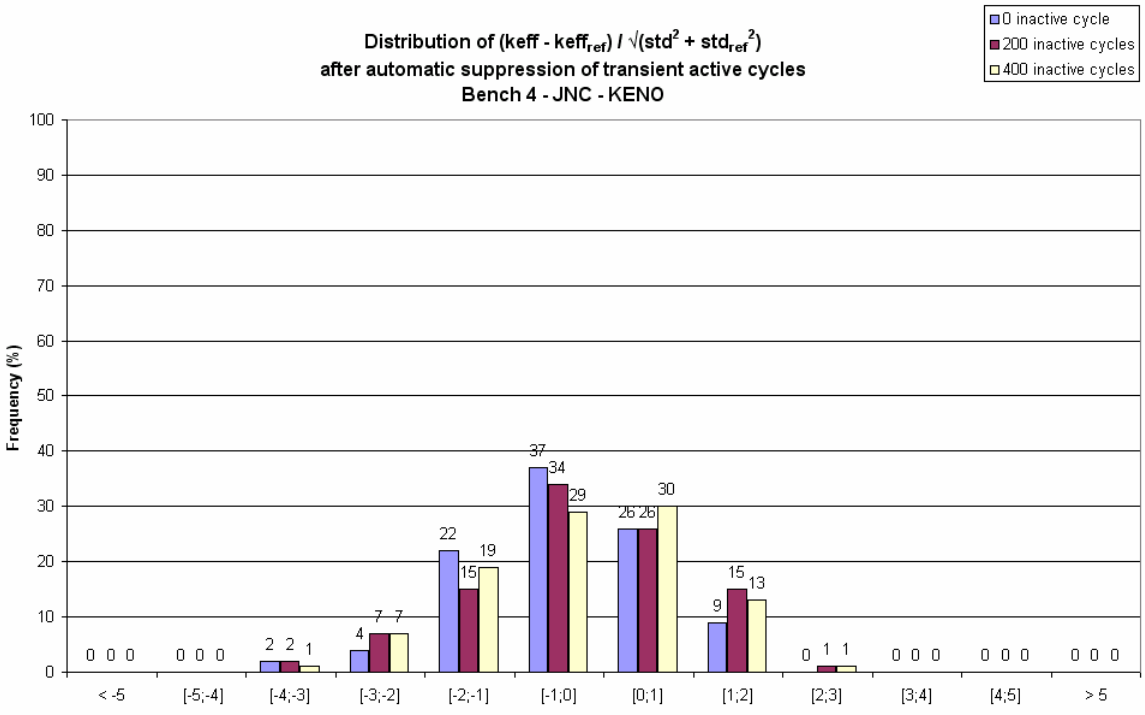

LANL / MCNP

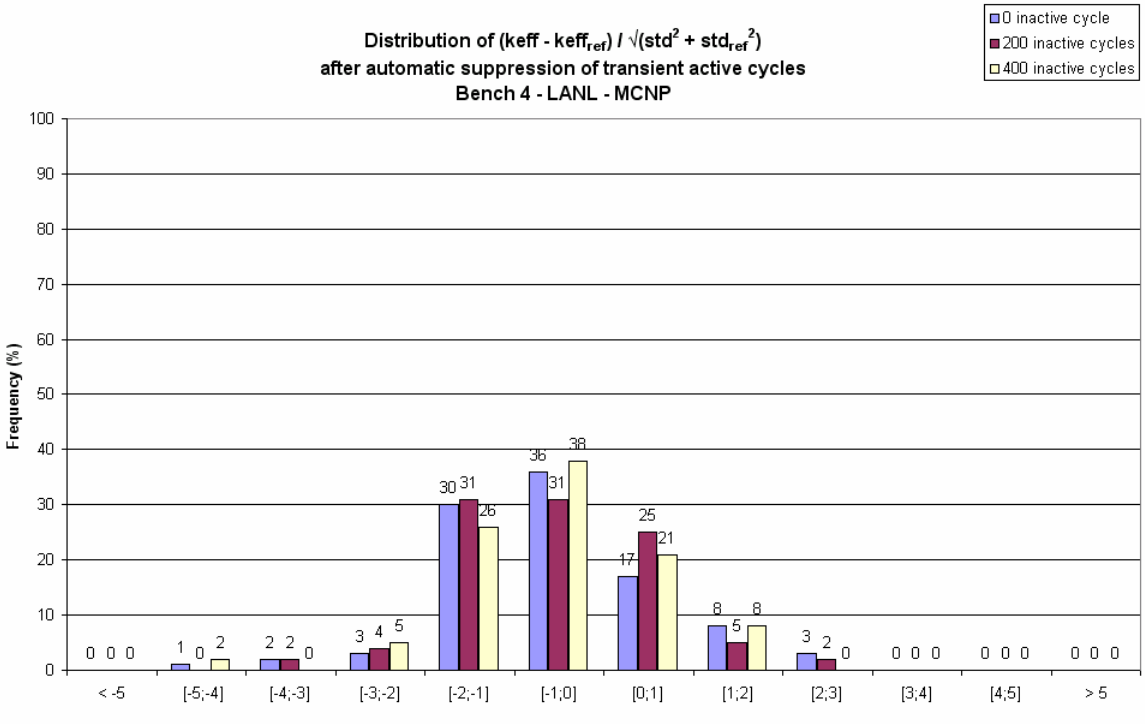

ORNL / KENO

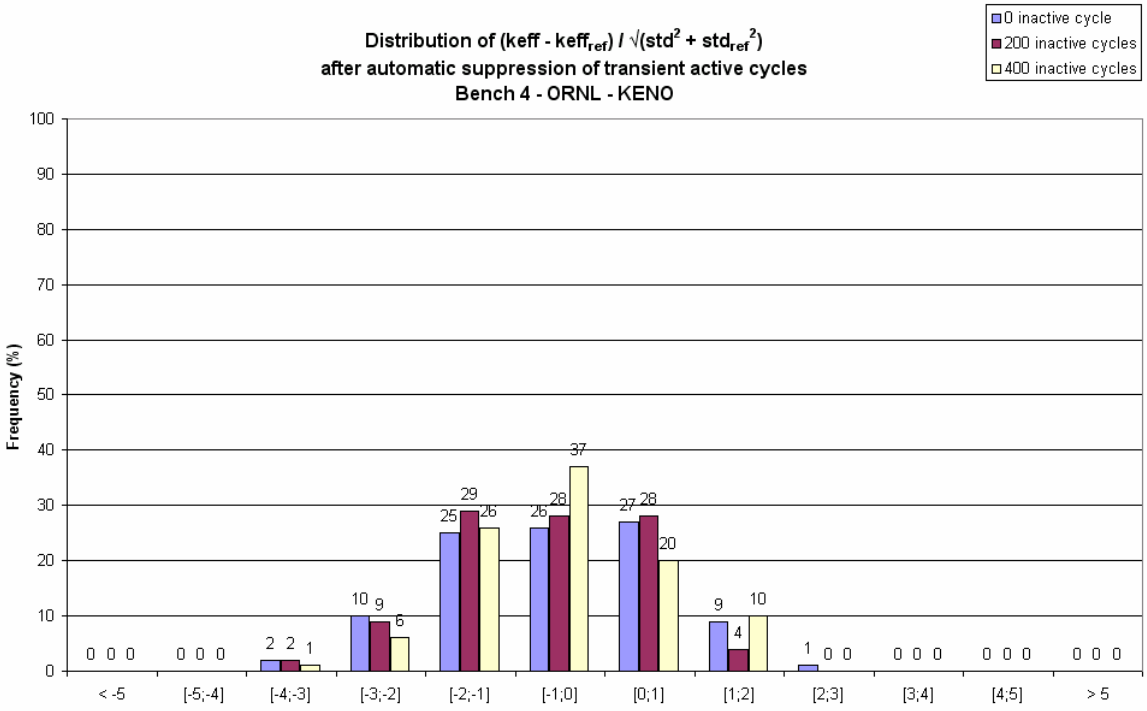

Chapter 6

SOURCE CONVERGENCE TEST PROBLEMS CONCLUSIONS

When a multiplying system has loosely coupled components, or many fissionable pieces, great care is required in the performance of criticality calculations, especially Monte Carlo calculations. We outline here a simple set of computational practices that will be of use in identifying such systems and will help the analyst to quickly develop a robust computational strategy. Because these techniques do not require any special algorithms or code features, they are accessible to anyone using the various criticality safety codes available today. They are aimed at two questions the analyst must answer: (1) Is the fission source sufficiently converged, and (2) Are the uncertainty estimates distorted by serial correlation?

Loose coupling occurs either if the multiplying component pieces are neutronically separated or if the system is much larger than a neutron migration length. As usual, the best defense against misleading calculational results is a thorough understanding of the physical properties of the system. The analyst should always inspect multiplying systems for loose coupling and undersampling effects. In the checkerboard problem, for example, the layout suggests that the multiplying cells are nearly isolated from each other. Moreover, if one compares the reflecting properties of water and concrete, it will be apparent that the corner cell bounded on two sides by concrete is probably the dominant cell in a converged calculation. This difference in reflection is well-known to experienced criticality safety analysts, but the effect can be easily evaluated using simple calculations of a single fuel pin bundle with the two different reflectors.

One reliable technique is to repeat a calculation with several different initial sources, and compare the results. For example, in test problem 2, the depleted pin cell, one should place the initial source first in the bottom half of the problem and then in the top half. If the calculations do not converge the source, they will produce significantly different k_{eff} values and fission distributions. If no significant eigenvalue differences are seen, then the problem is probably symmetric or nearly so, and any non-conservatism introduced by incomplete source convergence will be minimal. If the results do differ, the obvious conservative strategies are to (1) increase the number of skip generations until the starting source distribution no longer has an effect on the results, or (2) put the initial source entirely or predominantly in the high-worth end of the pins (identified in the preliminary calculation), and adjusting the number of skip generations.

A second technique can be used to complement the first. If there are many fissionable components, the procedure outlined in the previous paragraph can be laborious. In stead of an exhaustive search, one can perform a single calculation with a uniform starting source. If there are relatively few components that will eventually dominate the fission distribution, it should be possible to identify them. In the checkerboard problem, for example, it is clear even from the unconverged fission source after tens of generations that the corner location will be the most reactive. Obviously, one should try a source concentrated in location (1,3). The uniform initial source results can be used to identify a small set of starting distributions for use in the first technique if there are several reactive components. Care must be taken that the high-worth zones are not merely local maxima.

Third, one can test whether changing the Monte Carlo computational control parameters changes a supposedly converged k_{eff} or fission distribution. The simplest is to increase the number of skip generations and/or tally generations to see if k_{eff} or the fission distribution changes significantly. If there are many fissionable components, the number of histories per generation can be increased to check for undersampling problems. Many codes show the evolution of the eigenvalue estimates during the calculation, information which can be helpful but does not definitively show source convergence.

Two simple techniques can be used to assess the quality of uncertainty estimates. First, if either batching or the superhistory method is being used, the number of generations per batch or stage can be increased, while keeping the total number of histories tallied constant. If batching increases the estimated uncertainties, then the original ones were probably underestimated due to serial correlation between batches. The larger number of generations per batch should then be adopted to improve uncertainty estimates. The second technique is to perform a set of independent calculations (replicas) that are identical except for the random number sequence. After correcting for the increased total number of histories included in the set of replicas, the uncertainty estimates of the ensemble of results are compared with those from the Monte Carlo code.

Experience with the source convergence test problems also indicates that statistical tests should be employed with caution. There are fairly simple, long- and widely-used tests in use in some codes that are designed to detect unconverged eigenvalues or fission source distributions, but these are outside of the scope of this report. In general, statistical tests of eigenvalue estimates are not very sensitive. When a calculation fails such a test, it should be taken seriously, but if it passes not much assurance should be taken. Statistical tests usually perform better on fission distributions, but they are generally still not reliable enough to justify blind reliance on them. It is frequently the case that they perform much better when the number of histories per generation is very large.

Better statistical tests are currently being developed and tested that show great promise. The Shannon entropy methods [1,2] are useful partly because they provide a single number that reflects the state of convergence of the fission distribution – a very useful property for systems with many fissionable zones. The Brownian Bridge technique [3], by contrast, is used to detect eigenvalue drift and to adjust the number of skip generations retroactively to limit tallies to the post-convergence portion of the Monte Carlo calculation.

Advanced source convergence methods are worth using in difficult problems, but are not always effective. For example, stratified sampling and the superhistory method improve at least the probability that the fission source will converge. In general, however, the more difficult the problems, the less efficacious they are. Just as statistical tests are not a panacea, neither are these algorithms.

As new convergence methods and statistical tests are developed and used, they may be shown to be sufficiently robust to guarantee convergence or to detect inadequate convergence in criticality safety calculations, but for now they are no substitutes for sound engineering judgment, understanding the physics of individual systems, careful application of appropriate computational techniques, and healthy skepticism of one's results.

References

[1] “Stationarity Diagnostics Using Shannon Entropy in Monte Carlo Criticality Calculation I: F Test”, by T. Ueki and F. B. Brown, Trans. Am. Nucl. Soc., 87, 156 (2002).

[2] “Stationarity and Source Convergence Diagnostics in Monte Carlo Criticality Calculation”, by T. Ueki and F. B. Brown, Proceedings of M&C 2003, Nuclear Mathematical and Computational Sciences: A Century in Review, A Century Anew, Gatlinburg, Tennessee, April 6-11, 2003.

[3] “Automated Suppression of the Initial Transient in Monte Carlo Calculations based on Stationarity Detection using the Brownian Bridge Theory”, by Y. Richet, O. Jacquet and X. Bay, Proceedings of the Seventh International Conference on Nuclear Criticality Safety, Vol. II, 578-583, Tokai, Ibaraki, Japan, October 20-24, 2003.

OECD PUBLICATIONS, 2 rue André-Pascal, 75775 PARIS CEDEX 16
Printed in France.